

microscop
Lats2
Nijmegen
cytokinese
kloneren
celbiologie
volhouden
literatuur
substraat
evolutie
paranimf
ureum/glycerol-PAGE
copromotoren stagiaires
celdeling

DMPK E and Lats2 in the cell division cycle

Study of two AGC kinases

mitose
Western blot
celweek
dagje-uit
peptide-array
blunderbokaal
vrijdagmiddagborrel
celcyclus
proefschrift
relativeren
Noordwijkerhout cryptogram
contractiele ring
feest
PDZ domein
AGC-kinases
pipetteren
kerst diner
you-tube knaller
MLC2
doorzetten
DMPK
incasseren
Southern blot
Lieke Gerrits
isovormen
centrosomen
ladies movie night
promotor

DMPK E and Lats2 in the cell division cycle

Study of two AGC kinases

DMPK E and Lats2 in the cell division cycle

Study of two AGC kinases

The studies described in this thesis were performed at the department of cell biology, Nijmegen Centre for Molecular Life Sciences, Radboud University Nijmegen Medical Centre (RUNMC), The Netherlands. Financial support was obtained from RUNMC grant 2006-12.

ISBN/EAN: 9789461082701

Cover design: Mirthe Erkens, Marieke Willemse and Lieke Gerrits

Printed by: Gildeprint Drukkerijen - The Netherlands

DMPK E and Lats2 in the cell division cycle

Study of two AGC kinases

Een wetenschappelijke proeve op het gebied van de Medische Wetenschappen

Proefschrift

ter verkrijging van de graad van doctor
aan de Radboud Universiteit Nijmegen
op gezag van de rector magnificus prof. mr. S.C.J.J. Kortmann,
volgens besluit van het college van decanen
in het openbaar te verdedigen
op donderdag 5 april 2012 om 15.30 uur precies

door
Jacqueline Wilhelmien Gerrits
geboren op 26 augustus 1981
te Noordwijkerhout

Promotor:

Prof. dr. B. Wieringa

Copromotoren:

Dr. D.G. Wansink

Dr. W.J.A.J. Hendriks

Manuscriptcommissie:

Prof. dr. J.M.J. Kremer (voorzitter)

Prof. dr. M.A. Huynen

Dr. F.N. van Leeuwen

To live is to choose. But to choose well, you must know who you are and what you stand for, where you want to go and why you want to get there.

- Kofi Annan -

TABLE OF CONTENTS

Chapter 1	General introduction	9
	1. Reversible protein phosphorylation	
	2. The AGC kinase group	
	3. Protein interaction domains	
	4. Cell cycle	
	5. Myosin II	
Chapter 2	Phosphorylation target site specificity for AGC kinases DMPK E and Lats2	35
Chapter 3	Phosphorylation of myosin regulatory light chain by a cytosolic isoform of Dystrophia Myotonica Protein Kinase (DMPK)	65
Chapter 4	Gene duplication and conversion events shaped three homologous differentially expressed myosin regulatory light chain (MLC2) genes	95
Chapter 5	Lats2 contains a phosphorylation-regulated PDZ domain-binding motif	127
Chapter 6	Summarizing discussion	149
	References	163
	Nederlandse samenvatting	187
	Abbreviations	191
	Publications	194
	Curriculum vitae	195
	Dankwoord	196

Chapter 1

General introduction

cell cycle
Lats2 chromosome missegregation
NDR kinases MLC2
tumorigenesis
DMPK kinases cytokinesis
PDZ domain II PDZ domain aneuploidy
reversible protein phosphorylation
cell cycle
NDR kinases
Myosin II
aneuploidy
DMPK
cell division
contractile ring
aneuploidy
protein interaction domains
contractile ring
AGC kinases
DMPK kinases
MLC2
cell cycle
DMPK
centrosome
PDZ domain
MLC2 regulation
Lats2
AGC kinases
cytokinesis
cell division
contractile ring
tumorigenesis
Myosin II
AGC kinases
DMPK kinases
reversible protein phosphorylation
centrosome
tumorigenesis
Lats2
PDZ domain
DMPK
Lats2
cell cycle
aneuploidy
cell division
MLC2
contractile ring
AGC kinases
protein interaction domains

Coordination of cellular processes requires accurate control of interplay between components of signalling pathways. These components are proteins and small molecules, including peptides, nucleotide derivatives, steroids, phospholipids and ions. In signal transfer often enzymes are involved that modify specific amino acid residues in their substrate proteins, leading to a change in substrate protein conformation or stability. This in turn affects activity or interaction characteristics of the substrate(s). Amino acid residues that can get modified are often part of motifs that serve as binding sites for protein-protein interaction (reviewed in Pawson and Nash, 2003). In this way, catalytic domains and interaction domains on different proteins work together to transduce signals.

A topic of main interest of my work described in this thesis are signalling events that are involved in cell cycle control. The cell cycle encompasses the entire sequence of processes that occur in a cell from the time it is formed from its parent cell till the time of its own division. A vast series of protein-protein interaction and protein modification events steer these processes, which will ultimately - but only when strictly regulated - lead to the generation of two daughter cells, each with an exact copy of the mother cell's genome. In this thesis, focus will be on two enzymes that modify their substrates via phosphorylation: protein kinases DMPK E and Lats2. Results obtained provide insight into the mechanisms via which they influence cell cycle progression. Before presenting an outline of this thesis, relevant information about the mechanism of protein phosphorylation, structure-function relationships in DMPK E and Lats2, the cell cycle and cell division (in particular cytokinesis) and the role of the newly identified DMPK E substrate MLC2 will be presented in this chapter.

1. REVERSIBLE PROTEIN PHOSPHORYLATION

Many signalling pathways involve phosphorylation of target proteins. Already in 1906 evidence of presence of phosphate in proteins was found (Levene and Alsberg, 1906), but it took another 40-50 years to discover that the removal and addition of phosphate groups was mediated by proteins themselves (Burnett and Kennedy, 1954; Simoni *et al.*, 2002). Subsequently, in the mid 1950s Krebs and Fisher discovered that the attachment and removal of phosphate groups to and from enzymes can reversibly alter their activity (reviewed in Krebs and Beavo, 1979). This process, called reversible protein phosphorylation (Figure 1), turned out to be a key mechanism in the regulation of cellular signalling pathways (Hunter, 2000; Ubersax and Ferrell, 2007).

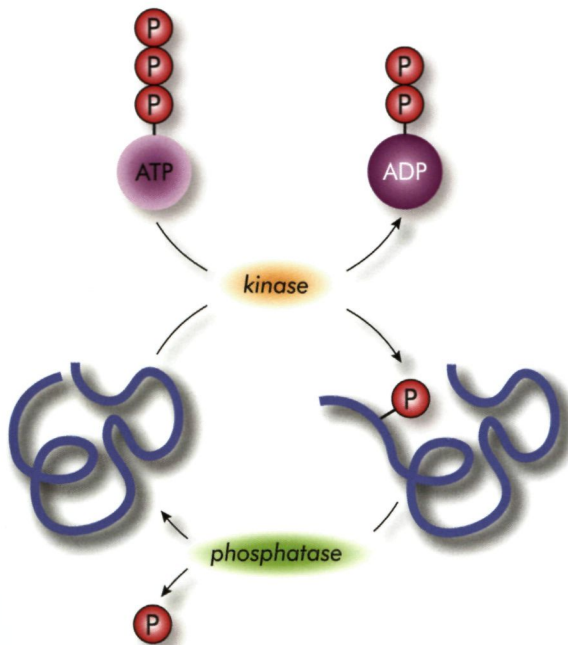


Figure 1: Reversible protein phosphorylation. Kinases mediate coupling of the terminal phosphate group of ATP to serine, threonine or tyrosine residues. Phosphatases are responsible for the removal of these phosphate groups. In this way, proteins can cycle between phosphorylated and unphosphorylated states which often differ in their conformation. Reversible phosphorylation is crucial in regulation of protein activity and stability.

Protein phosphorylation depends on the activity of two different classes of phospho-transfer enzymes: protein kinases and protein phosphatases. Protein kinases catalyze transfer of the terminal (γ) phosphate group of an ATP molecule to the hydroxyl group of a serine, threonine or tyrosine side chain of a substrate protein. Phosphorylation of histidine, lysine and arginine residues has also been described (Ciesla *et al.*, 2011; Steeg *et al.*, 2003; Wieland *et al.*, 2010), but mainly in prokaryotes. As this activity seems to be of minor influence in mammalian protein signalling, it will not be further discussed here. Protein phosphatases catalyze the removal of phosphate groups. The phosphorylation state of an amino acid residue in any given target protein at any moment thus depends on the relative activities of protein kinases and phosphatases that are directed towards that site. Most kinases exhibit a specificity for phosphorylation of either serine/threonine or tyrosine residues, although dual-specificity kinases do exist. The same holds true for phosphatases. This introduction will continue with a detailed description of the structure and biological significance of members of a particular group of kinases, the AGC kinases, two of which have been subject of study in this thesis.

2. THE AGC KINASE GROUP

AGC kinases form one of the groups of protein kinases that were defined by Manning

in 2002 based on sequence homology between the individual kinase domains (Manning *et al.*, 2002). The AGC group of protein kinases comprises multiple related (sub)families of protein serine/threonine kinases, including the NDR and DMPK families studied here (Figure 2). Nowadays, more than 500 human kinases have been identified, 60-70 of which belong to the AGC kinase group (Hergovich *et al.*, 2006b; Manning *et al.*, 2002). The term AGC is derived from the three archetypical members of this group, protein kinase A (PKA), PKG and PKC (Hanks and Hunter, 1995).

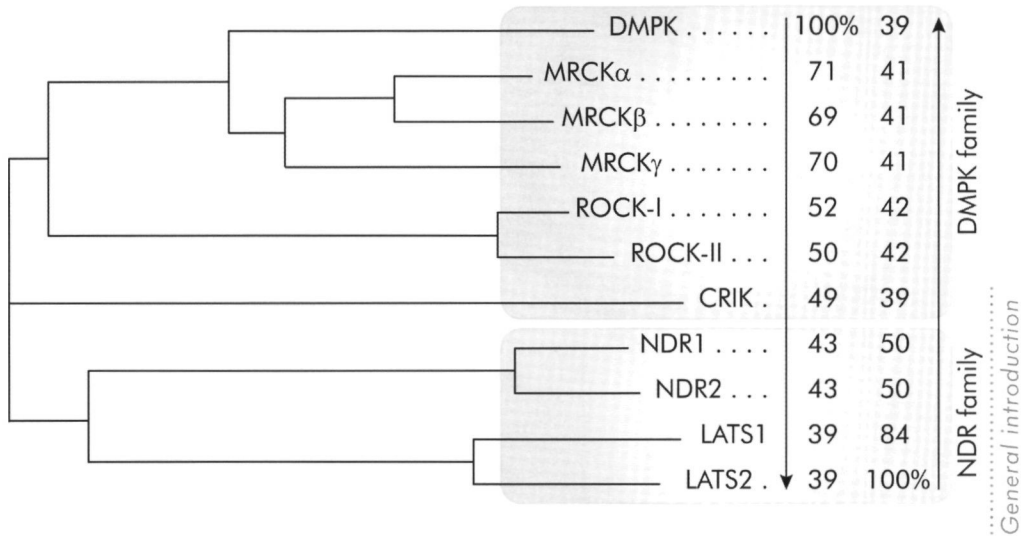


Figure 2: Evolutionary relationship between DMPK and NDR families of the AGC kinase group.

Phylogenetic tree of DMPK (DMPK, MRCK α , - β , - γ , ROCK-I and -II, and CRK) and NDR (NDR1 and -2 and LATS1 and -2) families of the AGC kinase group. The tree was created with ClustalW and mouse sequences were used. Percentages indicate sequence identity related to DMPK's (left column) or LATS2's (right column) kinase domain (set at 100%). The tree is drawn to scale. Adapted from Wansink *et al.*, 2006.

The folded AGC kinase domain consists of an amino-terminal small lobe of mostly β -sheets and a carboxy-terminal large lobe of mainly α -helices (Figure 3). The ATP binding cleft is located between these two lobes. Activation of most AGC kinases requires phosphorylation of two highly conserved sequences, the activation segment (also known as the T- or activation loop) and the hydrophobic motif. The activation segment resides in the catalytic domain and its phosphorylation induces a conformational change that leads to formation of an interaction network between a glutamate residue in one of the α -helices (α C), a lysine residue in the small lobe and the phosphate groups of ATP, which is essential for kinase activity (Komander *et al.*, 2005; Pearce *et*

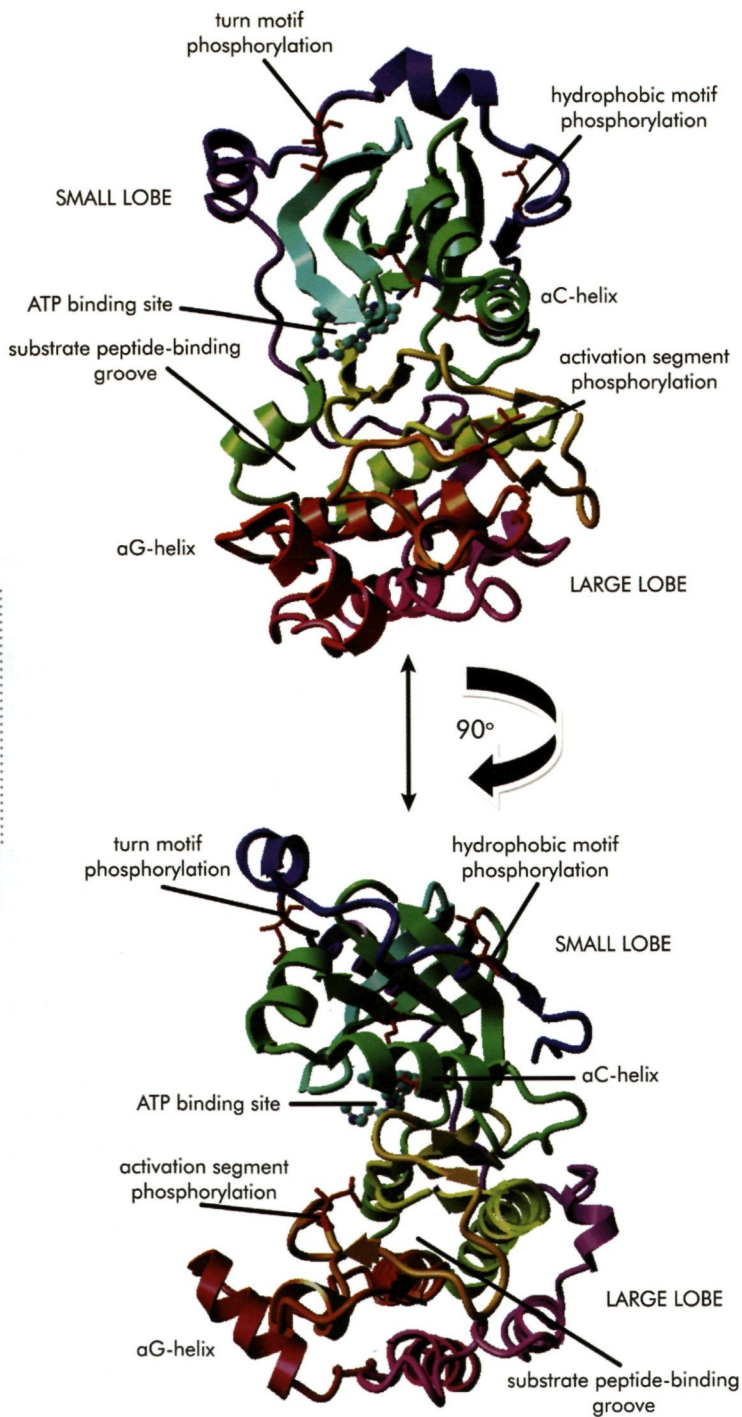


Figure 3: Structural features of the kinase domain of AGC kinases. The most important structural features of the kinase domain of AGC kinases are exemplified in the structure of protein kinase C $\beta 2$ (PDB 2I0E). The phosphorylation target residues in the turn motif, hydrophobic motif and activation segment that are important for kinase activation are indicated in red. The glutamate residue in the αC helix and the lysine residue in the small lobe that form a network with the phosphates of ATP which is required for catalytic activity are also indicated in red. In some AGC kinases, the αG helix is also involved in interactions with substrates. The same structure is shown from two different angles which are rotated 90° with respect to each other.

al., 2010; Yang *et al.*, 2002a). The hydrophobic motif is located outside the catalytic domain and buried in a hydrophobic pocket. Its phosphorylation stimulates both kinase activity and protein stability (Yang *et al.*, 2002a; Yang *et al.*, 2002b). Another phosphorylatable motif that is found in some AGC kinases is the turn motif which also contributes to kinase stability and in addition is thought to prevent dephosphorylation of the hydrophobic motif (Grodsky *et al.*, 2006; Hauge *et al.*, 2007; Pearce *et al.*, 2010), thereby contributing to an increased kinase activity.

There are several ways in which AGC kinases can interact with their substrates. A substrate peptide-binding groove is located near the active site (Yang *et al.*, 2002b), but a protruding helical structure in the large lobe (α G-helix) can also mediate interaction with substrates (Komander *et al.*, 2008). The presence of other structural domains or binding motifs contribute to a higher affinity and specificity between AGC kinases and their substrates (Pearce *et al.*, 2010).

Some members of the AGC group of kinases have been subject of extensive research (Pearce *et al.*, 2010) and knowledge of substrates provided insight in the diversity of signalling pathways in which they are involved. However, the role of other AGC kinases is relatively unknown and identification of substrates is a crucial step in elucidating their function. NDR and DMPK kinase families are typical examples of families in the AGC kinase group that comprise members for which little knowledge exists about relevant signalling pathways.

2.1 The NDR family of kinases

The NDR (nuclear Dbf2-related) kinases form a family within the AGC group of kinases. This family comprises four human members (NDR1, NDR2, LATS1 and LATS2) and their highly conserved orthologues in a wide variety of organisms, varying from mammals, invertebrates, yeasts, fungi, plants to protozoa (Hergovich *et al.*, 2006b). For their activation, phosphorylation of the activation segment and the hydrophobic motif are required (Figure 4, with LATS2 as an example).

NDR family members have some unique features that make them stand out amongst the AGC kinases. They contain a 30-60 amino acid insertion between kinase subdomains VII and VIII. The primary sequence of this insert is poorly conserved but for all NDR family members it contains a region at its C-terminal side that is rich in positively charged residues and that negatively affects kinase activity. Therefore, this sequence is called the auto-inhibitory sequence (AIS). In addition, NDR kinases contain a SMA (S100B/hMOB1 association) domain, also known as the NTR (N-terminal regulatory) domain, proximal to the kinase domain. Activation of NDR family kinases requires autophosphorylation of the activation segment and subsequent phosphorylation of the hydrophobic motif by MST kinases. MST kinases also phosphorylate MOB proteins which facilitates their

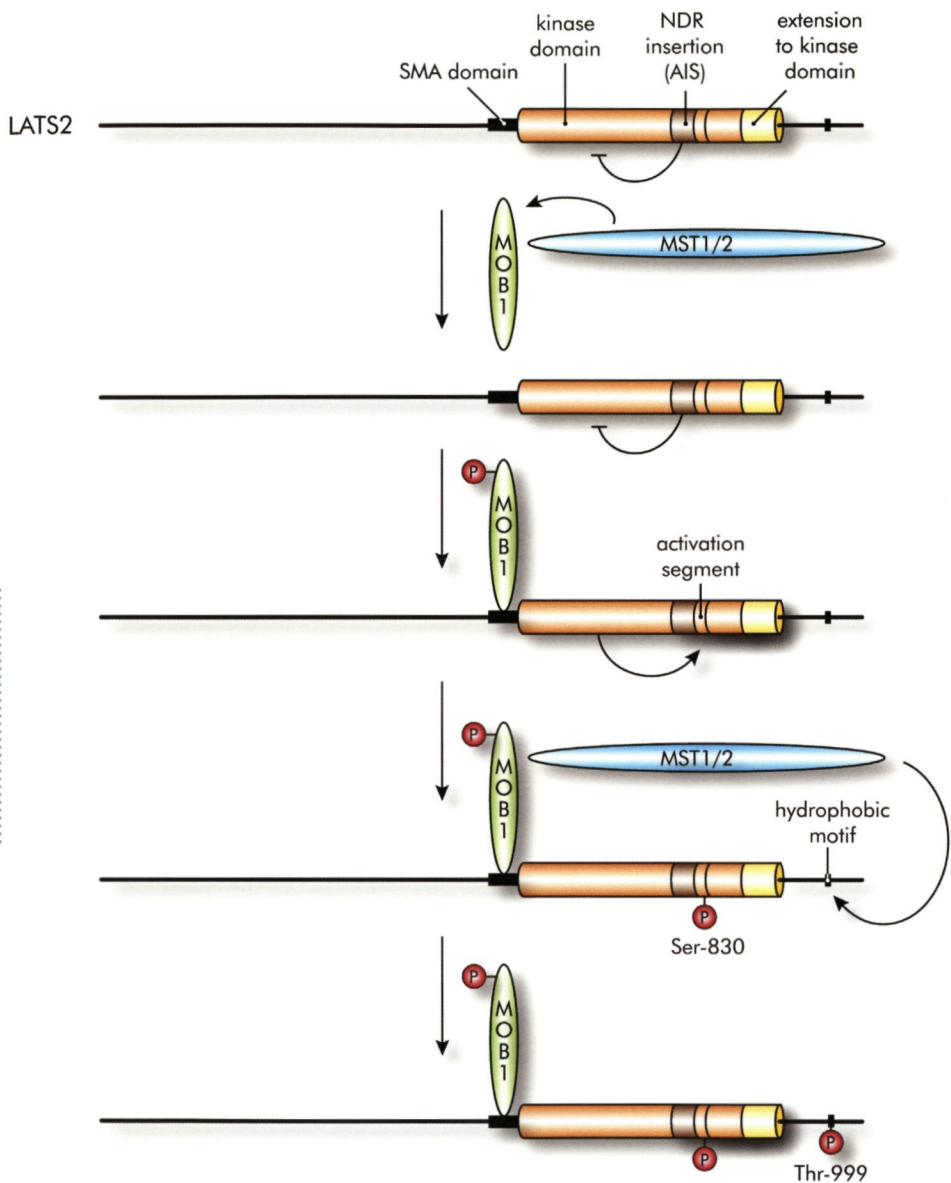


Figure 4: Domain structure and activation mechanism of LATS2. Binding of MOB to the SMA domain of LATS2 is promoted by phosphorylation of MOB by MST1/2 and releases inhibition by the auto-inhibitory sequence (AIS). This subsequently leads to activation of autophosphorylation activity which results in phosphorylation of the activation segment at Ser830. Additional phosphorylation of the hydrophobic motif at Thr999 by MST1/2 results in further activation and stabilization of the kinase. Amino acid numbers correspond to the positions in the mouse LATS2 sequence.

binding to the SMA domain. This binding leads to release of autoinhibition, and thereby promotes autophosphorylation activity. Another important function of the interaction between MOB proteins and NDR family kinases is the targeting of NDR kinases to the plasma membrane, a process that directs interaction with upstream kinases (reviewed in Hergovich *et al.*, 2008; Hergovich and Hemmings, 2009; Hergovich *et al.*, 2006b; Tamaskovic *et al.*, 2003a).

A common function of NDR family kinases is the regulation of aspects of cell morphogenesis, including maintenance of cell shape and cell polarity and the organization of the actin and tubulin cytoskeleton. NDR kinase family members also share involvement in the regulation of the cell cycle (Tamaskovic *et al.*, 2003a). Furthermore, a role in centrosome functioning has been proposed since NDR kinase family members localize to these structures. Their exact function in this process still remains elusive (Hergovich *et al.*, 2008; Hergovich *et al.*, 2007).

2.1.1 LATS2 protein structure

LATS2 (Large tumour suppressor 2) is a ~120 kDa protein with a serine/threonine kinase domain at the C-terminus as the only known protein domain with structural homology to other proteins (Figure 4). LATS2 is one of the two mammalian homologues of the *Drosophila* warts/lats protein, the other homologue being LATS1, with which it shares a high sequence similarity in the kinase domain (85% amino acid identity between the human forms; (Hori *et al.*, 2000)). The N-terminal parts of LATS1 and LATS2 are much less conserved (Hori *et al.*, 2000; Yabuta *et al.*, 2000).

Activation of LATS2 (Figure 4) requires binding of MOB1 to the LATS2 SMA-domain, which is promoted by phosphorylation of MOB1 by MST1/2 protein kinases (Bao *et al.*, 2009; Hergovich and Hemmings, 2009). This leads to release of auto-inhibition by the LATS2 AIS and subsequent autophosphorylation of a residue in its activation segment (Ser-830). Additional phosphorylation of a residue in the hydrophobic motif (Thr-999) by MST2 further promotes kinase activity and contributes to kinase stability.

2.1.2 LATS2 function

The gene encoding human LATS2 was mapped to region 13q11-q12, a region that frequently exhibits loss of heterozygosity in many primary cancers (Yabuta *et al.*, 2000). Downregulation of LATS2 expression was found to occur in human astrocytoma (Jiang *et al.*, 2006), acute lymphoblastic leukemia (Jimenez-Velasco *et al.*, 2005), prostate cancer (Powzaniuk *et al.*, 2004), oesophageal cancer (Lee *et al.*, 2009), breast cancer (Takahashi *et al.*, 2005) and gastric cancer (Cho *et al.*, 2009). Also a role of LATS2 in the development of testicular germ cell tumours was suggested (Voorhoeve *et al.*,

2006). Together, these data strongly suggest that deregulation of LATS2 contributes to tumourigenesis.

LATS2 protein locates at centrosomes (Abe *et al.*, 2006; McPherson *et al.*, 2004; Toji *et al.*, 2004) and interaction of LATS2 with Ajuba was found to play a role in recruitment of γ -tubulin to centrosomes during mitosis and in mitotic spindle organization (Abe *et al.*, 2006; Das Thakur *et al.*, 2010). Other LATS2 interacting proteins that have been described include Aurora-A kinase (Toji *et al.*, 2004), androgen receptor (Powzaniuk *et al.*, 2004), MST2, YAP, TAZ and MDM2. Interaction with MST2, YAP and TAZ makes LATS2 a component of the Salvador-Warts-Hippo tumour suppressor signalling pathway (Chan *et al.*, 2011; Dong *et al.*, 2007; Hergovich *et al.*, 2008; Hergovich and Hemmings, 2009; Zhao *et al.*, 2007). Essential for activation of this pathway is that MST2, a mammalian homolog of the *Drosophila* Hippo protein kinase, phosphorylates the hydrophobic motif of LATS2. In turn LATS2 then phosphorylates the transcriptional coactivators YAP and TAZ (Lei *et al.*, 2008; Zhao *et al.*, 2007), leading to suppression of cellular transformation (Chan *et al.*, 2008; Dong *et al.*, 2007).

General introduction

Interaction with MDM2 makes LATS2 a player in p53 signalling. This interaction inhibits MDM2's ubiquitin ligase activity, which protects p53 from ubiquitination and subsequent degradation. Increased p53 levels in turn promote LATS2 expression (Aylon *et al.*, 2006), providing a positive feedback loop. Involvement of LATS2 in p53 signalling is further supported by the interaction of LATS2 with ASPP1, a key mediator of the nuclear p53 apoptotic response (Aylon *et al.*, 2010). In addition, it was recently suggested that two miRNAs (miR-372 and miR-373), which can function as oncogenes by neutralizing p53-mediated CDK inhibition, inhibit expression of LATS2 (Voorhoeve *et al.*, 2006).

Based on high sequence similarity between *Drosophila* warts/lats, LATS1 and LATS2 other putative interactors might include CSK (Stewart *et al.*, 2003), CDC2 (Morisaki *et al.*, 2002; Tao *et al.*, 1999), zyxin (Hirota *et al.*, 2000), Omi (Kuninaka *et al.*, 2005) and LIMK1 (Yang *et al.*, 2004). Considering the variety of interactors that was found for LATS2 it is to be expected that this protein plays a role in diverse processes, many of which are apparently linked to the regulation of cell cycle. Indeed, LATS2 was found to be involved in events like G2/M transition (Kamikubo *et al.*, 2003), G1/S transition (Li *et al.*, 2003) and the completion of cytokinesis (Yabuta *et al.*, 2007). Also the observation that LATS2 is specifically phosphorylated during mitosis (Hori *et al.*, 2000) is in agreement with this role. Furthermore, LATS2 plays a role in induction of apoptosis (Kamikubo *et al.*, 2003; Ke *et al.*, 2004), centrosome duplication, maintenance of mitotic fidelity and genomic stability (McPherson *et al.*, 2004).

2.2 The DMPK family of kinases

The DMPK (Dystrophia Myotonica Protein Kinase) kinases form another family in the group of AGC kinases. The intensely examined human kinases ROCK-I and -II (Riento and Ridley, 2003) as well as the less well-studied kinases MRCK α , - β , and - γ (Leung *et al.*, 1998; Ng *et al.*, 2004), CRK (Madaule *et al.*, 1998) and DMPK and their orthologues in a wide variety of other organisms belong to this family. In all members an N-terminal leucine-rich domain precedes the conserved serine/threonine kinase domain which is in turn followed by a coiled-coil domain (Riento and Ridley, 2003; Zhao and Manser, 2005) (Figure 5, with DMPK as an example). The N-terminal leucine-rich domain is thought to contribute to catalytic activity (Leung *et al.*, 1996; Riento and Ridley, 2003; Tan *et al.*, 2001b; Wansink *et al.*, 2006). The coiled-coil region is involved in multimerization which is crucial for catalytic activity (Bush *et al.*, 2000; Chen *et al.*, 2002; Riento and Ridley, 2003; Tan *et al.*, 2001b). Several other features are shared by the DMPK family members. They all display autophosphorylation activity (Bush *et al.*, 2000; Di Cunto *et al.*, 1998; Ishizaki *et al.*, 1996; Tan *et al.*, 2001b; Wansink *et al.*, 2003), have the ability to interact with small GTPases of the Rho family (Di Cunto *et al.*, 1998; Leung *et al.*, 1996; Leung *et al.*, 1998; Shimizu *et al.*, 2000) and influence actomyosin dynamics via phosphorylation of MLC2 (myosin regulatory light chain) and/or MYPT (myosin phosphatase targeting subunit) (Amano *et al.*, 1996; Gally *et al.*, 2009; Kawano *et al.*, 1999; Kimura *et al.*, 1996; Leung *et al.*, 1998; Muranyi *et al.*, 2001; Tan *et al.*, 2001a; Totsukawa *et al.*, 1999; Velasco *et al.*, 2002; Wilkinson *et al.*, 2005; Yamashiro *et al.*, 2003).

2.2.1 DMPK protein structure

DMPK is the protein product of the *DMPK* gene, which is mutated in myotonic dystrophy type 1 (DM1) patients (Brook *et al.*, 1992; Fu *et al.*, 1992; Mahadevan *et al.*, 1992). Much research has been done on the molecular pathogenesis underlying this multisystemic neuromuscular disorder (Sicot *et al.*, 2011), which is now generally accepted to mainly involve an RNA gain-of-function mechanism (Ranum and Cooper, 2006; Wheeler and Thornton, 2007). Expansion of a (CTG) n trinucleotide repeat in the affected *DMPK* gene results in large (CUG) n repeat-containing toxic DMPK mRNA products that are trapped together with splice and transcription factors in aggregates within the nucleus (Davis *et al.*, 1997; Hamshire *et al.*, 1997; Taneja *et al.*, 1995). These factors can therefore no longer exert their normal function, leading to deregulation of gene expression (Cho and Tapscott, 2007; Ebralidze *et al.*, 2004), in particular due to abnormal RNA splicing. A role for DMPK proteins in the pathogenesis of DM1 is still unclear. Although coding mutations have been found in tumours of non-DM1 patients (<http://www.sanger.ac.uk/genetics/CGP/cosmic/>), no mutations in *DMPK* coding parts have been described in DM1 patients. It cannot be

excluded that protein haploinsufficiency due to transcript retention in the nucleus may contribute to certain DM1 symptoms (Benders *et al.*, 1997; Berul *et al.*, 1999; Jansen *et al.*, 1996; Kaliman and Llagostera, 2008; Llagostera *et al.*, 2009; Llagostera *et al.*, 2007; Reddy *et al.*, 1996).

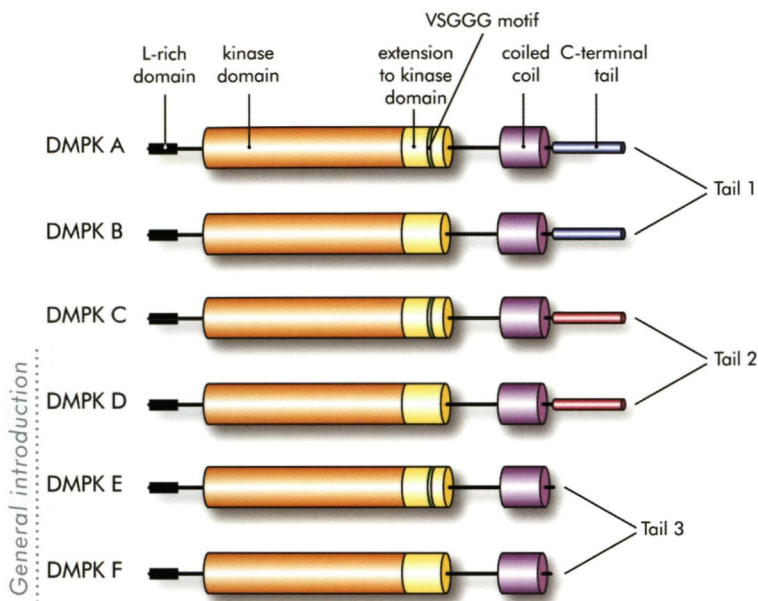


Figure 5: Domain structure of six major DMPK splice isoforms. DMPK protein isoforms are produced as the result of alternative splicing of DMPK pre-mRNA. Shown are schematic pictures of the six major DMPK isoforms (A-F) and their structural domains. All isoforms contain an N-terminal leucine (L) rich domain, a serine/threonine kinase domain, a kinase extension

domain and a coiled coil domain. Isoforms A, C, and E contain the five-amino-acid sequence VSGGG in the kinase domain due to use of an alternative splice site in exon 8. The distinct C-terminal tails that further define the various DMPK isoforms are the result of alternative splicing events in the exon 12-15 region and determine the subcellular localization: DMPK A-D are membrane proteins and located at mitochondria or the ER (van Herpen *et al.*, 2005; Wansink *et al.*, 2003), while DMPK E-F are present in the cytosol (Wansink *et al.*, 2003).

The DMPK protein was originally described as either a membrane-bound (Dunne *et al.*, 1996; Mussini *et al.*, 1999; Salvatori *et al.*, 1997; Shimokawa *et al.*, 1997; Ueda *et al.*, 1999) or a soluble (Pham *et al.*, 1998; Ueda *et al.*, 1999) protein. This apparent contradiction could later be explained by the identification of six different major splice isoforms, DMPK A-F (Figure 5) (Groenen *et al.*, 2000; van Herpen *et al.*, 2005; Wansink *et al.*, 2003). All isoforms share the N-terminal leucine-rich domain, the serine/threonine protein kinase domain and the coiled-coil region,

but differ in the presence or absence of a Val-Ser-Gly-Gly-Gly sequence (the VSGGG motif) and the nature of their C-terminal tail (Groenen *et al.*, 2000; van Herpen *et al.*, 2005; Wansink *et al.*, 2003). These differences arise by the use of three alternative splice sites within the 15 exons of the *DMPK* gene. The first alternative splice site determines whether the VSGGG motif is included (DMPK A, C, and E) or excluded (DMPK B, D, and F). The VSGGG motif was shown to contribute to autophosphorylation activity, possibly by inducing a conformational change in DMPK upon phosphorylation of the serine residue in this motif (Wansink *et al.*, 2003). A second alternative splice site is responsible for the sequence of the C-terminal tail resulting in either a hydrophobic C-terminus (tail 1; DMPK A and B) or a relatively hydrophilic C-terminus (tail 2; DMPK C and D), respectively. A truncated C-terminal tail results from a third alternative splice event which leads to the occurrence of an early stop codon (tail 3; DMPK E and F). A seventh, minor, isoform (DMPK G) seems to occur only in humans and contains yet another C-terminus (tail 4) as the result of use of a fourth alternative splice site (Tiscornia and Mahadevan, 2000; Wansink *et al.*, 2003). The nature of the C-terminus is an important determining factor for localization of the DMPK splice isoforms (i.e., long isoforms are found at the ER or mitochondrial membrane while short isoforms E and F are present in the cytosol) and also influences kinase activity (van Herpen *et al.*, 2005; Wansink *et al.*, 2003).

2.2.2 DMPK function

Despite the detailed knowledge on DMPK's molecular composition, not much is known about its biological function. There are indications that DMPK is involved in skeletal muscle integrity (Carrasco *et al.*, 2002), glucose metabolism (Llagostera *et al.*, 2007), cardiac atrioventricular conduction (Berul *et al.*, 1999; Pall *et al.*, 2003; Saba *et al.*, 1999) and regulation of actomyosin dynamics (Kaliman and Llagostera, 2008; Llagostera *et al.*, 2007; Mulders *et al.*, 2011), but the best described function is regulation of ion homeostasis (Kaliman and Llagostera, 2008). DMPK has been found to influence several types of ion channels. The current of rat voltage-gated Na⁺- channels was altered upon co-expression with human DMPK in *Xenopus* oocytes (Chahine and George, 1997; Mounsey *et al.*, 1995). In addition, a reduced Na⁺ current amplitude and late reopening of Na⁺-channels was observed in skeletal muscle and skeletal myocytes of *DMPK*^{+/-} and *DMPK*^{-/-} mice (Mounsey *et al.*, 2000a). DMPK was also suggested to be involved in voltage-dependent Ca²⁺ release, since an increased cytoplasmic calcium concentration was detected in DM1 patient muscle cells (Jacobs *et al.*, 1990) and in myotubes derived from *DMPK*^{-/-} mice (Benders *et al.*, 1997). More evidence for a role in ion homeostasis comes from the finding that DMPK phosphorylates phospholamban, a muscle specific Ca²⁺ ATPase inhibitor (Kaliman *et al.*, 2005). This event leads to inactivation of phospholamban and results

in sequestration of Ca^{2+} in the sarcoplasmic reticulum, as confirmed in ventricular homogenates of *DMPK*^{-/-} mice (Kaliman *et al.*, 2005). A role in Cl^- homeostasis was proposed via phosphorylation of phospholemman, a regulator of the $\text{Na}^+/\text{Ca}^{2+}$ exchanger and Na^+/K^+ ATPase, by DMPK (Geering, 2006). Expression of phospholemman in *Xenopus* oocytes induces Cl^- currents, which are reduced upon coexpression with DMPK.

DMPK relatives (ROCKs, CRIK and MRCKs) play a role in actomyosin remodelling in a variety of processes, including cytokinesis, cell motility, neurite outgrowth, and muscle contraction (Amano *et al.*, 2000; Chen *et al.*, 1999; Di Cunto *et al.*, 1998; Leung *et al.*, 1998; Madaule *et al.*, 1998; Riento and Ridley, 2003; Wilkinson *et al.*, 2005; Yasui *et al.*, 1998; Zhao and Manser, 2005). These kinases are activated by members of the family of small GTPases (Leung *et al.*, 1998; Madaule *et al.*, 1998; Riento and Ridley, 2003), which have an even better established function in the regulation of actomyosin dynamics (reviewed in Etienne-Manneville and Hall, 2002). The observation that DMPK is activated by binding to the small GTPase Rac1 and phosphorylation by Raf1 (Shimizu *et al.*, 2000), suggests that also DMPK contributes to actomyosin remodelling. This hypothesis is further supported by the notion that apoptotic blebbing and reorganization of the actin cytoskeleton occurs in lens cells upon DMPK overexpression (Jin *et al.*, 2000). Overexpression of an enzymatically inactive DMPK mutant caused disassembly of actin stress fibres in HeLa cells (Llagostera *et al.*, 2007), whereas expression of the cytosolic DMPK E isoform in *DMPK*^{-/-} myotubes induced formation of stellar-shaped stress fibres during differentiation (Mulders *et al.*, 2011). This latter effect was not observed when the mitochondrial tail-anchored DMPK C isoform was overexpressed, suggesting that involvement in actomyosin dynamics is indeed isoform-specific. A possible explanation at the molecular level for DMPK control over actomyosin dynamics comes from the identification of MYPT (a subunit of myosin phosphatase, see section 5) as a substrate of DMPK (Muranyi *et al.*, 2001). MYPT also serves as a substrate for most other DMPK family members (Gally *et al.*, 2009; Kawano *et al.*, 1999; Kimura *et al.*, 1996; Tan *et al.*, 2001a; Velasco *et al.*, 2002; Wilkinson *et al.*, 2005) and some of these can also directly phosphorylate MLC2 (section 5) (Amano *et al.*, 1996; Leung *et al.*, 1998; Totsukawa *et al.*, 1999; Yamashiro *et al.*, 2003). The latter was not demonstrated for DMPK, although MLC2 was found as DMPK interaction partner in mass spectrometric (Forner *et al.*, 2010) and yeast two-hybrid experiments (Groenen and Wieringa, 1998).

The function of interactions between DMPK and other proteins that are not involved in ion homeostasis and actomyosin-dynamics is often much less clear. MKBP (DMPK binding protein), a protein thought to be involved in stress response in muscle, was identified as a DMPK activator (Suzuki *et al.*, 1998). Additionally, other proteins

involved in stress response have been found as interactors with mass spectrometry approaches, but at present it is unknown whether these act as activators or as effectors (Forner *et al.*, 2010). Similarly, SRF (serum response factor) and CUG-BP (CUG-binding protein; a protein that also binds expanded DMPK transcripts) are among the candidate substrates (Iyer *et al.*, 2003; Roberts *et al.*, 1997), but the exact significance of all these findings remains unknown.

3. PROTEIN INTERACTION DOMAINS

Modular interaction domains are essential protein building blocks found in regulatory proteins - like the kinases - and in the interactors discussed above. In fact most aspects of protein behaviour, like subcellular partitioning, recognition of posttranslational modifications, formation of complexes, but also characteristics like folding conformation, activity and substrate specificity of enzymes depend on the presence of interaction domains (Pawson and Nash, 2003). The presence of multiple interaction domains within one protein contributes to specificity in cellular signalling and diversification of function. Some interaction domains may recognize different types of motifs, like SH2 domains which can simultaneously bind phosphorylated tyrosine residues and SH3 domains. Conversely, some types of motifs are recognized by different interaction domains, like the case of phosphorylated serines which can be recognized by 14-3-3, WW, and MH2 domains. The interaction domains named here are only a few of the more than eighty different protein interaction domains that have been classified thus far (<http://pawsonlab.mshri.on.ca/>). SH2, SH3, PTB and PH domains are among the most extensively studied protein interaction domains. The most widespread occurring type of binding domain is the PDZ domain.

General introduction

3.1 The PDZ domain

Like classical protein interaction domains, PDZ domains can fold independently into a globular conformation with their N- and C-termini close together and are therefore easily incorporated in proteins (Harris and Lim, 2001; Pawson and Nash, 2003). The name PDZ is an acronym of PSD-95/SAP90, Discs-large and ZO-1, the first three proteins in which a PDZ domain was identified (Kennedy, 1995). PDZ domains occur in all kingdoms, including plants, yeast and bacteria (Jelen *et al.*, 2003). They mediate interactions between proteins mainly via the recognition of a C-terminal peptide, but interactions with internal peptides that may mimic a C-terminus have been described (Jelen *et al.*, 2003; van Ham and Hendriks, 2003).

PDZ domains typically consist of 80-100 amino acids, which form six β -strands (β A- β F) and two α -helices (α A and α B), which fold into a six-stranded β -sandwich domain. A C-terminal peptide recognized by a PDZ domain fits as an anti-parallel

β -strand into a groove between β -strand B and α -helix B, a mechanism known as β -strand addition (Harrison, 1996; Jelen *et al.*, 2003). The four C-terminal amino acids (P^0 - P^3) in this peptide contain the major recognition determinants, but there are also examples in which residues upstream of P^3 are involved in PDZ domain interactions (Birrane *et al.*, 2003; Kozlov *et al.*, 2002; Songyang *et al.*, 1997; Walma *et al.*, 2002). Besides C-terminal peptides and peptides that mimic a C-terminus, PDZ domains can also bind phosphatidylinositol 4,5-bisphosphate (PIP_2) (Zimmermann *et al.*, 2002) and other protein-protein interaction domains (spectrin repeats (Xia *et al.*, 1997), ankyrin repeats (Maekawa *et al.*, 1999) and LIM domains (Cuppen *et al.*, 1998; Cuppen *et al.*, 2000; Murthy *et al.*, 1999)). Also head-to-tail dimerization of PDZ domains has been described (Hillier *et al.*, 1999).

Peptide sequences that bind PDZ domains are referred to as PDZ binding motifs (PDZ-BM) and they can be divided into four classes, all with their own consensus sequence: $-(S/T)-X-\Phi$ (Class I), $-(\Phi/\Psi)-X-\Phi$ (Class II), $-(D/E)-X-V$ (Class III) and $-X-\Psi-(D/E)$ (Class IV); X in these sequences represents any amino acid, Φ a hydrophobic residue and Ψ an aromatic residue (Vaccaro and Dente, 2002). Many PDZ-BMs contain a serine, threonine or tyrosine residue suggesting that phosphorylation of these residues might play a role in regulation of PDZ-mediated interactions. Indeed for some PDZ interactions it was demonstrated that they are influenced by the phosphorylation status of the PDZ-BM (Cao *et al.*, 1999; Choi *et al.*, 2002; Chung *et al.*, 2000; Cohen *et al.*, 1996; Hall *et al.*, 1998a; Matsuda *et al.*, 1999; Popovic *et al.*, 2010; Sulka *et al.*, 2009; Vazquez *et al.*, 2001), but whether this is a general mechanism to regulate PDZ interactions is unclear at present. In all known cases phosphorylation of the PDZ-BM was found to impair binding to PDZ domains. A study of the PDZ-BM in PTEN suggested that its phosphorylation causes a conformational change that results in the masking of the PDZ-BM. This will, in turn, lead to decreased binding to PTEN's interaction partner MAGI-2 (Vazquez *et al.*, 2001). Such a conformational change leading to masking of the interaction surface might prove to be a general consequence of PDZ-BM phosphorylation.

Multiple PDZ domains are often found in one protein (Harris and Lim, 2001). Differential binding specificity of individual PDZ domains makes these multiple PDZ domain-containing proteins excellent scaffolds for protein signalling complexes (Sheng and Sala, 2001). As such, PDZ proteins can function in a wide variety of cellular processes. Well-described general functions of PDZ proteins include maintenance of cell polarity (Fanning and Anderson, 1999), protein targeting to sites of cell-cell communication (Harris and Lim, 2001; Sheng and Sala, 2001) and organization of postsynaptic densities in neurons (Feng and Zhang, 2009). Some PDZ proteins have a role in cell cycle regulation, a process that will be discussed in the next section.

4. CELL CYCLE

The cell cycle consists of four stages: G1-, S-, G2- (together called interphase) and M-phase. Upon stimulation by growth factors, a cell in G1 will verify that internal and external conditions are suitable to proceed with S-phase during which the genomic material is duplicated. During G2 the cell prepares itself for M-phase, again by checking internal and external conditions. If these are favourable the cell will enter M-phase, during which two genetically identical daughter cells are formed.

4.1 Cell division

M-phase can be divided in prophase, prometaphase, metaphase, anaphase, telophase (together called mitosis or karyokinesis) and cytokinesis (Figure 6). Although M-phase is a relatively fast event, it encompasses the most striking and prominent structural changes of the whole cell cycle. After their duplication in S-phase, chromosomes consist of two sister chromatids and the start of prophase is marked by their condensation. In addition, the movement of the centrosomes to opposite poles of the cell and formation of the mitotic spindle occurs during this step of mitosis. Prometaphase starts with breakdown of the nuclear envelope. In this phase a subset of microtubules from the mitotic spindle attach to the kinetochores on the chromosomes. Kinetochore microtubules connect the kinetochores of sister chromatids to the opposing spindle poles. Alignment of the chromosomes at the equator of the mitotic spindle occurs during metaphase. In anaphase the connection between the sister chromatids is broken and by movement of the centrosomes and shortening of the microtubules the chromatids become separated. When the sister chromatids arrive at the two poles of the mitotic spindle, a nuclear envelope is reassembled at both poles during telophase and the chromosomes start to decondense, resulting in the formation of two nuclei.

Cytokinesis is the division of the cytoplasm and depends on formation of a structure called the contractile ring, which is mainly composed of actin filaments and myosin II. Specification of the position of the contractile ring occurs during anaphase and assembly of the contractile ring starts in telophase, midway between the spindle poles (Alberts, 2002; Cooper, 2000). Contraction of the ring leads to formation of a cleavage furrow, which further ingresses upon continued contraction. Eventually this leads to creation of an intercellular bridge which contains compacted microtubules from the mitotic spindle. The region where these antiparallel microtubules overlap is called the midbody, which is thought to function in the recruitment of essential proteins for proper execution of the final step of cytokinesis, abscission (Glotzer, 2009; Steigemann and Gerlich, 2009). Abscission is not understood in much detail and several models exist to explain this last step of cytokinesis, including simple rupture of the two daughter cells by mechanical force and targeted delivery of membrane by vesicles. Another model involves disassembly of microtubules in the midbody

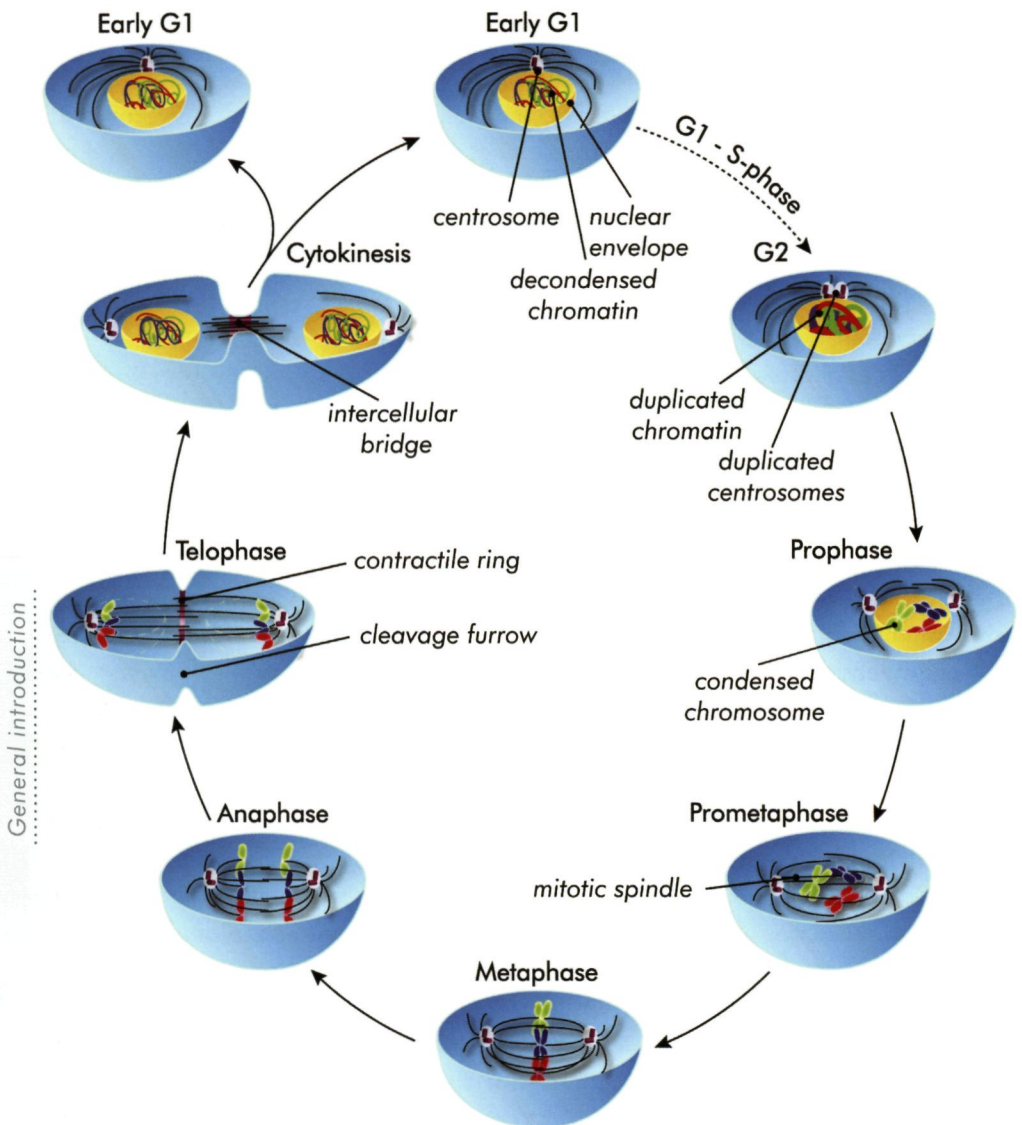


Figure 6: Different stages of M-phase in animal cells. M-phase encompasses mitosis (prophase to telophase) and cytokinesis and results in the formation of two daughter cells, each with an exact copy of the mother cell's genomic material. Details of events in the specific subphases are given in the text. The most important structures are indicated.

coordinated with plasma membrane ingression, followed by hemifusion and fission of opposing plasma membrane regions (Montagnac et al., 2008; Steigemann and

Gerlich, 2009). Movement of centrosomes to the midbody has also been proposed to play a role in abscission (Mack and Rattner, 1993; Montagnac *et al.*, 2008; Piel *et al.*, 2001). The aforementioned DMPK family member ROCK was shown to be involved in this centrosomal migration (Chevrier *et al.*, 2002).

Proper execution of the mechanistic events that regulate mitosis and cytokinesis depends on strict regulation of cytoskeleton dynamics, aspects of which will be discussed in more detail further on.

4.2 Chromosome missegregation, aneuploidy and tumourigenesis

The ultimate goal of mitosis and cytokinesis is to generate two daughter cells that both contain an exact copy of the mother cell's genetic material. To achieve this, correct segregation of the sister chromatids of every chromosome during mitosis is essential. A very important mechanism that controls chromosome segregation, is the mitotic checkpoint (or spindle assembly checkpoint) (Chi and Jeang, 2007; Holland and Cleveland, 2009; Kops *et al.*, 2005; Taylor *et al.*, 2004). The mitotic checkpoint ensures that proper attachment of chromosomes to the microtubules of the mitotic spindle is being monitored. Start of anaphase is delayed until all chromosomes are attached with equal tension to both poles of the bipolar spindle. When this is achieved, the anaphase-promoting complex (APC) is activated. This eventually leads to disruption of the cohesion between sister chromatids and triggers, as the name of the complex indicates, the onset of anaphase (Peters, 2002). One single unattached kinetochore is sufficient to activate the mitotic checkpoint. Dereglulation of the monitoring processes of the mitotic checkpoint leads to chromosome missegregation.

Other mechanisms that can result in chromosome missegregation include defects in the machinery that controls sister chromatid cohesion (leading to e.g. premature loss of cohesion between sister chromatids) (Barber *et al.*, 2008; Pei and Melmed, 1997; Tao *et al.*, 1999; Yu *et al.*, 2003; Zhang *et al.*, 2008), merotelic attachment of kinetochores to microtubules (the attachment of a single kinetochore to microtubules emanating from both spindle poles) (Cimini, 2008; Cimini *et al.*, 2001; Gregan *et al.*, 2011; Holland and Cleveland, 2009; Kops *et al.*, 2005; Ruchaud *et al.*, 2007), and the presence of more than two centrosomes (Chi and Jeang, 2007; Holland and Cleveland, 2009; Kops *et al.*, 2005).

Since centrosomes form the poles of the mitotic spindle, the presence of more than two centrosomes can result in the formation of a multipolar mitotic spindle. This can lead to the generation of three or more daughter cells each with an aberrant number of chromosomes, a phenomenon known as aneuploidy. Aneuploidy is a common characteristic of tumour cells but whether it is a cause or consequence of tumourigenesis is still under debate (Bannon and Mc Gee, 2009; Chi and Jeang, 2007; Holland and Cleveland, 2009; Kolodner *et al.*, 2011). Multiple pathways can lead to

the acquisition of extra centrosomes, including centrosome overduplication, cell-cell fusion and cytokinesis failure (Holland and Cleveland, 2009). The aforementioned members of the NDR family of AGC kinases are known to play a role in centrosome duplication. Overexpression of NDR1 and 2 was found to result in centrosome overduplication (Hergovich *et al.*, 2007), whereas overexpression of LATS2 was found to suppress centrosome duplication (McPherson *et al.*, 2004).

4.3 Centrosome structure and function

Centrosomes in animal cells consist of an orthogonally organized pair of centrioles surrounded by a matrix of proteins that is termed pericentriolar material (PCM; Figure 7A). A centriole is a cylinder-shaped structure that contains microtubule triplets grouped in a nine-fold symmetrical arrangement. Directly after mitosis a centrosome consists of a mature (mother) and an immature (daughter) centriole. Duplication of both centrioles starts during S-phase and is completed in G2 (Azimzadeh and Bornens, 2007). During M-phase, the duplicated centrosomes each move towards one of the poles of the mitotic cell. There they function as the microtubule organizing centres (MTOC) and as such are crucial for proper formation of the mitotic spindle (Azimzadeh and Bornens, 2007; Debec *et al.*, 2010).

Centrosomes also function as MTOC in other phases than M-phase and are therefore involved in cellular processes that entail the microtubule cytoskeleton, such as determination and maintenance of cell polarity and organization of intracellular trafficking. Besides being essential components of centrosomes, centrioles are also found in axonemes (the inner core) of flagella and cilia and are then called basal bodies. Cilia can be found in most mammalian cell types and are involved in for example sensing signals from surrounding cells (Debec *et al.*, 2010). Absence of or mutations in cilia often leads to development of disease, the so-called ciliopathies (Fliegauf *et al.*, 2007).

4.4 Contractile ring assembly and structure

Another key structure during mitosis is the contractile ring (Figure 7A). Formation of the contractile ring starts at telophase at the cell cortex. Specification of its position is already determined during anaphase by accumulation of RhoA-activator ECT in the midzone (Glotzer, 2009; Yuce *et al.*, 2005), the region midway between the opposing spindle poles which contains overlapping polar microtubules from the mitotic spindle. Accumulation of ECT at the midzone leads to localized activation of RhoA and this is thought to activate a protein of the formin family, which in turn acts as a scaffold for the assembly of actin filaments and myosin II to form the contractile ring (Chang *et al.*, 1997; Guertin *et al.*, 2002; Yuce *et al.*, 2005). Formins were also postulated to tether the contractile ring to the plasma membrane (Pollard, 2010). Myosin II then

generates the force necessary to contract actin filaments in the contractile ring and actin filaments most likely depolymerise during constriction. It is generally thought that contraction of the contractile ring works via the same principles as contraction of linear actomyosin bundles in muscle sarcomeres but the exact mechanism remains to be established (Pollard, 2010).

5. MYOSIN II

Besides being crucial for force production during contraction of the contractile ring, myosin II motor activity is involved in a wide variety of other processes, including muscle contraction, cell migration, cell shape change, cell-cell adhesion, and cell division (Conti, 2008; De Lozanne and Spudich, 1987; Mabuchi and Okuno, 1977; Spudich, 1994). Myosin II is a prominent member of the large myosin family of motor proteins and one of the primary motor proteins in cells. Myosin II exists as several closely related isoforms, each comprising six protein subunits: two myosin heavy chains II (MHCII), two essential light chains (ELC or MLC1), and two regulatory light chains (RLC or MLC2; Figure 7B). MHCII contains a globular subfragment 1 (S1) and a rod-shaped tail domain. Dimerization of the tail domains of two MHCII molecules within one myosin II complex leads to formation of a coiled-coil rod that is responsible for multimerization of multiple myosin II complexes into myosin II filaments (Figure 7A). The MHCII S1 domain contains the head domain - the site of actin-binding and ATP hydrolysis - and the neck domain. The energy resulting from ATP hydrolysis is converted to mechanical force at the junction of the head and neck domain, causing movement of the head domain relative to the neck domain. This promotes sliding of the myosin II complex along the actin microfilaments. The neck domain of each MHCII molecule provides binding sites for one MLC1 molecule and one MLC2 molecule. Binding of MLC1 is generally thought to increase the stability of MHCII, while MLC2 plays a crucial role in the regulation of myosin II activity (discussed below) and the formation of myosin II filaments (Burgess *et al.*, 2007; Craig and Woodhead, 2006; Scholey *et al.*, 1980; Vicente-Manzanares *et al.*, 2009; Wendt *et al.*, 2001; Woodhead *et al.*, 2005).

The group of myosin II proteins include cardiac, skeletal muscle, smooth muscle and nonmuscle isoforms. Smooth muscle (sm) and nonmuscle (nm) myosin II are found in many different cell types and result from the combination of different sm and nm MHCII, MLC1 and MLC2 types of subunits. For example, nm and sm type of MHCII subunits are products from four different genes encoding nonmuscle A (MYH9), nonmuscle B (MYH10), nonmuscle C (MYH14) and smooth muscle (MYH11) MHCII, each of which is subject to alternative splicing (reviewed in Eddinger and Meer, 2007). Two MLC1 isoforms exist, which are generated by alternative splicing

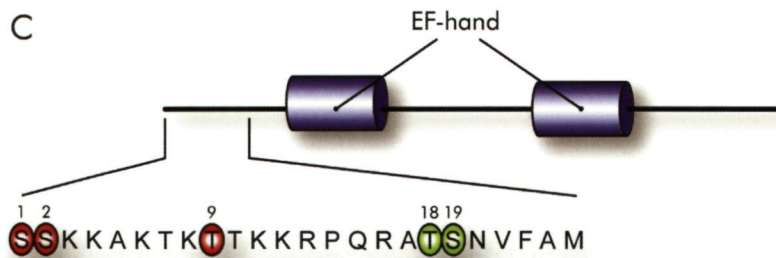
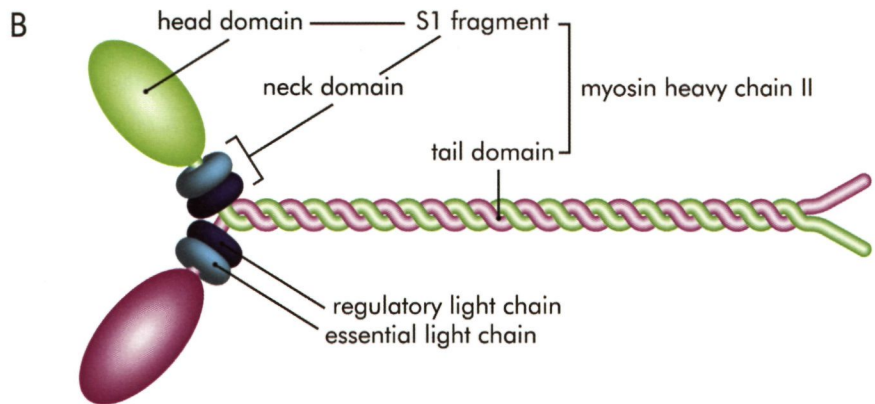
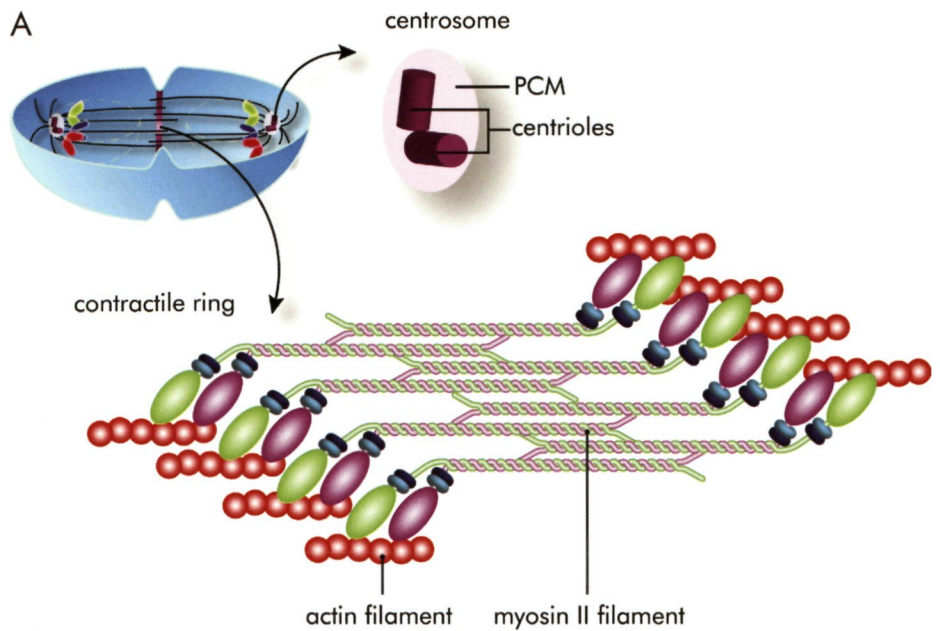


Figure 7: Details of cytoskeletal structures that are crucial for proper completion of M-phase. (A) Close up of centrosomes and contractile ring in a telophase cell. One centrosome contains two centrioles and is surrounded by the pericentriolar material (PCM). The contractile ring is composed of myosin II and actin filaments. The assembly of myosin II complexes into bipolar filaments is mediated by multimerization of the coiled-coil rod domains. The bipolar filaments bind to actin filaments to form thick bundles and movement of the MHCII head domains results in actomyosin sliding. (B) A myosin II complex is composed of two copies of myosin heavy chain II (MHCII), essential light chain (ELC) and regulatory light chain (MLC2). The long coiled-coil domain in MHCII is important for dimerization. For sake of clarity, the two MHCII molecules each have a different colour. (C) Domain structure of an MLC2 molecule. The N-terminus contains two activating phosphorylation sites (green) and three putative inactivating (red) phosphorylation sites. Two EF-hand domains are present in MLC2, which are responsible for Ca^{2+} binding. Depicted here is human nonmuscle MLC2.

of transcripts from one single gene (Lash *et al.*, 1990; Lenz *et al.*, 1989; Nabeshima *et al.*, 1987) and there are multiple MLC2 genes, encoding different MLC2 subunit isoforms (Collins, 2006; Eddinger and Meer, 2007).

Together, this complexity of protein isoforms results in an enormous number of possibilities for formation of differentially composed myosin II complexes, but it is not known exactly which combinations exist in nature or can coexist in cells (Conti, 2008). Since myosin II contractile properties were found to be influenced by MHCII isoform expression (Arner *et al.*, 2003; Babu *et al.*, 2000; Conti, 2008; Karagiannis and Brozovich, 2003) it is likely that differentially assembled complexes have different contractile characteristics. Whether distinct light chain isoforms also affect myosin contractility to a different extent, is unclear at present. Generating more insight into expression distribution profiles and levels of individual MLC2 isoforms in different cell types will ultimately contribute to a better understanding of functional differences between the many myosin II complexes.

General introduction

5.1 MLC2 regulation

As mentioned, MLC2 plays a crucial role in regulation of myosin II activity. MLC2 proteins are ~20 kDa in size and their N-terminus contains several phosphorylation sites. Phosphorylation of MLC2 is essential for activation of nonmuscle (nm) and smooth muscle (sm) myosin II as this modification induces a conformational change in the MHCII heads, which is coupled to a strong increase in their ATPase activity (Burgess *et al.*, 2007; Craig and Woodhead, 2006; Jung *et al.*, 2008b; Wendt *et al.*, 2001; Woodhead *et al.*, 2005). In skeletal muscle and cardiac myosin II ATPase activity is regulated by an actin-bound Ca^{2+} -sensitive protein (troponin). Ca^{2+} -binding

induces a conformational change in troponin, which renders actin filaments accessible for binding to myosin II, which in turn activates myosin II ATPase activity (Kamm and Stull, 2011). MLC2 phosphorylation in these myosins modulates Ca^{2+} -sensitivity and Ca^{2+} /troponin-dependent force generation thereby influencing contractile properties (Scruggs and Solaro, 2011; Stull *et al.*, 2011).

Phosphorylation of nonsarcomeric MLC2 proteins has been described to occur on serine 19 (Ser19) and threonine 18 (Thr18) and to a lesser extent on Ser1, Ser2 and Thr9. Phosphorylation of Ser19 and additional phosphorylation of Thr18 (Vicente-Manzanares *et al.*, 2009) is necessary for myosin II activation, whereas phosphorylation of the three other residues has been shown to inhibit myosin II activity (Figure 7C). These inhibitory sites can be phosphorylated by PKC and Cdc2 *in vitro* (Bengur *et al.*, 1987; Ikebe *et al.*, 1987; Kawamoto *et al.*, 1989; Nishikawa *et al.*, 1984; Satterwhite *et al.*, 1992), but the relevance of these phosphorylation events *in vivo* has not been established (Shuster and Burgess, 1999). Several kinases responsible for phosphorylation of Ser19 and Thr18 have been identified, including MLCK, PAK, DAK, ILK and the DMPK subfamily members CRIK, ROCK and MRCK (reviewed in Matsumura, 2005). Whether DMPK itself is capable of phosphorylating MLC2 remains to be investigated.

Only one phosphatase for MLC2, called myosin phosphatase (already earlier mentioned in section 2.2.2 as a DMPK substrate), has been identified thus far. This protein contains three subunits, a 38 kDa protein phosphatase catalytic subunit (the δ isoform of type 1 protein phosphatase, PP1c), a ~ 120 kDa non-catalytic subunit known as MYPT1 (myosin phosphatase targeting subunit) or MBS (myosin binding subunit), and a 20 kDa subunit (M20) of undefined function. As the name implies, MYPT1 is the subunit responsible for targeting myosin phosphatase to MLC2 (reviewed in Matsumura, 2005) and (Matsumura and Hartshorne, 2008)). Interestingly, MYPT1 is inhibited by phosphorylation, a process exerted by several of the same kinases that phosphorylate MLC2 (a schematic overview can be found in Matsumura, 2005), including ROCK (Kimura *et al.*, 1996) and MRCK (Tan *et al.*, 2001a). These activities act synergistically and result in a strong net increase in MLC2 phosphorylation. The possible involvement of members of the DMPK kinase family in MLC2 modification has been discussed earlier, in section 2.2.

5.2 MLC2 and cytokinesis

Phosphorylation, and thus activation, of MLC2 has been described to fluctuate in a cell-cycle dependent manner (Matsumura *et al.*, 2001; Satterwhite *et al.*, 1992; Yamakita *et al.*, 1994). When cells enter mitosis, phosphorylation levels of Ser19 and Thr18 are low, but when cytokinesis starts, these residues are quickly phosphorylated (Yamakita *et al.*, 1994). In analogy with other events that require actomyosin

dynamics, the same processes and actors discussed above are involved in cytokinesis. Indeed MYPT is specifically activated during mitosis and inactivated during cytokinesis (Totsukawa *et al.*, 1999). In addition, mono- and diphosphorylated MLC2 (Dean and Spudich, 2006; DeBiasio *et al.*, 1996; Komatsu *et al.*, 2000; Matsumura *et al.*, 1998; Yamashiro *et al.*, 2003) as well as MYPT phosphorylated at an inhibitory site were shown to be enriched at the cleavage furrow (Kawano *et al.*, 1999; Yokoyama *et al.*, 2005).

Further evidence supporting an important role for regulation of MLC2 Ser19 and Thr18 phosphorylation in the coordination of cytokinesis comes from various reports using unphosphorylatable or phosphomimetic mutants of MLC2. Overexpression of an unphosphorylatable MLC2 mutant leads to multinucleation in COS-7 and NRK cells, most likely by formation of an abnormal cleavage furrow leading to incomplete cytokinesis (Komatsu *et al.*, 2000). In *Drosophila* S2 cells, an elegant study was performed in which endogenous MLC2 expression was knocked-down and expression of either wild type MLC2 or an unphosphorylatable or phosphomimetic form of MLC2 was introduced. Only expression of the unphosphorylatable MLC2 mutant led to binucleation, suggesting that phosphorylation of MLC2 is crucial for proper cytokinesis (Dean and Spudich, 2006). In *Drosophila* oocytes, phosphorylation of especially Ser21, which corresponds to Ser19 in vertebrate MLC2, was essential for proper cytokinesis (Jordan and Karess, 1997). In cancer cells low levels of phosphorylated MLC2 were associated with cytokinesis defects. These defects could be rescued by the expression of an MLC2 phosphomimetic (Wu *et al.*, 2010). Interestingly, evidence is accumulating that myosin II activity also impacts on other aspects of the mitotic process, including separation of chromosomes (Hashimoto *et al.*, 2008; Komatsu *et al.*, 2000) and the positioning of centrosomes (Rosenblatt *et al.*, 2004).

6. AIM AND OUTLINE OF THIS THESIS

In the course of earlier studies at the department of cell biology, preliminary evidence had been provided for the involvement of two AGC kinases, LATS2 and DMPK isoform E, in regulation of the cell cycle. The aim of the work described in this thesis was to unravel the mechanisms by which this regulation is achieved. First, we needed more insight in the identity and role of possible candidate substrates for LATS2 and DMPK E. In Chapter 2, I describe the search for such potential targets for each of the two kinases exploiting a peptide array that allows large scale substrate screening. I also describe how we used these data for determination of consensus phosphorylation motifs recognized by LATS2 and DMPK E. One of the DMPK E candidate substrates identified in Chapter 2 is MLC2. In Chapter 3, I describe how we further investigated

this interaction and its biological significance, using *in vitro* and *in vivo* approaches. During this study three highly homologous MLC2 isoforms were found to exist that appeared poorly annotated in literature. In Chapter 4 I therefore continue with a description of methods to distinguish between these three isoforms at the protein and RNA level. In this same chapter I will also describe how we subsequently employed this methodological knowledge for the analysis of isoform expression levels in tumour-derived and non-transformed cell lines. LATS2 is known to affect various aspects of cell division, but the molecular mechanisms by which this occurs were largely unknown at the beginning of this study. In Chapter 5, the discovery of a phosphorylation sensitive PDZ-binding motif at the very C-terminus of LATS2, which has impact on cell cycle progression, is described. Finally, Chapter 6 summarizes the findings of the work described in this thesis and discusses the main conclusions in a broader context.

Phosphorylation target site specificity for AGC kinases DMPK E and Lats2

Lieke Gerrits^a, Hanka Venselaar^b, Bé Wieringa^a, Derick G. Wansink^a,
and Wiljan J.A.J. Hendriks^a,

^aDepartment of cell biology and ^bCentre for Molecular and Biomolecular Informatics, Nijmegen Centre for Molecular Life Sciences, Radboud University Nijmegen Medical Centre, Nijmegen, The Netherlands.

Journal of Cellular Biochemistry - in press

ABSTRACT

Serine/threonine kinases of the AGC group are important regulators of cell growth and motility. To examine the candidate substrate profile for two members of this group, DMPK E and Lats2, we performed *in vitro* kinase assays on peptide arrays. Substrate peptides for both kinases exhibited a predominance of basic residues surrounding the phosphorylation target site. 3D homology modeling of the kinase domains of DMPK E and Lats2 indicated that presence of two negative pockets in the peptide binding groove provides an explanation for the substrate preference. These findings will aid future research towards signaling functions of Lats2 and DMPK E within cells.

Phosphorylation target site specificity for AGC kinases DMPK E and Lats2

2

Protein kinases catalyze transfer of the terminal phosphate group of ATP to the hydroxyl group on serine, threonine or tyrosine residues in target proteins. This process is a key mechanism in the regulation of signaling cascades and, hence, in many cellular processes (Ubersax and Ferrell, 2007). Aberrant phosphorylation can be involved in the etiology of disease (Hunter, 2000) and improving our knowledge about kinases and their substrate specificities would help explain molecular consequences and identify therapeutic targets.

Most kinases are either serine/threonine- or tyrosine-directed, but dual-specificity kinases also exist. One group of kinases with Ser/Thr specificity is known as the AGC (protein kinase A, -G, -C) group (Manning *et al.*, 2002). Activation of many AGC kinases depends on phosphorylation of two highly conserved motifs within these enzymes, i.e. the activation segment and the hydrophobic motif (Pearce *et al.*, 2010). Interactions with substrate proteins are largely defined by the substrate peptide binding groove located near the active site (Yang *et al.*, 2002b), but other structural domains or binding motifs may also shape substrate affinity and specificity of AGC kinases (Pearce *et al.*, 2010).

The AGC group comprises several families, including NDR (nuclear Dbf2-related) and DMPK (Dystrophia Myotonica Protein Kinase) kinases, of which Lats2 (large tumor suppressor 2) and DMPK E, respectively, are representative members (Manning *et al.*, 2002). Lats2 has been subject of intense research since its expression was found to be down-regulated in multiple cancer types (Cho *et al.*, 2009; Lee *et al.*, 2009; Voorhoeve *et al.*, 2006). Lats2 is a component of the mammalian tumor suppressor Salvador-Warts-Hippo pathway (Hergovich and Hemmings, 2009) and participates also in p53 signaling (Aylon *et al.*, 2006; Voorhoeve *et al.*, 2006). Functional studies suggest roles for Lats2 in cell cycle regulation (Kamikubo *et al.*, 2003; Li *et al.*, 2003; Yabuta *et al.*, 2007), induction of apoptosis (Kamikubo *et al.*, 2003; Ke *et al.*, 2004), centrosome duplication and maintenance of mitotic fidelity and genomic stability (McPherson *et al.*, 2004). Despite the many studies on Lats2's function and interaction partners, at present only YAP (yes-associated protein) and TAZ (transcriptional co-activator with PDZ-binding motif), two additional components of the Salvador-Warts-Hippo pathway, have been identified as substrates (Hergovich and Hemmings, 2009).

DMPK E is one of the kinase isoforms encoded by the *DMPK* gene, which is mutated by an expanded, non-coding (CTG)_n repeat in myotonic dystrophy type 1 patients (Sicot *et al.*, 2011). Alternative splicing of *DMPK* transcripts gives rise to several DMPK isoforms which differ in the presence of a five-amino-acid VSGGG insertion in the kinase domain and in the nature of their C-terminus (Groenen *et*

et al., 2000). Not much is known about DMPK's biological function, but available data point towards roles in ion homeostasis (Benders *et al.*, 1997; Geering, 2006; Kaliman *et al.*, 2005; Mounsey *et al.*, 2000b) and actomyosin dynamics (Jin *et al.*, 2000; Mulders *et al.*, 2011). Identified substrates include phospholamban (a muscle-specific Ca^{2+} ATPase inhibitor) (Kaliman *et al.*, 2005), phospholemman (a regulator of the $\text{Na}^{+}/\text{Ca}^{2+}$ exchanger and $\text{Na}^{+}/\text{K}^{+}$ ATPase) (Mounsey *et al.*, 2000a), MYPT (myosin phosphatase targeting subunit) (Muranyi *et al.*, 2001), SRF (serum response factor) (Iyer *et al.*, 2003) and CUG-BP (CUG-binding protein) (Roberts *et al.*, 1997). The significance of phosphorylation modification of these target proteins remains largely unknown.

Here, we report on the application of peptide array technology and homology modeling to acquire insight into the substrate specificity profiles of AGC kinases DMPK E and Lats2.

Generation of expression plasmids

Plasmid pEBG-DMPK E, encoding N-terminally GST-tagged DMPK E, was generated by ligation of the *Bgl*III-digested DMPK E cDNA insert from pSG8-DMPK E (Groenen *et al.*, 2000) in-frame into *Bam*HI-digested pEBG vector (Tanaka *et al.*, 1995). Plasmid pEBG-DMPK E KD (kinase dead; the enzymatically inactive mutant) was created in a similar manner using the cDNA insert from pSG8-DMPK E KD (Wansink *et al.*, 2003).

Plasmid pEYFP-C1-Lats2 CD, encoding YFP fused N-terminally to a truncated Lats2 version representing its C-terminal catalytic domain (CD), was created by cloning a *Bgl*III-digested PCR fragment (spanning position 2209 - 2780 of mouse Lats2 cDNA, acc. nr. NM_015771) into pEYFP-C1. Primers used were 5'-ATGAGATCTGCTGGGCTCTGTGAGGCCG-3' (sense, *Bgl*III site in bold) and 5'-CTTAGATCTAGTACTTGAATTGTGAGTCC-3' (antisense, *Bgl*III site in bold, *Scal* site underlined). Mammalian expression plasmid pSG8-VSV-mLats2 had been constructed by subcloning a PCR-generated mouse Lats2 (mLats2) cDNA fragment (nucl. pos. 134-3262 in acc. nr. NM_015771) in-frame into *Bam*HI-digested pSG8-VSV vector (Cuppen *et al.*, 1998). To complement the pEYFP construct with the remaining 3'-part of Lats2 cDNA, it was linearized with *Scal* and *Bam*HI and ligated with a *Scal*/*Bam*HI-digested Lats2 fragment (spanning position 2781 to the 3' end) from pSG8-VSV-mLats2. Plasmid pEBG-Lats2 CD, encoding an N-terminally GST-tagged version of the Lats2 catalytic domain, was constructed from pEYFP-C1-Lats2 CD by releasing the kinase domain insert (spanning position 2209 to the 3' end, encoding amino acids 592-1042, of mouse Lats2) using *Bam*HI and *Bgl*III and ligating this into vector pEBG (Tanaka *et al.*, 1995). In parallel, construct pEYFP-C1-Lats2 CD KD (encoding the enzymatically inactive mutant) was generated exploiting the partial Lats2 cDNA insert from pSG8-VSV-mLats2-KD bearing a Lys655Ala mutation. Likewise, pEYFP-C1-Lats2 CD KD enabled the creation of pEBG-Lats2 CD KD via *Bam*HI-*Bgl*III cloning into pEBG.

To generate pGEX-4T-3-MLC2-nm, the nm-MLC2 coding sequence was obtained by *Eco*RI/*Xho*I digestion from expression construct pSG8Δ*Eco*RI-h/m-nm (Gerrits *et al.*, 2012b) and ligated into *Eco*RI/*Xho*I-digested pGEX-4T-3. Plasmids pEBG-PTP-PEST WT and pS65T-lamA have been described elsewhere (Broers *et al.*, 1999; Halle *et al.*, 2007).

Cell culture and transient transfection

COS-1 cells (ATCC #CRL1650) were cultured in DMEM (Gibco/Invitrogen, Paisley, UK) supplemented with 10% (v/v) FCS at 37°C and 7.5% CO₂. Transfection of COS-1 cells was done using DEAE-Dextran as described (van Ham *et al.*, 2003). Cells

expressing wild type (WT) or kinase-dead (KD) GST-Lats2 CD were treated with 1 μ M okadaic acid for 1h prior to lysis (Millward *et al.*, 1999).

GST pull-down

COS-1 cells expressing GST-tagged proteins were washed once with ice-cold PBS and lysed in ice-cold lysis buffer (50 mM Tris-HCl, pH 7.5; 150 mM NaCl; 1% NP-40; 25 mM NaF; 1 mM sodium pyrophosphate; 0.1 mM NaVO_3 ; 2 μ M microcystin LR (Alexis Biochemicals/Enzo Life Sciences, Farmingdale, NY); 1 mM PMSF and protease inhibitor cocktail (Roche, Basel, Switzerland)) 1-2 days after transfection. Cell debris was pelleted by centrifugation for 30 min at 15,000 rpm. Glutathione Sepharose 4B beads were added to cleared lysates and incubated overnight at 4°C while rotating. Before being used in the kinase assay, beads were washed once in lysis buffer containing 0.5 M NaCl, once in lysis buffer, and finally once in 50 mM Tris-HCl, pH 7.5; 1 mM DTT; 1 mM benzamidine. In case GST-fusion kinases were to be used for a peptide array, proteins were eluted with 10 mM reduced glutathione in 50 mM Tris-HCl, pH 8.0, diluted in kinase storage buffer (50% glycerol; 1 μ M DTT; 1 μ M EDTA; 200 μ g/ μ l bovine serum albumin), snap frozen and stored at -80°C.

Peptide array and data analysis

To determine DMPK E and Lats2 CD activity towards a peptide library, PepChip Kinase I arrays (Pepscan PRESTO, Lelystad, The Netherlands) were used according to the manufacturer's instructions. Enzymatically inactive mutants were included to determine background phosphorylation caused by potentially co-purifying endogenous kinases.

In short, the concentration of eluted GST fusion proteins of DMPK E (WT or KD) and Lats2 CD (WT or KD) was determined on a Coomassie Brilliant Blue (CBB) stained SDS gel by comparison with standard BSA concentrations. GST fusion proteins were diluted in a 1:1 mixture of glutathione elution buffer and kinase storage buffer yielding a recombinant protein concentration of 100 ng/ μ l (Lats2 CD WT or KD) or 150 ng/ μ l (DMPK E WT or KD). The kinase reaction contained 5 (Lats2 CD WT or KD) or 8 (DMPK E, WT or KD) μ g kinase, 1x kinase master mix (50 mM Hepes, pH 7.4; 10 mM MgCl_2 ; 10% glycerol; 0.01 mg/ml BSA; 0.01% Brij-35; 2.5 mM MnCl_2 ; 1 μ M microcystin), 1 μ M PKA inhibitor peptide (Bachem, Bubendorf, Switzerland), 10 μ M ATP and 300 μ Ci/ml γ - ^{33}P -ATP. Two-thirds of the total reaction volume (60 μ l) was applied to the PepChip Kinase I slide and the remaining one-third was used for SDS-PAGE to confirm kinase input levels. Slides were then coverslipped and incubated for 4 hrs at 30°C in a humidified chamber. Slides were washed once for 5 min with PBS containing 1% Triton X-100 (PBS-Tx), twice with NaCl-Tx (2 M NaCl; 1% Triton X-100) and three times with water. Finally, slides were air dried and exposed to a phosphor-imager screen (Bio-Rad, Berkeley, CA). Spot intensities were measured with GenePix

software (Axon instruments/Molecular Devices, Sunnyvale, CA) and the average intensity of duplicate spots and standard deviation were calculated.

Antibodies

Endogenous Cdc2 was immunoprecipitated (1:100) and detected on western blot (1:1,000) with anti-Cdc2 antibody A17 (Ab18, Abcam, Cambridge, UK). Polyclonal anti-DMPK antibody B79 antibody (1:10,000 (Groenen *et al.*, 2000)) was used to detect GST-DMPK E (WT or KD) on western blot. Polyclonal anti-GST-GFP antiserum (Cuppen *et al.*, 2000) was used to immunoprecipitate GFP-Lamin A (in a 1:250 dilution) and to detect GST-tagged proteins on western blot (1:5,000). To detect GFP-Lamin A on western blot, monoclonal anti-GFP antibody was used (sc-9996, Santa Cruz Biotechnology, Santa Cruz, CA; dilution 1:5,000). All primary antibodies for western blotting were diluted in blocking buffer.

Immunoprecipitation

Protein immunoprecipitation from cleared lysates of transfected COS-1 cells was performed as described for GST pull-down, but now antibody-coupled protein A beads were used. Polyclonal anti-GFP antiserum or Cdc2 antibody was coupled to beads by overnight rotation at 4°C in PBS. Unbound antibodies were removed from the beads by brief centrifugation and washing at 4°C in PBS, before loaded beads were added to the lysates. After overnight immunoprecipitation, beads were washed five times with PBS containing 1% NP-40 and immediately used in an *in vitro* kinase assay.

Bacterial GST-protein production and purification

Competent BL21(DE3)pLysS cells were transformed with plasmid pGEX-4T-3-MLC2-nm and subsequently grown to log phase in LB medium at 37°C, induced with 1 mM IPTG, and grown for an additional 3 hrs. Bacteria were pelleted by centrifugation at 5000 rpm for 5 min, resuspended in ice-cold PBS and subjected to three freeze-thaw cycles and three sonication steps of 10 sec with an interval of 1 minute on ice in between steps. Cell debris was pelleted by centrifugation at 9500 rpm for 15 min and supernatant was incubated with glutathione-Sepharose 4B beads overnight. Subsequently, beads were washed extensively with PBS and GST-fusion proteins were eluted from the beads using 10 mM reduced glutathione in 50 mM Tris-HCl, pH 8.0, snap frozen and stored at -80°C.

SDS-PAGE and western blotting

Protein samples were mixed with 5x SDS-PAGE sample buffer (2.5 M DTT; 25% glycerol; 150 mM Tris-HCl, pH 6.8; 5% (w/v) SDS), boiled for five min and subjected to SDS-

PAGE. Subsequently, proteins were electro-blotted onto PVDF membrane (Millipore, Billerica, MA). For immunodetection purposes, membranes were blocked with 5% (w/v) non-fat dry milk in TBS-T (10 mM Tris-HCl, pH 8.0; 150 mM NaCl; 0.05% Tween-20 (Sigma-Aldrich; St. Louis, MO)) for 30-60 min, incubated with primary antibodies overnight at 4°C and then washed three times with TBS-T. Subsequently, the appropriate secondary antibodies - goat anti-mouse or anti-rabbit IRDye® 600 or 800 (LI-COR Biosciences (Lincoln, NE), dilution 1:10,000) - were applied and incubated for 1 hr at room temperature. Following three successive washes with TBS-T, detection of fluorescent signals was done on an Odyssey infrared Imaging System (LI-COR Biosciences). For Coomassie Brilliant Blue (CBB) staining of proteins, membranes were incubated with CBB staining solution (0.25% (w/v) CBB; 50% methanol; 10% acetic acid) for 1 min and then destained with 50% methanol.

3D-modeling

A 3D model of the Lats2 catalytic domain was created using the automatic homology modeling script in the YASARA & WHAT IF Twinset (Krieger *et al.*, 2002; Vriend, 1990). As a template for this model, we used PDB file 1XH9, containing the structure of cAMP-dependent protein kinase catalytic subunit alpha (Breitenlechner *et al.*, 2005). The 3D structure of DMPK E catalytic domain has been solved experimentally and can be found in PDB file 2VD5 (Elkins *et al.*, 2009). Peptide docking onto DMPK E and Lats2 catalytic domains was based on GSK3 peptide position in PKB (PDB file 1O6K) and optimized using energy minimizations in the YASARA & WHAT IF Twinset.

In vitro kinase assay

In vitro kinase assay was performed as described (Wansink *et al.*, 2003). Briefly, substrate-coated beads (Cdc2, Lamin A, PTP-PEST) were washed once with lysis buffer containing 0.5 M NaCl, once with lysis buffer, and once with 50 mM Tris-HCl, pH 7.5; 1 mM DTT, 1 mM PMSF; 1 mM benzamidine. Beads were then aliquoted in the desired number of kinase reaction samples and subjected to the final washing step before being added to 20 μ l 2x kinase assay buffer (100 mM Tris-HCl, pH 7.5; 20 mM MgCl₂; 4 mM MnCl₂; 2 mM DTT; 2 μ M PKA inhibitor peptide; 2 μ M PMSF; 2 μ M benzamidine; 4 μ M microcystin LR). Likewise, eluted MLC2 substrate was aliquoted in the desired number of kinase reaction samples and diluted in 20 μ l 2x kinase assay buffer. Beads containing GST-coupled kinase or the enzymatically inactive mutant were added to the substrate and H₂O was added to a final volume of 40 μ l. To determine specific activities, 500 ng eluted GST-fusion kinase was used in an *in vitro* kinase assay and the final peptide concentration was 30 μ M. Reactions were started by adding 5 μ l 0.5 mM γ -³²P-ATP and continued for 30 min at 30°C. Reactions were stopped by the addition of 5x SDS-PAGE sample buffer and samples were used for

2

Phosphorylation target site specificity for AGC kinases DMPK E and Lats2

RESULTS

Purification of DMPK E and Lats2 protein

In order to gain insight into DMPK E and Lats2 kinase specificity both kinases need to be obtained in their active, i.e. properly phosphorylated, state. To this end, kinases were expressed in COS-1 cells as GST-fusion proteins and subsequently purified via glutathione beads. Full-length Lats2 protein was found to be very inefficiently produced and purified, thus an N-terminally truncated version representing the essential catalytic domain (referred to as Lats2 CD) was used instead. Localisation of ectopically expressed Lats2 CD in the cell matched that of full-length Lats2 (data not shown) and also Lats2 CD depended on okadaic acid treatment of cells to acquire an active state. This indicates that regulatory kinases and phosphatases did not noticeably discriminate between the two forms and supports use of Lats2 CD to identify potential substrates. Next to wild type (WT) versions of both kinases also enzymatically inactive mutants (KD, kinase dead) were included to be able to monitor any contribution of potentially co-purifying kinases (Fig. 1A).

Prior to determining specificity profiles for Lats2 CD and DMPK E, enzymatic

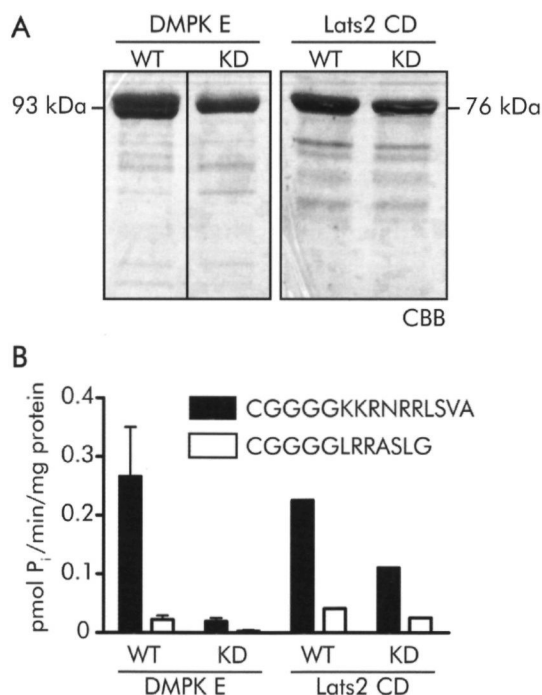


Figure 1: Purified DMPK E and Lats2 CD are enzymatically active. (A) GST fusion proteins of DMPK E and Lats2 CD (i.e., an N-terminally truncated version representing the essential catalytic domain), both in a WT and an enzymatically inactive version (KD, kinase dead), were produced in COS-1 cells and purified via GST pull-down. GST-DMPK E WT, but not KD, appears as a broad doublet band, indicative of autophosphorylation activity (Wansink et al., 2003). Protein purity and concentration were determined on a CBB-stained SDS gel by comparison with standard BSA concentrations. (B) Kinase activity of DMPK E and Lats2 CD towards two different peptides determined in an *in vitro* kinase assay ($n=2$ for DMPK E, $n=1$ for Lats2 CD).

activity of purified proteins was assessed via an *in vitro* kinase assay in which two peptide substrates were included: (i) standard NDR substrate peptide CGGGGKKRNRRLSVA (Millward *et al.*, 1998) - also known to be phosphorylated by DMPK E (Wansink *et al.*, 2003) - and (ii) PKA substrate kemptide CGGGGLRRASLG as negative control (Wansink *et al.*, 2003). Specific activity of Lats2 CD and DMPK E towards the NDR kinase substrate peptide was approximately 0.25 pmol P/min/ μ g kinase (Fig. 1B). Background activity in the DMPK E KD protein preparation was marginal, but some residual activity was detected in the Lats2 CD KD preparation. Kinase activity towards kemptide was insignificant for both kinases. These data confirmed our expectation that purified recombinant WT forms of DMPK E and Lats2 CD are enzymatically active and that DMPK E KD - and to a lesser extent Lats2 CD KD - may serve as specificity controls.

Peptide array screening

Purified recombinant kinases were subsequently used to phosphorylate peptides on an arrayed library. Most of these peptides represent genuine *in vivo* phosphorylation targets (www.phosphosite.org). The array glass surface, onto which two duplicate sets of 1152 different peptide sequences were printed, was incubated with purified kinase in the presence of γ -³³P-ATP (Fig. S1). Resulting ³³P incorporation was quantified using a phosphorimager device. Incubation with DMPK E WT resulted in several distinct spots representing phosphorylated peptides, while incubation with DMPK E KD revealed only minor background phosphorylation (Fig. 2A). On the array incubated with Lats2 CD WT much more peptides were labeled. Also, the slide incubated with Lats2 CD KD revealed a considerable number of radiolabeled spots (Fig. 2B). These data imply that the Lats2 kinase domain, outside the context of the full-length protein, displays broader substrate specificity than DMPK E. We cannot exclude that some of these spots reflect contributions of kinases that co-purified with Lats2 CD.

To extract a cogent set of substrate peptides from these array data, we applied three selection criteria. First, the average signal intensity for a substrate peptide should match at least 5% of the highest average intensity of duplicate spots obtained for the WT kinase. Second, to exclude peptide sequences with high background phosphorylation levels in the KD arrays, average labeling intensity for duplicate spots should be at least twice as high on the WT array as on the KD array. Third, to exclude poorly reproducible signals, the standard deviation of duplicate spots on the WT array should not exceed the average signal for those spots. Peptides that matched all three criteria were manually checked to exclude influences from strong radiation of neighboring spots or non-specific smears on the array surface. This resulted in a list of 47 candidate DMPK E substrate peptides (Table S1). For Lats2 CD 243 peptides met the criteria and the top 40 sequences are listed in Table S2.

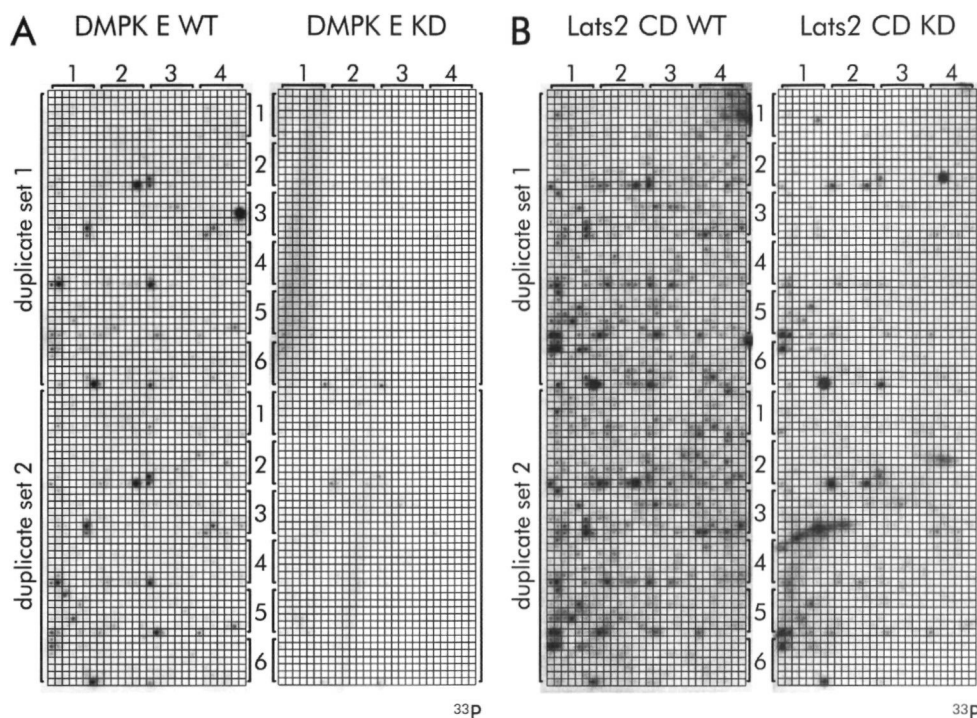


Figure 2: Testing kinase specificity for DMPK E and Lats2 using a peptide array. The grid of the peptide array carrying two duplicate sets of 1152 kinase substrate peptides was overlaid with phosphorimager results of in vitro phosphorylation with DMPK E WT or KD (A), or Lats2 CD WT or KD (B).

DMPK E and Lats2 prefer basic residues flanking their target phosphorylation site

Almost all peptides phosphorylated by DMPK E contained a Ser or Thr phosphoacceptor site next to a Lys or Arg at position -2 and frequently also a Lys/Arg at positions -1, -3 or -4 (Table S1). This consensus indicated a preference of DMPK E activity for Ser/Thr residues just C-terminal of basic residues (Fig. 3A). Besides, Lys/Arg residues were often present at positions +1 to +4 as well. Hydrophobic residues were encountered at position +1.

Also the vast majority of peptides in the top list of candidate Lats2 CD substrates (Table S2) contained at least one Lys/Arg residue at position -2 and -3 (Fig. 3B) but compared to DMPK E, positively charged residues were less frequent at position -1. As for DMPK E, Lys/Arg residues were also observed at positions +2 to +4 in Lats2 substrate peptides. In contrast to DMPK E substrates, hydrophobic residues were encountered at position -1 and +3 in Lats2 substrates.

We used homology modeling to relate our observations regarding DMPK E

Phosphorylation target site specificity for AGC kinases DMPK E and Lats2

2

and Lats2 preferences for peptide sequences containing Lys/Arg residues at positions -1 to -3 (Fig. 3) to 3D structures of the respective kinase domains (Krieger *et al.*, 2002). The structure for the DMPK E kinase domain has been solved (PDB file 2VD5; Elkins *et al.*, 2009). PDB file 1XH9, containing cAMP-dependent protein kinase catalytic subunit alpha (Breitenlechner *et al.*, 2005) was used as a template to model the Lats2 catalytic domain. Due to high sequence identity between the kinase domains of DMPK E and Lats2, the published active site of DMPK E (Elkins *et al.*, 2009) could be used to predict location of the active site and hence the peptide binding groove of Lats2.

Two negative pockets exist in the region where the N-terminus of the target peptide is expected to bind (Fig. 4). The region that should harbor the C-terminus of the peptide, a hydrophobic pocket, is also present. We subsequently docked preferred target peptides into the 3D structures of the catalytic domains. As shown in Fig. 4 B/C

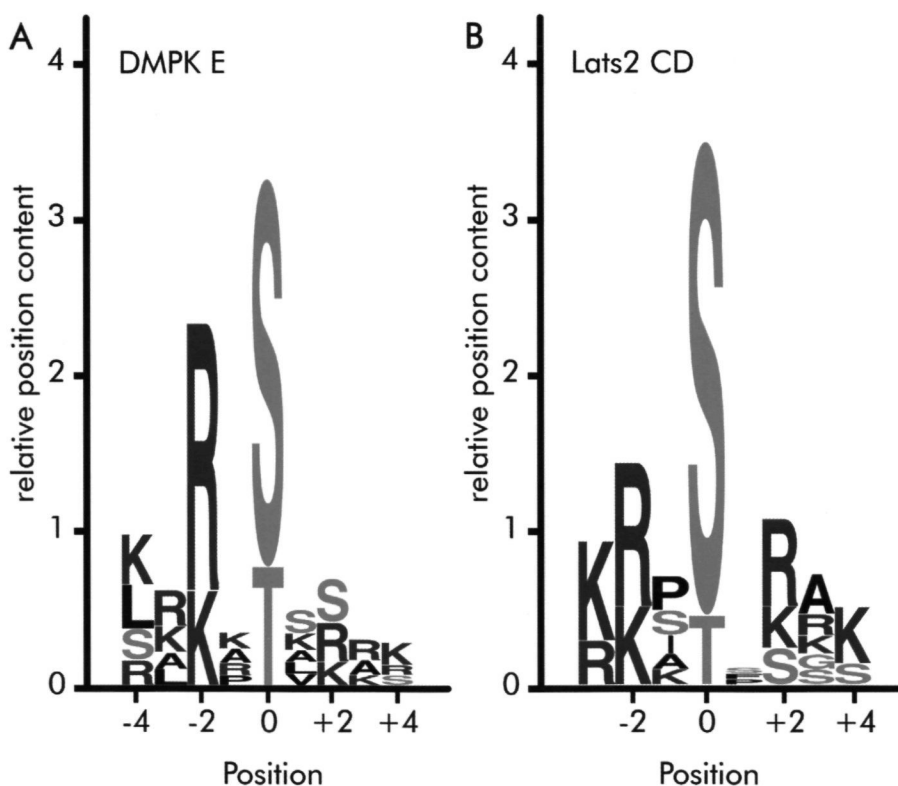


Figure 3: Consensus phosphorylation target sequence of (A) DMPK E and (B) Lats2, generated using the LOGO algorithm (<http://weblogo.berkeley.edu/>). The phosphoacceptor site is located at position 0, residues positioned N-terminal (-) or C-terminal (+) of the phosphorylated residue are indicated. The Y-axis represents the relative position content.

and E/F, the positively charged residues in docked peptides nicely fill the negative pockets on the catalytic domains. This provides an explanation for the experimental observation that peptides with Lys/Arg residues N-terminal of the target Ser/Thr site are favored by DMPK E and Lats2.

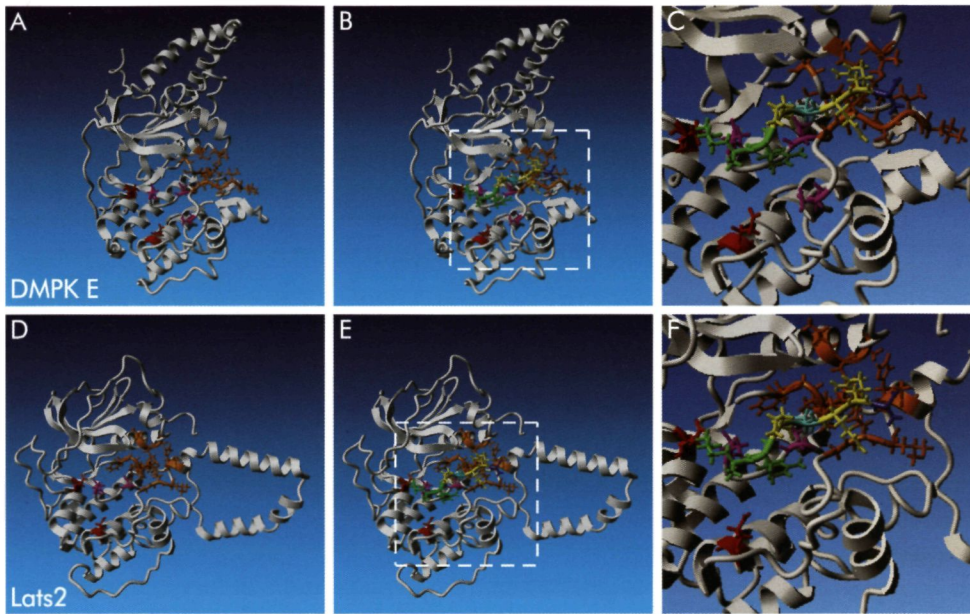


Figure 4: Three-dimensional model of DMPK E and Lats2 catalytic domains. (A) 3D structure of DMPK E (PDB 2VD5) with negatively charged residues of the two negative pockets indicated in red and magenta and the hydrophobic residues of the hydrophobic pocket in orange. (B) DMPK E in complex with peptide KRPTQRA. (C) Close-up of the area indicated with the white dashed box shown in (B), representing the peptide binding-groove of DMPK E. (D) 3D model of the Lats2 catalytic domain (created by homology modeling) with negatively charged residues of the two negative pockets indicated in red and magenta and the hydrophobic residues of the hydrophobic pocket in orange. (E) Lats2 catalytic domain in complex with peptide KRPTQRA. (F) Close-up of the area indicated with the white dashed box shown in (E), representing the peptide binding-groove of Lats2. Positively charged residues in the peptide that fit in the negative pockets of the kinases are indicated in green, hydrophobic residues are indicated in blue and the phosphoacceptor residue is indicated in cyan.

Comparison of highly similar DMPK E substrate peptide sequences

The peptide array data provided a list of potential substrates for the kinases under study (Tables S1 and S2). Use of the full-length DMPK E protein in the kinase assay resulted

in a more refined phosphorylation pattern than obtained with the Lats2 catalytic domain. We therefore decided to use DMPK E to further validate our experimental findings and theoretical predictions. We noted that a difference of one or two amino acids within a peptide sequence could lead to marked differences in phosphorylation activities. Therefore clusters of peptides with highly similar sequences were selected to extract information on exclusion principles that guide DMPK E target sequence selectivity (Fig. 5).

Data from the cluster depicted in Fig. 5A suggest that DMPK E has a preference for Thr over Ser. This finding may appear to contradict the consensus sequence depicted in Fig. 3A, but one should bear in mind that the latter is based on a 4-5 times overrepresentation of Ser relative to Thr phosphoacceptor sites in the peptide collection on the array. Data from cluster 5A also suggest that, at least in the context of this peptide, a tyrosine at the C-terminus is favored over alanine. Other comparisons reveal that the presence of a polar residue at position +1 negatively influences phosphorylation by DMPK E (Fig. 5B). Panel 5C underscores the importance of a basic residue at -2: it explains why only the C-terminal one of the two Thr residues in the two upper peptides is phosphorylated by DMPK E. Additional positive charges N-terminal of the target site further boost phosphorylation by DMPK E. One may argue that the target site in the shorter peptide is simply less accessible for the kinase (Fig. 5C) but this is not likely as the second peptide in cluster A contains even less amino acids N-terminal to the phosphorylation site. Fig. 5D shows that the N-terminal Ser residue in YRKSSLKSR is phosphorylated by DMPK E, although also the adjacent Ser is positioned relative to a positively charged amino acid at position -2. The C-terminal Ser in this peptide is not phosphorylated by DMPK E, underscoring the -2 Arg/Lys requirement (Fig. 5D).

In some peptides multiple possible phosphorylation target sites that fit the -2 Arg/Lys rule are present. For instance, in the first peptide in cluster E a Ser as well as a Thr residue (indicated by dashed boxes) is preceded by a positively charged residue at position -2. The second peptide in this cluster is not phosphorylated (Fig. 5E) but it is impossible to distinguish between two likely causes. The presence of a negatively charged glutamate in the proximity of the N-terminal Ser may well hinder its phosphorylation. Alternatively, in case the Thr residue represented the DMPK E phosphorylation site, its sheer absence in the second peptide explains the lack of signal. Peptides in cluster F also contain multiple possible phosphorylation target sites, two of which contain an Arg residue at position -2 (Fig. 5F). Since three residues N-terminally of the phospho-target site suffices for phosphorylation (Fig. 5A,B) and the middle Ser residue in all cluster F peptides is preceded by an Arg at position -2, it comes as a surprise that the RRSSVGVI peptide is not phosphorylated. This points to the most N-terminally located Ser residue as the most likely target site, whose

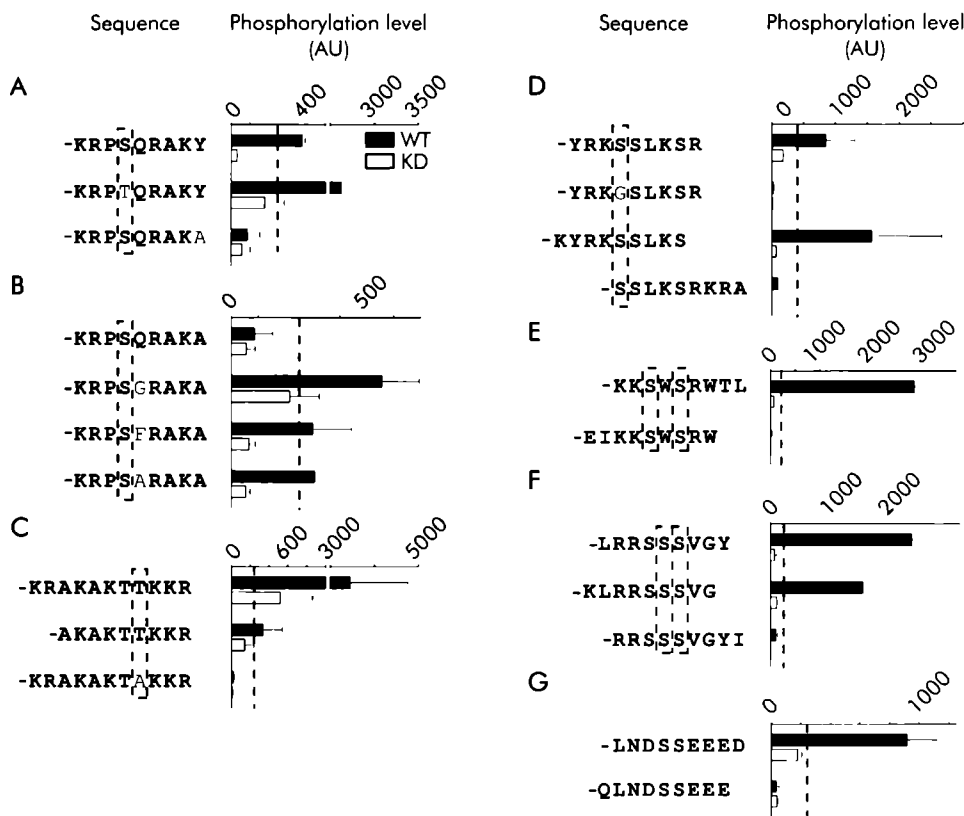


Figure 5: Analysis of kinase activity towards highly similar peptides grouped in clusters (A-G). Peptide sequences are shown with the common target residue in dashed boxes. In case multiple possible target residues may reside within one peptide, this is indicated with multiple dashed boxes. Only Ser/Thr residues with a Lys/Arg at position -2 were considered possible target sites. The hyphen at the N-terminal end of peptide sequences symbolizes the covalent link to the glass surface of the array. Amino acids in normal font reflect single residue differences with the top sequence in the cluster. Graphs on the right represent average signal intensities (arbitrary units \pm SD) for the given peptides measured on the DMPK E WT (black bars) or KD (white bars) arrays (Fig. 2A). A dashed line in the graph indicates the cut-off value for substrate selection (5% of highest average signal on WT array).

phosphorylation in the third peptide may be hampered by insufficient N-terminal residues. In agreement with the results of cluster D, the presence of an extra positive charge at -4 of the phosphorylation site had no significant influence on phosphorylation levels (compare first and second peptide in cluster F).

The only phosphorylated substrate that did not match the DMPK E target site consensus is the first peptide shown in cluster G, which does not carry a positively charged residue at -2 (Fig. 5G). Instead, five negatively charged residues surround the candidate serines. This finding suggests that in addition to the known peptide binding groove of DMPK E, other regions may contribute to peptide recognition as well.

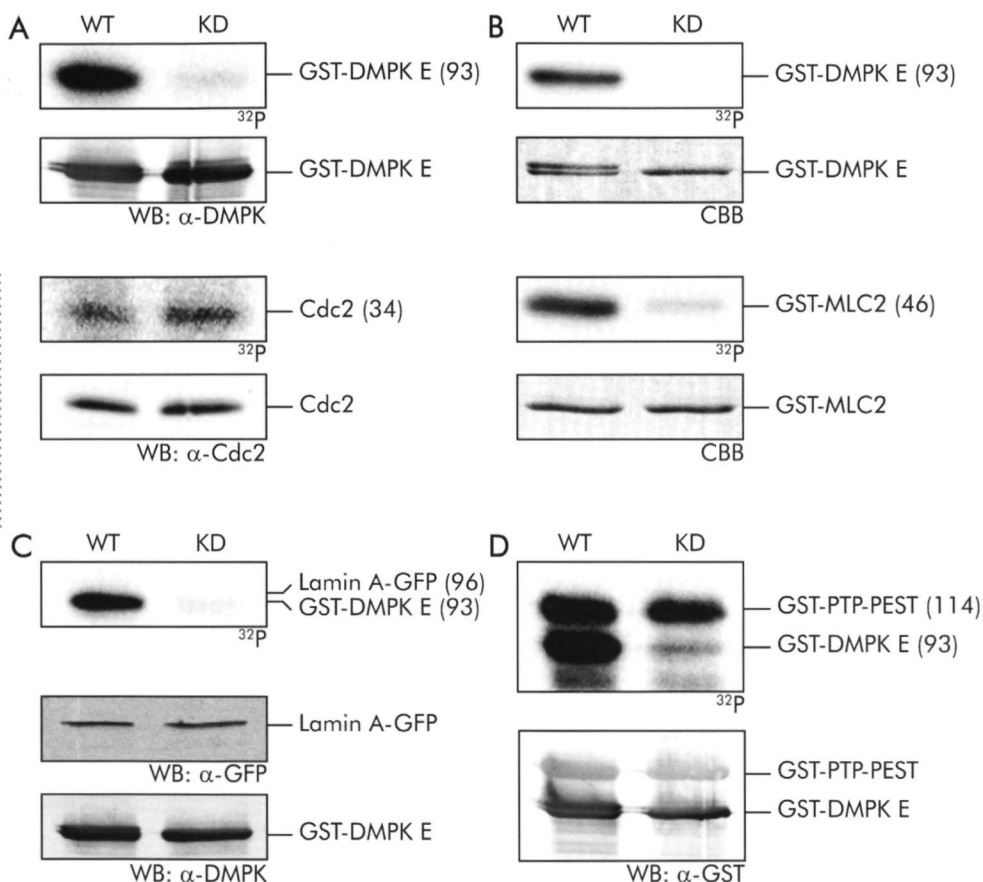


Figure 6: Testing full-length candidate protein substrates in an *in vitro* DMPK E kinase assay. Cdc2 (A), nm-MLC2 (B), Lamin A (C) and PTP-PEST (D) were isolated and incubated with either DMPK E WT (WT) or KD (KD) in an *in vitro* kinase assay. Panels show phosphorylation of DMPK E (i.e., autophosphorylation) and candidate proteins (^{32}P). Protein input levels were determined by western blotting (WB) or Coomassie Brilliant Blue staining (CBB). Numerals between brackets indicate the predicted molecular weight in kDa.

***In vitro* testing of full-length candidate substrates for DMPK E**

To investigate if data obtained with the array can be extrapolated to full-length substrate proteins, the activity of DMPK E against four proposed candidates (Table S1) was tested. Availability of proper antibodies allowed immunoprecipitation of endogenous Cdc2 from COS-1 cells. Furthermore, the non-muscle isoform of MLC2 was produced as a GST fusion protein in bacteria, purified and released from glutathione beads. In addition, Lamin A-GFP and GST-tagged PTP-PEST were produced and purified from COS-1 cells with immunoprecipitation and GST pull-down, respectively. The four candidate proteins were tested in *in vitro* kinase assays in the presence of purified DMPK E WT or KD. Protein input levels were verified by western blotting or Coomassie Brilliant Blue (CBB) staining, while phosphorylation was measured using a phosphorimager. Autophosphorylation of DMPK E served as a control for assay conditions. DMPK E-specific phosphorylation of candidate substrate Cdc2, if at all present, did not reach a level above background as observed in the KD samples (Fig. 6A). The same holds for recombinant Lamin A and PTP-PEST proteins (Fig 6C and D). Recombinant MLC2 protein, on the contrary, displayed significant specific phosphate incorporation upon incubation with DMPK E WT (Fig. 6B).

In this study we demonstrate that AGC kinases DMPK E and Lats2 have a similar, yet distinct, target consensus sequence. Both kinases prefer to phosphorylate peptides in which the target residue is surrounded by positively charged amino acids. Preference for this type of sequences is reflected by the presence of two negative pockets in the peptide binding groove that were identified by analysis of 3D models of the kinase domains involved.

The phosphorylation consensus sequences that were delineated from Tables S1 and S2 are in line with reported consensus target sequences for other AGC kinases (Hao *et al.*, 2008; Mah *et al.*, 2005; Millward *et al.*, 1998; Turner *et al.*, 2002). Comparison of DMPK E and Lats2 phosphorylation profiles in parallel array screens aids the assessment of substrate specificities for these two AGC kinases. Both share a preference for positively charged residues at positions -2 and/or -3 and additional positive charges further N-terminal. In particular, for DMPK E a basic residue at position -2 is highly preferred. The DMPK E consensus sequence described here agrees well with the one discussed in our earlier work (Wansink *et al.*, 2003), although in the present study we could not confirm a preference for Lys/Arg at position -1 concurrently with -3. Another study yielded a consensus sequence with an Arg at position -3, but this sequence was based on phosphorylation analysis of five peptides only (Bush *et al.*, 2000). All DMPK full-length substrates for which the phosphorylation target sites have been determined indeed display Arg residues at position -2 and -3 (AIRRASTIEMP in phospholamban (Kaliman *et al.*, 2005), KLRRYTTFSKR in SRF (Iyer *et al.*, 2003) and RQSRRSTQGV in MYPT1a (Muranyi *et al.*, 2001); phospho-acceptor sites in bold). Interestingly, phospholamban was represented on the peptide array by peptides IRRASTIEM and RRASTIEMP but phosphorylation levels did not meet our criteria. The phospholamban target site was identified in the full-length protein (Kaliman *et al.*, 2005) suggesting that DMPK E-mediated phosphorylation of phospholamban may require the full-length protein context. Target requirements for Lats2 appear less discriminative than for DMPK E: at least one basic residue at position -2 or -3. In the Lats2 substrates TAZ and YAP multiple Lats2 target sites were found, each matching the consensus sequence HXRXXS (X represents any amino acid; (Hergovich and Hemmings, 2009; Lei *et al.*, 2008)). Only two peptides that obey this consensus are present on the peptide array: THERSPSPS and HKRKSSQAL, but their phosphorylation levels did not exceed background signal, explaining why the HXRXXS consensus did not emerge from the current screen.

In our study 70% (DMPK E) to 87% (Lats2) of the substrate peptides contain positively charged amino acids at both sides of the phosphorylation target site, even though the array does not seem to be enriched for this type of peptides. In addition,

peptide LRRASLRG is a DMPK E substrate, but LRRASLAG not, confirming a preference for positive charges at both sides of the target site. Such a preference has not been described before for any AGC kinase. This observation could point towards the possibility of bidirectional binding of peptides in the peptide binding groove (Chan *et al.*, 1982; Torshin, 2000; Zaliani *et al.*, 1998). This would also explain why some peptides that only contain positively charged residues downstream of the target site (e.g. GGSVTKRRK) were still phosphorylated by DMPK E and Lats2.

Four candidate substrates that resulted from the peptide array screening were examined for phosphorylation by DMPK E in an *in vitro* kinase assay. For three of these (Cdc2, PTP-PEST and Lamin A) phosphorylation levels were not detectably increased by DMPK E. It is not uncommon that only a limited number of candidate proteins that result from peptide screens actually turn out to be *bona fide* substrates (Mah *et al.*, 2005). After all, extrapolation of array data towards full-length target proteins very much depends on the structural context of the corresponding sequence in the substrate. Recently, co-immunoprecipitation of Lamin A with a DMPK isoform that differs from DMPK E was reported (Harmon *et al.*, 2011), but the ability of this isoform to phosphorylate Lamin A was not investigated.

For nm-MLC2 we found convincing evidence that DMPK E was able to phosphorylate the full-length protein. On the PepChip Kinase I array the MLC2 protein was represented by several peptides spanning the position 9 threonine residue for which phosphorylation has been reported (Bengur *et al.*, 1987). Thr18 and Ser19 are the best-studied MLC2 phosphoacceptor sites (Vicente-Manzanares *et al.*, 2009) but these were not represented in the peptide collection. We investigated whether phosphorylation of full-length MLC2 by DMPK E did occur on this Thr9. Substitution of Thr9 by alanine indeed resulted in a 50% reduction of MLC2 phosphorylation levels, confirming that MLC2 Thr9 is a DMPK E target site but also indicating that phosphorylation at positions Thr18/Ser19 is probably mediated by DMPK E as well (L.G. and D.G.W.; unpublished data).

One of the limitations of peptide array technology is that only a restricted number of proteins can be represented. There could be many more proteins out there that serve as substrates and contain sequences resembling consensus DMPK E and Lats2 target sites. We explored this by performing a motif search in a database of phosphorylated peptides (at phospho.elm.eu.org) which yielded an overwhelming number of possible candidates. To be effective, such an approach would require the delineation of a much more detailed consensus target sequence, for instance by screening additional custom-made peptide clusters. In addition, structural information on substrate candidates is required to incorporate surface accessibility of the identified peptide sequences in such search algorithms. (Semi-)quantitative phosphoproteomics may therefore represent a more feasible way of expanding and refining the list of

DMPK E and Lats2 substrates to provide additional insight into their biological function.

In summary, our findings provide insight into the identity of possible Lats2 and DMPK E substrate proteins and a basis to search for other candidate substrate proteins. More research will be necessary to investigate the phosphorylation capacity of DMPK E and Lats2 towards these proteins. Knowledge on their phosphorylation site preferences will aid in understanding via which molecular pathways Lats2 and DMPK E may exert their activity.

2

Acknowledgments

GST-PTP-PEST constructs were a kind gift from dr. Michel Tremblay (Goodman Cancer Centre, Montreal, Quebec, Canada) and GFP-Lamin A constructs were kindly provided by drs. Guillaume van Eys and Frans Ramaekers (University of Maastricht, Maastricht, The Netherlands). This work was funded by grant RUNMC 2006-12 from the Radboud University Nijmegen Medical Centre.

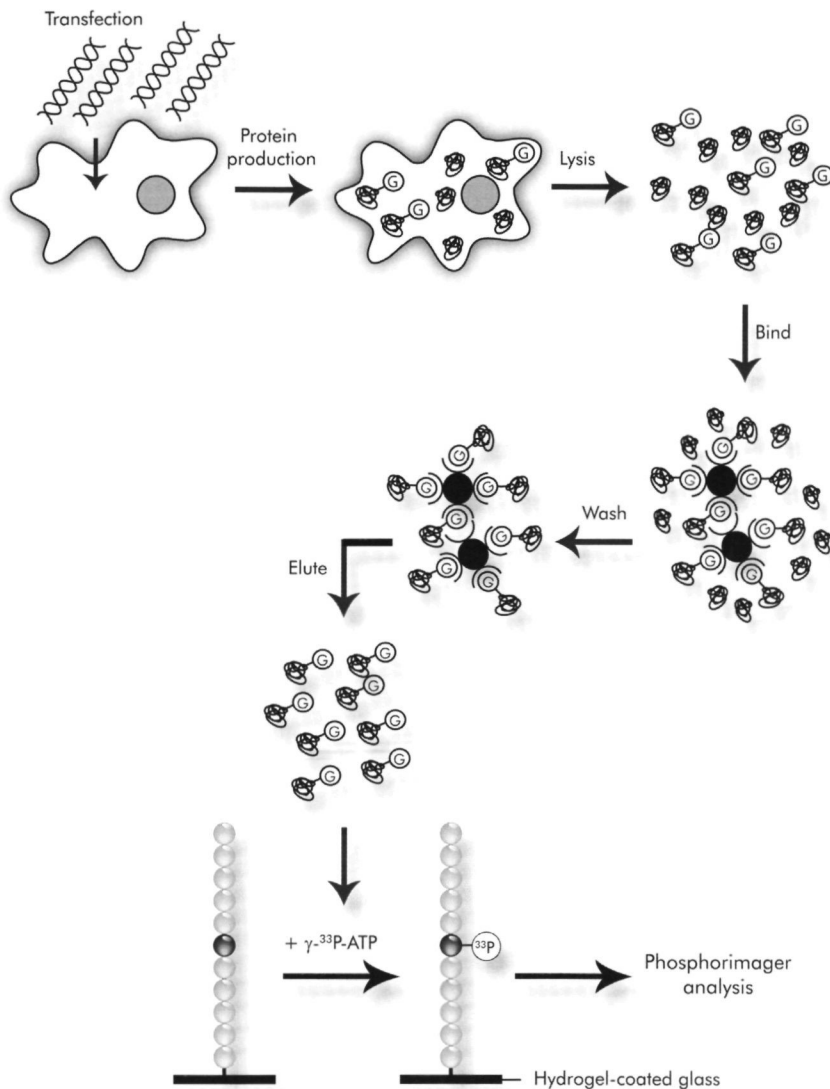


Figure S1: Graphical summary of the array methodology used. Mammalian cells were transfected with DNA encoding GST-tagged kinase and protein was produced for one or two days followed by cell lysis. GST-tagged kinase was purified by GST pull-down. GST-tagged kinase was eluted from the beads by reduced glutathione and applied to the peptide array in the presence of $\gamma\text{-}^{33}\text{P}\text{-ATP}$. After washing and exposure of the peptide array to a phosphorimager screen, labeled peptides could be identified.

Table S1: Substrate specificity of DMPK E. List of 47 peptides that were selected as substrates using the criteria described in the text.

Sequence	Protein nr. (organism)	Common name	Phosphosite ⁺	Slide signal (norm.) [*]
KTTASTRKV	P13569 (<i>Homo sapiens</i>)	Cystic fibrosis transmembrane conductance regulator	KTTA <u>S</u> TRKV	100.0
KRAKAKTTKKR	P02612 (<i>Gallus gallus</i>)	Myosin regulatory light chain 2, smooth muscle major isoform	KRAKAK <u>T</u> KKR (H/R/M)	73.0
KKSWSRWTL	P25107 (<i>Didelphis virginiana</i>)	Parathyroid hormone 1 receptor	KK <u>S</u> W <u>S</u> RWTL (H/R/M)	62.3
KRPTQRAKY	P02687 (<i>Bos taurus</i>)	Myelin basic protein	Artificial peptide derived from KR <u>P</u> SQR <u>S</u> KYL	56.4
LRRSSSVGY	P02718 (<i>Torpedo californica</i>)	Acetylcholine receptor subunit delta	LRR <u>S</u> <u>S</u> SVG <u>Y</u>	52.2
SRRQSVLVK	Q13002 (<i>Homo sapiens</i>)	Glutamate receptor, ionotropic kainate 2	SRRQ <u>S</u> VLVK	44.9
KLRRSSSVG	P02718 (<i>Torpedo californica</i>)	Acetylcholine receptor subunit delta	KLRR <u>S</u> SVG	34.2
KYRKSSLKS	P22613 (<i>Ovis aries</i>)	spermatid nuclear transition protein 1	KYRK <u>S</u> SLK <u>S</u>	33.8
LRRASLRG	(<i>Bos taurus</i>)	(Bovine) liver pyruvate kinase (fragment)	x	24.9
GGSVTKKRK	P11516 (<i>Mus musculus</i>)	lamin A/C	GG <u>S</u> V <u>T</u> KKRK	21.3
KRRSSSYHV	P04775 (<i>Rattus norvegicus</i>)	Sodium channel protein type 2 subunit alpha	KRR <u>S</u> <u>S</u> SYHV	20.6

Phosphorylation target site specificity for AGC kinases DMPK E and LatA2

2

LNDSSSEED	P03129 (Human papillomavirus type 16)	Protein E7	Viral protein, no mammalian ortholog found	19.7
PPRSSIRN	P14598 (<i>Homo sapiens</i>)	NADPH oxidase organizer 2	PPRR <u>S</u> IRN	19.4
KAKVTGRWK	P13789 (<i>Bos taurus</i>)	Troponin T, cardiac muscle isoform	KAKV <u>T</u> GRWK	18.8
YRKSSLKSR	P22613 (<i>Ovis aries</i>)	spermatid nuclear transition protein 1	YRK <u>S</u> SLK <u>S</u> R	18.3
KAKTTKKRP	P02612 (<i>Gallus gallus</i>)	Myosin regulatory light chain 2, smooth muscle major isoform	KAK <u>T</u> TTKKRP (H/R/M)	18.2
KRAASPRKS	P02256 (<i>Parechinus angulosus</i>)	Histone H1, gonadal	Worm protein, No mammalian ortholog found	13.1
LRRASLGAA	(<i>Bos taurus</i>)	(Bovine) liver pyruvate kinase (fragment)	x	12.6
KRPSGRAKA	P02687 (<i>Bos taurus</i>)	Myelin basic protein	KRP <u>S</u> GRAKA	11.9
AKRISGKMA	P13863 (<i>Gallus gallus</i>)	Cdc2	AKRI <u>S</u> GKMA	10.8
SLRASTSKS	P08227 (<i>Mus musculus</i>)	40S ribosomal protein S6	<u>S</u> LR <u>A</u> ST <u>S</u> K <u>S</u>	10.2
PSPSSRVTV	P20700 (<i>Homo sapiens</i>)	lamin B	P <u>S</u> P <u>S</u> SRVTV	10.1
KISASRKLQ	P08057 (<i>Bos taurus</i>)	Troponin I, cardiac muscle isoform	KI <u>S</u> AS <u>R</u> KLQ	10.0
SRRSSLGSL	P07293 (<i>Oryctolagus cuniculus</i>)	voltage-dependent L-type calcium channel alpha-1S subunit	No, only other residues in full-length protein	9.3
GVLRRASVA	P12928; P04763; Q64618 (<i>Rattus norvegicus</i>)	Pyruvate kinase isozymes R/L	GVLRR <u>A</u> SVA	9.1
KSKISASRK	P08057 (<i>Bos taurus</i>)	Troponin I, cardiac muscle isoform	K <u>S</u> KI <u>S</u> AS <u>R</u> K	9.1

Phosphorylation target site specificity for AGC kinases DMPK E and Lats2

2

RVRKTKGKY	P19490 (<i>Rattus norvegicus</i>)	Glutamate receptor ionotropic, AMPA 1	No, only other residues in full-length protein	8.8
LRLSTKYR	Q05209 (<i>Homo sapiens</i>)	PTP-PEST	LRL <u>S</u> TKYR	8.7
KASASPRRK	P02256 (<i>Parechinus angulosus</i>)	Histone H1, gonadal	Worm protein. No mammalian ortholog found	8.1
KRPSQRAKY	P02687 (<i>Bos taurus</i>)	Myelin basic protein	KRP <u>S</u> QRAKY	8.1
RQRKSRRTI	P01589 (<i>Homo sapiens</i>)	interleukin 2 receptor, alpha	RQRK <u>S</u> RRTI	8.0
QRVSSYRRT	P02542 (<i>Gallus gallus</i>)	Desmin	QRV <u>S</u> SYRRT	7.9
ARKSTRRSI	P08567 (<i>Homo sapiens</i>)	Pleckstrin	ARK <u>S</u> TRRSI	7.7
LRRFSLATM	P00176 (<i>Rattus norvegicus</i>)	cytochrome P-450b type b	LRRF <u>S</u> LATM	7.6
LELSDDDD	A34928 (<i>Bos taurus</i>)	myosin heavy chain, brain (peptide)	LE <u>S</u> DDDD (H/R/M)	7.2
KRKQISVRG	P11217 (<i>Homo sapiens</i>)	Glycogen phosphorylase, muscle form	KRKQI <u>S</u> VRG	7.2
AKAKTTKKR	P02612 (<i>Gallus gallus</i>)	Myosin regulatory light chain 2, smooth muscle major isoform	AKAKT <u>T</u> KKR (H/R/M)	7.2
LRRASLGAF	(<i>Bos taurus</i>)	(Bovine) liver pyruvate kinase (fragment)	x	7.1
KRPSARAKA	P02687 (<i>Bos taurus</i>)	Myelin basic protein	KRP <u>S</u> ARAKA	6.6
KRPSFRAKA	P02687 (<i>Bos taurus</i>)	Myelin basic protein	KRP <u>S</u> FRAKA	6.4
LSYRRYSL	x	x	x	6.3
FRKFTKSER	P00516 (<i>Bos taurus</i>)	cGMP-dependent protein kinase 1, alpha isozyme	FRKF <u>T</u> KSER	6.1

KTRSSRAGL	P02261 (<i>Homo sapiens</i>)	H2A histone family, member C	No, only other residues in full-length protein	5.8
SRSRTPSLP	x	x	x	5.8
RVRKSKGKY	P19491 (<i>Rattus norvegicus</i>)	glutamate receptor, ionotropic, AMPA 2	RVRK <u>S</u> KGKY	5.5
LRRASVAQL	P12928; P04763; Q64618 (<i>Rattus norvegicus</i>)	Pyruvate kinase isozymes R/L	LRRAS <u>V</u> AQL	5.5
GKSSSYSKQ	P02671 (<i>Homo sapiens</i>)	Fibrinogen alpha chain	No, only other residues in full-length protein	5.4

+ bold and underlined residues indicate which Ser, Thr and/or Tyr residues are annotated as *in vivo* phosphorylation sites (www.phosphosite.eu). When the protein of the indicated organism was not found but an ortholog was present in the database this is indicated. Also, when no orthologs were found in the phosphosite database, this is indicated. H, *homo sapiens*; R, *rattus norvegicus*; M, *mus musculus*; x, not listed.

* represents the average signal of two duplicate spots on the DMPK E WT array normalized to the highest average value (set at 100).

Table S2: Substrate specificity of Lats2. List of 40 highest scoring peptides out of the 243 peptides that were selected as substrates using the criteria described in the text.

Sequence	Protein nr. (organism)	Common name	Phosphosite ⁺	Slide signal (norm.)*
AKRISGKMA	P13863 (<i>Gallus gallus</i>)	Cdc2	AKRI <u>S</u> GKMA	100.0
KRPTQRAKY	P02687 (<i>Bos taurus</i>)	Myelin basic protein	Artificial peptide derived from KRPS <u>Q</u> RSKYL	76.4
KRRSSSYHV	P04775 (<i>Rattus norvegicus</i>)	Sodium channel protein type 2 subunit alpha	KRRSS <u>S</u> YHV	74.2
KISASRLQ	P08057 (<i>Bos taurus</i>)	Troponin I, cardiac muscle isoform	KI <u>S</u> ASRLQ	70.7
KKWSRWTL	P25107 (<i>Didelphis virginiana</i>)	Parathyroid hormone 1 receptor	KK <u>S</u> WSRWTL (H/R/M)	65.3
YRKSSLKSR	P22613 (<i>Ovis aries</i>)	spermatid nuclear transition protein 1	YRK <u>S</u> SLKSR	65.1
KSKISASRK	P08057 (<i>Bos taurus</i>)	Troponin I, cardiac muscle isoform	KSKI <u>S</u> ASRK	65.0
LNDSEED	P03129 (Human papillomavirus type 16)	Protein E7	Viral protein, no mammalian ortholog found	64.6
KLRRSSSVG	P02718 (<i>Torpedo californica</i>)	Acetylcholine receptor subunit delta	KLRR <u>S</u> SSVG	61.9
KYRKSSLKS	P22613 (<i>Ovis aries</i>)	spermatid nuclear transition protein 1	KYRK <u>S</u> SLKS	61.4
KRPSNRAKA	P02687 (<i>Bos taurus</i>)	Myelin basic protein	KRP <u>S</u> NRAKA	59.9
KASASPRRK	P02256 (<i>Parechinus angulosus</i>)	Histone H1, gonadal	Worm protein, no mammalian ortholog found	56.6
KIQASFRGH	P35722 (<i>Bos taurus</i>)	neurogranin	KIQA <u>S</u> FRGH	53.8

Phosphorylation target site specificity for AGC kinases DMPK E and Lats2

2

RTKRSGSV	x	x	x	52.7
SRPSSNRSY	P20152 (<i>Mus musculus</i>)	Vimentin	<u>SRPSSNRSY</u>	52.1
KRPSQRAKY	P02687 (<i>Bos Taurus</i>)	Myelin basic protein	KRPSQRAKY	52.0
KSPA K TPVK	P12957 (<i>Gallus gallus</i>)	Caldesmon	KSPA K TPVK (T absent in full-length protein)	49.6
KRAASPRKS	P02256 (<i>Parechinus angulosus</i>)	Histone H1, gonadal	Worm protein, no mammalian ortholog found	47.6
KRFGSKAHM	P29476 (<i>Rattus norvegicus</i>)	Nitric oxide synthase, brain	No, only other residues in full-length protein	47.4
SKDSSKRGR	P27573 (<i>Mus musculus</i>)	Myelin protein P0	SKDSS K GRGR	46.3
KRPSLRAKA	P02687 (<i>Bos Taurus</i>)	Myelin basic protein	KRPS L RAKA	44.1
KKLGSKKPQ	P04775 (<i>Rattus Norvegicus</i>)	Sodium channel protein type 2 subunit alpha	No, only other residues in full-length protein	43.3
SPRKSPKKS	P02256 (<i>Parechinus angulosus</i>)	Histone H1, gonadal	Worm protein, no mammalian ortholog found	42.8
RKQITVR	P11217 (<i>Homo sapiens</i>)	Glycogen phosphorylase, muscle form	T absent in full-length protein	42.8
GKSSSYSKQ	P02671 (<i>Homo sapiens</i>)	Fibrinogen alpha chain	No, only other residues in full-length protein	42.4
AKGGTVKAA	P08132 (<i>Sus scrofa</i>)	Annexin A4	No, only other residues in full-length protein	41.7
KAKVTGRWK	P13789 (<i>Bos taurus</i>)	Troponin T, cardiac muscle isoform	KAKV T GRWK	41.4

DSRSSLRK	P08183 (<i>Homo sapiens</i>)	Multidrug resistance protein 1	DSRSSLRK	41.4
KRPSKRAKA	P02687 (<i>Bos Taurus</i>)	Myelin basic protein	KRPSKRAKA	39.7
KRPSDRAKA	P02687 (<i>Bos Taurus</i>)	Myelin basic protein	KRPSDRAKA	38.9
KRPSFRAKA	P02687 (<i>Bos Taurus</i>)	Myelin basic protein	KRPSFRAKA	38.5
KSFGSPNRI	P20911 (<i>Xenopus laevis</i>)	Cyclin-dependent kinase 7	KSFGSPNRI (H/R/M)	37.8
KRPSARAKA	P02687 (<i>Bos Taurus</i>)	Myelin basic protein	KRPSARAKA	35.3
LTRRASFSQA	P07248 (<i>Saccharomyces cerevisiae</i>)	Regulatory protein ADR1	Yeast protein, no mammalian ortholog found	35.2
SLRASTSKS	P08227 (<i>Mus musculus</i>)	40S ribosomal protein S6	SLRASTSKS	34.9
KRKQISVRG	P11217 (<i>Homo sapiens</i>)	Glycogen phosphorylase, muscle form	KRKQISVRG	34.4
KRPSQRAKA	P02687 (<i>Bos taurus</i>)	Myelin basic protein	KRPSQRAKA	34.2
PRKGSPRKG	P06146 (<i>Lytechinus pictus</i>)	Histone H2B.2, sperm	No, only other residues in full-length protein (H)	34.1
TKKQSFQKT	P13569 (<i>Homo sapiens</i>)	Cystic fibrosis transmembrane conductance regulator	TKKQSFQKT	33.2
ARKSTRRSI	P08567 (<i>Homo sapiens</i>)	Pleckstrin	ARKSTRRSI	32.0

* bold and underlined residues indicate which Ser, Thr and/or Tyr residues are annotated as *in vivo* phosphorylation sites (www.phosphosite.eu). When the protein of the indicated organism was not found but an ortholog was present in the database this is indicated. Also, when no orthologs were found in the phosphosite database, this is indicated. H, *Homo sapiens*; R, *Rattus norvegicus*; M, *Mus musculus*; x, not listed.

* represents the average signal of two duplicate spots on the Lats2 CD WT array normalized to the highest average value (set at 100).

Chapter 3

Phosphorylation of Myosin Regulatory Light Chain by a cytosolic isoform of Dystrophia Myotonica Protein Kinase (DMPK)

Lieke Gerrits, René E.M.A. van Herpen, Susan A.M. Mulders, Remco van Horssen, Ronny C. Derks, Wiljan J.A.J. Hendriks, Bé Wieringa, Derick G. Wansink

Department of cell biology, Nijmegen Centre for Molecular Life Sciences, Radboud University Nijmegen Medical Centre, Nijmegen, The Netherlands.

[illegible]

SUMMARY

Proper functioning of the mitotic spindle and cleavage furrow machinery is essential for successful completion of cell division. Regulation of myosin II motor activity via phosphorylation of its regulatory light chain subunit (MLC2) is actively involved in this process. We show here that the cytosolic dystrophin myotonia protein kinase (DMPK) isoform E - but not membrane-bound isoforms - can phosphorylate MLC2 at multiple sites. Monophosphorylated MLC2 concentrates at the contractile ring during telophase and cytokinesis. Diphosphorylated MLC2 localizes predominantly at centrosomes, the microtubule organizing centers that direct formation of the mitotic spindle. Forced expression of DMPK E results in mitotic spindle defects, multinucleation and cell death. We propose that MLC2 hyperphosphorylation as a result of DMPK activity hampers the cell's ability to faithfully pass through M-phase, presumably by disturbing the *modus operandi* of centrosomes during cytokinesis.

Phosphorylation of Myosin Regulatory Light Chain by a Cytosolic Isoform of Dystrophin Myotonia Protein Kinase

3

Actomyosin sliding is an important aspect of cytoskeletal dynamics and involved in a wide variety of cellular processes that require movement and shape changes (Vicente-Manzanares *et al.*, 2009) in interphase and during cell division (De Lozanne and Spudich, 1987; Mabuchi and Okuno, 1977). Cell division encompasses nuclear division (mitosis) and cytoplasmic division (cytokinesis), which together define the M-phase of the cell cycle. During cytokinesis actin network dynamics and myosin II motor activity are mechanistically combined to generate the force that drives constriction of the contractile actomyosin ring, thus forming the cleavage furrow (Glotzer, 2005). Assembly of the ring starts at late anaphase and furrow ingression proceeds until spindle microtubules are compacted into a structure called the cytoplasmic bridge. The last step of cytokinesis, called abscission, results in the actual formation of two daughter cells. Mechanisms underlying abscission are not understood in much detail, but membrane trafficking events and directed movement of centrosomes are known to play a role (Montagnac *et al.*, 2008; Piel *et al.*, 2001). Besides being important for constriction of the contractile ring, myosin II filaments are involved in positioning of centrosomes and in chromosome separation (Fabian and Forer, 2007; Komatsu *et al.*, 2000; Rosenblatt *et al.*, 2004; Snyder *et al.*, 2010).

Myosin II filaments are formed by multimerization of hexameric myosin II complexes. One complex is composed of two copies each of MLC2 (myosin regulatory light chain), MLC1 (myosin essential light chain) and MHCII (myosin heavy chain II). Different myosin II isoforms exist. Activity of non-sarcomeric (nonmuscle and smooth muscle) myosin II forms is regulated through phosphorylation of the MLC2 subunits on serine 19 followed by phosphorylation of threonine 18 (Ikebe and Hartshorne, 1985; Ikebe *et al.*, 1986).

There is now evidence that these phosphorylation events are timed in a cell-cycle dependent manner (Komatsu *et al.*, 2000; Matsumura *et al.*, 2001). At the entry of mitosis the degree of phosphorylation of Thr18/Ser19 residues of MLC2 is relatively low, but levels greatly increase as cells enter cytokinesis (Yamakita *et al.*, 1994). Expression of non-phosphorylatable MLC2 mutants in mammalian and *Drosophila* cells induces failure of cytokinesis (Jordan and Karess, 1997; Komatsu *et al.*, 2000). In cancer cells, cytokinesis failure was found to be associated with reduced phosphorylation levels of MLC2, while expression of a phosphomimetic mutant of MLC2 rescued this phenotype (Wu *et al.*, 2010). Thus, MLC2 phosphorylation needs tight control and is crucial for successful completion of cell division.

Among the kinases that are able to phosphorylate MLC2 on Thr18/Ser19 (Matsumura, 2005) are several members of the DMPK (dystrophia myotonica protein kinase) family of the AGC group of kinases (Leung *et al.*, 1998; Riento and Ridley,

2003; Yamashiro *et al.*, 2003). This family comprises ROCK -I and -II, CRIK, MRCK- α , - β , and - γ and DMPK itself (Manning *et al.*, 2002). DMPK exists as six different isoforms which result from alternative splicing (Groenen *et al.*, 2000). The most important difference between these isoforms is the nature of the C-terminus, which determines the cellular localization of the kinases. Isoforms with a long C-terminal tail are membrane-bound, while isoforms lacking such tail region distribute throughout the cytosol, notably splice form DMPK E (Wansink *et al.*, 2003). Several DMPK family members are regulated by small GTPases of the Rho family, proteins with a known role in actomyosin remodeling (Di Cunto *et al.*, 1998; Jin *et al.*, 2000; Leung *et al.*, 1998; Riento and Ridley, 2003; Shimizu *et al.*, 2000). Reports on the importance of ROCKs (Riento and Ridley, 2003) and CRIK (Di Cunto *et al.*, 1998; Madaule *et al.*, 2000) in cell division have been issued, but whether the archetypical member of the family - DMPK itself - is engaged in cell division is still uncertain.

Here, we describe that expression of the cytosolic DMPK isoform, but none of the membrane-bound forms, induces formation of aberrant mitotic spindles, cytokinesis errors and multinucleation. We demonstrate that DMPK E is capable of phosphorylating MLC2 directly and provide evidence that diphosphorylated MLC2 colocalizes with centrosomes from prophase until cytokinesis and with the contractile ring during telophase and cytokinesis. We propose that cytosolic DMPK activity influences cell division directly through MLC2 phosphorylation and that hyperphosphorylation perturbs centrosome and contractile ring functioning.

Cell culture, transfection, and transduction

HeLa, COS-1 and neuroblastoma cells were cultured in DMEM (Gibco/Invitrogen; Carlsbad, CA) containing 10% (v/v) FCS, 2.5 mM pyruvate and 1 mM glutamine at 37°C in 7.5% CO₂. DMPK^{-/-} myoblasts were cultured as described (Mulders *et al.*, 2011). Adenoviral expression of N-terminally YFP-tagged DMPK isoforms or the enzymatically inactive (kinase dead; kd) mutant was performed as described (van Herpen *et al.*, 2005). Expression of C-terminally YFP-tagged MLC2 fusion proteins and N-terminally GST-tagged DMPK E proteins was achieved via DEAE-dextran transfection (van Ham *et al.*, 2003). Neuroblastoma cells were transfected using Lipofectamine (Invitrogen) according to the manufacturer's instructions.

Cell synchronization

HeLa cells were synchronized by applying a double thymidine block (Knehr *et al.*, 1995). In short, 200,000 cells were seeded in a 60 mm culture dish in which two glass coverslips were placed for later use in an immunofluorescence assay. After 24 hrs, 2 mM thymidine was added to the medium to arrest cells in S-phase. At ~48 hrs, cells were released by provision of regular medium and cultivated for another 12 hrs. Next, a second thymidine block of 14 hrs was applied. Viral transduction was started 3 hrs before the second thymidine block ended. The second release phase started by replacing the virus-containing medium with regular medium and cultivation was continued for 10, 12 or 14 hrs. At those time points, cells on coverslips were fixed and cells in the dish were used for TCA precipitation. A schematic overview of the protocol is depicted in Fig. 3A.

Expression plasmids

Expression construct pEBG-DMPK E, encoding N-terminally GST-tagged DMPK E was constructed by cloning a DMPK E-encoding *Bgl*III fragment (Groenen *et al.*, 2000) in frame into *Bam*HI-digested pEBG vector (Tanaka *et al.*, 1995). The inactive version, pEBG-DMPK E kd, was constructed in a similar manner (Wansink *et al.*, 2003).

Expression construct pEYFP-N1-ΔATG-MLC2-h/m-nm, encoding human/mouse nonmuscle MLC2 with a C-terminal YFP-tag, has been described (Gerrits *et al.*, 2012b). This plasmid was used as template in the QuikChange® Site Directed Mutagenesis Kit (Agilent Technologies, Santa Clara, CA) according to the manufacturer's instructions to generate MLC2 mutants. Primers used are listed in Table S1. Expression constructs generated by PCR were verified by DNA sequence analysis to exclude undesired mutations.

Immunofluorescence microscopy and image analysis

Cells on coverslips were washed once with PBS and fixed for 20 min at room temperature in 4% (w/v) formaldehyde in 0.1 M phosphate buffer (pH 7.4) containing 0.5% (w/v) Triton X-100. Cells were then washed three times in PBS. Free aldehyde groups were blocked by incubation in 0.1 M glycine in PBS for 15 min. Aspecific antibody binding was inhibited through incubation in blocking buffer (10% (v/v) normal goat serum in TBS (10 mM Tris-HCl, pH 8.0, 150 mM NaCl)). Cells were incubated with primary antibody for 1 hr at room temperature and then washed in TBS-Tx (0.05% (w/v) Triton X-100 in TBS) followed by incubation with the appropriate Alexa-Fluor-tagged secondary antibody (Molecular Probes/Invitrogen, 1:500) for 1 hr at room temperature. Subsequently, cells were washed three times in TBS-Tx, once in MilliQ, and once in methanol. Coverslips were air-dried and mounted in Mowiol supplemented with DAPI (0.6 μ g/ml) to visualize DNA. The mitotic spindle was detected with a monoclonal antibody against β -tubulin (E7; Developmental Studies Hybridoma Bank, University of Iowa; 1:5). Other primary antibodies used for immunofluorescence were monoclonal anti-phospho-MLC2-Ser19 (3675; Cell Signaling Technology, Danvers, MA; 1:50), polyclonal anti-phospho-MLC2-Thr18/Ser19 (3674; Cell Signaling Technology; 1:50) and monoclonal anti- γ -tubulin (Clone GTU-88; Sigma-Aldrich; St. Louis, MO). All primary and secondary antibodies were diluted in blocking buffer. Immunofluorescence with anti-NuMA antibody 1H1 was performed as described (Compton *et al.*, 1991).

Images were obtained using a Zeiss Axiophot2 fluorescence microscope with an Axiocam MRm CCD camera and Axio Vision 3.1 software (Zeiss, Thornwood, NY). DMPK-positive cells were identified by their YFP staining. Confocal images of aberrant mitotic spindles were obtained using an Olympus FV1000 (Olympus, Tokyo, Japan) or a Zeiss LSM510 metaConfocal Laser Scanning Microscope (Zeiss).

To analyze cell division failure of *DMPK*^{-/-} myoblasts, time lapse microscopy was performed for 24 hrs in a microscope stage incubator (Oko-Lab; Ottaviano, Italy) on a Nikon DiaPhot microscope (Nikon; Melville NY) equipped with a Hamamatsu C8484-05G digital camera (Hamamatsu, Hamamatsu City, Japan). Imaging was started 4 hrs after adenoviral transduction and pictures were taken every 10 min using Time Lapse Software (Oko-Lab), version 2.7, with a 10x objective. Movies were constructed from image sequences using ImageJ software. Each division event was scored in one of the five categories defined in Fig. 2C. For every DMPK isoform, at least one hundred mitotic events were analyzed in two independent experiments. Time point zero was defined as the start of rounding up for mitosis.

GST pull-down and immunoprecipitation

Pull-down of GST or GST-DMPK fusion proteins was performed by incubating

Glutathione-Sepharose 4B beads with cleared lysates of COS-1 cells expressing GST-tagged proteins. To this end, cells were washed once with ice-cold PBS and lysed with ice-cold lysis buffer (50 mM Tris-HCl, pH 7.5, 150 mM NaCl, 1% (w/v) NP-40, 25 mM NaF, 1 mM sodium pyrophosphate, 0.1 mM NaVO_3 , 2 μM microcystin LR (Alexis Biochemicals/Enzo Life Sciences, Farmingdale, NY), 1 mM PMSF and protease inhibitor cocktail (Roche, Basel, Switzerland)) 1-2 days after transfection. Cell debris was pelleted by centrifugation for 30 min at 15,000 rpm. Beads and cleared lysates were incubated by overnight rotation at 4°C. Subsequently, beads were washed five times with PBS containing 1% (w/v) NP-40 before eluting proteins with 10 mM reduced glutathione in 50 mM Tris-HCl (pH 8.0). Eluates were diluted 1:1 with kinase storage buffer (50% glycerol, 1 mM DTT, 1 mM EDTA, 0.2 mg/ml BSA) and stored at -80°C after snap freezing in liquid N_2 .

To immunoprecipitate YFP or YFP-tagged MLC2 proteins from COS-1 cells, cell-free extracts were prepared in lysis buffer as described above. GFP antibodies (Cuppen *et al.*, 2000) were coupled to protein A beads by overnight rotation at 4°C in PBS and then incubated with cleared lysates. Bead-coupled YFP or YFP-MLC2 fusion proteins were subsequently prepared for use in an *in vitro* kinase assay.

***In vitro* kinase assay**

In vitro kinase assays were performed as described (Wansink *et al.*, 2003). Briefly, immunoprecipitation reactions were washed once with lysis buffer containing 0.5 M NaCl, once in lysis buffer and once in 50 mM Tris-HCl, pH 7.5, 1 mM DTT, 1 mM PMSF, 1 mM benzamidine. Beads were divided over the desired number of kinase reactions. After the last washing step, beads were taken up in 20 μl 2x kinase assay buffer (100 mM Tris-HCl, pH 7.5, 20 mM MgCl_2 , 4 mM MnCl_2 , 2 mM DTT, 2 μM PKA inhibitor peptide (Bachem, Bubendorf, Switzerland), 2 μM PMSF, 2 μM benzamidine, 4 μM Microcystin LR) and either 500 ng GST-kinase or GST alone was added to the substrate in a total volume of 40 μl . Reactions were started by adding 5 μl 0.5 mM γ - ^{32}P -ATP and continued for 20 min at 30°C. Reactions were stopped by the addition of 5x SDS-PAGE sample buffer (2.5 M DTT, 25% glycerol, 150 mM Tris, pH 6.8, 5% (w/v) SDS) and boiling for 5 min before separation on SDS-PAGE followed by Western blotting.

Urea/glycerol polyacrylamide gel electrophoresis and Western blotting

Urea/glycerol PAGE was performed essentially as described (Mulders *et al.*, 2011). Membranes were blocked in 5% (w/v) milk powder in TBS-T (10 mM Tris-HCl, pH 8.0, 150 mM NaCl, 0.05% Tween-20 (Sigma-Aldrich)) 30-60 min prior to incubation with primary antibodies. MLC2 antibody K19 (Mulders *et al.*, 2011) was diluted 1:5,000 in blocking buffer and incubated overnight at 4°C. Membranes were washed three times

with TBS-T and then incubated with secondary antibody goat anti-rabbit IRDye®800; (LI-COR Biosciences, Lincoln, NE, 1:10,000) for 1 hr at room temperature, followed by two TBS-T washes and one TBS wash. Detection of immunoreactive bands was done on an Odyssey infrared Imaging System (LI-COR Biosciences).

SDS-PAGE and Western blotting

Kinase assay products were run on 15% SDS-PAGE gels and transferred to PVDF membrane for immunodetection. Membranes were blocked as described for membranes generated with urea/glycerol polyacrylamide gel electrophoresis. Immunodetection of GST and GST-DMPK E fusion proteins was done with a polyclonal GST antiserum (Cuppen *et al.*, 2000). YFP and YFP-MLC2 fusion proteins were detected on blot with a GFP monoclonal antibody (sc-9996; Santa Cruz Biotechnology, Santa Cruz, CA; 1:5,000).

Statistics

Bars represent mean values \pm SEM. For comparison of the percentage of normal cell divisions after expression of different DMPK isoforms a two-tailed unpaired t-test was performed. The percentages of aberrant spindles in cell cultures expressing different DMPK isoforms were also analyzed with a two-tailed unpaired t-test. Differences in MLC2 phosphorylation were analyzed by a Chi-square test. Differences were considered significant when $p < 0.05$ (*: $p < 0.05$; **: $p < 0.01$; ***: $p < 0.001$; n.s.: not significant). Statistical analyses were performed with GraphPad Prism 4 software.

DMPK E induces multinucleation

In our studies on the subcellular localization and effects of catalytically active DMPK isoforms (Wansink *et al.*, 2003), we noticed that transient expression of cytosolic isoform E in transfected cells induced multinucleation. The most pronounced effect was observed in *DMPK*^{-/-} myoblasts, which lack DMPK proteins and therefore represent a good cell model to examine function of distinct DMPK isoforms (Oude Ophuis *et al.*, 2009b). At least 60% of DMPK E-expressing myoblasts displayed a multinuclear appearance 24 hrs after adenoviral transduction (Fig. 1A-B). In contrast, less than 10% of DMPK-positive cells appeared multinucleated upon expression of membrane-bound isoforms (DMPK A or C, Fig. 1A, C-D). These data clearly indicate that subcellular localization of the DMPK protein is an important factor in inducing M-phase abnormalities.

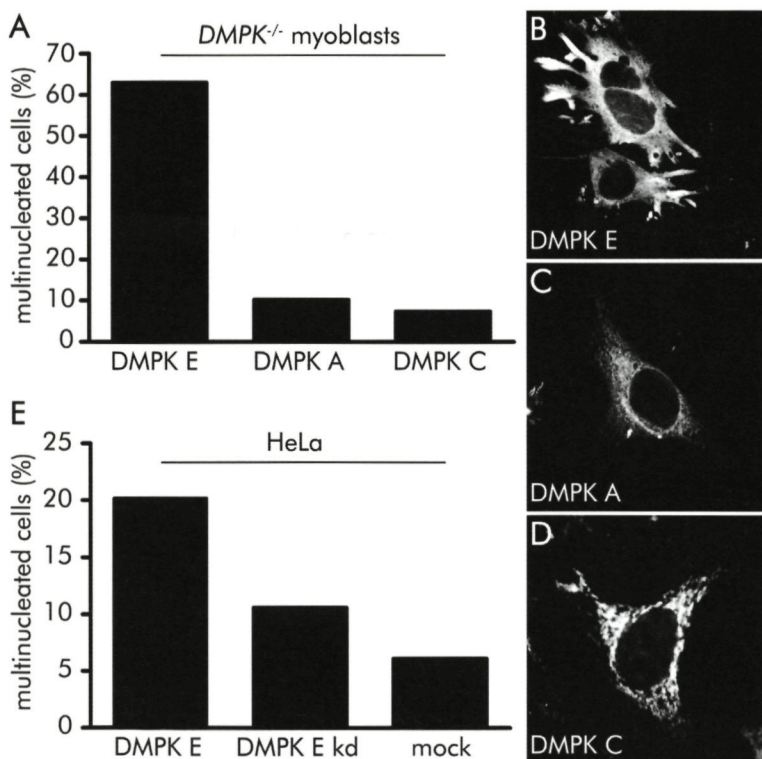


Figure 1: DMPK E induces formation of multinucleated cells. (A) *DMPK*^{-/-} myoblasts were transduced with DMPK E, A or C via adenoviral gene transfer and fixed 24 hrs after infection. In *DMPK*^{-/-} myoblasts transfected with DMPK E the percentage of multinucleated cells was ~60%, whereas this percentage was less than 10% in cells transduced with either DMPK A or C. At least

200 YFP-positive cells were counted per isoform. **(B-D)** Confocal images of DMPK^{-/-} myoblasts expressing N-terminally YFP-tagged DMPK E, A, or C. DMPK E displayed a cytosolic localization **(B)**, DMPK A localized to the ER **(C)**, and DMPK C showed a mitochondrial localization **(D)**. **(E)** HeLa cells were transduced with DMPK E or its catalytically inactive mutant form (DMPK E kd) via adenoviral gene transfer and fixed 24 hrs after infection. ~20% of HeLa cells that expressed DMPK E had a multinuclear phenotype, whereas this percentage was ~10% in cells that expressed DMPK E kd. At least 250 YFP-positive cells were counted per condition.

The multinucleation effect could be reproduced in other cell types as well. In neuroblastoma cells, almost 30% of DMPK E-expressing cells were multinucleated versus less than 10% in DMPK A/C-expressing cells (Fig. S1A). FACS analysis to quantify DNA content confirmed that the amount of tetraploid cells was 1.6-fold higher in the DMPK E-transfected population (Fig. S1B). Furthermore, the amount of aneuploid (>4N) cells was strongly increased.

DMPK E-induced multinucleation was also observed in HeLa cells (Fig. 1E). In HeLa cells that expressed an enzymatically inactive (kinase dead; kd) DMPK E mutant, multinucleation was observed to a much lower extent, pointing to a requirement of kinase activity. Occurrence of multinucleation also seemed to be rather independent of cellular DMPK E concentration, since it was observed in cells with high as well as in cells with low DMPK E expression levels (data not shown).

Expression of catalytically active DMPK E affects proper completion of mitosis

To obtain more insight into how multinucleated cells developed as a result of DMPK E expression, time lapse microscopy was performed. DMPK^{-/-} myoblasts were transduced with adenoviruses encoding either DMPK isoform E, E kd, or C and were monitored for 24 hrs, starting 4 hrs after virus addition (Fig. 2A-B, Fig. S2 and Movies). Following rounding up of the cells during pro/metaphase we observed, next to the normal process of cell division (route I, Movie I), two different routes leading to formation of multinucleated cells. One route (incomplete furrow ingression or abscission failure, IIa; Normand and King, 2010) is illustrated in Movie IIa_1; the other (absence of furrow ingression, IIb; Normand and King, 2010) in Movie IIb. Note the divergent time scales between route I and routes IIa and b (Fig. 2B, Fig. S2).

Cytokinesis defects can occur during any of the four subphases of cytokinesis, i.e., during specification of the cleavage plane, cleavage furrow ingression, midbody formation or abscission (Normand and King, 2010). We studied many aberrant events in detail and found that in cells that followed route IIa cytokinesis usually failed before a clear intercellular bridge was formed (Movie IIa_1), but occasionally this occurred even after formation of a very thin cytoplasmic bridge (Fig. 2B, panel IIa_2; Fig. S2; Movie IIa_2).

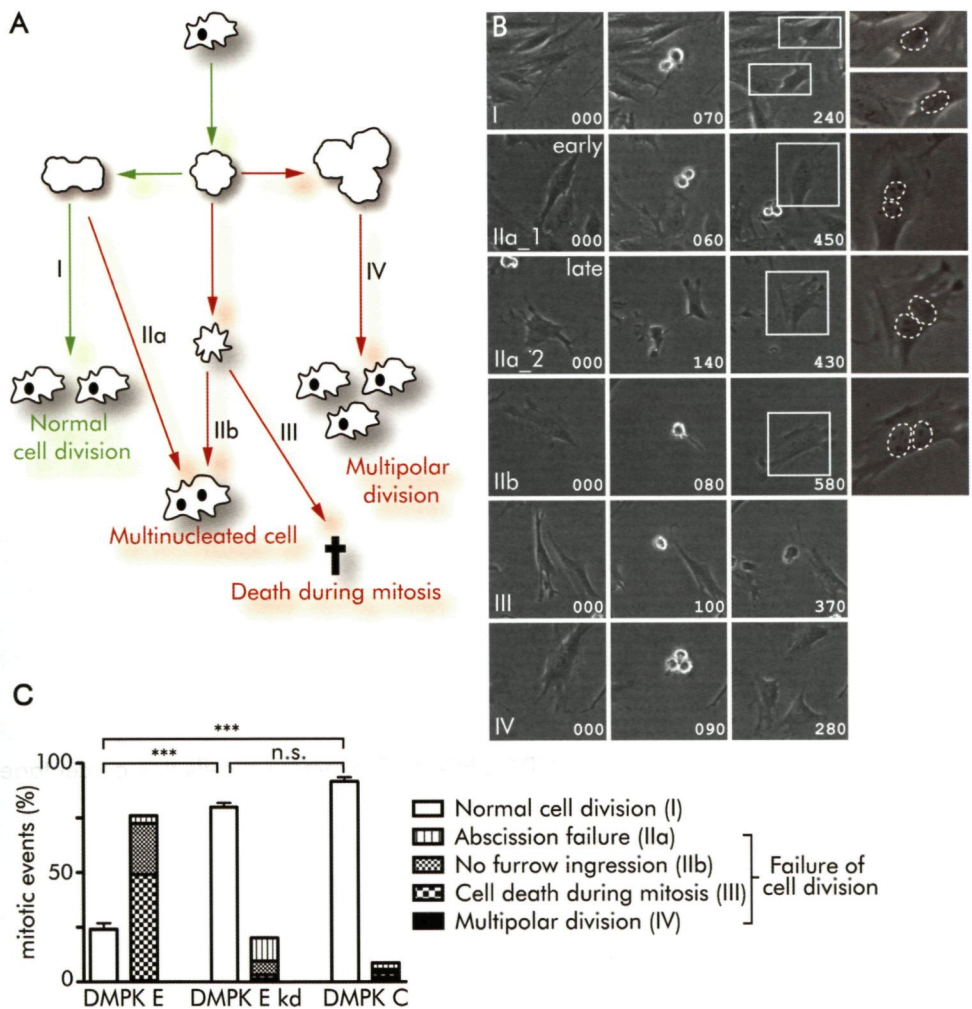


Figure 2: DMPK E expression leads to defects in cell division. DMPK^{-/-} myoblasts were transduced with DMPK E, E kd, or C and mitotic events were monitored by live cell microscopy. **(A)** Schematic picture of cell division and possible fates of DMPK E-expressing cells that entered M-phase. Cells that divided normally gave rise to two mononucleated daughter cells (route I). Four types of abnormal cell division events were observed: generation of multinucleated cells via abscission failure (IIa), absence of furrow ingression (IIb), entry in mitosis shortly followed by cell death (route III) and multipolar cell division resulting in the generation of at least three daughter cells (IV). **(B)** Stills from movies illustrating typical outcomes shown in **(A)** for dividing DMPK E-expressing myoblasts. White rectangles illustrate position of magnification in next panel. Positions of nuclei are indicated by dashed circles. Roman numerals refer to scenarios depicted

in (A). Arabic numerals indicate time in min since start of mitosis (rounding up of cells). More stills from these movies are depicted in Fig. S2 and movies can be viewed as supplementary data. (C) White bars represent the percentage of M-phase events that proceeded normally. Filled bars represent the percentage of failure of cell division. Every filled bar is composed of four categories as indicated.

Other abnormal M-phase events in DMPK E expressing cells involved mitotic entry culminating in cell death (route III, Movie III) and multipolar mitosis resulting in the formation of three or more daughter cells (route IV, Movie IV). Cells that followed route III could be easily distinguished from regular apoptotic cells (Movie V). Rounding up went fast, but the whole process took much longer to complete than regular apoptosis (compare Figs. S2 and S3, and Movies III and V). Importantly, the percentage of cells undergoing a mitotic event was equal for all DMPK isoform constructs examined (data not shown). This supports the conclusion that cells along route III indeed died during mitosis - presumably around metaphase - and not as a result of apoptosis during another phase of the cell cycle.

To compare effects of individual isoforms, we did a quantitative analysis and scored all mitotic events in YFP-DMPK positive myoblast cells as either normal or as failure of cell division (Fig. 2C). In DMPK E-expressing cells only about 25% of all cell divisions was normal, whereas in DMPK E kd- or C-expressing cells this percentage was 80-90% ($p < 0.001$). Seventy percent of dividing cells expressing DMPK E involved the ruffled intermediate cell type (routes IIb+ III), some of which reattached to the substratum and spread as binuclear cells without undergoing noticeable furrow ingression (route IIb; 22% of all mitotic events). In DMPK E kd- or C-expressing cells this percentage was much lower (8% and 4%, respectively). Mitotic cells in a ruffled intermediary stage that did not reattach to the substratum, died (route III). In case of DMPK E expression this accounted for ~50% of all mitotic events, whereas in the case of DMPK E kd or C expression this was only ~2%. Multipolar cell divisions were rarely observed, under all conditions (1-2% of all mitotic events), as has been described for many cell lines (Ganem *et al.*, 2009).

Taken together, our observations suggest that DMPK E activity perturbs cell division, mainly via inhibition or collapse of the cytokinetic process. Ultimately this leads to a multinucleated phenotype or cell death.

DMPK E-expressing cells display mitotic spindle abnormalities

To complete our picture of possible morphological abnormalities associated with DMPK E expression, we analyzed mitotic spindle morphology using fluorescence confocal microscopy on fixed HeLa cells that were transduced with YFP-DMPK E, E kd or C.

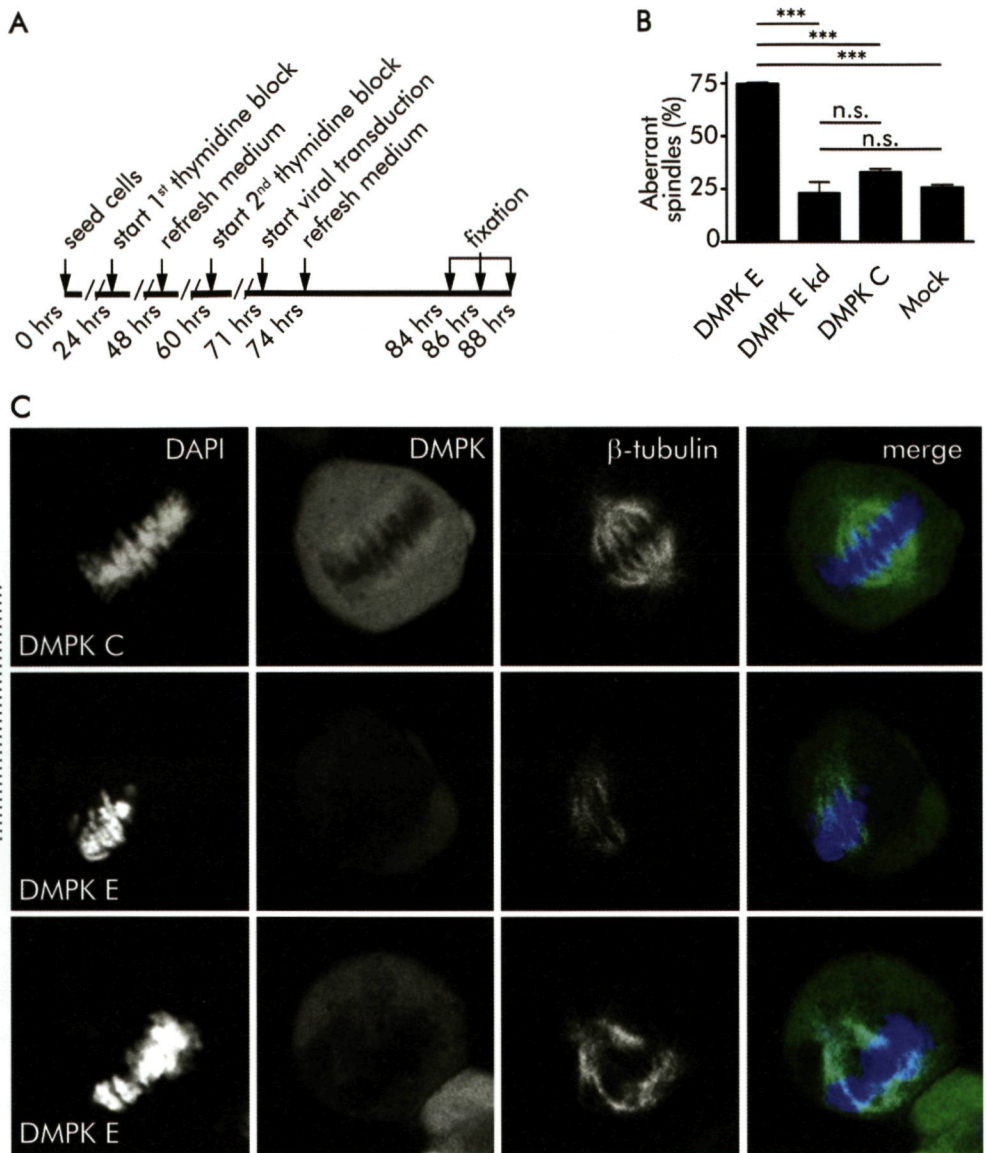


Figure 3: DMPK E induces mitotic spindle aberrancies. (A) Synchronization and transduction protocol. HeLa cells were subjected to a double thymidine block followed by release. Viral transduction was performed 3 hrs before the second release and cells were fixed 10, 12 or 14 hrs after the second release to be sure to capture cells in all different phases of mitosis. (B, C) Mitotic spindles were stained with an antibody against β -tubulin. DNA was stained with DAPI. Every mitotic spindle was scored as normal or aberrant. The percentage aberrant spindles is depicted in graph (B). In cultures overexpressing DMPK E the

percentage of mitotic cells with a defective spindle was three times higher than in DMPK E kd- or C-expressing cultures. (C) Typical examples of a normal spindle (top panels; DMPK C expression) and mitotic spindle defects (bottom two series, DMPK E expression) are shown.

To enrich for mitotic cells, HeLa cells were synchronized in mitosis using a double thymidine block followed by a release for 10, 12 or 14 hrs (Fig. 3A). HeLa cells were chosen because they are commonly used for cell cycle studies. Synchronization protocols to obtain a mitotically enriched HeLa cell population are well established (Knehr *et al.*, 1995). Simultaneous β -tubulin and DNA staining revealed that up to 75% of all mitotic DMPK E-transduced cells showed spindle defects (Fig. 3B), ranging from skewed to disintegrated or distorted spindles (Fig. 3C). In mock-treated cells or cells transduced with DMPK E kd/C only ~25% of all mitotic cells contained an atypical spindle structure ($p < 0.001$). These observations suggest that occurrence of mitotic cell death and collapse of cytokinesis may be related to aberrant spindle formation.

DMPK E can phosphorylate MLC2 *in vivo*

The actomyosin cytoskeleton is strongly involved in cleavage furrow ingression and a function for myosin II in spindle formation is supported by experimental evidence (Komatsu *et al.*, 2000; Mabuchi and Okuno, 1977). Based on this knowledge and on own published findings (Mulders *et al.*, 2011), we hypothesized that maintenance of the diphosphorylated state of MLC2 by sustained activity of DMPK E might contribute to the aberrant cell division phenomena.

Lysates of DMPK E-, E kd- or mock-transduced HeLa cells were analyzed for phospho-MLC2 levels to investigate whether DMPK E indeed contributed to MLC2 phosphorylation. We used urea/glycerol-polyacrylamide gel electrophoresis (UG-PAGE) to separate 2P-MLC2 from 1P-MLC2 and unphosphorylated MLC2 (0P-MLC2) (Garcia *et al.*, 1995) (Fig. 4A). The MLC2 signal originated from distinct MLC2 paralogs - nonmuscle (nm), nonmuscle-like (nml) and smooth muscle (sm) MLC2, which differ in only a few amino acids, but all contain phosphoacceptor sites Thr18 and Ser19 (Gerrits *et al.*, 2012b). The complex signal was composed of three doublets, each representing MLC2 isoforms of one specific phosphorylation state (0P: top two bands; 1P: middle two bands; 2P: lower two bands). In mock-transduced HeLa cells, ~50% of MLC2 protein was in the 0P state, while the 1P and 2P forms each made up about 25% of total MLC2. When HeLa cells expressed DMPK E, the MLC2 phosphorylation status changed completely ($p < 0.001$); almost 70% of MLC2 protein was in the 2P state, 20% in the 1P state and only 10% remained unphosphorylated. Surprisingly, even a very rare 3P-MLC2 form appeared (Fig. 4A, band indicated by asterisks), presumably carrying an additional phosphate at Thr9

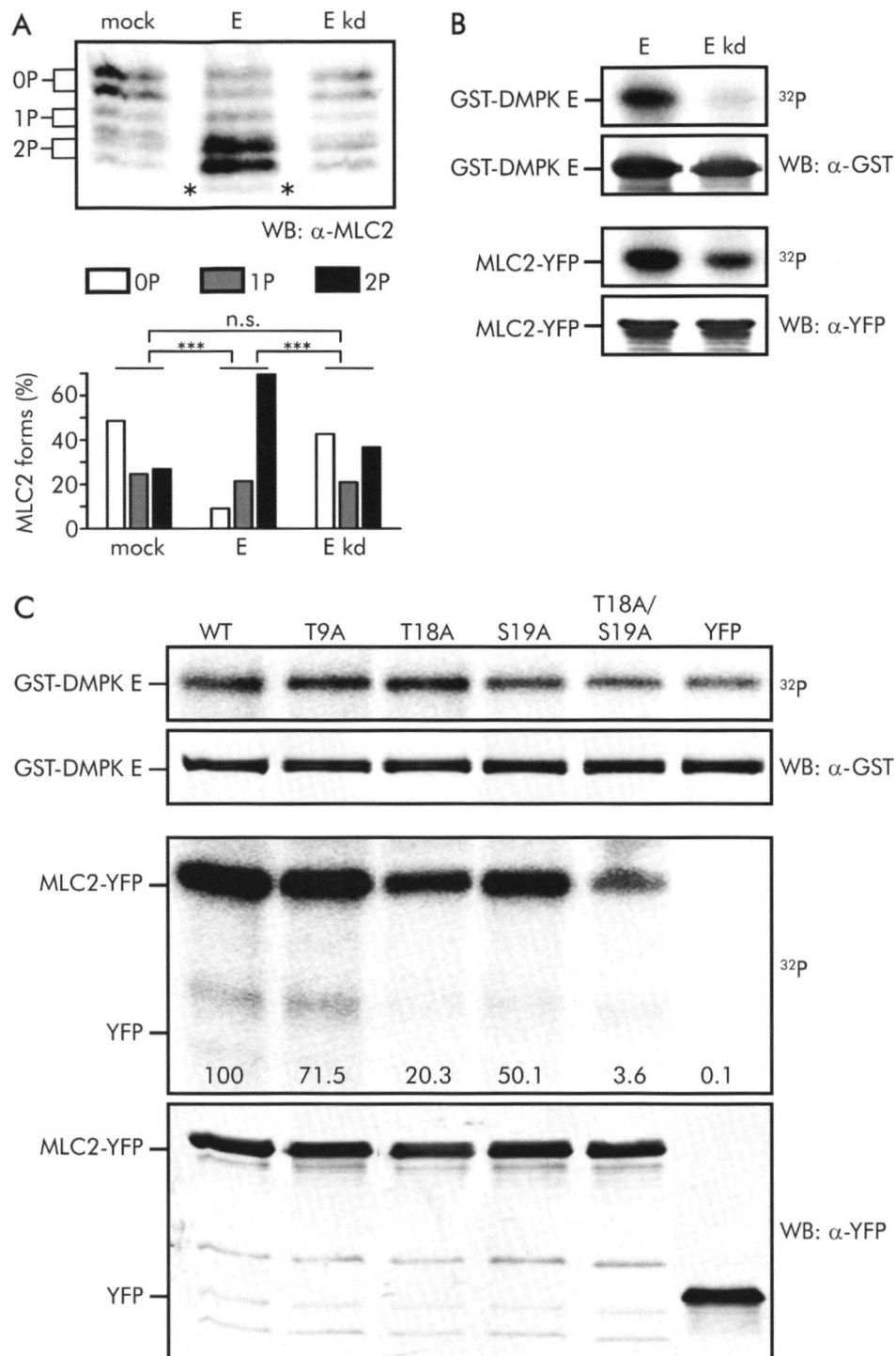


Figure 4: MLC2 is a DMPK E substrate. (A) DMPK E expression results in MLC2 phosphorylation *in vivo*. 0P- (top two bands), 1P- (middle two bands) and 2P-MLC2 (bottom two bands) proteins were separated by urea/glycerol-PAGE and visualized on Western blot using an α -MLC2 antibody (upper panel). Each MLC2 phosphorylation state was quantified as the fraction of total MLC2 protein present in each sample (lower panel). The band between asterisks represents a putative triphosphorylated state of MLC2. (B) MLC2 is an *in vitro* substrate of DMPK E. Purified GST-DMPK E or E kd and MLC2-YFP were combined in an *in vitro* kinase assay. Reaction products were loaded on SDS-PAGE and 32 P-labeled proteins were quantified to determine autophosphorylation activity and phosphorylation of MLC2 (32 P panels). Protein input was verified on Western blot (WB panels). (C) MLC2 phosphomutants were generated in which one or two known phosphorylation sites were mutated. GST-DMPK E was combined with MLC2-YFP proteins in a kinase assay and analyzed as described for (B). 32 P panels illustrate phosphate incorporation in GST-DMPK E (autophosphorylation) or MLC2 proteins. WB panels illustrate protein input. Numerals represent the relative amount of phosphate incorporation compared to WT (set at 100).

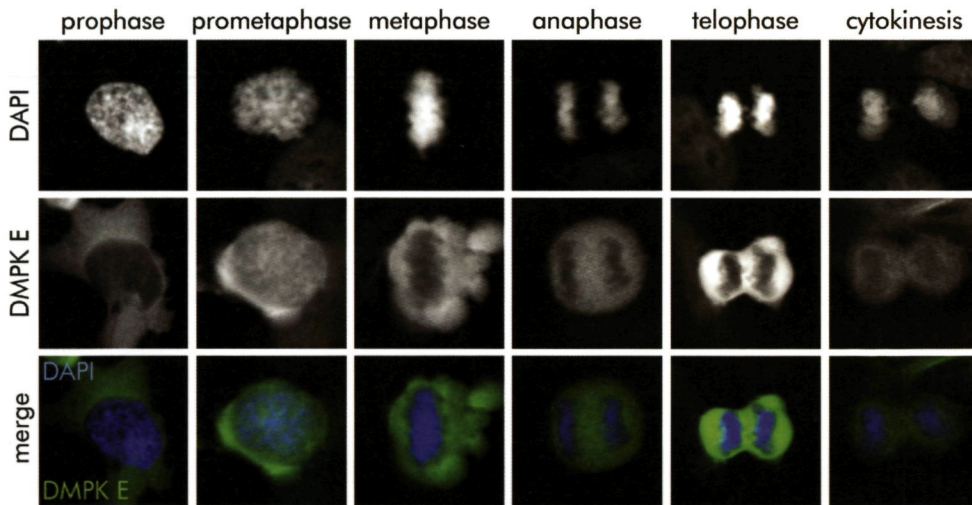


Figure 5: Localization of DMPK E during mitosis. HeLa cells were transduced with YFP-DMPK E, synchronized according to the protocol depicted in Fig. 3A and fixed. DNA was stained with DAPI. DMPK E localized throughout the cytoplasm during all phases of mitosis.

(Obara *et al.*, 2008). No significant change in phospho-MLC2 levels occurred when HeLa cells expressed DMPK E kd ($p=0.34$).

DMPK is known to phosphorylate MYPT1 leading to inhibition of myosin phosphatase activity (Muranyi *et al.*, 2001), which in turn may also contribute to increased MLC2 phosphorylation. To examine whether DMPK E is able to phosphorylate MLC2 directly, an *in vitro* kinase assay was performed using isolated proteins. DMPK E autophosphorylation served as activity control (Wansink *et al.*, 2003) and inclusion of the kinase-dead mutant allowed specificity assessment (Fig.

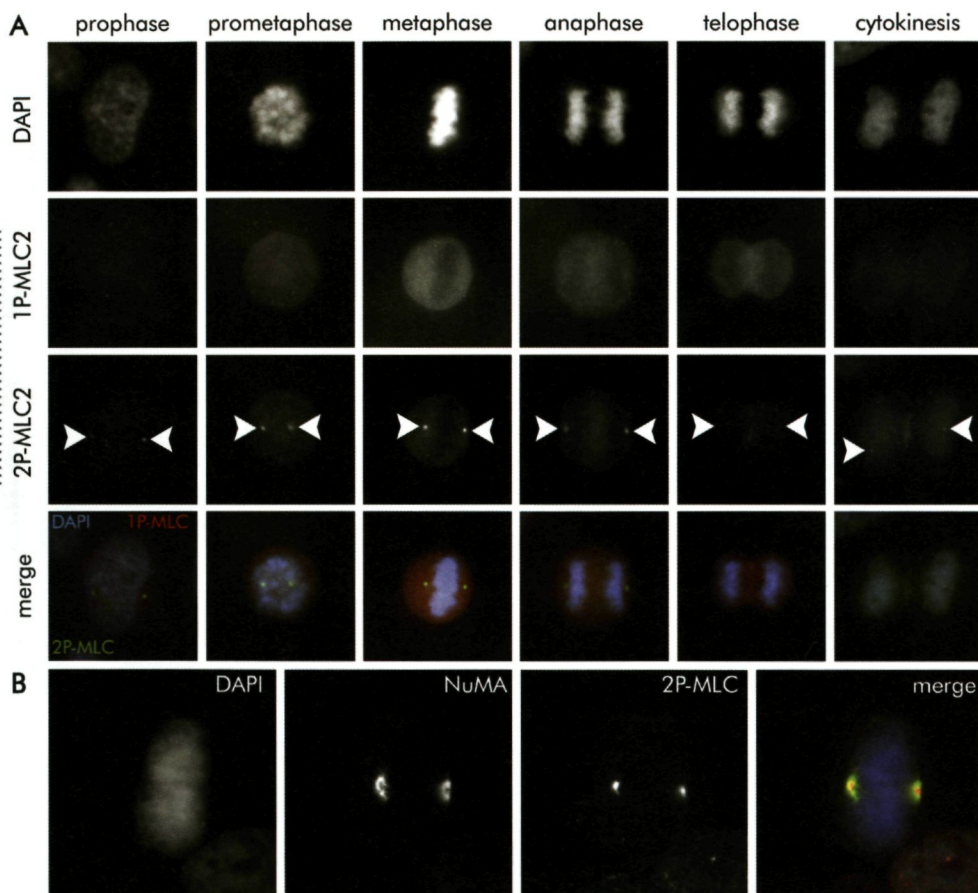


Figure 6: Localization of mono- and diphosphorylated MLC2 during mitosis. (A) HeLa cells were fixed and stained for endogenous 1P- and 2P-MLC2 using phosphorylation-specific MLC2 antibodies. DAPI-stained DNA was used to distinguish different mitotic phases. Centrosomes are indicated by arrowheads. **(B)** HeLa cells were fixed and stained for 2P-MLC2 and NuMA to confirm 2P-MLC2's centrosomal localization. DNA was counterstained with DAPI.

4B, top ^{32}P panel). MLC2 phosphorylation was prominent in presence of DMPK E (Fig. 4B, lower ^{32}P panel). As the kd mutation renders DMPK catalytically completely inactive (Wansink *et al.*, 2003), background phosphate incorporation obtained in presence of DMPK E kd probably resulted from some co-purifying kinase activity. To assess in detail which residues in MLC2 were subject to phosphorylation by DMPK E, YFP-MLC2 point mutants were generated that carried alanine instead of the phosphorylatable serine or threonine residues. YFP protein only was used as a negative control. Phosphorylation level was highest for MLC2-WT and almost similar to that for the T9A mutant (Fig. 4C). Mutation of either Thr18 or Ser19 resulted in a strong decrease in MLC2 phosphorylation, while virtually no phosphate was detected in the T18A/S19A mutant.

Taken together, these data present experimental evidence that DMPK E is able to phosphorylate MLC2 *in vivo* at Thr18 and Ser19, and maybe also Thr9. Forced DMPK E activity during mitosis may thus perturb completion of cell division by hyperphosphorylation of MLC2.

Localization of DMPK E and MLC2 during mitosis

We wondered whether MLC2 hyperphosphorylation and cytokinesis effects could be correlated and explained by the partitioning behavior of MLC2 and DMPK E during mitosis. To this end, the subcellular localization of DMPK E, 1P- and 2P-MLC2 was analyzed in HeLa cells during different stages of M-phase. We found that DMPK E remained diffusely present throughout the entire cell in all stages, including cytokinesis (Fig. 5). Endogenous 1P-MLC2 showed a diffuse cytosolic staining during mitosis, with a mild enrichment at the midzone and contractile ring during telophase (Fig. 6A). A similar cytosolic localization and enrichment at the cleavage furrow was observed for endogenous 2P-MLC2 (Fig. 6A). A highly pronounced 2P-MLC2 signal was detected at two distinct spots, which were identified as centrosomes using NuMA (Gaglio *et al.*, 1995; Whitehead *et al.*, 1996) and γ -tubulin staining (Fig. 6B and Fig. S4, respectively). Centrosomal localization of 2P-MLC2 was observed from early prophase up to cytokinesis. Combined, these data show that phosphorylated MLC2 concentrates at the midzone and contractile ring at late mitosis and cytokinesis and that 2P-MLC2 in particular is enriched at centrosomes from early mitotic stages onwards.

Thus, we demonstrated that DMPK E phosphorylates MLC2 *in vivo* and that forced DMPK E activity leads to formation of aberrant mitotic spindles. Centrosomes are the microtubule organizing centers during mitosis and are involved in proper spindle formation. We therefore decided to investigate 2P-MLC2 localization in mitotic DMPK E-expressing HeLa cells. Indeed, in cells with abnormal mitotic spindle morphology, numerical and structural centrosome abnormalities were obvious (Fig. 7). These findings can be explained by assuming that DMPK E activity can distort

normal control over phospho-MLC2 levels at centrosomes, ultimately resulting in centrosome and spindle abnormalities.

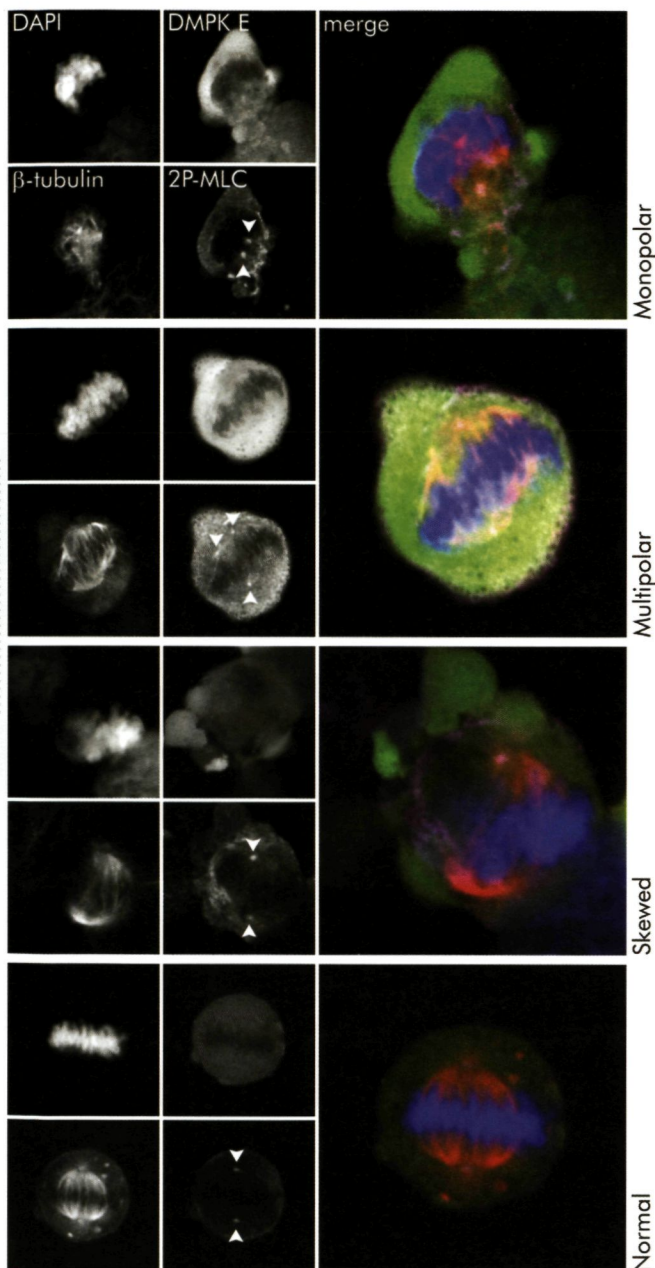


Figure 7: Centrosome abnormalities in DMPK E-expressing cells with aberrant mitotic spindles. HeLa cells were transduced with YFP-DMPK E and synchronized at mitosis (see Fig. 3A). DNA was stained with DAPI. Mitotic spindles were visualized with an antibody against β -tubulin and centrosomes with an antibody against 2P-MLC. Depicted are three categories of mitotic spindle abnormalities: monopolar, multipolar and skewed spindles. In all cases, centrosomes (arrowheads) were mislocalized. For comparison, a normal mitotic spindle is shown in the lower panels.

DISCUSSION

Actin and myosin II filaments are the main components of the contractile ring and their activity plays a key role in completion of M-phase. Centrosome positioning and chromosome separation depend also on myosin II function (Fabian and Forer, 2007; Komatsu *et al.*, 2000; Rosenblatt *et al.*, 2004; Snyder *et al.*, 2010). Diphosphorylation of its MLC2 subunits is required for myosin II activity. In this study, we demonstrate that DMPK E expression contributes to MLC2 diphosphorylation, presumably via direct phosphorylation. Diphosphorylated, but not monophosphorylated MLC2 was found to be enriched at centrosomes during mitosis. Ectopic DMPK E expression led to errors in several aspects of the cell division process, resulting in mitotic spindle defects, multinucleation and cell death.

Multinucleation was observed in multiple cell types, albeit to a different extent. Most likely this reflects variation in cell type-dependent factors important for manifestation of the DMPK E-induced phenotype. Multinucleation was dependent on DMPK localization and kinase activity. For that reason, a recent study describing effects of a DMPK truncation mutant on nuclear envelope integrity is difficult to relate to our findings, as these effects were also seen with an inactive version of the truncated protein (Harmon *et al.*, 2011). In our study, M-phase defects occurred irrespective of DMPK E expression levels, since it was observed in cells with relatively low protein expression too. This finding indicates to us that low DMPK E activity already suffices to induce cell division defects and argues against a mere overexpression effect. The fact that *DMPK*^{-/-} myoblasts divide normally in absence of DMPK E indicates that the DMPK E isoform is not essential for cell division, presumably because many other kinases can phosphorylate MLC2 as well (Matsumura, 2005).

By scoring cell division events as normal or abnormal, we observed three types of abnormal outcomes: cell death during mitosis, multipolar division and generation of multinucleated cells. The last category harbors two types of errors as their outcome is the same: i) cleavage furrow regression in case of two almost separated daughter cells, connected only by a thin intracellular bridge; and ii) absence of any detectable cytokinesis. In *DMPK*^{-/-} myoblasts, we observed by live cell imaging that 50% of all mitotic events resulted in the generation of multinucleated cells, closely matching the percentage of multinucleated cells observed in fixed cell preparations 24 hrs after transduction. Interestingly, in synchronized HeLa cells, anaphases were underrepresented, suggesting that cells that underwent an abnormal mitotic event could not pass the metaphase checkpoint and either were arrested or died.

Abnormal events during mitosis, similar to those observed in our study, have been reported by others. For example, proper metaphase to anaphase transition was disturbed upon expression of a MLC2 T18A/S19A mutant (Komatsu *et al.*, 2000). Cell

death during mitosis is a phenomenon currently known as mitotic catastrophe and can occur when cells prematurely or inappropriately enter mitosis (Vakifahmetoglu *et al.*, 2008). Finally, also chromosome missegregation can cause multinucleation due to furrow regression (Shi and King, 2005).

Several different MLC2 proteins exist, most of which show a cell-type specific expression (Collins, 2006). The nonmuscle isoform was used in the *in vitro* kinase assays. Nm-MLC2 shows a high degree of sequence identity with nml- and sm-MLC2 (Gerrits *et al.*, 2012b). Currently no antibodies exist that can distinguish between these homologous isoforms, but a combination of urea/glycerol-PAGE and immunoblot analysis allowed the discrimination of MLC2 isoforms and phosphorylation levels.

The phosphorylation assay using HeLa cells revealed that DMPK E contributes to phosphorylation of nm-MLC2 and likely also nml- and sm-MLC2 isoforms. *In vitro* kinase assays clearly demonstrated that MLC2 is a direct, *bona fide* DMPK E substrate. The apparent contradiction with literature data stating that MLC2 is not a DMPK substrate, may best be explained by the fact that a different MLC2 (atrial) isoform was used or by lack of activity of bacterially produced DMPK (Bush *et al.*, 2000; Tan *et al.*, 2011; Wansink *et al.*, 2003). The phosphoacceptor sites in atrial MLC2 differ from those in nm/nml/sm-MLC2. Furthermore, it is known that reversible phosphorylation of MLC2a does occur but is not critical for cardiac muscle contractility (Takashima, 2009). Perhaps MLC2 isoforms other than nm/nml/sm are less prone to DMPK E phosphorylation.

Importantly, the nm-MLC2 segment bearing the phosphoacceptor sites (SSKRAKAKTTTKRPQRATSNVF; Thr9, Thr18 and Ser19 underlined) closely resembles the DMPK consensus substrate sequence that was established in earlier studies: threonine/serine residues with a number of positively charged amino acids at the N-terminal side (Bush *et al.*, 2000; Wansink *et al.*, 2003). Our kinase assay with MLC2 phosphorylation mutants revealed that Thr18 is the most important target site for DMPK E. We cannot exclude the possibility, however, that the T18A mutation hampers detection of phosphorylation on other sites by DMPK E (Fig. 4C). Although mainly Thr18 and Ser19 phosphorylation have been studied, our results point to the existence of a triphosphorylated MLC2 species, in line with an earlier report (Obara *et al.*, 2006). There are indications that the third phosphorylation site is Thr9 (Obara *et al.*, 2008), but it may also be Ser1 or Ser2. Phosphorylation of Ser1, Ser2 and Thr9 is thought to inhibit myosin II activity (Ikebe *et al.*, 1987) and would therefore disagree with parallel phosphorylation of activating phosphosites Ser19 and Thr18. Mass spectrometry may shed light on the combinations of phosphorylated residues that actually exist in cells.

It is of note that DMPK E may contribute to increased phospho-MLC2 levels also via inhibitory phosphorylation of MYPT1 (Muranyi *et al.*, 2001; Wansink *et*

al., 2003), the regulatory subunit of myosin phosphatase. For DMPK homologues ROCK and MRCK such a double effect on MLC2 phosphorylation has been described (Amano *et al.*, 1996; Totsukawa *et al.*, 1999; Velasco *et al.*, 2002; Wilkinson *et al.*, 2005).

Analysis of localization of mono- and diphosphorylated MLC2 during different steps of mitosis revealed a very clear and bright 2P-MLC2 signal in centrosomes, from prophase to cytokinesis, and an enriched signal in the midzone/contractile ring, during anaphase to cytokinesis. 2P-MLC2 location at the cleavage furrow has been well established in literature (Dean and Spudich, 2006; DeBiasio *et al.*, 1996; Komatsu *et al.*, 2000; Yamashiro *et al.*, 2003). A centrosomal localization for MLC2 has not been well described, but evidence is accumulating that MLC2 fulfils a function at centrosomes, for example in the complete separation of duplicated centrosomes (Rosenblatt *et al.*, 2004). The contractile actomyosin cortex residing at the poles of dividing cells also influences positioning of the cleavage furrow and disruption of this cortex results in cytokinesis errors and aneuploidy (Sedzinski *et al.*, 2011). Finally, diphosphorylated MLC2 affects separation of chromosomes from the equator at metaphase and formation of the mitotic spindle (Hashimoto *et al.*, 2008; Komatsu *et al.*, 2000).

Isoform DMPK C is a membrane-bound protein during interphase, but often displays a cytosolic localization during mitosis, similar to DMPK E. However, only DMPK E expression induced cell division defects. This may suggest that interaction between MLC2 and DMPK E in the preceding cell cycle affects upcoming cell division. Alternatively, the C-terminal tail of DMPK C may preclude an interaction with MLC2 during mitosis.

Even though DMPK E displays a general cytoplasmic staining during mitosis and is thus present at contractile ring, midbody and centrosomes, the kinase is not specifically enriched at these structures, unlike its homologues CRIK and ROCK (Kosako *et al.*, 1999; Madaule *et al.*, 2000). It may therefore be that local availability of activators at the midzone, contractile ring and centrosomes explains the influence of DMPK E on cell division. Despite evidence presented here, we cannot exclude that the observed effects on cell division are regulated through DMPK E substrates that were not investigated. We anticipated that if MLC2 hyper-phosphorylation is the cause of the observed cell division defects, these errors should be recapitulated upon overexpression of MLC2 phosphomimetic mutants (e.g., T18D/S19D). Unfortunately, cells expressing this MLC2 mutant were not viable, precluding scoring of any mitotic events. Similar results were obtained upon overexpression of wild-type MLC2.

In sum, our data underscore a phosphorylation-dependent centrosomal function for MLC2. We hypothesize that DMPK E-mediated hyperphosphorylation of MLC2 leads to disturbance of centrosomal and contractile ring function during mitosis,

resulting in mitotic spindle defects followed by instant cell death or multinucleation. Future research should aim at further elucidating the role of MLC2 phosphorylation in centrosome functioning.

Table S1: Primers used to generate pEYFP-N1-ΔATG-MLC2 constructs via site directed mutagenesis. Crucial nucleotides to introduce the desired mutations are underlined.

Construct name	Forward primer	Reverse primer
pEYFP-N1-ΔATG-MLC2-T9A	5'-AAAGCGAAGACCAAGGC-CACCAAGAAGCGCC-3'	5'-GGCGCTTCTTGGTG-GCCTTGGTCTTCGCTTT-3'
pEYFP-N1-ΔATG-MLC2-T18A	5'-GCGCCCTCAGCGCGCG-GCGTCCAATGTGTTGCC-3'	5'-GGCGAACACATTGGAC-GCCGCGCGCTGAGGGC-GC-3'
pEYFP-N1-ΔATG-MLC2-S19A	5'-GCGCCCTCAGCGCG-CAACTGCGAATGTGTTTCGC-CATG-3'	5'-CATGGCGAACACATTGG-CAGTTGCGCGCTGAGGGC-GC-3'
pEYFP-N1-ΔATG-MLC2-T18A/S19A	5'-CCCTCACGCGCAGCAG-CAAATGTGTTGCC-3'	5'-GGCGAACACATTGCT-GCTGCGCGCTGAGGG-3'

SUPPLEMENTARY DATA

Movies I, IIa_1, IIa_2, IIb, III, IV and V can be downloaded from <http://home.kpn.nl/j.gerrits38>:

Movie_I: normal cell division

Movie_IIa_1: regression of cleavage furrow before formation of midbody

Movie_IIa_2: regression of cleavage furrow after formation of midbody

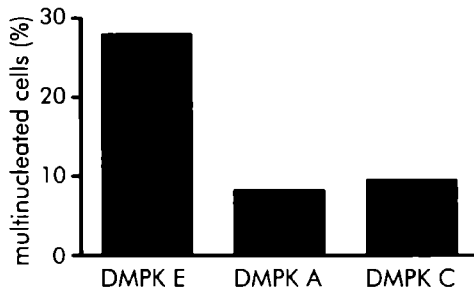
Movie_IIb: lack of furrow ingression

Movie_III: cell death during mitosis

Movie_IV: multipolar division

Movie_V: regular apoptosis during interphase

A



B

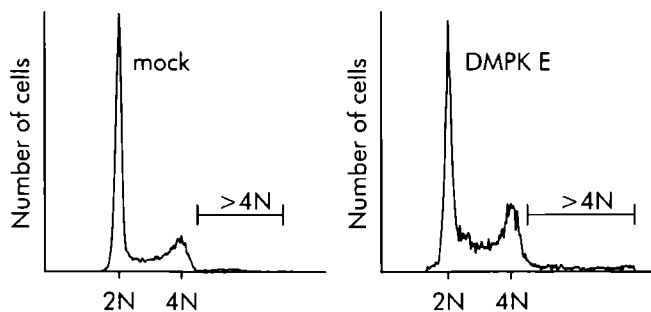
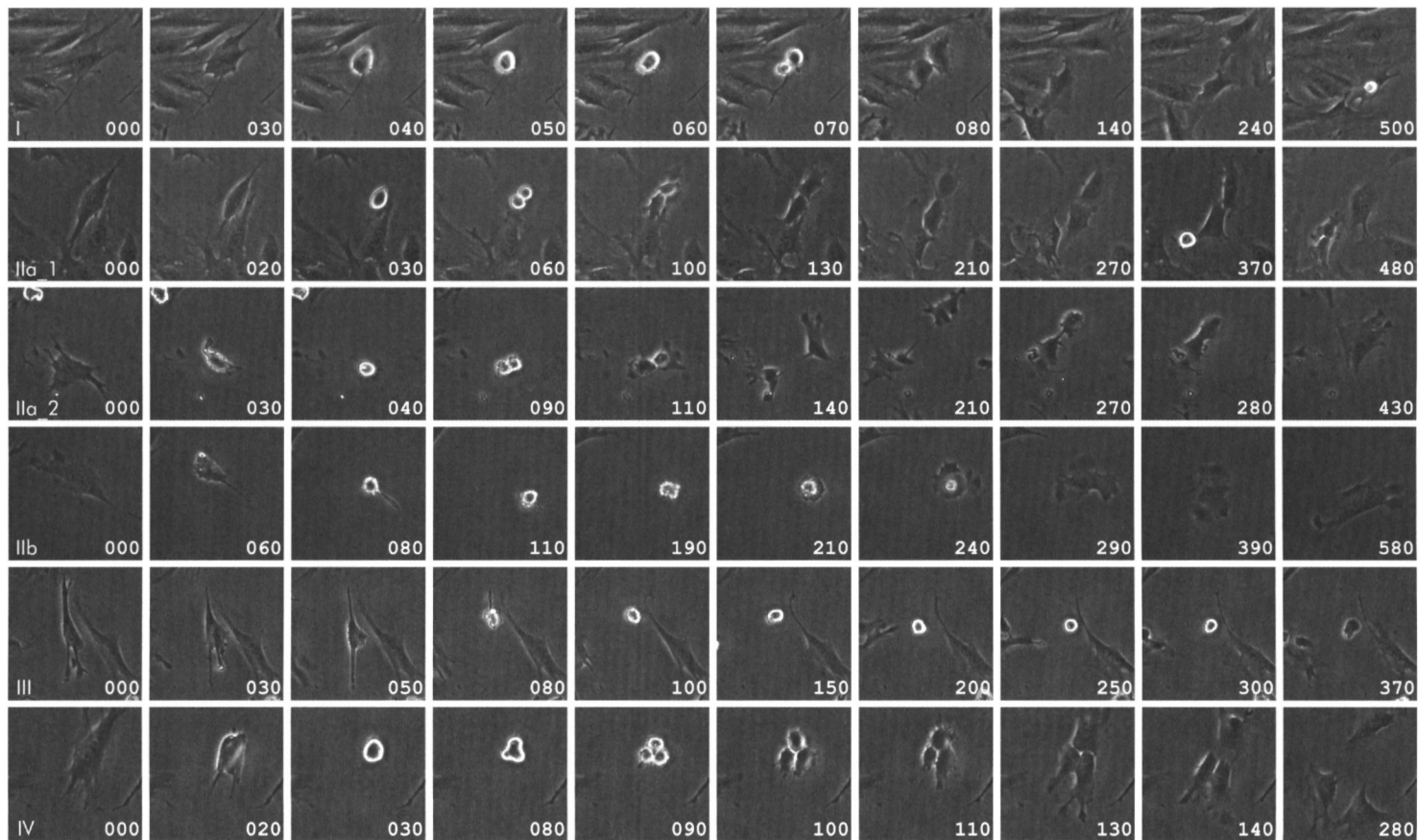


Figure S1: DMPK E induces multinucleation in neuroblastoma cells.

(A) Neuroblastoma cells were transfected with DMPK isoforms and cultured for 24 hrs. The fraction of multinucleated cells increased to almost 30% upon transfection with DMPK E, whereas cultures transfected with DMPK A or C displayed ~10% multinucleated cells.

(B) Flow cytometric analysis of mock- or

DMPK E-transfected neuroblastoma cells. Transduction efficiency was >75%. Cells were stained with propidium iodide to visualize DNA content (>6500 cells analyzed). The DMPK E-transfected culture showed a 1.6-fold increase in the amount of tetraploid cells and also the number of cells containing >4N DNA was strongly increased upon DMPK E expression.



Phosphorylation of Myosin Regulatory Light Chain by a cytosolic isoform of Dystrophia Myotonica Protein Kinase

Figure S2: Stills from movies made from dividing DMPK E-expressing myoblasts illustrating division outcomes shown in Fig. 2A. Roman numerals refer to the outcomes drawn in Fig. 2A. Arabic numerals indicate the time in min since start of mitosis (rounding up of cells). Stills depicted in Fig. 2B are a selection from the stills shown here.

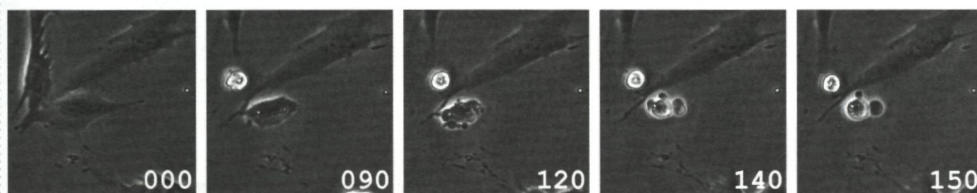


Figure S3: Stills from a movie showing a DMPK E-expressing myoblast dying from apoptosis during interphase. Arabic numerals indicate the time in min since rounding up of the cell. Note the large bleb appearing after 120 min.

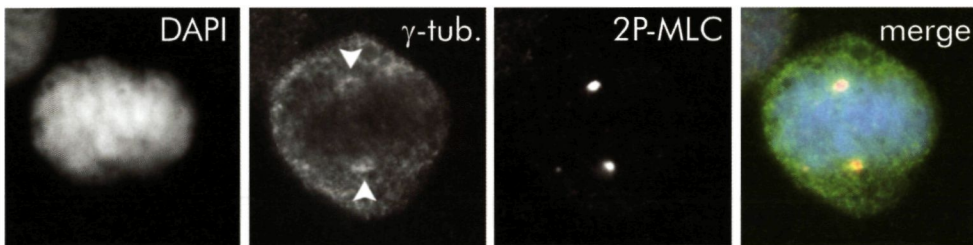


Figure S4: 2P-MLC2 localizes to centrosomes. HeLa cells were fixed and stained for 2P-MLC2 and γ -tubulin, which was used as a centrosomal marker. DNA was stained with DAPI. Centrosomes are indicated with arrowheads.

Chapter 4

Gene duplication and conversion events shaped three homologous, differentially expressed Myosin Regulatory Light Chain (MLC2) genes

Lieke Gerrits, Gijs J. Overheul, Ronny C. Derks, Bé Wieringa, Wiljan J.A.J. Hendriks, Derick G. Wansink

Department of cell biology, Nijmegen Centre for Molecular Life Sciences, Radboud University Nijmegen Medical Centre, Nijmegen, The Netherlands.

European Journal of Cell Biology - in press

ABSTRACT

Myosin II is a hexameric protein complex consisting of two myosin heavy chains, two myosin essential light chains and two myosin regulatory light chains. Multiple subunit isoforms exist, allowing great diversity in myosin II composition which likely impacts on its contractile properties. Little is known about the evolutionary origin, expression pattern and function of myosin regulatory light chain (MLC2) isoforms. We analyzed the evolutionary relationship between smooth muscle (sm), nonmuscle (nm) and nonmuscle-like (nml) MLC2 genes, which encode three homologous proteins expressed in nonmuscle cells. The three genes arose by successive gene duplication events. The high sequence similarity between the tandemly arranged nm- and nml-MLC2 genes is best explained by gene conversion. Urea/glycerol-polyacrylamide gel electrophoresis and RNA analysis were employed to monitor expression of sm-, nm- and nml-MLC2 in human and mouse cell lines. Conspicuous differences between transformed and non-transformed cells were observed, with sm-MLC2 being suppressed in Ras-transformed cells. Our findings shed light on the evolutionary history of three homologous MLC2 proteins and point to isoform-specific cell growth-related roles in nonmuscle cell myosin II contractility.

Gene duplication and conversion events shaped three homologous, differentially expressed MLC2 genes

4

Members of the myosin super family play a role in a wide variety of cell dynamical processes, including migration, intercellular adhesion, polarization, division and contraction (Berg *et al.*, 2001). Class II myosins (myosin II) are called conventional myosins and are involved in bipolar filament formation. Myosin II has been found in all eukaryotes (Sellers, 2000) and its structure is well conserved throughout evolution (Jung *et al.*, 2008), indicative of a crucial function for diverse forms of eukaryotic life. Different forms of myosin II exist in higher eukaryotes (Kovacs *et al.*, 2003): sarcomeric forms are abundantly present in striated skeletal muscle fibres and heart cells, while nonmuscle (nm) and smooth muscle (sm) forms are widely expressed in various cell types and organs, including stomach, heart, intestine and urinary bladder (Eddinger and Meer, 2007; Inoue *et al.*, 1992).

All forms of myosin II exist as hexameric complexes comprised of two copies of myosin II heavy chains (MHCII), two myosin essential light chains (ELC) and two myosin regulatory light chains (MLC2). Vertebrate smooth muscle, muscle precursor and nonmuscle cells produce MHCII proteins that are encoded by four different genes that each display alternative splicing: nonmuscle A (MYH9), nonmuscle B (MYH10), smooth muscle (MYH11) and nonmuscle C (MYH14). For the ELC subunits, two variants exist which are generated from a single gene by alternative splicing (Lenz *et al.*, 1989) and multiple genes encode a collection of different MLC2 isoforms (Collins, 2006). All these subunit variants can be combined into distinct hexameric myosin II complexes, each presumably with unique contractile properties, allowing fine-tuning of cellular contractile processes. Better understanding of myosin II characteristics therefore requires insight into the properties of the separate subunits. A correlation between MHCII isoform expression and sm- and nm-myosin II contractility has been described (Babu *et al.*, 2000; Karagiannis and Brozovich, 2003) and different light chain isoforms are thought to modulate myosin II contractile properties in a distinct way, but experimental evidence is scarce. The extent and role of isoform variation in non-sarcomeric cells is even less well explored.

In MHCII molecules a globular subfragment (S1) and a rod-shaped tail domain can be distinguished. Tail domains dimerize to form a coiled-coil rod domain which is involved in multimerization of myosin II into so-called thick filaments. MHCII's globular S1 domain contains the motor domain - the site of actin-binding and ATP hydrolysis - and the neck domain. Energy resulting from ATP hydrolysis leads to mechanical movement at the junction of the motor and neck domain, resulting in movement of the motor domain relative to the neck domain, thus promoting active sliding of the entire molecule along actin filaments (Huxley, 2000; Huxley, 2004). The neck domain of each MHCII molecule provides binding sites for one ELC and one

MLC2 molecule. Binding of ELC is generally thought to increase the stability of the myosin II complex (Vicente-Manzanares *et al.*, 2009).

In nonmuscle and smooth muscle myosin II MLC2 is able to modulate myosin-actin interaction in a phosphorylation-dependent manner, causing a conformational change with a strong increase in the ATPase activity of the head domain and effects on filament formation (Craig and Woodhead, 2006). This regulation involves sequential phosphorylation of an essential serine residue at position 19 (Ser19; generating monophosphorylated MLC2) and a threonine residue at position 18 (Thr18; resulting in diphosphorylated MLC2) (Vicente-Manzanares *et al.*, 2009). In cardiac and skeletal muscle myosin II contractility is regulated by a Ca^{2+} -induced conformational change in actin-bound troponin that makes the actin filaments accessible for myosin II binding. MLC2 phosphorylation in these myosins has no significant effect on myosin ATPase activity but rather modulates Ca^{2+} -sensitivity and Ca^{2+} /troponin-dependent force generation, thereby influencing contraction properties (Scruggs and Solaro, 2011; Stull *et al.*, 2011).

To come to a better understanding of the functional significance of homologous non-sarcomeric myosin II complexes, we studied the different MLC2 isoforms found in nm- and sm-myosin II complexes in various mammalian cell types. Three highly conserved MLC2 genes could be discerned, two of which are oriented head-to-tail on the chromosome and reflect concerted evolution by means of gene conversion. Expression of the paralogous MLC2 proteins is differentially regulated in non-transformed and tumourigenic cell types, pointing towards distinct growth-related roles.

MATERIALS AND METHODS

Cell culture

C2C12 (mouse myoblast), HeLa (human adenocarcinoma), HT-1080 (human fibrosarcoma), A375 (human melanoma), B16-F10 (mouse melanoma) and U251 (human glioma) cells were cultured at 37°C in Dulbecco's Modified Eagle Medium (DMEM; Gibco/Invitrogen; Carlsbad, CA) supplemented with 10% (v/v) foetal calf serum (FCS). Immortalized mouse myoblasts (from *DMPK*^{-/-} mice) were cultured as described (Jansen *et al.*, 1996). Immortalized mouse iliac and aorta smooth muscle cells (isolated essentially as described (Campbell *et al.*, 1989)), were kindly provided by dr. G. van Eijs (Dept. Genetics and Cell Biology, Maastricht University, The Netherlands) and were cultured at 33°C in DMEM supplemented with 10% FCS and 0.01 IU/ml γ -interferon. MMT (mouse mammary carcinoma) cells (Tsuji *et al.*, 2006) were cultured at 37°C in Eagle's Minimum Essential Medium supplemented with 10% FCS. C-5120 primary human fibroblasts (Distelmaier *et al.*, 2009) were cultured in HEPES (25 mM)-buffered M199 medium (Gibco/Invitrogen) supplemented with 10% FCS, 100 IU/ml penicillin and 100 IU/ml streptomycin. Dombi human primary keratinocytes were cultured as described (Amigo *et al.*, 2006). Generation and propagation of the collection of mouse embryonic fibroblasts, which represent different stages of oncogenic progression (Prim-MEF, Imm-MEF, TBX2-MEF, Ras-LP, Ras-HP, and Ras-TUM) was described by de Groof *et al.* (de Groof *et al.*, 2009). All cell lines were cultured at 7.5% CO₂ and 20% O₂.

Antibodies

As MLC2 antibodies we used (i) an antibody recognizing unphosphorylated (0P), monophosphorylated (1P) and diphosphorylated (2P) MLC2 (K19; Mulders *et al.*, 2011); (ii) an antibody against 1P (Ser19) MLC2 (#3675; Cell signaling technology; Danvers, MA); (iii) an antibody against 2P (Thr18/Ser19) MLC2 (#3674; Cell signaling technology). All three MLC2 antibodies recognized sm-, nm- and nml MLC2.

Salirasib treatment of Ras-LP cells

Salirasib (Cayman Chemical, Ann Arbor, MI) stock of 75 mM was made in DMSO. Cells were treated at a final concentration of 75 μ M in culture medium. Control cells were treated with 0.1% DMSO. Doubling times were calculated by counting cell numbers after trypsinization. Salirasib- and DMSO-containing media were refreshed every 2-3 d. Treatment was continued for 16 d during which cells were split five times and after which RNA isolation was performed as described below.

Expression plasmids and transfection

cDNAs encoding human and mouse nm-, sm- and nml-MLC2 were obtained by RT-PCR using appropriate forward primers containing an *EcoRI* site and appropriate reverse primers containing a *XhoI* site. Details on primer sequences and accession numbers of mouse and human nm-, sm- and nml-MLC2 cDNA sequences can be found in Tables S1 and S2, respectively. PCR products were cloned into an *EcoRI/XhoI*-digested pSG8Δ*EcoRI* vector (Groenen *et al.*, 2000). The constructs were named pSG8Δ*EcoRI*-MLC2 including h (human) or m (mouse) to specify the species and sm, nm or nml to indicate the isoform. Since protein sequences of mouse and human nm-MLC2 are 100% identical, only the mouse nm-MLC2 variant construct was generated.

pSG8Δ*EcoRI*-MLC2 constructs were used as template in a PCR with appropriate *EcoRI* site-containing forward and *BamHI* site-containing reverse primers to create a no-stop mutation. The resulting PCR fragments were cloned into an *EcoRI/BamHI*-digested pEYFP-N1 vector (Clontech Laboratories, Mountain View, CA) from which the start codon was removed by PCR (pEYFP-N1-ΔATG). The resulting plasmids encode C-terminally YFP-tagged MLC2 isoforms from human and mouse and were named accordingly.

HeLa cells were transfected using jetPEI™ transfection reagent (Polyplus-transfection, Illkirch, France) according to the manufacturer's instructions. B16F10 cells were transfected with Lipofectamine (Invitrogen) according to the manufacturer's instructions.

Fluorescence microscopy

Transfected HeLa cells expressing YFP-tagged MLC2 proteins were fixed for 20 min in 2% (w/v) formaldehyde in 0.1 M phosphate buffer (pH 7.4). To visualize stress fibres, cells were permeabilized with 0.1% Triton X-100 in PBS for 20 min at room temperature (rt) and stained with Alexa-568 conjugated phalloidin (A12380, Molecular Probes/Invitrogen, Carlsbad, CA) for 30 min at rt. Following three washes with PBS, cells were mounted on glass slides using Mowiol containing DAPI (0.6 μg/ml) and 2.5% (w/v) NaN₃. Images were obtained using a Zeiss Axiophot2 fluorescence microscope (Zeiss, Thornwood, NY) with an Axiocam MRm CCD camera and Axio Vision 3.1 software (Zeiss).

In vitro transcription/translation

Generation of proteins via *in vitro* transcription/translation was done using the TNT®T7 Quick Coupled Transcription/Translation System (Promega, Madison, WI) according to the manufacturer's instructions. In short, 40 μl TNT® Quick Master Mix was mixed with 1 μg circular plasmid DNA template and methionine was added to a final concentration of 20 μM. Nuclease-free water was added to a final volume of 50

μ l. The reaction proceeded for 1.5 hrs at 30°C. 3 μ l of the reaction mix was used for analysis on urea/glycerol-polyacrylamide gel electrophoresis (UG-PAGE) (Mulders et al., 2011).

RT-PCR and Southern blotting

RNA isolation was done with the Aurum Total RNA mini kit (BioRad, Berkeley, CA) according to the manufacturer's instructions. 500 ng RNA was used in a standard reverse transcriptase reaction using Superscript II Reverse Transcriptase (Invitrogen). The resulting cDNAs were used in a PCR reaction with primers 5'-GGAGGACCTGCACGACAT-3' (forward) and 5'-CGGTGCCCCATGGTGGT-3' (reverse) which allowed simultaneous amplification of all three mouse MLC2 paralogues. PCR products were separated on a 2% (w/v) agarose gel and transferred to Hybond-N+ membrane (Amersham/GE healthcare, Munich, Germany). Membrane was prehybridized at 42°C for at least 1h in 2x SSC containing 1% SDS and then incubated o/n at 42°C in the same buffer with either ³²P-labelled 5'-AGGTAGGCATCAGTGGGATT-3' oligonucleotide probe for nm-MLC2, 5'-TCATGCCCTCCAGATACTCGTCTGT-3' for sm-MLC2, or 5'-GTTGGGTTTTTCCCATTGACG-3' for nml-MLC2 DNA while rotating. After washing the membrane in 2x SSC containing 0.2% SDS at 42°C, the membrane was exposed to a PhosphorImager K-screen (Bio-Rad). Radiolabelled DNA bands were detected using a Bio-Rad personal Fx PhosphorImager (Bio-Rad) and analyzed using Quantity One software (Bio-Rad). Stripping of the membrane was done for 30 min at 80°C in 0.2x SSC containing 0.2% SDS, after which the procedure was repeated for the next MLC2-isoform-specific probe. To compensate for pipetting or blotting variations, actin PCR product was added as an internal control in all samples at equal amounts. This product was obtained by PCR using actin primers 5'-GCTAYGAGCTGCCTGACGG-3' (forward) and 5'-GAGGCCAGGATGGAGCC-3' (reverse) on cDNA generated from RNA of TBX2-MEF cells. For detection on Southern blot the forward actin probe was labelled and used as described above.

Urea/glycerol polyacrylamide gel electrophoresis and Western blotting

Urea/glycerol-PAGE (UG-PAGE) was performed essentially as described (Mulders et al., 2011). In short, to preserve existing posttranslational protein modifications and prevent enzymatic protein degradation prior or during electrophoretic analysis, cells were washed with ice-cold PBS and scraped on ice in 12% TCA/10 mM DTT in acetone (-80°C). Precipitates were collected in Eppendorf tubes and centrifuged for 20 min (15,000 rpm; 4°C). Pellets were washed once with 10 mM DTT in acetone (20 min, 20,000g, 4°C) and air dried. Pellets were either stored at -80°C or immediately used for analysis on UG-PAGE. This was done by mechanically dissolving pellets in urea sample buffer (8 M urea; 125 mM Tris-HCl, pH 6.8; 5% β -mercapto-ethanol (v/v); 2%

saturated bromophenol blue (v/v)) at rt at least 1 h before loading on gel. Samples were then separated on a 16% acrylamide/bis-acrylamide (37.5:1) gel containing 40% (v/v) glycerol and 375 mM Tris-HCl (pH 8.8). The stacking gel consisted of 40% glycerol, 4% acrylamide/bis-acrylamide (37.5:1) and 125 mM Tris-HCl (pH 6.8). Gels were run for 16 hrs at rt in running buffer (25 mM Tris; 192 mM glycine; 1 mM DTT; pH 8.5-8.8) at 5 mA. Proteins were transferred to PVDF membrane (Millipore; Billerica, MA) for 4 hrs in ice-cold blotting buffer (48 mM Tris, 39 mM glycine, 0.037% SDS, 20% (v/v) methanol) at 300 mA. If TCA-lysates needed to be analyzed on SDS-PAGE, samples were mixed with 5x SDS sample buffer (250 mM Tris-HCl, pH 6.8; 500 mM DTT; 10% SDS; 50% glycerol; 0.5% bromophenol blue) to a final concentration of 2x SDS sample buffer and left at rt for 2 hrs before loading on gel.

Membranes were blocked in 5% milk powder (for antibody K19) or 3% bovine serum albumin (for antibodies against Ser19-MLC2 and Thr18/Ser19-MLC2) in TBS-T (10 mM Tris-HCl, pH 8.0, 150 mM NaCl, 0.05% Tween-20 (Sigma-Aldrich; St. Louis, MO)) 30-60 min prior to incubation with primary antibodies. Antibodies were diluted in blocking buffer and incubated overnight at 4°C. Next, membranes were washed three times with TBS-T and then incubated with secondary antibody (goat anti-mouse or goat anti-rabbit IRDye® 680 or 800; LI-COR Biosciences; Lincoln, NE) 1:10,000 for 1 h at rt, followed by two TBS-T washes and one TBS (10 mM Tris-HCl, pH 8.0, 150 mM NaCl) wash. Detection of immunoreactive bands was done on the Odyssey infrared Imaging System (LI-COR Biosciences).

Homology and phylogenetic analysis

Sequences were aligned with MUSCLE (v3.7) software configured for highest accuracy (default settings). Ambiguous regions (i.e., containing gaps and/or poorly aligned) were removed from the alignment with Gblocks (v0.91b) using the following parameters: minimum length of a block after gap cleaning was ten; no gap positions were allowed in the final alignment; all segments with contiguous nonconserved positions bigger than eight were rejected; minimum number of sequences for a flank position was 85%. The phylogenetic tree was created on www.phylogeny.fr (Dereeper *et al.*, 2008) and reconstructed using the maximum likelihood method implemented in the PhyML program (v3.0 aLRT). The default substitution model was selected assuming a proportion of no invariant sites and four gamma-distributed rate categories to account for rate heterogeneity across sites. The gamma shape parameter was estimated directly from the data (gamma=1.196). Reliability for internal branch was assessed using the aLRT test (SH-Like). Accession numbers of used sequences are listed in Table S2.

Conservation of homologous MLC2 isoforms

Interpretation of published data on the repertoire of myosin regulatory light chain (MLC2) variants that is expressed in vertebrate nonmuscle cells is complicated by species differences and the use of many different and confusing names. Literature suggests that mammals express three MLC2 isoforms in nonmuscle cells (Gaylinn *et al.*, 1989; Grant *et al.*, 1990; Monical *et al.*, 1993) and the NCBI database indeed lists three human MLC2 genes; *MYL9*, *MYL12A* and *MYL12B*. Protein products of *MYL9* and *MYL12B* are commonly referred to as smooth muscle (sm) and nonmuscle (nm) MLC2, respectively, although other ambiguous names have been used (e.g., muscle myosin, myosin light chain regulatory C for sm-MLC2 and similar to myosin regulatory light chain or myosin light chain regulatory B for nm-MLC2). No proper equivalent name is coined for the protein encoded by gene *MYL12A*. We propose here to name the *MYL12A* protein product nonmuscle-like (nml) MLC2, based on the strong sequence similarity with its nm paralogue (Fig. 1).

Phylogenetic studies on myosin II have focused almost exclusively on the MHCII proteins (Berg *et al.*, 2001). To analyse the evolutionary relationship between sm-, nm- and nml-MLC2 proteins in more detail, we searched for homologues in a variety of organisms and performed Blast searches with human MLC2 protein sequences in both NCBI and Ensembl databases. In *D. discoideum*, *A. queenslandica*, *C. elegans*, *D. melanogaster*, *S. kowalevskii*, *B. floridae* and *C. intestinalis* only a single protein corresponded to the human sm-, nm- and nml-MLC2 sequences. In *X. tropicalis* two homologues could be detected. Four MLC2 homologues were found in *D. rerio*, but only three related sequences could be detected in *T. nigroviridis*, of which only the *Myl9* protein product was annotated. Also in *T. rubripes* and *G. aculeatus* three homologues were identified (not shown). In birds and mammals, orthologues for all three human MLC2 sequences were encountered. The *G. gallus* *MYL9* and *MYL12A* protein products were properly annotated, but we had to assemble the full-length *MYL12B* sequence from two partial sequence entries (see Table S2). *M. musculus* sm- and nm-MLC2 were properly annotated, but the protein product of gene *Myl12A* was listed under a confusing name. Alignment of MLC2 protein sequences demonstrated that sm-, nm-, and nml-MLC2 isoforms contain 171 to 172 amino acids and are highly conserved during evolution (Fig. S1).

The paralogous nm- and nml-MLC2 proteins share a high degree of identity and differ in only three (plus one amino acid deletion) and four amino acid residues in human or mouse, respectively (Fig. 1; Fig. S1). Sm-MLC2 protein and either nm- or nml-MLC2 proteins differ at 10-12 amino acid positions in human and mouse. Interspecies differences between orthologues are also very small: only one or three

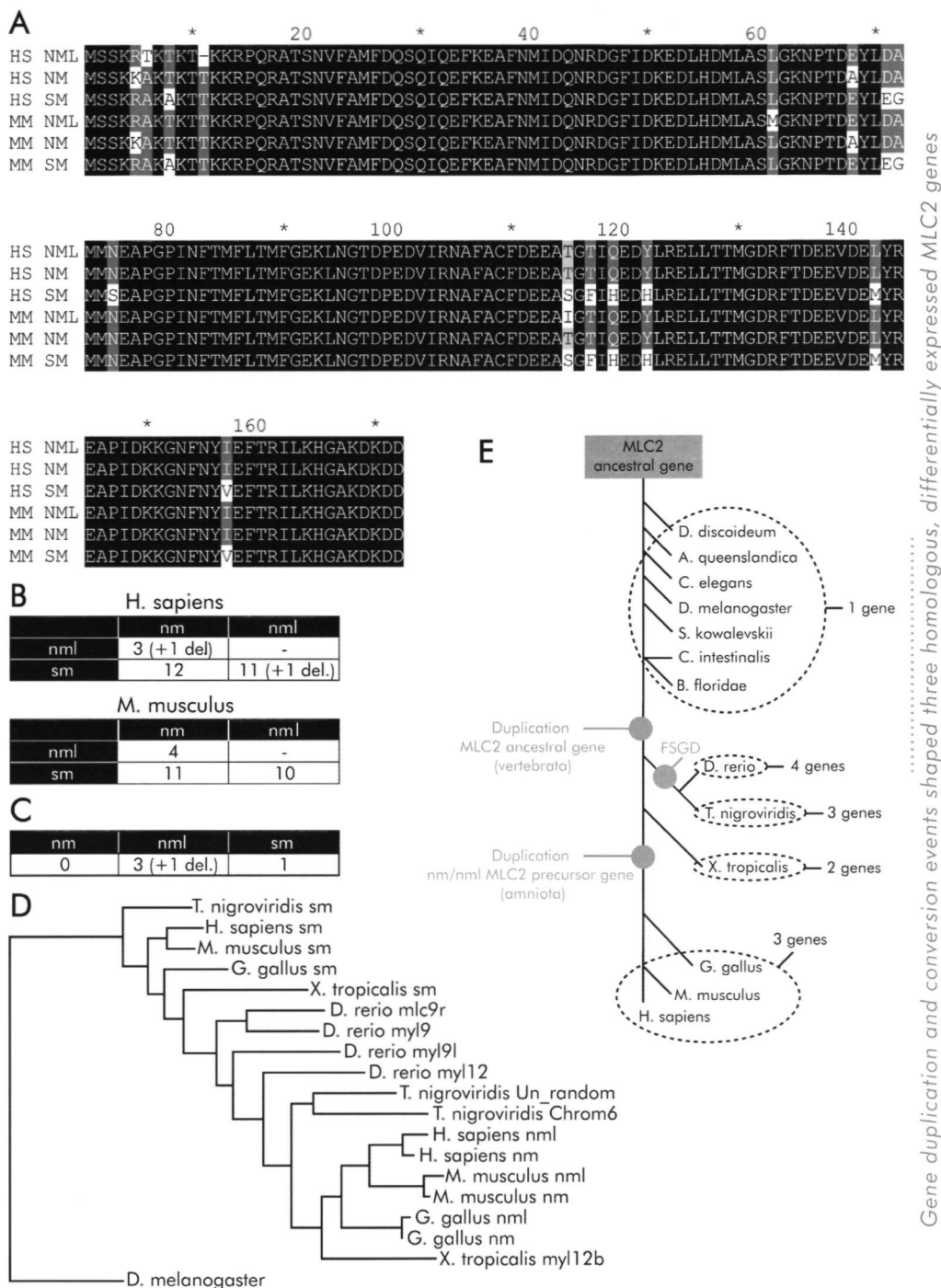


Figure 1: Three MLC2 genes in man and mouse are highly conserved throughout evolution

and result from two gene duplication events. (A) Alignment of human (HS) and mouse (MM) sm-, nm- and nml-MLC2 protein sequences. Conservation of amino acid sequences within and between species is very high, indicative of high evolutionary pressure. White characters on a black background represent identical residues in all aligned proteins; white characters on a dark grey background represent the most common amino acid at a certain position (>50% occurrence); black characters on a light grey background represent amino acids with an occurrence of ≤50%. **(B)** Summary of the total number of divergent residues between sm-, nm- and nml-MLC2 in *H. sapiens* (upper panel) and *M. musculus* (lower panel). **(C)** Summary of the number of divergent residues between sm-, nm- and nml-MLC2 of *H. sapiens* and *M. musculus*. **(D)** Phylogenetic tree based on sequences shown in Fig. S1: Sm-, nm- and nml-MLC2 are highly conserved throughout evolution in a wide variety of species. The MLC2 protein sequence from *D. melanogaster* was used to root the tree. Accession numbers of sequences are listed in Table S2. **(E)** Evolutionary model showing how nm/nml-MLC2 and sm-MLC2 precursor genes resulted from one ancestral MLC2 gene through two subsequent gene duplication events. FSGD=fish-specific genome duplication, sm=smooth muscle, nm=nonmuscle, nml=nonmuscle-like, del.=deletion.

(plus one amino acid deletion) amino acids differ between mouse and human sm- or nml-MLC2, respectively, and mouse and human nm-MLC2 protein sequences are 100% identical (Fig. 1A and C; Fig. S1). It is therefore no surprise that also high conservation is found at phosphorylation sites that are essential for regulation of myosin II activity: Thr18 and Ser19 are conserved in virtually all isoforms and organisms (Vicente-Manzanares *et al.*, 2009). Phosphoacceptor sites Ser1, Ser2 and Thr9 - which received very little attention in literature thus far (Bengur *et al.*, 1987) - are also conserved among most MLC2 proteins.

Model for the evolutionary history of multiple MLC2 isoforms

Alignment of cDNA sequences encoding vertebrate sm-, nm- and nml-MLC2 proteins was used to create a phylogenetic tree (Fig. 1D). Because it is distantly related to the MLC2 sequences under study, the single MLC2 gene of *D. melanogaster* (*mlc2p*) was used to root the tree. As expected from the protein sequence comparisons, sm-MLC2 orthologues were clustered in the evolutionary tree. In contrast, nm- and nml-MLC2 cDNA sequences appeared clustered per organism rather than per isoform. A scenario of duplications of nml/nm-MLC2 precursor genes occurring independently in all species, however, is highly unlikely. Similar observations have been made for hsp70, attacin, alpha-amylase, gamma-crystallin, RHCE, RHD and alpha-2-fucosyltransferase genes (Abrantes *et al.*, 2009; Bettencourt and Feder, 2002; Innan, 2003; Inomata *et al.*, 1995; Lazzaro and Clark, 2001; Plotnikova *et al.*, 2007) and are thought to reflect gene conversion events (Brown *et al.*, 1972). In this process,

duplicated genes within a species evolve in concert because the two copies exchange DNA sequence information regularly, thus keeping inter-copy variation low (Innan, 2009). Gene conversion usually occurs between gene copies located in close proximity on the same chromosome. Analysis of the chromosomal location indeed showed that the nm- and nml-MLC2 genes in birds and mammals are arranged as a single head-to-tail tandem.

Assuming gene conversion-based concerted evolution of nm- and nml-MLC2 genes, the following evolutionary model becomes apparent (Fig. 1E): only one prototype MLC2 gene was present in the genome of the most recent common ancestor of animals. Early during the divergence of the vertebrate lineage, a duplication of this ancestral gene must have occurred, which led to the separate smooth muscle and nonmuscle-type MLC2 ancestral genes. In amphibians (*X. tropicalis*) these two MLC2 gene types are still detected but during evolution towards the common ancestor of birds and mammals a further, intrachromosomal gene duplication must have occurred for one of these two ancestral MLC2 genes, creating the nm- and nml-MLC2 ancestral genes. This scenario is in line with the presence of three homologous MLC2 proteins in *G. gallus*, *M. musculus* and *H. sapiens*, and is substantiated by the identification of three homologous MLC2 proteins in *T. guttata* (Zebra Finch) and *B. taurus* (cattle; data not shown). In fish, the lineage-specific whole-genome duplication explains the occurrence of four nonsarcomeric MLC2 genes in *D. rerio*. The fact that only three MLC2 variants were detected in three other teleosts may reflect loss of one MLC2 copy in these species but could also be an artefact of the low sequencing depth of current fish genome data. The notion that fish nm/nml-type MLC2 gene pairs do not display the extreme concerted evolution as observed for nm and nml genes in birds and mammals (Fig. 1D) further supports the evolutionary scenario we propose in Fig. 1E.

We also checked for MLC2-related sequences in the most complete genome data available for reptiles. *A. carolensis*, the anole lizard, was found to contain complete nml- and sm-MLC2 DNA and protein sequences. A third, incomplete sequence was also identified which showed strong sequence similarity to nml- and sm-MLC2 and thus may represent the C-terminal part of a nm-type MLC2 protein.

Subcellular localization of MLC2 protein isoforms

To reveal whether mammalian sm-, nm- and nml-MLC2 proteins have distinct functions in the cell we expressed individual mouse and human variants as C-terminally YFP-tagged proteins and determined their subcellular localization. For nm-MLC2 only the mouse cDNA was included, as the protein sequences of mouse and human nm-MLC2 are 100% identical. C-terminal fusions were chosen in order to prevent interference with documented phosphorylation events at the MLC2 N-terminus and because other studies successfully used C-terminal tagging to study MLC2 interactions (Chan *et al.*,

2005b; Komatsu *et al.*, 2000; Wu *et al.*, 2010). In interphase HeLa cells, MLC2-YFP fusion variants mainly located along actin stress fibres, as revealed by phalloidin

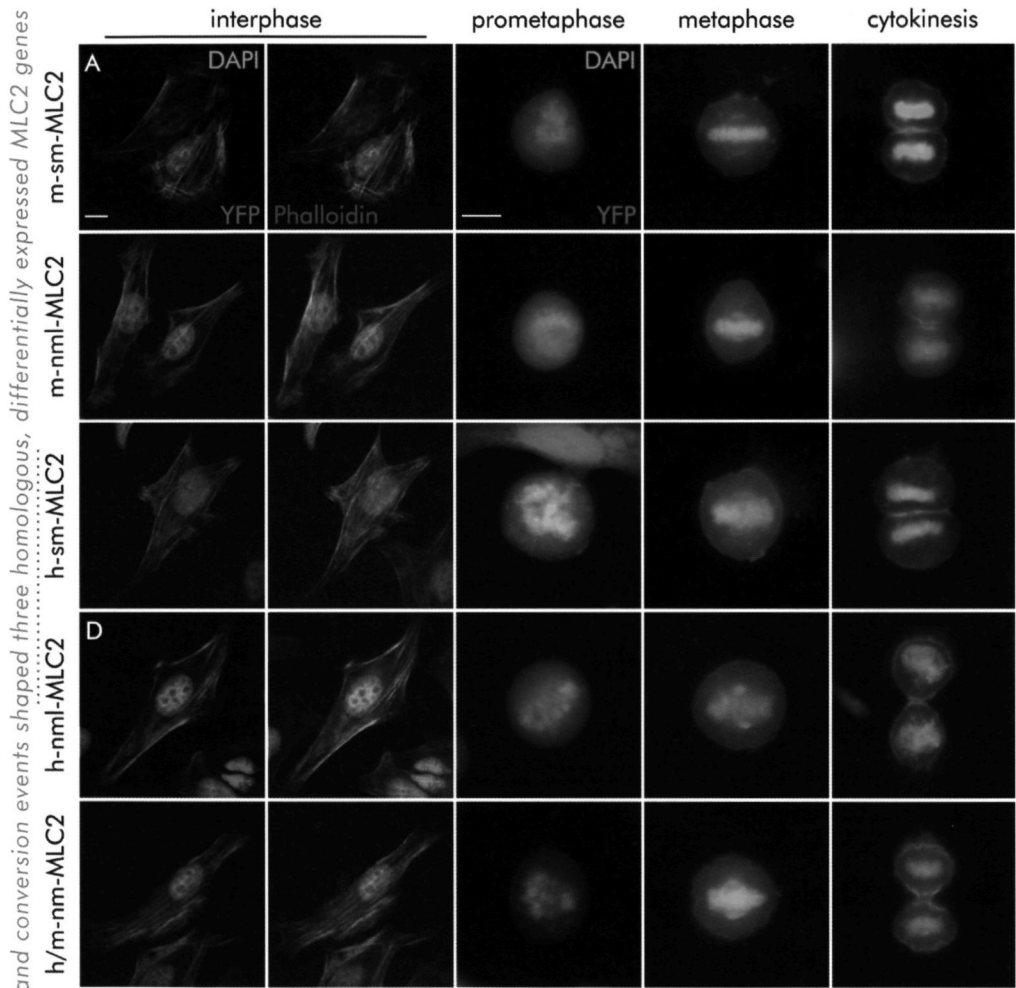


Figure 2: Cell cycle-dependent localization of MLC2 isoforms in HeLa cells. YFP-tagged human (h) or murine (m) sm-, nm- and nml-MLC2 proteins were transiently expressed in HeLa cells. Nuclei were counterstained by DAPI. During interphase, all MLC2 isoforms localized to fibre-like structures (first column), which were shown to be actin stress fibres by phalloidin staining (merged DAPI, YFP and phalloidin in second column). During mitosis, a diffuse cytoplasmic staining could be observed, including enrichment at polar crescents of the spindle during metaphase and at the midzone during cytokinesis (third, fourth and fifth column). Localization to the cortical cytoskeleton was observed during metaphase and cytokinesis. Bars are 5 μ m.

staining (Fig. 2; first and second column), indicating that the presence of a C-terminal YFP-tag did not interfere with MLC2's incorporation into myosin II complexes. Also in mouse B16-F10 melanoma cells, localization to actin stress fibres was predominant, again with no obvious differences between the distinct isoforms (Fig. S2).

During mitosis, localization to fibres vanished and a diffuse intracellular localization became apparent for all human and mouse isoforms (Fig. 2; third, fourth and fifth column). During metaphase the MLC2-YFP signals were enriched in crescents at the poles of the spindle (Zeng, 2000). During cytokinesis, MLC2 signals appeared strongest in the cleavage furrow, in agreement with immunofluorescence studies that used an MLC2 antiserum recognizing all three MLC2 isoforms (Matsumura *et al.*,

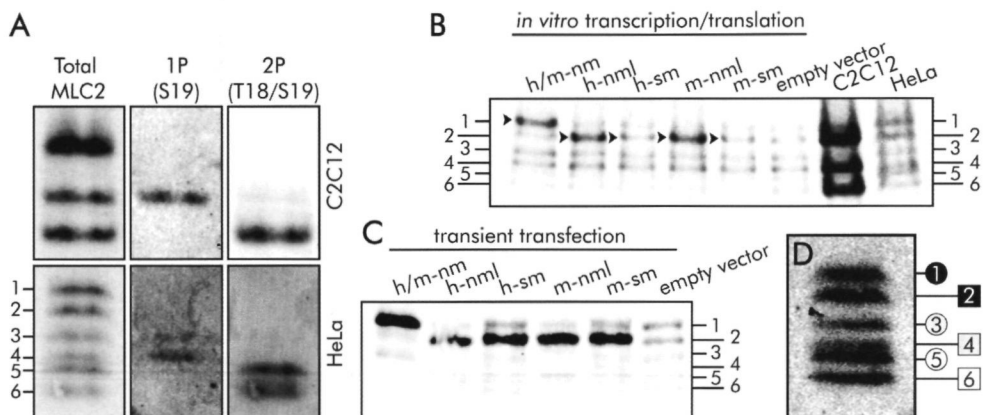


Figure 3: Identification of sm-, nm- and nml-MLC2 protein by urea/glycerol-PAGE. (A) Whole cellular protein extracts of C2C12 cells (upper panels) and HeLa cells (lower panels) were separated by urea/glycerol-PAGE. Western blotting was performed using a total MLC2 antibody (left panels), a phospho-Ser19-MLC2 antibody (middle panels) and a diphospho-Thr18/Ser19-MLC2 antibody (right panels). These three antibodies recognized sm-, nm- as well as nml-MLC2. (B) Plasmids encoding human (h) or mouse (m) sm-, nm- or nml-MLC2 were used to produce MLC2 proteins by *in vitro* transcription and translation. UG-PAGE followed by Western blotting using a total MLC2 antibody revealed migration behaviour of individual MLC2 isoforms relative to endogenous MLC2 proteins expressed in C2C12 or HeLa cells as controls. Arrowheads indicate the signal of interest. (C) HeLa cells were transiently transfected with plasmids used in (B). Whole cellular protein was run on UG-PAGE and MLC2 proteins were visualized as in (B). (D) Summarizing scheme of the identity of the different MLC2 signals seen on urea/glycerol-PAGE after Western blotting with total MLC2 antibody. Circles represent nm-MLC2, squares represent comigrating nml- and sm-MLC2 forms. Black shapes indicate unphosphorylated MLC2, grey shapes monophosphorylated MLC2 and white shapes indicate diphosphorylated MLC2.

1998). In the transition from metaphase to cytokinesis, partitioning of MLC2 variants to the submembranous, cortical actin cytoskeleton also became apparent in the vast majority of cells, but again with no obvious differences between individual human and mouse MLC2 isoforms. Similar mitotic distribution patterns were seen in mouse B16-F10 cells (Fig. S3).

Identification of MLC2 proteins by urea/glycerol-polyacrylamide gel electrophoresis

Antibodies that distinguish between sm-, nm- and nml-MLC2 proteins are not available. We therefore employed urea/glycerol-polyacrylamide gel electrophoresis (UG-PAGE) followed by Western blotting for further study of expression of MLC2 variants. UG-PAGE exploits differences in net negative protein charge and is commonly used to separate unphosphorylated MLC2 from mono- and diphosphorylated forms (Seto and Sasaki, 1990). We reasoned that UG-PAGE might also discriminate between unmodified MLC2 variants, as sm- and nml-MLC2 isoforms carry one extra negative charge compared to nm-MLC2 isoforms.

Surprisingly, when a C2C12 cell lysate was analyzed with UG-PAGE for endogenous MLC2 expression, three distinct bands were revealed whereas no less than six bands were detected in HeLa cell lysates (Fig. 3A, left panels). Upon probing of the same membranes with antibodies recognizing either monophosphorylated (Ser19) or diphosphorylated (Thr18/Ser19) MLC2 (note that phosphoacceptor epitopes are identical in all three MLC2 isoforms) the middle band of the C2C12 pattern was identified as monophosphorylated MLC2, while the fastest migrating (bottom) band was recognized as diphosphorylated MLC2 (Fig. 3A, upper middle and upper right panels). As the slowest migrating (top) band did not react with phosphospecific antibodies, we concluded that this band contained MLC2 that was not phosphorylated on Thr18 or Ser19. The monophosphorylated signal in the HeLa cell extract presented as a doublet (bands #3 and #4, counted from the top), while the lowest two bands (bands #5 and #6) corresponded to diphosphorylated MLC2 (Fig. 3A, lower middle and right panels). The two slowest migrating bands (bands #1 and #2) represented unphosphorylated MLC2 protein. Direct comparison of C2C12 and HeLa extracts in adjoining lanes on UG-PAGE demonstrated that the three MLC2 signals from C2C12 corresponded with the lower bands of the three doublets (i.e., bands #2, #4 and #6) in HeLa extracts (Fig. 3B).

To investigate how these signals from endogenous proteins relate to the MLC2 variants identified in sequence databases, we compared their UG-PAGE migration pattern to that of unphosphorylated MLC2 proteins produced *in vitro*. Amidst the background originating from immunoreactive proteins in the transcription/translation kit (see empty vector lane), human/mouse nm-MLC2 migrated as band #1 in HeLa cell extracts, while mouse and human sm- and nml-MLC2 migration corresponded

with HeLa protein band #2. Note that, for unknown reasons, sm-MLC2 expression consistently yielded a very weak signal just above background (i.e., empty vector lane). Analysis of UG-PAGE migration behaviour of MLC2 variants produced in transfected HeLa cells (Fig. 3C) further confirmed that nm-MLC2 migrated as band #1, while human and mouse sm- and nml-MLC2 comigrated as band #2. This migratory behaviour agrees with the observation that nm-MLC2 carries one negative charge less than sm and nml forms.

The Western blot data are summarized in Fig. 3D. UG-PAGE is able to separate unphosphorylated nm-MLC2 (band #1) from unphosphorylated sm- and nml-MLC2 variants (which comigrate as band #2) due to a net charge difference. The same reasoning applies to their respective monophosphorylated and diphosphorylated variants (bands #3/#5 versus bands #4/#6, respectively).

MLC2 expression in a collection of human and mouse cell lines

The former results imply that C2C12 cells do not express nm-MLC2, whereas all three MLC2 genes may be expressed in HeLa cells. To know more about cell-type dependent expression of MLC2 variants, we analyzed a broad range of human and mouse cell lines. In all human samples tested, six different MLC2 signals were observed (Fig. 4A). This indicated presence of unphosphorylated and phosphorylated nm-MLC2 together with analogous versions of sm- and/or nml-MLC2. Under the culture conditions used, the phosphorylation status of MLC2 proteins varied between cell lines, and - except for primary human fibroblasts (C-5120) - unphosphorylated forms dominated. In the mouse cell collection, the sm/nml-MLC2 signal was prevailing and nm-MLC2 protein (bands #1/#3/#5) was barely detectable in non-tumourigenic cells (Fig. 4B). Notably, two mouse cell lines with a tumourigenic origin (B16-F10 and MMT) displayed six rather than three MLC2 signals.

To test the hypothesis that MLC2 isoform expression is related to growth behaviour or oncogenic character *per se*, we analysed cells from a panel of six interrelated pools at different stages of transformation, all originating from the same primary mouse embryonic fibroblast (MEF) culture (de Groof *et al.*, 2009). Cell lines in this panel were primary MEFs, spontaneously immortalized MEFs, TBX2-immortalized MEFs and three types of Ras-V12/E1A-transformed fibroblasts at different stages of tumourigenesis. Doubling times of the Ras-transformed cell lines (Ras-LP, -HP and -TUM) ranged from twelve to seventeen hrs, whereas those of the three untransformed cell lines spanned twenty to twenty-four hrs (de Groof *et al.*, 2009). Remarkably, the expression level of nm-MLC2 protein (bands #1/#3/#5) was rather similar for all six cell lines, but the cumulative signal for sm- and nml-MLC2 was dramatically higher for non-tumourigenic lines than for the Ras-transformed lines (Fig. 4C).

To further distinguish between regulation of sm-, nm- and nml-MLC2

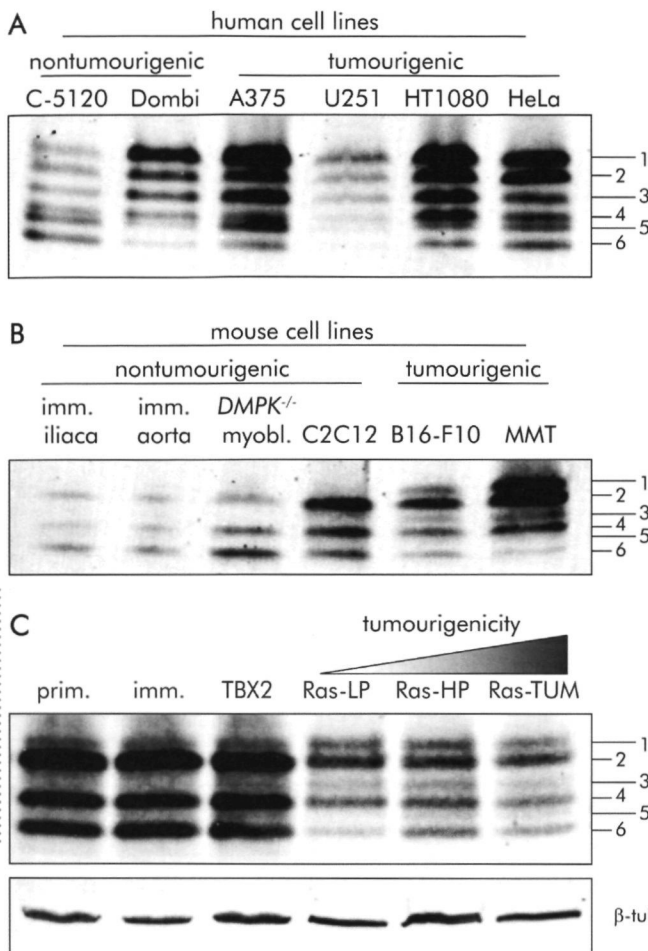


Figure 4: MLC2 isoform expression in a collection of human and mouse cell lines. Whole cell extracts of a diverse set of human and mouse cell lines were prepared by TCA precipitation and analyzed by urea/glycerol-PAGE followed by Western blotting with an MLC2 antibody. MLC2 patterns of human (A) and mouse (B) cultures were grouped based on tumourigenic or non-tumourigenic character of the cell lines. In all human samples six discrete bands could be observed. Patterns in mouse cell samples differed between non-tumourigenic (three bands) and tumourigenic (six bands) cell types. (C) MLC2 protein expression in a mouse cell panel consisting of six cell

lines, originating from the same primary MEF culture (i.e., prim.) and characterized by an increasing degree of tumourigenicity as indicated. MLC2 staining was done as in (A) and (B). The sm-/nml-MLC2 signal (bands #2/#4/#6) was down-regulated in Ras-transformed MEFs. prim.=primary; imm.=immortalized; myobl.=myoblast. Total protein loading was determined by analysis of β-tubulin levels in whole cell extracts used in the upper panel on SDS-PAGE (lower panel).

expression, RNA of all lines in the MEF panel was isolated and used in an RT-PCR analysis in which transcripts of all three MLC2 paralogues were amplified using a single set of primers. Resulting PCR products were then blotted and hybridized to MLC2 isoform-specific probes (Fig. 5A). Nm-MLC2 RNA levels were rather low in the non-transformed cell lines and five to twenty-fold higher in the Ras-transformed cell

lines (Fig. 5B and C). In contrast, expression of sm-MLC2 RNA was prominent in non-transformed cells, but virtually undetectable in transformed lines. Nml-MLC2 transcript signals appeared similar in all cell types in the panel, irrespective of tumourigenic status.

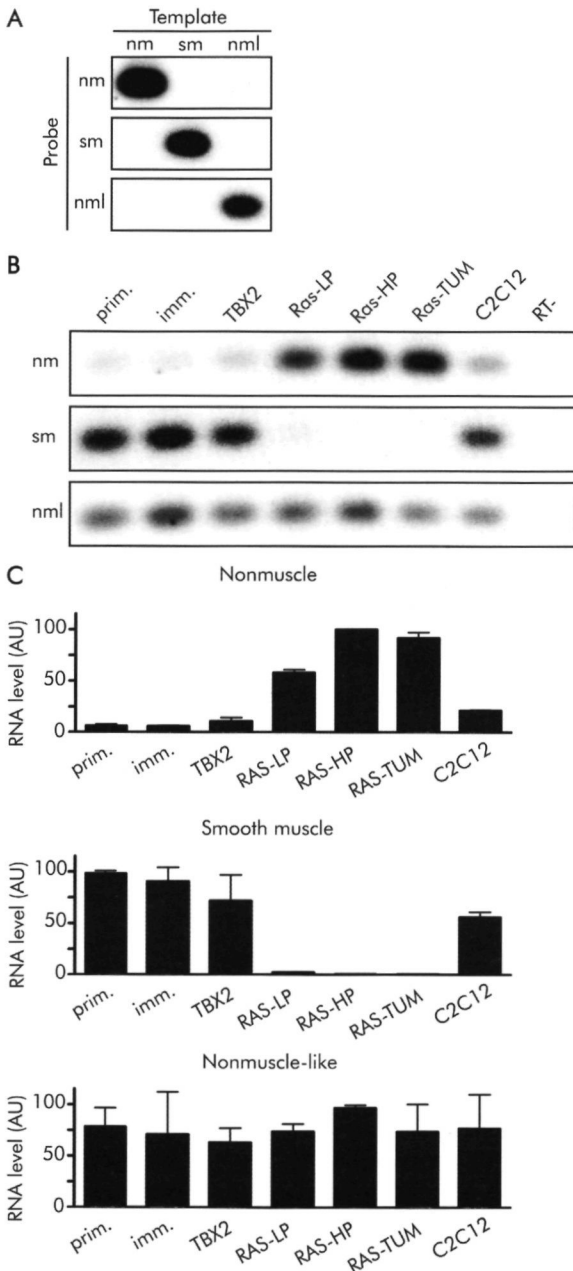


Figure 5: Differential expression of sm- and nm-MLC2 transcripts in a MEF cell panel. (A) Specificity of MLC2 isoform-specific oligo probes in Southern blotting (isoform type of oligos indicated at the left). Isoform-specific MLC2 DNA was obtained by PCR using individual MLC2 expression vectors as template (isoform types indicated on top). **(B)** MLC2 RNA expression in MEF panel. RT-PCR products based on RNA isolated from six cell lines from the MEF panel and C2C12 cells as reference were used in Southern blotting as tested in **(A)**. One set of MLC2 PCR primers was used, which amplified corresponding fragments from sm-, nm- and nml-MLC2 cDNA. A sample in which reverse transcriptase was omitted, served as negative control (RT-). **(C)** Quantification of experiment shown in **(B)**. Relative expression levels of the MLC2 isoforms in the cell lines from the MEF panel ($n=2$). For each oligo the strongest signal was set at 100%.

Ras inhibition in Ras-transformed cells induces sm-MLC2 RNA expression

We hypothesized that there is a relationship between Ras-mediated growth signalling (Haklai *et al.*, 1998) and expression of MLC2 isoform transcripts and that inhibition of Ras in Ras-transformed cells would lead to increased sm-MLC2 and decreased nm-MLC2 transcript levels. To test this hypothesis, Ras-LP cells were cultured for 16 d in presence of Salirasib, a well-known inhibitor of Ras effects (Weisz *et al.*, 1999). Salirasib treatment indeed significantly raised cell doubling time (Fig. 6A) and concomitantly augmented sm-MLC2 transcript expression (Fig. 6B). Nm- and nml-MLC2 expression remained unaltered (Fig. 6B). In conclusion, these findings provide evidence for a correlation between cellular growth rate and differential MLC2 isoform expression.

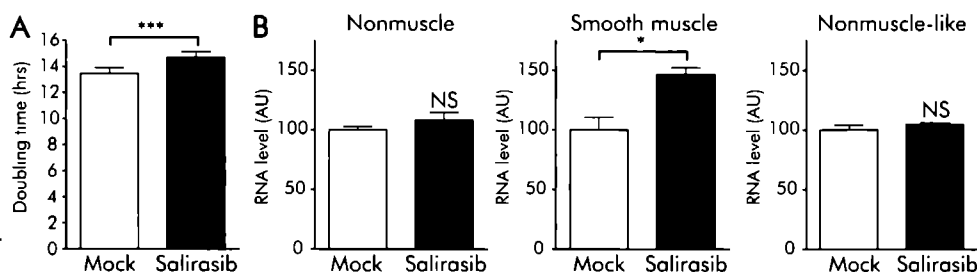


Figure 6: Ras inhibition reduces growth rate and sm-MLC2 transcript levels in Ras-transformed MEFs. RAS-LP MEFs were treated with Ras inhibitor Salirasib for 16 days prior to RNA isolation. Cell number was determined every 2-3 days. **(A)** Average doubling time for mock and Salirasib-treated RAS-LP MEF cells ($n=15$; ***. $p<0.001$) **(B)** Sm, nm- and nml-MLC2 transcript levels after 16 days of Salirasib treatment ($n=3$; *: $p<0.05$) RT-PCR analysis, Southern blotting and quantification were performed as for Fig. 5.

DISCUSSION

Occurrence of multiple gene products and splice variants for each of the subunits of the hexameric myosin II motor protein creates an enormous potential for fine regulation of cell shape transitions and cell motility in higher multicellular organisms. The current study contributes to understanding biological significance of different MLC2 proteins in actomyosin-based cell dynamics of nonmuscle cells. We compared expression patterns of three conserved MLC2 genes, designated here as smooth muscle (sm), nonmuscle (nm) and nonmuscle-like (nml), and found an interesting correlation between MLC2 isoform levels and growth rate and transformation in mouse cells.

Analysis of phylogeny and evolution of the three nonsarcomeric MLC2 genes and proteins revealed that the creation of nm- and nml-MLC2 variants took place in a common ancestor of birds and mammals after diverging from fish and amphibians in the vertebrate lineage. Furthermore, the head-to-tail juxtaposition of the nm- and nml-MLC2 genes and their extraordinary sequence identity suggests duplication within an ancestral chromosome segment and minimization of subsequent divergence via regular gene conversion. Other studies describing gene convergence demonstrate that this can occur between more than two genes thereby leading to concerted evolution of whole gene families (Teshima and Innan, 2004). Remarkably, in many examples of gene convergence pseudogenes participate in the process, which could lead to inactivation of the functional gene (Abrantes *et al.*, 2009; Plotnikova *et al.*, 2007). It is also common that only part of the gene sequence (i.e., an exonic region) is involved in the convergence process (Abrantes *et al.*, 2009; Plotnikova *et al.*, 2007). In our study nm- and nml-MLC2 genes were both found to be actively transcribed and gene convergence apparently spanned the complete coding sequence.

The high degree of similarity between nm-, nml- and sm-MLC2 proteins suggests that the evolutionary constraint on structure and function of each MLC2 must be considerable. What could be gained by introducing a third MLC2 protein variant? When duplicated genes are preserved, this is often because a higher dosage of the gene product is advantageous (selection for more of the same), because both copies have distinct functions (neofunctionalization) or because the ancestral gene's subfunctions are partitioned over the duplicated genes (subfunctionalization) (Innan, 2009). Expression of nml-MLC2 appeared rather cell-type independent. Modulation of cell growth rate or cell transformation did not affect its levels, suggesting that nml-MLC2 fulfils an important basal task. In that case, nm-MLC2 might reflect the newest evolutionary development towards a more specialized role, e.g. in the regulation of myosin II features like stability, force generation or shortening velocity, much like what was shown for ELC isoforms (Reiser and Bicer, 2006). The conservation of the primary

Gene duplication and conversion events shaped three homologous, differentially expressed MLC2 genes

MLC2 sequences contrasts with the markedly distinct regulation of expression. Hence, we favour the possibility that nml-MLC2 safeguards basal nonsarcomeric myosin II functionality, while switching between nm-MLC2 and sm-MLC2 expression may allow cells to specialize their contractile apparatus.

Up till now, no clear distinction between different MLC2 gene products has been made in publications on MLC2 structure and function in early muscle, smooth muscle and nonmuscle cells. This is likely due to the high rate of conservation and the lack of isoform-specific antibodies which render identification of individual MLC2 isoforms difficult. Even with proteomic mass-spectroscopic approaches a conclusive MLC2 isoform analysis is hard to achieve, due to the similarity of the variants, generating many identical peptides. Typically, Western blot studies using UG-PAGE revealed three MLC2 immunoreactive bands in some publications (Guo *et al.*, 2007; Mizutani *et al.*, 2009; Shivanna *et al.*, 2010), but six in others (Bao *et al.*, 2002; Di Ciano-Oliveira *et al.*, 2003; Huang *et al.*, 2004). Not much attention was spent on the identity of the additional MLC2 signals. Di Ciano-Oliveira *et al.* assigned the six bands to three doublets, and proposed that each doublet represents one phosphorylation state of two different isoforms (Di Ciano-Oliveira *et al.*, 2003), but also in this study no isoform specification was given. In other publications, presence of multiple bands (i.e., #1/#3/#5 on UG-PAGE/Western blots as we show in Figs 3 and 4) was simply ignored (Bao *et al.*, 2002; Huang *et al.*, 2004). Our findings reported here may very well contribute to reinterpretation of existing data.

Differential expression of individual MLC2 isoforms in animal species and tissues has been addressed in some publications (Grant *et al.*, 1990; Monical *et al.*, 1993; Park *et al.*, 2007; Yuen *et al.*, 2009), but studies in which expression of all three isoforms was analysed simultaneously are scarce. Recently, Park *et al.* (Park *et al.*, 2011) demonstrated that nml- and nm-MLC2 are involved in maintenance of cellular integrity and stabilization of MHC IIs and ELCs. The role of the third MLC2 member, sm-MLC2, was not investigated in that study.

Could there be a distinctive role in the regulation of cell motility or cell morphodynamics for any of the three MLC2 variants? The association to actin fibres in migrating interphase cells was seen for all MLC2 forms alike and matches commonly reported endogenous MLC2 and myosin II localization (Naumanen *et al.*, 2008), indicating that the YFP-tagged MLC2 variants incorporate normally into myosin II complexes and filaments. We cannot exclude, however, that small local concentration differences in MLC2 variants may exist and play a role in for example leading versus trailing edge functioning (Vicente-Manzanares *et al.*, 2009). During metaphase, we observed MLC2-YFP at the poles of the mitotic spindle, the so-called polar crescents (Zeng,

2000). This localization has been reported for diphosphorylated MLC2, but the MLC2 isoforms involved were not specified (Yamashiro *et al.*, 2003).

Actin involvement in spindle assembly and positioning is generally accepted (Kunda and Baum, 2009) and it is likely that actin and myosin II act in concert at these spindle sites. In addition, there are indications that myosin II activity is required for positioning of duplicated centrosomes (Hashimoto *et al.*, 2008; Rosenblatt *et al.*, 2004) and subsequent chromosome separation (Komatsu *et al.*, 2000). Claims that myosin II is located at the mitotic spindle (Fujiwara and Pollard, 1978) support the hypothesis that control over its activity - presumably by association to distinct MLC2 variants - may be necessary. Further study is thus needed to reveal functional significance of individual MLC2 isoforms - and the specific actin-myosin II structures in which they co-operate - at polar crescents.

Comparison of transcript and protein isoform levels of MLC2 in cells of our MEF panel revealed interesting features. In Ras-transformed cells, we found higher nm-MLC2 transcript levels, but the protein levels remained constant, independent of growth rate. This suggests to us that expression of nm-MLC2 in these cells is primarily regulated at the translational level. Findings with sm- and nml-MLC2 are more difficult to interpret, since these two isoforms cannot be separated at the protein level. As the level of sm-MLC2 RNA is decreased but the level of nml-MLC2 RNA is maintained, reduced synthesis of sm-MLC2 gene products may account for the loss of signal intensity for the combined sm/nml-MLC2 protein in transformed cells with highest growth rates, but we cannot exclude other types of effects. Our data are in agreement with published findings (Kumar and Chang, 1992) on a decrease in sm-MLC2 transcript levels upon transformation of human fibroblasts. In contrast, examination of the Gene Expression Omnibus (GEO) indicated that sm-MLC2 gene expression was not affected by Ras-transformation (GDS3456, GDS3455, GDS1306). In the same data sets nm-MLC2 expression was found to be downregulated upon Ras-transformation, which also contradicts our findings. The nml-MLC2 gene is not included on Affymetrix platforms, but one study describes an upregulation of nml-MLC2 in Ras-transformed cells (Cobellis *et al.*, 2001). Kumar *et al.* (Kumar and Chang, 1992) claim that reduced sm-MLC2 expression depends on the mechanisms leading to transformation. It would therefore be interesting to investigate MLC2 expression in primary MEFs transformed via alternative mechanisms or with an altered growth rate without being transformed.

We noted a significant increase in sm-MLC2 transcript levels upon inhibition of Ras activity in Ras-transformed MEFs using Salirasib. Noticeably, Ras inhibition resulted in a ~1.5-fold increase, while sm-MLC2 transcript levels in non-transformed cells were ~100-fold higher than in transformed cells in the MEF cell-panel. This indicates that the effects of Salirasib were only partial, presumably because a

genuine non-transformed state in Ras-LP cells cannot be reached anymore using this single compound. This assumption is strengthened by the observation of an altered doubling time of Salirasib-treated cells, which is still significantly lower than that of untransformed cells in the panel. The effect of Salirasib was obviously not sufficient to cause a decrease in nm-MLC2 transcript levels.

Two characteristics of transformed cells - invasiveness and a disorganization of the cytoskeleton (Gimona, 2008) - may couple to MLC2 functions. Cells with myosin II complexes that contain high levels of nm-MLC2 could have a higher invasive capacity and a less organized cytoskeleton. For nm-myosin II it is known that different types of complexes (containing either MHC-NM IIA, B or C; Conti, 2008) have a different *in vitro* motility. For other contractile proteins a change in expression levels was also observed upon transformation (Cobellis *et al.*, 2001). Likely different MLC2 variants will also influence cell motility behaviour and other myosin II characteristics. Testing this hypothesis will require careful imaging of migrating cells expressing individual MLC2 variants.

In sum, we describe here for the first time an examination of specific characteristics of the three nonsarcomeric MLC2 isoforms at transcript and protein levels. Homology between these MLC2 genes is best explained by a combination of gene duplication and gene conversion events. We provide experimental evidence that expression levels are related to growth rate and suggest a role for MLC2 isoforms in tumourigenic transformation. To elucidate whether this role is active or passive, sophisticated tools to manipulate growth rate and oncogenic transformation will be required. Data reported here will contribute to better awareness about the complexity of MLC2 biology and ultimately help to provide detailed insight into the biological significance of MLC2 isoforms in mammals.

Acknowledgments

C-5120 primary human fibroblasts were kindly provided by F. Valsecchi (Dept. Biochemistry, NCMLS, Nijmegen). Dombi primary keratinocytes were kindly provided by D. Rodijk-Olthuis (Dept. Dermatology, NCMLS, Nijmegen). Immortalized iliaca and aorta smooth muscle cells were a kind gift from G. van Eijs (Dept. Genetics and Cell Biology, Maastricht University, Maastricht, The Netherlands). Mouse mammary tumour cells were kindly provided by A. Khalil (Dept. Cell Biology, NCMLS, Nijmegen). We are grateful to W. de Jong for helpful discussion on interpretation of evolutionary data. This work was financed by a RUNMC grant (2006-12) to WJAJH, DGW and BW.

SUPPLEMENTARY MATERIALS AND METHODS

Table S1. Primers used in this study. Sequences of primers used to generate constructs encoding untagged human and mouse *sm-*, *nm-* and *nml-MLC2* proteins (pSG8ΔEcoRI constructs) and C-terminally YFP-tagged *sm-*, *nm-* and *nml-MLC2* proteins (pEYFP-N1-ΔATG constructs). In the forward primers EcoRI sites are in *italic* and start codons are underlined. In the reverse primers XhoI and BamHI sites are in *italic*.

Construct	Forward primer (5' → 3')	Reverse primer (5' → 3')
pSG8ΔEcoRI-h/m-nm	CAGGAATTCCGCCACCATGTC- GAGCAAAAAGC	GAGCTCGAGTCAGTCATCTTT- GTCTTTCGC
pSG8ΔEcoRI-m-nml	AAAGAATTCATTTAACC GCCAC- CATGTCT	AAACTCGAGCGGGAG- CAATGGGCTGGA
pSG8ΔEcoRI-m-sm	AAAGAATTCATTTAACC GCCACCAT- GTCGAGCAAGAGAGCCAAGG	AAACTCGAGGATGGGGTCTAG- GCACTG
pSG8ΔEcoRI-h-nml	AAAGAATTCATTTAACC GCCACCAT- GTCGAGCAAAAAGAA	AAACTCGAGAAGGAACGTTTG- GCTGGAATTT
pSG8ΔEcoRI-m-sm	AAAGAATTCATTTAACC GCCACCAT- GTCCAGCAAGCGGGCCAAAG	AAACTCGAGGGCTGGGGTGT- CAGGG
pEYFP-N1-ΔATG-h/m-nm	CAGGAATTCCGCCACCATGTC- GAGCAAAAAGC	GGTGGATCCCCGTCATCTTT- GTCTTTCGCGC
pEYFP-N1-ΔATG-m-nml	CAGGAATTCCGCCACCATGTCTAG- CAA	GGTGGATCCCCGTCATCTTT- GTCTTTCGCGC
pEYFP-N1-ΔATG-m-sm	CAGGAATTCCGCCACCATGTC- GAGCAA	GGTGGATCCCCGTCGTCCTT- GTCCTTGCGC
pEYFP-N1-ΔATG-h-nml	CAGGAATTCCGCCACCATGTC- GAGCAA	GGTGGATCCCCGTCATCTTT- GTCTTTGGCTCC
pEYFP-N1-ΔATG-h-sm	CAGGAATTCCGCCACCATGTC- GAGCAA	GGTGGATCCCCGTCGTCCTT- TATCCTTGCGC

Gene duplication and conversion events shaped three homologous, differentially expressed MLC2 genes

Table S2. Accession numbers. NCBI accession numbers of MLC2 sequences used to construct the phylogenetic tree in Fig. 1 and alignment in Fig. S1. n.a. = not applicable.

Organism	MLC2 isoform	NCBI accession number
<i>Dictyostelium discoideum</i>	n.a.	M25251.1
<i>Amphimedon queenslandica</i>	n.a.	XM_003383919
<i>Caenorhabditis elegans</i>	n.a.	NM_065299.3
<i>Drosophila melanogaster</i>	n.a.	NM_078502.2
<i>Saccoglossus kowalevskii</i>	n.a.	XM_002740053
<i>Ciona intestinalis</i>	n.a.	XM_002123773
<i>Branchiostoma floridae</i>	n.a.	XM_002593491
<i>Xenopus tropicalis</i>	sm	NM_001102780.1
	nm	NM_001004813.1
<i>Gallus gallus</i>	sm	NM_205278
	nm	XM_001233328*
	nml	NM_205341
<i>Mus musculus</i>	sm	NM_172118
	nm	NM_023402.2
	nml	NM_026064.2
<i>Homo sapiens</i>	sm	NM_006097
	nm	NM_001144944
	nml	NM_006471
<i>Tetraodon nigroviridis</i>	sm	CR701929
	nm-type (Chrom6)	**
	nm-type (Un_random)	***

Genetic drift and conversion events shaped three homologous, differentially expressed MLC2 genes

<i>Danio rerio</i>	mlc9r	NM_001006027
	myl9	NM_213212.1
	myl9l	NM_214699.1
	myl12.2	NM_001130589.1
<i>Taeniopygia guttata</i>	sm	XM_002189773
	nm	XM_002192655
	nml	XM_002192757.1
<i>Bos taurus</i>	sm	NM_001075234
	nm	XM_002706947
	nml	NM_001015640.2
<i>Anolis carolinensis</i>	sm	XM_003220495
	nm	****
	nml	XM_003219685

* The N-terminal 115 amino acids of this sequence correspond to the N-terminal part of the *G. gallus* nm-MLC2 sequence. The remaining 57 C-terminal amino acids are located on chromosome 2 (+), bp 103992390-103992561.

** This nm-type MLC2 encoding sequence can be found at chromosome 6, positions 5,430,576 (+) to 5,432,095 (+)

*** This nm-type MLC2 encoding sequence can be found at chromosome Un_random positions 20,812,488 (-) to 20,813,247 (-).

**** C-terminal sequence of *Anolis carolinensis* nm-MLC2 can be found on scaffold GL343470.1, positions 472422 to 472502 (+) and 472546 to 472731 (+).

Gene duplication and conversion events shaped three homologous, differentially expressed MLC2 genes

		80	*	100	*	120
D. discoideum :	KQFVFVMDQIDMFASADTTKSGAGPEPMS	MSRRMKQTSNFIQLNFTKPTFG	NG			
A. queenslandica :	ASLIGKQPSADVMDMEAGP	P	INFTMFLITMFGKLTGDPEDVIRNAFACFDEAG	OV		
C. elegans :	ASLIGKVEQFIDSMINEAGAP	P	INFTMFLITMFGKLTGDPEDVIRNAFACFDE	DNSG		
D. melanogaster :	ASLIGNKPTDYLDDMMNEAGP	P	INFTMFLITMFGKLTGDPEDVIRNAFACFDE	MG		
S. kowalevskii :	ASLIGNKPTDYLDDMMNEAGP	P	INFTMFLITMFGKLTGDPEDVIRNAFACFDE	AG		
C. intestinalis :	ASLIGKVSDDVILKMCAGAP	P	INFTMFLITMFGKLTGDPEDVIRNAFACFDE	GTG		
B. floridae :	ASLIGNKPTDYLDDMMNEAGP	P	INFTMFLITMFGKLTGDPEDVIRNAFACFDE	DGSG		
D. rerio mC9r :	ASLIGNKPTDYLDDMMNEAGP	P	INFTMFLITMFGKLTGDPEDVIRNAFACFDE	AG		
D. rerio myl9r :	ASLIGNKPTDYLDDMMNEAGP	P	INFTMFLITMFGKLTGDPEDVIRNAFACFDE	GS		
D. rerio myl9r :	ASLIGNKPTDYLDDMMNEAGP	P	INFTMFLITMFGKLTGDPEDVIRNAFACFDE	GS		
D. rerio myl12.2 :	ASLIGNKPTDYLDDMMNEAGP	P	INFTMFLITMFGKLTGDPEDVIRNAFACFDE	GS		
T. nigroviridis sm :	ASLIGNKPTDYLDDMMNEAGP	P	INFTMFLITMFGKLTGDPEDVIRNAFACFDE	GS		
T. nigroviridis nm :	ASLIGNKPTDYLDDMMNEAGP	P	INFTMFLITMFGKLTGDPEDVIRNAFACFDE	GS		
T. nigroviridis nml :	ASLIGNKPTDYLDDMMNEAGP	P	INFTMFLITMFGKLTGDPEDVIRNAFACFDE	GS		
X. tropicalis sm :	ASLIGNKPTDYLDDMMNEAGP	P	INFTMFLITMFGKLTGDPEDVIRNAFACFDE	GS		
X. tropicalis myl2b :	ASLIGNKPTDYLDDMMNEAGP	P	INFTMFLITMFGKLTGDPEDVIRNAFACFDE	GS		
G. gallus sm :	ASLIGNKPTDYLDDMMNEAGP	P	INFTMFLITMFGKLTGDPEDVIRNAFACFDE	GS		
G. gallus nml :	ASLIGNKPTDYLDDMMNEAGP	P	INFTMFLITMFGKLTGDPEDVIRNAFACFDE	GS		
G. gallus nm :	ASLIGNKPTDYLDDMMNEAGP	P	INFTMFLITMFGKLTGDPEDVIRNAFACFDE	GS		
M. musculus sm :	ASLIGNKPTDYLDDMMNEAGP	P	INFTMFLITMFGKLTGDPEDVIRNAFACFDE	GS		
M. musculus nml :	ASLIGNKPTDYLDDMMNEAGP	P	INFTMFLITMFGKLTGDPEDVIRNAFACFDE	GS		
M. musculus nm :	ASLIGNKPTDYLDDMMNEAGP	P	INFTMFLITMFGKLTGDPEDVIRNAFACFDE	GS		
H. sapiens sm :	ASLIGNKPTDYLDDMMNEAGP	P	INFTMFLITMFGKLTGDPEDVIRNAFACFDE	GS		
H. sapiens nml :	ASLIGNKPTDYLDDMMNEAGP	P	INFTMFLITMFGKLTGDPEDVIRNAFACFDE	GS		
H. sapiens nm :	ASLIGNKPTDYLDDMMNEAGP	P	INFTMFLITMFGKLTGDPEDVIRNAFACFDE	GS		

4

Figure S1: Sm-, nm- and nml-MLC2 are highly conserved throughout evolution in a wide variety of species. Alignment of MLC2 protein sequences used to construct the evolutionary model in Fig. 1E. White characters on a black background represent residues conserved in all aligned proteins; white characters on a dark grey background represent the most common amino acid at a certain position (>50% occurrence); black characters on a light grey background represent amino acids at a certain position with an occurrence of $\leq 50\%$.

Gene duplication and conversion events shaped three homologous, differentially expressed MLC2 genes

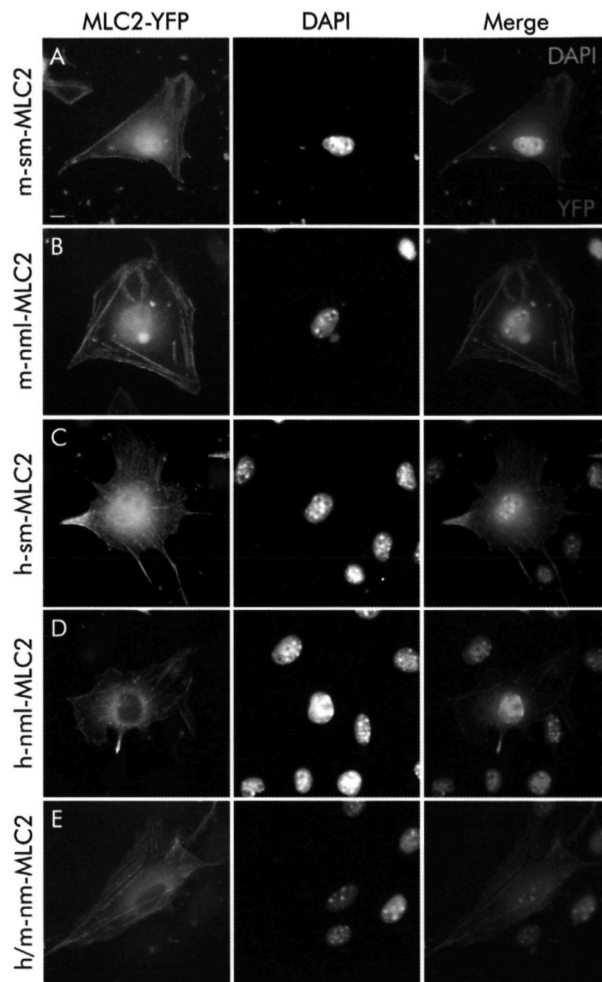


Figure S2: Localization of human and mouse sm-, nm- and nml-MLC2 in B16F10 cells during interphase. YFP-tagged human (h) or murine (m) sm-, nm- and nml-MLC2 were expressed in mouse B16F10 cells using transient transfection. Cells were fixed ~20 h after transfection. Nuclear DNA was counterstained with DAPI. All MLC2 isoforms localized to stress fibres. Bar = 5 μ m.

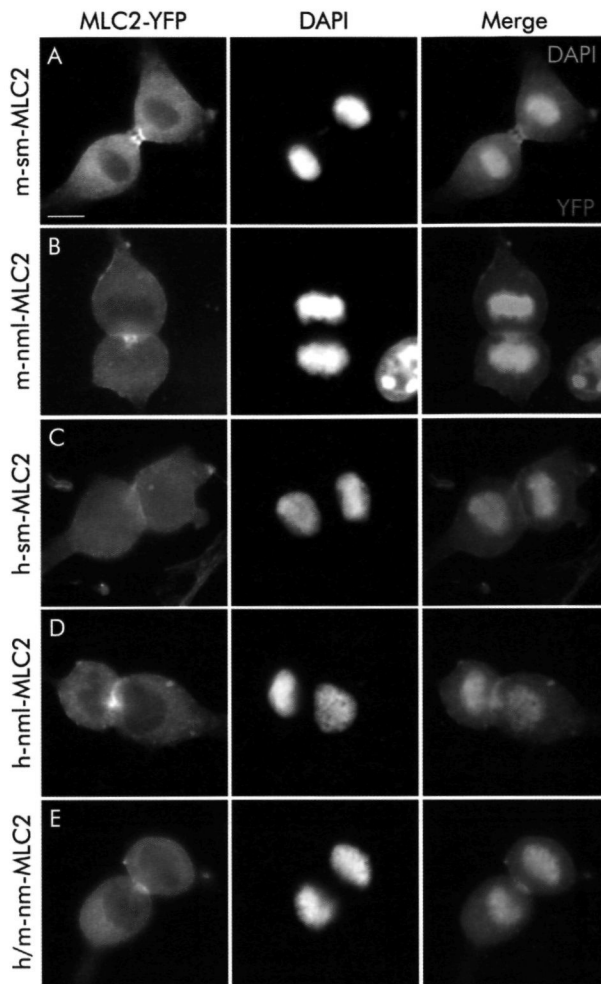


Figure S3: Localization of human and mouse sm-, nm- and nml-MLC2 in B16F10 cells during cytokinesis. YFP-tagged human (h) or murine (m) sm-, nm and nml-MLC2 were expressed in B16F10 cells using transient transfection. Cells were fixed ~20 h after transfection. Nuclear DNA was counterstained with DAPI. All MLC2 proteins displayed a cytoplasmic localization with an enrichment in the midzone. Bar = 5 μ m.

Chapter 5

Lats2 contains a phosphorylation-regulated
PDZ domain-binding motif

Lieke Gerrits^a, Lieke C.J. van den Berk^a, Piet E.J. van Erp^b, Jan T.G. Schepens^a, Edwin P.J.G. Cuppen^a, Bé Wieringa^a, Derick G. Wansink^a, Wiljan J.A.J. Hendriks^a

^aDepartment of cell biology and ^bDepartment of dermatology, Nijmegen Centre for Molecular Life Sciences, Radboud University Nijmegen Medical Centre, Nijmegen, The Netherlands.

[illegible]

ABSTRACT

The mammalian serine/threonine kinase Lats2 is a potent cell cycle regulator. Correct functioning of its *Drosophila* homologue, the tumour suppressor warts/lats, requires phosphorylation of a C-terminal tyrosine residue. We describe here that in mouse Lats2 this penultimate residue (Y1041) resides within a C-terminal PDZ domain-binding motif (PDZ-BM) and can be phosphorylated *in vivo*. Presence of the PDZ-BM and its modification by phosphorylation impacted on a canonical interaction with PDZ domains, but did not affect Lats2 kinase activity or subcellular localization. Overexpression of wild type Lats2 in HeLa cells resulted in a marked reduction of cells in G2 and M phase and deletion of the PDZ-BM exacerbated this effect. Our findings point to a role for the PDZ-BM in cell cycle regulation, presumably mediated via protein interactions that depend on its phosphorylation status.

Lats2 contains a phosphorylation regulated PDZ domain-binding motif

5

INTRODUCTION

Lats2 (Large tumour suppressor 2) is a mammalian homologue of *Drosophila* warts/lats, and member of the NDR family of the AGC (protein kinase A/PKG/PKC) group of protein kinases (Hergovich *et al.*, 2006b; Pearce *et al.*, 2010; Tamaskovic *et al.*, 2003a). Activation of AGC kinases involves phosphorylation of two highly conserved regulatory elements, the hydrophobic phosphorylation motif (Yang *et al.*, 2002b) and the activation segment (Parker and Parkinson, 2001). The hydrophobic phosphorylation motif in NDR kinases is located C-terminal of the catalytic domain (Yang *et al.*, 2002b) and is phosphorylated by MST (mammalian sterile 20-like) kinase (Chan *et al.*, 2005a). The activation segment in NDR kinases (Hergovich and Hemmings, 2009; Tamaskovic *et al.*, 2003b) lies within the catalytic domain and is phosphorylated by autophosphorylation. Full activation of these kinases also requires release of inhibition by the auto-inhibitory sequence, which is located in a 30-60 amino-acid insertion between kinase subdomains VII and VIII characteristic for NDR kinases (Bichsel *et al.*, 2004). For Lats2 this conformational change is induced by binding of co-activator MOB (Mps one binder) to a conserved N-terminal sequence, called the SMA (S100B and MOB association) domain (Hergovich *et al.*, 2006a; Yabuta *et al.*, 2007).

Lats2 is a component of the Salvador-Warts-Hippo pathway (Dong *et al.*, 2007; Hergovich and Hemmings, 2009; Zhao *et al.*, 2007), which is involved in mammalian tumourigenesis (Chan *et al.*). In prostate (Powzaniuk *et al.*, 2004), esophageal (Lee *et al.*, 2009), breast (Takahashi *et al.*, 2005) and gastric cancer (Cho *et al.*, 2009), down-regulation of Lats2 expression was observed. Also a role for Lats2 in the development of testicular germ cell tumours has been proposed (Voorhoeve *et al.*, 2006). Furthermore, Lats2 was found to be involved in the regulation of various steps of the cell cycle, such as G2/M transition (Kamikubo *et al.*, 2003), G1/S transition (Li *et al.*, 2003) and completion of cytokinesis (Yabuta *et al.*, 2007). Lats2 has also been implicated in the induction of apoptosis (Kamikubo *et al.*, 2003; Ke *et al.*, 2004; Kuninaka *et al.*, 2005), centrosome duplication and maintenance of mitotic fidelity and genomic stability (McPherson *et al.*, 2004). Together, these data strongly suggest that deregulation of Lats2 contributes to tumourigenesis.

In *Drosophila*, phosphorylation of a single tyrosine residue within the highly conserved warts/lats C-terminus was found to be critical for proper functioning *in vivo* (Stewart *et al.*, 2003). Expression of a warts/lats mutant protein that lacked this phosphorylation site was insufficient to rescue lethality and large tissue phenotypes that were observed in *lats* mutant flies. For human Lats1 it was demonstrated that it binds via its C-terminus to the PDZ (acronym of PSD-95, Discs Large and Zonula Occludens 1) domain of the pro-apoptotic serine protease Omi/HtrA2, thereby enhancing Omi/

Lats2 contains a phosphorylation-regulated PDZ domain-binding motif

5

HtrA2 protease activity and contributing to the onset of apoptosis (Kuninaka *et al.*, 2005). PDZ domains are frequently occurring protein-protein interaction modules that regulate various cellular signalling processes through sequence-specific binding to a PDZ-binding motif (PDZ-BM) in the C-terminus of their target proteins (Jelen *et al.*, 2003). Four classes of PDZ-BMs can be discerned based on the type of amino acids at positions P⁻³ to P⁰ (Vaccaro and Dente, 2002).

We describe here that -in analogy to Lats1- also Lats2 can interact with PDZ domains via its C-terminal PDZ-BM. The Lats2 PDZ-BM contains a highly conserved tyrosine residue (Tyr-1041) that is amenable to phosphorylation. Cell transfection studies show that presence and phosphorylation status of this site impact on the interaction potential of Lats2 with PDZ domains and on Lats2-induced cell cycle arrest.

Lats2 contains a phosphorylation-regulated PDZ domain-binding motif

5

Yeast two-hybrid assay

Interaction-trap vectors and yeast strain EGY48 were kindly provided by Dr. Roger Brent and colleagues (Massachusetts General Hospital, Boston, MA). Construction of the PTP-BL PDZ domain-encoding bait plasmids has been described (Cuppen *et al.*, 1998). Prey construct hLats2-Cterm Δ C3 was made by PCR using clone hLats2-Cterm as a template and the reverse oligonucleotide 5'-CCCTCGAGTCAAGGCTGGCAGCCTTCAGT-3' (XhoI restriction site in bold) in combination with a pJG4-5 forward primer. The EcoRI-XhoI restriction fragment of the resulting amplicon was subcloned in pJG4-5. The prey construct encoding the mouse peptide corresponding to hLats2-Cterm was made by PCR using mouse EST clone W81967 as template and oligonucleotide 5'-GGGAATTCGTGGATGAAGAAAGCCCC-3' (EcoRI site in bold) in combination with a T3 primer. The resulting PCR product was digested with EcoRI and XhoI and subcloned in EcoRI/XhoI digested pJG4-5. All constructs generated by PCR were verified by DNA sequencing.

For two-hybrid interaction trap assays (Cuppen *et al.*, 1998; Gyuris *et al.*, 1993) plasmids were introduced in yeast strain EGY48 (MATa trp1 ura3 his3 LEU2::pLexAop6-LEU2) containing plasmid pSH18-34, which includes the reporter lacZ gene, and tested for an interaction as detected by growth and blue coloring on HUTL⁻ (lacking histidine, uracil, tryptophan and leucine) minimal agar-plates containing 2% galactose, 1% raffinose and 80 μ g/ml X-gal, buffered at pH 7.0.

Mammalian expression plasmids

Expression construct BL-PDZ 1-5 (encoding the five PDZ domains of PTP-BL and an N-terminal VSV-tag) has been described elsewhere (Cuppen *et al.*, 1998). Mammalian expression plasmid pSG8-VSV-mLats2 was constructed by subcloning a PCR-generated mouse Lats2 (mLats2) cDNA fragment (nucl. pos. 134-3262 in acc. nr. NM_015771) in-frame into BamHI-digested pSG8-VSV vector (Cuppen *et al.*, 1998). The GST-mLats2C mammalian expression plasmid was constructed by inserting a PCR-generated fragment, spanning pos. 2929-3262 of mouse Lats2 cDNA, into BamHI-digested pEBG vector (Tanaka *et al.*, 1995). mLats2- Δ C3 constructs were generated using 5'-CCGCTCGAGTTACGGCTGGCAGCCCTC-3' (XhoI restriction site in bold) as antisense primer. In a similar manner, the Y1041F mutation was introduced into full-length as well as C-terminal mLats2 constructs by performing a PCR using antisense primer 5'-TTGGATCCGGCTTACACGAACACCGGCTGGC-3' (BamHISite and Y1041F mutation site in bold) in combination with appropriate mLats2 sense primers. The Y1041E mutation was introduced into full-length mLats2 by performing a PCR using antisense primer 5'-CCACTAGTGGATCCTTACACCTCCACCGGCTGGCAGCCCTC-3' (SpeI

Lats2 contains a phosphorylation-regulated PDZ domain-binding motif

site and Y1041E mutation in bold, *Bam*HI site underlined). The full-length mLats2 variants were cloned in frame into pEYFP-C1 and pEBG vectors. All expression constructs generated by PCR were verified by DNA sequence analysis to exclude undesired mutations.

Tissue culture and transient cell transfections

COS-1 (ATCC #CRL1650) and HeLa cells (ATCC #CCL-2) were cultured in DMEM (Gibco/Invitrogen, Paisley, UK) supplemented with 10% fetal calf serum (FCS) at 37°C and 7.5% CO₂. Transfection of COS-1 cells was performed using DEAE-Dextran as described (van Ham *et al.*, 2003). COS-1 cells were treated with 1 μM okadaic acid for 1h before lysis in case lysates were used for an *in vitro* kinase assay. For determination of tyrosine phosphorylation of the mLats2 PDZ-BM, cells were treated with 1 mM BpV(phen) 20 minutes prior to lysis (see below). HeLa cells were transfected using jetPEI™ reagent (Polyplus-transfection, Illkirch, France) according to the manufacturer's instructions.

GST pull-down and immunoprecipitation

GST pull-down was performed by incubating Glutathione-Sepharose 4B beads with cleared lysates of COS-1 cells expressing GST-tagged proteins. To this end, cells were washed once with ice-cold PBS and lysed in ice-cold lysis buffer (50 mM Tris-HCl, pH 7.5; 150 mM NaCl; 1% NP-40; 25 mM NaF; 1 mM Na₄P₂O₇; 0.1 mM NaVO₃; 2 μM Microcystin LR (Alexis Biochemicals/Enzo Life Sciences, Farmingdale, NY), 1 mM PMSF and protease inhibitor cocktail (Roche, Basel, Switzerland)) 24-48h after transfection. Cell debris was pelleted by centrifugation for 30 minutes at 15,000 rpm. Beads and cleared lysates were incubated overnight rotating at 4°C. Subsequently, beads were washed once in lysis buffer containing 0.5 M NaCl, once in lysis buffer, and finally once in 50 mM Tris-HCl, pH 7.5; 1 mM DTT; 1 mM benzamidine before use in an *in vitro* kinase assay.

Immunoprecipitation of protein complexes from cleared lysates of transfected COS-1 cells was performed in a similar way as GST pull-down, but now antibody-coupled protein A beads were used. Either polyclonal anti-GFP antiserum (Cuppen *et al.*, 2000; van den Berk *et al.*, 2004) or monoclonal anti-VSV antibody (P5D4; Kreis, 1986) was coupled to the beads by overnight rotation at 4°C in PBS. After overnight immunoprecipitation, beads were washed five times with PBS containing 1% NP-40 and resuspended in 25-40 μl sample buffer (100 mM Tris-HCl, pH 6.8; 200 mM DTT; 4% SDS; 20% glycerol; 0.2% bromophenol blue) before being prepared for Western blotting.

Lats2 contains a phosphorylation regulated PDZ domain-binding motif

Western blotting

Proteins in sample buffer were boiled for five minutes and loaded onto an SDS-polyacrylamide gel for size separation by electrophoresis. Subsequently, proteins were transferred to a PVDF membrane (Millipore, Billerica, MA) by electro-blotting. Membranes were blocked in 5% (w/v) non-fat dry milk in TBS-T (10 mM Tris-HCl; pH 8.0; 150 mM NaCl; 0.05% Tween-20 (Sigma-Aldrich; St. Louis, MO)) for 30-60 minutes. Monoclonal anti-GFP antibody (sc-9996, Santa Cruz Biotechnology, CA, dilution 1:5,000) and polyclonal anti-VSV antibody (A190-131A, Bethyl laboratories, Montgomery, TX; 1:1,000) were used to detect YFP- and VSV-tagged proteins, respectively. Monoclonal antibody pY-20 (Santa Cruz Biotechnology, sc-508, dilution 1:1,000) was used to detect tyrosine-phosphorylated proteins.

Anti-VSV and anti-GFP antibodies were diluted in blocking buffer. pY-20 was applied in TBS containing 1% (w/v) BSA and 1% (w/v) milk powder. Membranes were incubated with primary antibodies overnight at 4°C and then washed three times with TBS-T (or TBS for the pY-20 antibody). Subsequently, the appropriate secondary antibodies - goat anti-mouse IRDye® 800 and/or goat anti-rabbit IRDye® 680 (LI-COR Biosciences (Lincoln, NE), dilution 1:10,000) - were applied and incubation was for 1 h at room temperature. Following three successive washes with TBS-T (or TBS for the pY-20 antibody), detection and quantification of immunoreactive bands were done on an Odyssey infrared Imaging System (LI-COR Biosciences).

In vitro kinase assay

The kinase assay was essentially done as described (Wansink *et al.*, 2003). GST-tagged proteins were captured by pull-down with Glutathione-Sepharose 4B beads. At the final wash after GST pull-down bead-coupled proteins were aliquoted in the desired number of reactions, final wash buffer was removed after centrifugation and beads were taken up in 40 µl kinase assay buffer (50 mM Tris-HCl, pH 7.5; 10 mM MgCl₂; 2 mM MnCl₂; 1 mM DTT; 1 µM PKA inhibitor peptide (Bachem, Bubendorf, Switzerland); 1 mM PMSF; 1 mM benzamidine; 2 µM Microcystin LR). Then 30 µM substrate peptide (CGGGGKKRNRRLSVA, representing a general artificial substrate for NDR kinases (Millward *et al.*, 1998)) was added. The reaction was started by adding 5 µl 0.5 mM ATP containing ~2 µCi [γ -³²P]ATP (specific activity: 3000 Ci (111 TBq)/mmol), continued for 1 h at 30°C while mixing, and stopped by adding 5 µl 0.5 M EDTA. To determine the level of transphosphorylation, beads were pelleted by centrifugation and 30 µl of the supernatant, containing the substrate peptide, was spotted on P81 phosphocellulose paper (Whatmann, Maidstone, UK). Filters were washed five times for five minutes in 1% phosphoric acid, once in acetone and then air dried. [³²P]-incorporation was determined in a liquid scintillation counter. To determine the level of autophosphorylation and protein input levels, the remaining beads were boiled in

sample buffer and extracts were run on SDS-PAGE and blotted onto PVDF membrane. The membrane was wrapped with SaranWrap and exposed to a PhosphorImager K-screen (Bio-Rad, Berkeley, CA) for 3 h. Phosphate-radiolabelled protein bands were detected using a Bio-Rad personal Fx PhosphorImager scanning apparatus and analysed using Quantity One software (Bio-Rad). Afterwards, the membrane was incubated with blocking buffer and subsequently with anti-GST antiserum (Cuppen *et al.*, 2000; van den Berk *et al.*, 2004; 1:5,000), and immunodetection was performed as described.

Flow cytometry

Adherently growing HeLa cells were detached by trypsinization and collected by centrifugation 24 h after transfection. Following three washes with PBS, cells were fixed for at least three hours in ice-cold 70% ethanol at -20°C. Cells were then washed twice with PBS and incubated for 20 minutes in DNA staining buffer (20 µg/ml propidium iodide, 0.2 mg/ml RNase A in PBS) at 37°C and stored o/n at 4°C. Cells were analysed for GFP expression level and DNA content on an EPICS Elite flow cytometer (Coulter, Luton, UK). An air-cooled argon laser (20 mW, 488 nm) was used for propidium iodide excitation. For detection, a 630-nm long-pass filter (red signal) and a photomultiplier were used. The area-to-peak ratio of the red signal combined with scatter parameters was used to exclude debris for further analysis and to discriminate between diploid cells, doublets and tetraploid cells. GFP positive and GFP negative cells were measured in the cell population from which debris and doublets were excluded. As a control, lymphocytes were measured and the data rate was set at 100 cells/s. Usually 10,000 events were measured. DNA histograms were constructed based on DNA content measured in the nuclei and were subsequently analysed using Modfit software (Verity Software House, Topsham, ME).

Fluorescence microscopy

Twenty-four hours after transfection, HeLa cells expressing YFP-tagged Lats2 protein variants were fixed for 20 minutes in 2% paraformaldehyde in 0.1 M phosphate buffer (pH 7.4). Following three washes with PBS, cells were mounted on glass slides using Mowiol supplemented with Dapi (0.6 µg/ml) and 2.5% sodium azide. Images were obtained using a Zeiss Axiophot2 fluorescence microscope (Zeiss, Thornwood, NY) equipped with an Axiocam MRm CCD camera and using Axio Vision 3.1 software (Zeiss).

Statistics

For statistical analysis of FACS experiments a two-tailed unpaired t-test was performed. To compare average auto- and trans-kinase activity a two tailed paired t-test was

used. Differences were considered significant when $p < 0.05$ (*: $p < 0.05$; **: $p < 0.01$; ***: $p < 0.001$). Statistical analyses were performed with GraphPad Prism 4 software. The number of replicates for each experiment is given in the figure legends.

5

Lats2 contains a phosphorylation-regulated PDZ domain binding motif

RESULTS

The C-terminus of Lats2 contains a PDZ-BM

Lats proteins from different organisms display extensive sequence variation, especially in regions outside the kinase domain (Hori *et al.*, 2000; Yabuta *et al.*, 2000). Their C-terminal residues, however, are highly conserved (Figure 1A). The ultimate three amino acids in *Drosophila* warts/lats, human and mouse Lats1 and Lats2 are Val-Tyr-Val, which matches the Φ/Ψ -X- Φ consensus sequence of a class II PDZ-BM in which Φ represents a hydrophobic residue, Ψ an aromatic residue and X any residue (Vaccaro and Dente, 2002). In order to verify PDZ domain-binding ability of the C-terminal -VYV_{COOH} motif of Lats2 we chose to use PTP-BL, a mouse protein tyrosine phosphatase that contains five PDZ-domains for which a broad and versatile binding ability – including class II target specificity– has been documented (van den Berk *et al.*, 2005; van den Berk *et al.*, 2007). Interactions were tested in a yeast two-hybrid setting. Using the ensemble of five PDZ domains of PTP-BL (BL-PDZ 1-5) as bait, a strong interaction was found with the C-terminal eighty amino acids of human and mouse Lats2 (hLats2-Cterm and mLats2-Cterm, respectively; Figure 1B). Deletion of the very last three residues of hLats2 (hLats2-Cterm Δ C3) fully eliminated this interaction, in line with a canonical PDZ-based interaction in which the C-terminal amino acids of hLats2 are essential for binding. Use of all five BL-PDZ domains separately as baits revealed that BL-PDZ-4 is responsible for hLats2 binding (Figure 1C). Together, these data demonstrate that the C-terminus of Lats2 represents a classical class II PDZ-BM.

The Lats2 PDZ-BM is subject to phosphorylation

Proper warts/lats functioning in *Drosophila* requires tyrosine phosphorylation of the conserved C-terminus (Stewart *et al.*, 2003). We therefore investigated whether the corresponding tyrosine in the PDZ-BM of mLats2 (Tyr-1041) is subject to phosphorylation as well. COS-1 cells expressing the YFP-tagged C-terminal portion of mLats2 were treated with phosphatase inhibitor BpV(phen) shortly before lysis and YFP-tagged proteins were immunoprecipitated and checked for phosphotyrosine content on Western blot using pY-20 antibody. As shown in Figure 2 (left panels) the mLats2 C-terminus was indeed strongly phosphorylated, whereas a Y1041F mutant version of this protein did not show any phosphorylation.

Multiple tyrosines in the 1042 amino-acids long mLats2 protein, including Tyr-1041, are predicted to be phosphoacceptor sites (NetPhos 2.0 Server; <http://www.cbs.dtu.dk/services/NetPhos/>). Two sites, which correspond to Tyr-81 and Tyr-272 in mLats2, have been experimentally identified in human Lats2 (Guo *et al.*, 2008; Moritz *et al.*, 2010) (www.phosphosite.org). To investigate the contribution of Tyr-1041 to overall mLats2 tyrosine phosphorylation, YFP-tagged full-length wild type mLats2 and

Lats2 contains a phosphorylation-regulated PDZ domain-binding motif

5

				GenBank ID	species
warts/lats	1091	KQPPDMTDDQAP	(Drosophila)	1105	NP_733403.1 drosophila
mLats1	1115	QHTSSDGNNRDL	(mouse)	1129	NP_034820.1 mouse
hLats1	1116	QNTGSEIKNRDL	(human)	1130	NP_004681.1 human
mLats2	1028	ADLEGAAEGCQP	(mouse)	1042	NP_056586.2 mouse
hLats2	1074	SDLVDQTEGCQP	(human)	1088	NP_055387.2 human

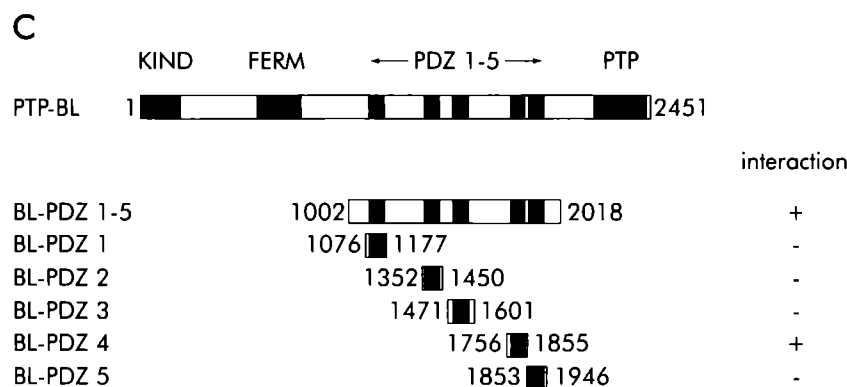
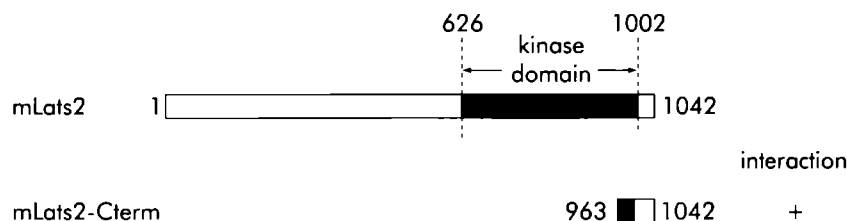
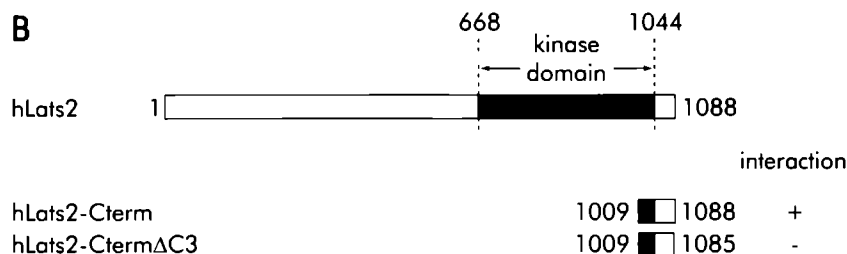


Figure 1: The C-terminus of Lats2 represents a PDZ-BM. (A) Alignment of the C-terminal 15 amino acids of *Drosophila* warts/lats, and mouse and human Lats1 and Lats2. Numbers flanking the sequences indicate amino acid positions in the full-length proteins (GenBank database entries are listed). (B) Schematic representation of Lats2 protein parts used in yeast two-hybrid analysis. PTP-BL PDZ 1-5 was used as bait and the 80 amino-acid long C-terminus of human Lats2 (hLats2-Cterm) or mouse Lats2 (mLats2-Cterm) served as preys. The hLats2 C-term fragment

lacking the three C-terminal residues (hLats2-Cterm Δ C3) was also used as prey. Position of the kinase domain in the full-length protein is indicated. (C) Schematic representation of different PTP-BL protein parts used as model baits for study of canonical interaction with hLats2-Cterm. KIND, FERM, PDZ, and PTP domains are indicated with black boxes and numbers refer to amino-acid positions in full-length PTP-BL (NM_011204). Interaction strengths observed in the two-hybrid assay are indicated with + (strong interaction) or - (no detectable interaction).

a Y1041F mutant were expressed in COS-1 cells. Following BpV(phen) treatment of cells and immunoprecipitation of YFP-tagged proteins, their phosphotyrosine content was determined on Western blot (Figure 2, right panels). Introducing the Y1041F mutation in full-length mLats2 caused a twofold reduction in signal strength when compared to wild type mLats2, strongly suggesting that the Tyr-1041 position is a major *in vivo* phosphorylation site in mLats2.

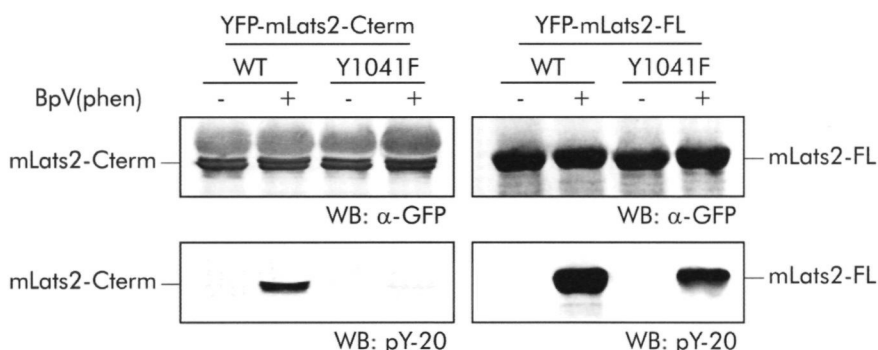


Figure 2: Lats2 Tyr-1041 is phosphorylated *in vivo*. COS-1 cells were transfected with constructs encoding a YFP-tagged C-terminal mLats2 fragment (left panels) or YFP-tagged full-length mLats2 (right panels). For both types of constructs wild type mLats2 (WT) and a mLats2-Y1041F mutant were used. Before being lysed, cells were either treated for 20 minutes with phosphatase inhibitor BpV(phen) (+) or left untreated (-). Following immunoprecipitation, Lats2 levels were detected on Western blot (WB) using an anti-GFP antiserum (top panels). Tyrosine phosphorylation levels in immunoprecipitates were detected using anti-phosphotyrosine antibody pY-20 (bottom panels).

Interaction between Lats2 and PDZ domains is regulated by phosphorylation of the PDZ-BM

Next, we examined whether phosphorylation of Tyr-1041 influenced binding of the mLats2 C-terminus to PDZ domains, again using the PDZ domains of PTP-BL as a

model. COS-1 cells were co-transfected with constructs encoding individual YFP-tagged mLats2 variants and the VSV-tagged PTP-BL segment spanning all five PDZ domains (VSV-BL-PDZ 1-5). Next to wild type mLats2 and its Y1041F mutant also a Y1041E mutant, in which Tyr-1041 is substituted by glutamic acid (Glu, to mimic constitutive phosphorylation) was included. Truncated mLats2 lacking its PDZ-BM (YFP-mLats2- Δ C3) served as a negative control. In addition, an enzymatically inactive (kinase dead) mLats2 mutant (YFP-mLats2-KD) was tested. Co-immunoprecipitation analysis revealed that the quantity of PDZ 1-5 segment captured by the mLats2-

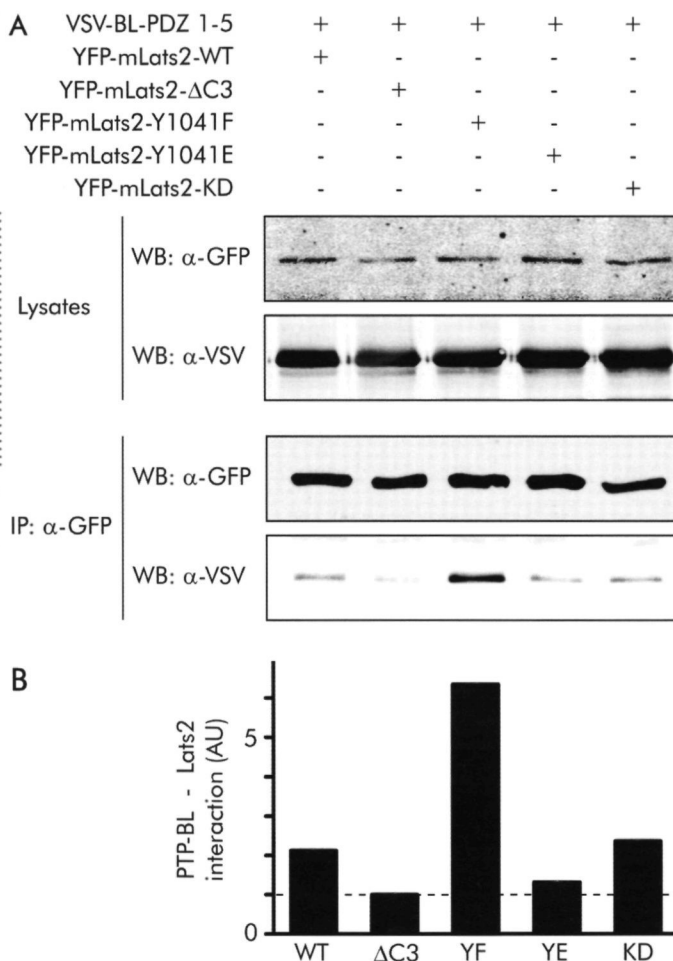


Figure 3: Tyr-1041 phosphorylation hampers Lats2 interaction with PDZ domains. (A) COS-1 cells were co-transfected with YFP-mLats2 and VSV-BL-PDZ 1-5 expression constructs and lysates were used for immunoprecipitation (IP) with polyclonal anti-GFP antiserum. Antibodies indicated on the left were used to detect proteins in lysates (upper two panels) and immunoprecipitates (bottom two panels) by Western blot (WB) analysis. (B) Quantification of the interaction capacity of the different mLats2 mutants and BL-PDZ 1-5 in arbitrary units (AU) as observed in (A). The ratio of co-precipitated BL-PDZ 1-5 versus the

corresponding amount of immunoprecipitated mLats2 was determined and values obtained were subsequently normalized to the value found for mLats2- Δ C3, which was set at 1. Representative images from one of two independent experiments are shown.

Y1041E mutant was close to background level, similar to that obtained with YFP-mLats2- Δ C3 as bait (Figure 3). YFP-mLats2-Y1041F, was at least six-fold more effective in co-precipitating VSV-BL-PDZ 1-5, outcompeting YFP-mLats2-WT by a factor of three (Figure 3). No difference in the amount of co-precipitated VSV-BL-PDZ 1-5 was observed when YFP-mLats2-KD and YFP-mLats2-WT were compared. Taken together, these data imply that PDZ domain binding to the mLats2 PDZ-BM is regulated through tyrosine phosphorylation of mLats2 Tyr-1041. Comparison of the binding efficiencies of wild type and Y1041F mutant mLats2 suggests that a considerable portion of mLats2 protein is phosphorylated under the conditions used here but it might also point to a preference by the PTP-BL PDZ moiety for phenylalanine over tyrosine at P⁻¹.

Lats2 kinase activity is not dependent on its PDZ-BM

Next, we investigated the possibility that the presence or phosphorylation status of Lats2 PDZ-BM influences Lats2 kinase activity and therewith its biological function. GST-mLats2 proteins were affinity purified from transfected COS-1 cells that had been treated with okadaic acid to trigger kinase activity (Millward *et al.*, 1999) and used in an *in vitro* kinase assay. GST-mLats2 variants were incubated in the presence of a substrate peptide (Millward *et al.*, 1998) and ³²P-labelled γ -ATP, and both trans- and autophosphorylation were measured. GST-mLats2-KD served as a negative control, revealing a low background signal that is likely attributable to activity of co-purifying kinases (Figure 4).

No significant differences in autophosphorylation were observed between mLats2 and different mutants tested (Figure 4A and B). Significant but small differences in transphosphorylation activity towards the substrate peptide were observed only for mLats2- Δ C3 (10% decrease) and mLats2-Y1041F (30% increase) when compared to mLats2-WT (Figure 4C). Together, these data suggest that Lats2 kinase activity is only marginally affected by presence or phosphorylation status of its PDZ-BM.

Lats2-induced G1/S cell cycle arrest is modulated by the Lats2 PDZ-BM

To investigate whether the PDZ-BM is of relevance for Lats2-induced cell cycle arrest (Kamikubo *et al.*, 2003; Li *et al.*, 2003), we expressed YFP-tagged wild type mLats2 (YFP-mLats2-WT) and YFP-mLats2- Δ C3 in HeLa cells and examined effects on cell cycle progression. YFP-mLats2-KD was taken along as control because it was reported not to induce a cell cycle arrest (Kamikubo *et al.*, 2003; Li *et al.*, 2003). Effects on cell proliferation were quantified based on flow-cytometric analyses of the DNA content of transfected cells, while the untransfected, YFP-negative fraction of cells was used for comparison. In line with published data (Li *et al.*, 2003) expression of YFP-mLats2-WT resulted in an increase of 11% in the proportion of cells in G0/G1 (Figure 5), indicative of increased arrest in G1- to S-phase transition or augmented exit from cell cycle.

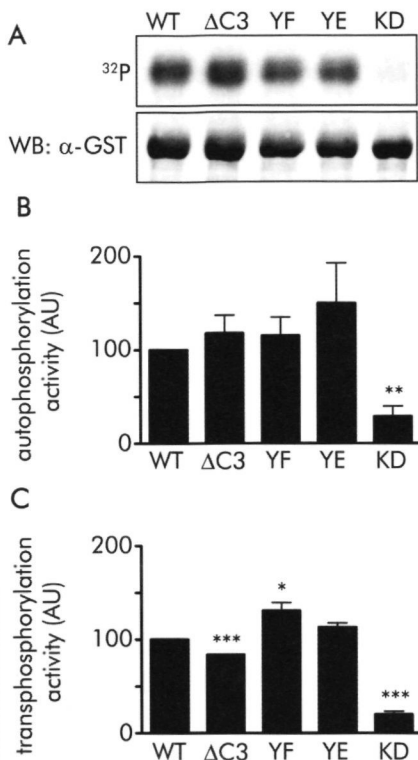
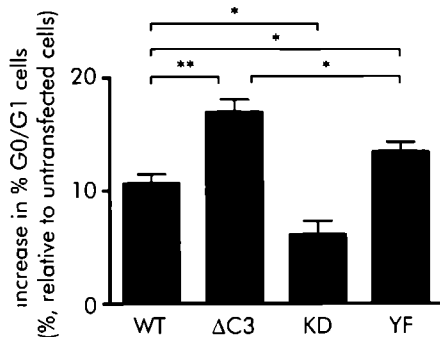


Figure 4: Lats2 kinase activity does not depend on its PDZ-BM. Purified GST-mLats2 proteins were used in an in vitro kinase assay. **(A)** Part of the kinase reaction was loaded on SDS-PAGE and ³²P-labeled GST-mLats2 proteins were detected with a phosphorimager screen to determine autophosphorylation activity (upper panel). Kinase input was verified on Western blot using an antibody against GST (lower panel). Images of a representative experiment are shown. **(B, C)** Autophosphorylation and transphosphorylation activity was expressed in arbitrary units (AU) and defined as the amount of phosphate incorporation in GST-mLats2 itself **(B)** or the peptide substrate **(C)** relative to the amount of GST-mLats2 input. For autophosphorylation and transphosphorylation activity the value calculated for GST-mLats2-WT was set at 100.

This effect depended on mLats2 kinase activity since a YFP-mLats2-KD-expressing cell population displayed an increase of only 6% in the proportion of cells in G0/G1 phase, probably reflecting effects of transfection and ectopic expression. Interestingly, YFP-mLats2-ΔC3 expression had a more pronounced effect, with 17% more cells arrested at G1/S. This indicates that the PDZ-BM is involved in modulation of Lats2-induced cell cycle effects.

Next, we investigated whether the phosphorylation status of Tyr-1041 would affect cell cycle progression, in further support of a role for the Lats2-PDZ-BM. The increase in G0/G1 cells was consistently less for mLats2-Y1041F than for mLats2-ΔC3. In the experiment shown in Figure 5 a higher percentage of G0/G1 cells was found when YFP-mLats2-Y1041F was expressed as compared to wild type protein, but this could not be reproduced in subsequent experiments. Effects of Tyr-1041 phosphorylation on Lats2-induced cell cycle arrest therefore remain unclear. Importantly, average YFP-Lats2 expression levels, reflected by YFP signal intensities during FACS analyses, were comparable for all constructs (100 (± 2.2), 90.1 (± 8.3), 93.5 (± 1.7) and 92.6 (± 2.0) for WT, ΔC3, KD and YF, respectively) and corroborate the Western blot findings (Figure 3).

A



B

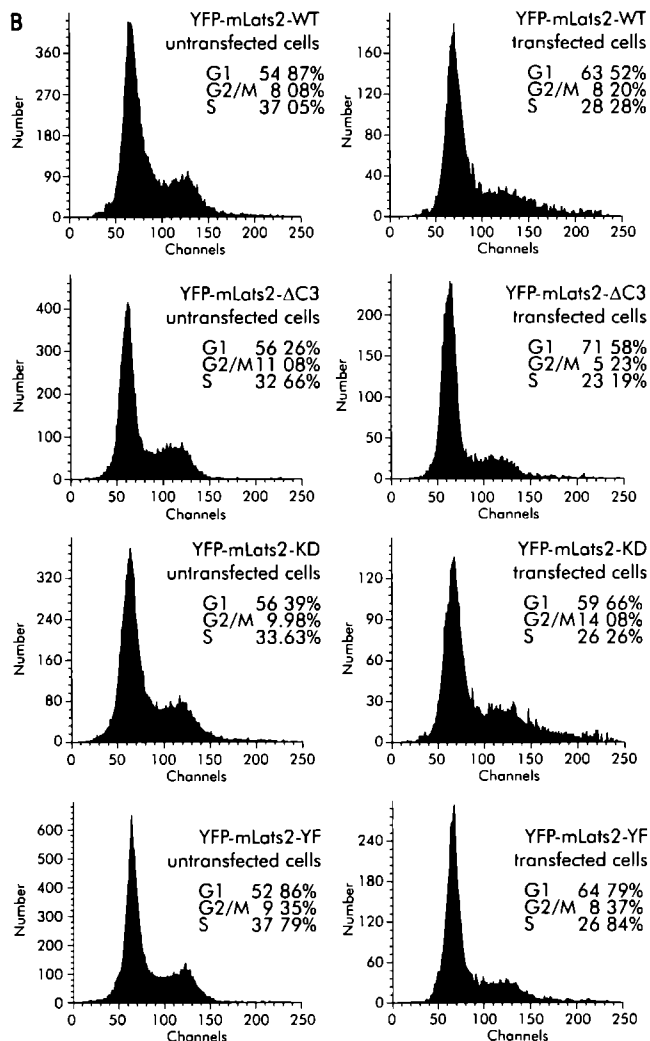


Figure 5: The PDZ-BM modulates effects of Lats2 on cell cycle. (A) HeLa cells were transfected with constructs encoding wild type YFP-mLats2 (WT), YFP-mLats2 lacking the three C-terminal residues (ΔC3) an enzymatically inactive version of YFP-mLats2 (kinase dead, KD) or YFP-mLats2 with a non-phosphorylatable PDZ-BM (YF). DNA content of untransfected (YFP-negative) and transfected (YFP-positive) cells within a sample was measured using FACS to establish the percentage of cells in G0/G1, S and G2/M. The mean difference (\pm SEM) in the percentage of cells in G0/G1 between transfected cells and untransfected cells is shown ($n=6$ for each construct). Average YFP expression levels (relative to YFP-mLats2-WT, which was set at 100) for the various constructs, as revealed in the FACS analyses, were $100 (\pm 2.2)$, $90.1 (\pm 8.3)$, $93.5 (\pm 1.7)$ and $92.6 (\pm 2.0)$ for WT, ΔC3, KD and YF, respectively. (B) Representative FACS profiles of DNA content after propidium iodide staining of HeLa cells transfected with YFP-mLats2 variants. Profiles of untransfected cells are shown for comparison.

Lats2 contains a phosphorylation regulated PDZ domain binding motif

5

Centrosomal localization of Lats2 is independent of the presence or phosphorylation state of its PDZ-BM

Finally, we investigated whether the PDZ-BM is a critical determinant of Lats2's subcellular localization and thereby mediates effects on cell proliferation (Kamikubo *et al.*, 2003; Li *et al.*, 2003; Figure 5). To this end, HeLa cells were transfected with constructs encoding the different YFP-mLats2 fusion variants. Although a general cytosolic localization was observed, a small fraction of YFP-mLats2-WT located at the centrosome (Figure 6A-C), in line with previous findings for fluorescent, c-Myc-tagged and endogenous Lats2 (Abe *et al.*, 2006; McPherson *et al.*, 2004; Toji *et al.*, 2004). This centrosomal localization was not markedly altered upon deletion of the PDZ-BM (Figure 6D-F), by mutating the penultimate residue (Figure 6G-I) or by abolishing kinase activity (Figure 6M-O). From these findings we conclude that phosphorylation of - or protein binding to-

the C-terminus has no major role in controlling Lats2's centrosomal localization, but we cannot exclude that this localization is an important determinant in Lats2's effects on cell cycle.

Lats2 contains a phosphorylation-regulated PDZ domain-binding motif

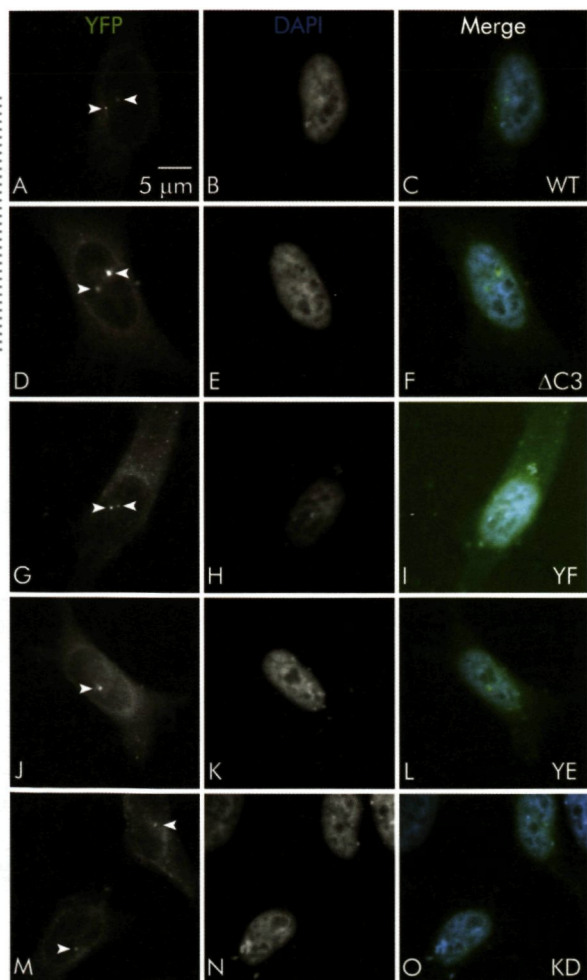


Figure 6: Lats2 PDZ-BM mutants display normal subcellular localization. HeLa cells were transfected with vectors encoding YFP-tagged wild type and mutant mLats2 proteins as indicated. Arrowheads indicate centrosomal location. Panels A, D, G, J, and M show the YFP-mLats2 signal. Panels B, E, H, K, and N show DAPI staining to visualize cell nuclei. Merged images are shown in panels C, F, I, L and O. Bar: 5 μ m.

DISCUSSION

In this study we demonstrated that mammalian Lats2 contains a C-terminal PDZ-BM and that phosphorylation of the penultimate residue in Lats2, Tyr-1041, impairs PDZ domain binding capacity, but subsequent major effects on Lats2 kinase activity or localization were not observed. Deletion of the entire PDZ-BM, however, significantly impaired normal traverse through cell cycle.

To reveal Tyr-1041 phosphorylation, cells were treated with the protein tyrosine phosphatase inhibitor BpV(phen) for 20 minutes. Without addition of this compound total phosphotyrosine levels in Lats2 proteins were below detection level, suggesting that under normal conditions Tyr-1041 phosphorylation may be a very specific event that e.g. only occurs during a small time window in the cell cycle or at a very specific subcellular location on only a fraction of molecules in the entire cell pool. The two known phosphotyrosine sites in human Lats2 (Tyr-82 and Tyr-286) are conserved in mouse and rat, supportive of a functional role. Our work reveals that Tyr-1041, which is also highly conserved throughout evolution, represents a third major phosphotyrosine site in full-length Lats2. Importantly, phosphorylation of the corresponding tyrosine residue in *Drosophila* warts/lats is required for proper control of cell proliferation (Stewart *et al.*, 2003). It remains to be investigated whether this impacts on the binding of *Drosophila* PDZ domain-containing proteins.

Evidence is accumulating that phosphorylation of threonine and serine residues in PDZ-BMs influences affinity for PDZ domains (Cao *et al.*, 1999; Cohen *et al.*, 1996; Hall *et al.*, 1998b; Matsuda *et al.*, 1999). At present there are only few studies describing the impact of PDZ-BM tyrosine phosphorylation on PDZ domain binding (Popovic *et al.*, 2010; Sulka *et al.*, 2009). Phosphorylation of the tyrosine residue at position -2 in the Jagged-1 C-terminus decreased affinity for the Afadin PDZ domain (Popovic *et al.*, 2010). Likewise, tyrosine phosphorylation of the C-terminal sequence of syndecan-1 impedes binding to the PDZ-domain of syntenin-1 (Sulka *et al.*, 2009). These examples suggest that tyrosine phosphorylation within a PDZ-BM will negatively influence the interaction with PDZ domains, possibly by negative charge repulsion or steric effects. Our data are in line with these findings.

The question whether the PDZ-BM would influence Lats2's subcellular localization and perhaps thereby affect Lats2-induced cell cycle arrest was also investigated. Strikingly, all Lats2 protein variants displayed similar subcellular localization, suggesting that the Lats2 PDZ-BM is likely not the major determinant in the proteins partitioning behaviour. However, in our studies the relevant - but thus far unknown - PDZ domain-containing partners for Lats2 were not provided and endogenous levels of these proteins may therefore not suffice to promote relocation of overexpressed Lats2 variants. We should therefore be careful not to over-interpret our

Lats2 contains a phosphorylation regulated PDZ domain-binding motif

findings. PDZ domain proteins often serve as scaffolds for large protein complexes (Sheng and Sala, 2001). It is likely that the Lats2 PDZ-BM enables the spatio-temporal regulation of its own micro-environment via local PDZ-mediated protein associations. As hypothesized before, Lats2 Tyr-1041 phosphorylation might be an event that occurs during a very specific time point during the cell cycle. More work, e.g. by applying time-lapse microscopy, is thus necessary to get insight in the role of Tyr-1041 phosphorylation during different phases of the cell cycle.

In cells that were not treated with BpV(phen), both $\Delta C3$ and Y1041E Lats2 mutants bind significantly less well to the PTP-BL PDZ model segment than non-phosphorylatable Y1041F mutant. Also wild type Lats2 binds 3-fold less well (Figure 3). One reason for this observation could be that binding is partly prevented because a considerable portion of wild type Lats2 is phosphorylated under our experimental conditions. However, since we could not detect any phosphotyrosines in wild type Lats2 under basal conditions (Figure 2) it may also be that PTP-BL domains prefer Lats2-Y1041F over non-phosphorylated wild type Lats2. Additionally, competition with endogenous PDZ domain-containing proteins may influence these data as well.

We anticipated that the Y1041F mutation would dampen the Lats2-WT-induced increase in G0/G1 phase arrest. However, we did not consistently observe a difference in the percentage of cells in G0/G1 between Lats2-WT and Lats2-Y1041F. It may therefore be that phosphorylation may perhaps induce a switch in binding to different partners, but that PDZ domain-mediated interactions with Lats2 per se are essential for normal cell cycle traverse. In such a hypothetical model only complete disruption of these interactions, as mimicked in our Lats2- $\Delta C3$ mutant, would affect the process. We exclude the possibility that differences in expression levels of Lats2 protein variants would underlie observed Lats2 PDZ-BM influences on cell cycle. Cells used in the flow-cytometric analyses were monitored for YFP fluorescence and showed comparable intensities for the different Lats2 mutants and this is corroborated by immunoblot analyses of expression levels in cell lysates.

We used PDZ domain-rich segment of PTP-BL as a model to demonstrate that tyrosine phosphorylation of the Lats2 C-terminus critically determines its binding to PDZ domain-containing proteins. Over the past years, several proteins that interact with Lats2 have been identified (Abe *et al.*, 2006; Aylon *et al.*, 2006; Powzaniuk *et al.*, 2004; Toji *et al.*, 2004; Yabuta *et al.*, 2007). Remarkably, Lats2 substrates YAP2 and TAZ also contain a PDZ-BM (Kanai *et al.*, 2000; Oka and Sudol, 2009) and perhaps these proteins bind in a competitive or cooperative manner to the same PDZ domain-containing proteins. None of the currently known Lats2 interactors contain a PDZ domain, but our findings put forward PTP-BL and other class II PDZ domain-containing proteins as candidate interactors. The fact that PTP-BL contains a protein tyrosine phosphatase domain, and can in that way influence Lats2 Tyr-1041 phosphorylation,

Lats2 contains a phosphorylation-regulated PDZ domain-binding motif

makes this a very interesting candidate. PDZ protein Omi/HtrA2 is known to bind the C-terminus of human Lats1 for which the three C-terminal residues of Lats1 (-VYV_{COOH}) are essential (Kuninaka *et al.*, 2005). The conservation of C-termini of Lats1 and Lats2 makes Omi/HtrA2 therefore a candidate interactor for Lats2 as well. Our data underscore that identification of PDZ domain-containing interaction partners for Lats2 is now an urgent next step towards a better understanding of its growth-suppressive role.

Acknowledgments

We thank Herlinde Gerrits, Marco van Ham and the late Wilma Peters for contribution during the early stages of these studies and Diana Rodijk-Olthuis for flow cytometrical data acquisition and analyses. Interaction trap vectors and yeast strains were kindly provided by Dr. Finley and Dr. Brent (Massachusetts General Hospital, Boston, MA). This work was supported in part by the Dutch Cancer Society (NKB-KWF grant KUN 95-900), the Dutch Organization for Earth and Life Sciences (NWO-ALW grant 809-38-004) and the Radboud University Nijmegen Medical Centre (grant UMCN 2006-12).

Chapter 6

Summarizing discussion

[illegible]

After sequencing and annotation of the complete human genome, about 500 genes were identified that encode a protein kinase. Together with protein phosphatases, kinases are responsible for reversible protein phosphorylation, a key mechanism in the regulation of crucial cellular processes. Deregulation of these processes is an important cause of human disease, including many types of cancer, neurodegenerative disorders and diabetes. Based on sequence homology, kinases are divided into several groups (Manning *et al.*, 2002). AGC kinases, which share the need to become phosphorylated themselves on conserved motifs in order to be activated, form one of these groups.

At the start of my PhD project, results of previous work at the department of Cell Biology suggested a role for two AGC kinases - Lats2 and DMPK E - in the regulation of cell cycle progression. Overexpression of Lats2 in HeLa cells induced a cell cycle arrest at the G1/S transition (van den Berk, 2005) and expression of DMPK E led to formation of multinucleated cells (van Herpen, 2006), indicative of a cytokinesis defect. In the study described in this thesis, we aimed at delineating the molecular mechanisms via which these kinases fulfil their roles.

The work described in Chapters 2-5 revealed that Lats2 and DMPK E have a similar, yet distinct consensus phosphorylation target sequence. The two kinases influence cell cycle progression at different stages, for which possible regulatory mechanisms were disclosed. MLC2 was identified as a *bona fide* DMPK E substrate. An intriguing correlation between oncogenic transformation and a specific pattern of MLC2 isoform expression was uncovered. In the current chapter these main findings will be discussed in a broader context. A graphical abstract of the findings described in this thesis is depicted in Figure 1.

Summarizing discussion

Kinase specificity and substrate discovery

In Chapter 2, identification of candidate substrates and derivation of a consensus target sequence for DMPK E and Lats2 are described based on data obtained using peptide array technology. Peptide arrays constitute an elegant tool to rapidly screen many potential substrate sequences simultaneously. In principle, two types of peptide arrays exist: knowledge-based arrays, containing peptide sequences derived from existing proteins and *de novo* designed arrays, often containing artificial peptide sequences with one or more defined amino acid positions and a number of variable residues (Thiele *et al.*, 2011). The PepChip Kinase I array used in our study is a knowledge-based array, a type of array that is primarily used for identification of potential substrate proteins. *De novo* designed arrays, on the other hand, are more suitable for determination of phosphorylation consensus sequences. A drawback of the PepChip Kinase I array - and likely also of other commercially available peptide arrays - is that the peptide library may be enriched for certain types of peptide

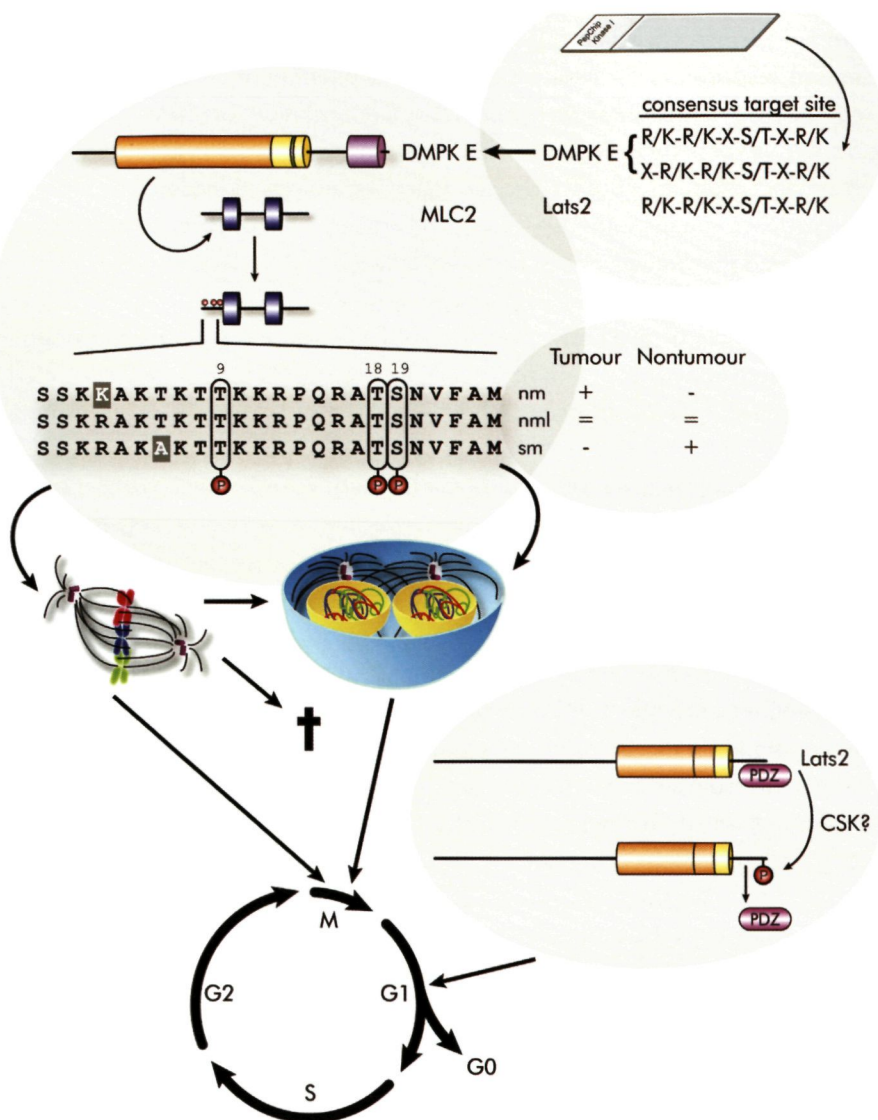


Figure 1: Graphical abstract of findings described in this thesis. Peptide array technology resulted in the identification of a consensus phosphorylation site for DMPK E and Lats2, and MLC2 was put forward as a candidate DMPK E substrate protein. MLC2 indeed is a bona fide DMPK E substrate containing three phosphoacceptor sites, Thr9, Thr18 and Ser19. MLC2 phosphorylation by DMPK E affects certain processes in M-phase, in particular spindle formation and cytokinesis. Three homologous MLC2 isoforms are expressed in higher organisms. Their protein and RNA expression patterns are different for cells of tumourigenic and nontumourigenic origin (+:high;

low; =:equal. A tyrosine residue in the C-terminus of Lats2 can be phosphorylated, the candidate tyrosine kinase being CSK. This phosphorylation abolishes Lats2's interaction with PDZ domains. Deletion of the C-terminal PDZ-binding motif induces G1/S arrest (see text for further details).

sequences, which might cause a bias in the derived consensus sequence. A complicating factor is that peptides may contain multiple potential phospho-acceptor sites, leaving questions open about which residue/s is/are truly phosphorylated by the kinase of interest (Schutkowski *et al.*, 2005; Thiele *et al.*, 2011). For a more accurate delineation of consensus sequences for DMPK E and Lats2 the use of a custom-designed array built from derivatives of the best substrates that arose from the PepChip Kinase I array would be the preferred approach. For each potential substrate at least one other peptide with only one amino acid mismatch should be included, to allow accurate and proper analysis of the importance of that amino acid at that position. Availability of a more stringent consensus sequence would help subsequent searches in protein databases for candidate substrate proteins.

The consensus sequences reported in Chapter 2 show strong similarity with known consensus sequences of AGC group family members. Like Lats2 and DMPK E, many AGC kinases favour a phospho-acceptor site flanked by a number of basic residues at the N-terminal side (Pearce *et al.*, 2010). Therefore, the consensus motif itself is not the sole discriminating factor that renders a protein a substrate for a specific AGC kinase. This is supported by our findings that only one of four tested candidate substrates - i.e. MLC2 - appeared to be a *bona fide* DMPK E substrate. Additional docking motifs and interaction domains or involvement of targeting subunits and scaffolds (Ubersax and Ferrell, 2007) might be even more important for kinase function. We also observed that some peptides that apparently matched the consensus phosphorylation sequence were not phosphorylated on the peptide array. For instance, the MLC2 peptide that tested positive as a DMPK E substrate (KRAKAKTTKKR) also fitted the Lats2 consensus sequence, yet was not identified as Lats2 candidate substrate. This must indicate that other mechanisms and features, including peptide conformation characteristics, contribute to protein phosphorylation specificity. A search for kinase substrates must therefore increasingly rely on 3D structure analysis of both kinase and candidate substrates. This type of analysis should for example provide information on whether the phospho-acceptor site is exposed on the surface of the substrate protein and fits into the peptide binding groove of the kinase of interest. Progress has been made in the development of phosphorylation site prediction tools that incorporate 3D information (e.g., PREDIKIN, PHOSIDA), but phosphorylation 3D motifs are not well defined yet (Via *et al.*, 2011) and 3D structures

are clearly not yet available for every kinase or potential substrate protein.

After extracting a list of potential candidate substrates from peptide array data, more experimental evidence is needed to conclude that a candidate protein is a *bona fide* kinase substrate. In analogy with the criteria for defining protein tyrosine phosphatase (PTP) substrates (Tiganis and Bennett, 2007), this work should address the following properties: (i) increased cellular substrate phosphorylation levels upon increased kinase activity, (ii) *in vitro* phosphorylation of the substrate by the purified kinase and (iii) direct interaction of the substrate with the kinase of interest. At present, no such universal criteria exist for defining protein kinase substrates. Since interactions between kinases and their substrates are often so-called 'kiss-and-run' interactions, the requirements for the third criterion are not easily fulfilled. An attractive approach would be the use of a mutated substrate protein in which the putative phospho-acceptor site has been changed into a reactive cysteine residue which, in combination with a cross-linker that interacts with the ATP-binding site, will lead to trapping of the kinase onto the substrate (Maly *et al.*, 2004; Statsuk *et al.*, 2008). Alternatively, the kinase of interest can be mutated in such a way that it can exploit an ATP γ S analogue and thiophosphorylate its substrate, which can be specifically detected with thiophosphate recognizing antibodies (Allen *et al.*, 2005; Allen *et al.*, 2007). Both methods are rather underexplored approaches to discover kinase-substrate pairs, but results of first studies e.g. by exploiting PKB/Akt and mutated substrate peptides (Statsuk *et al.*, 2008) and mutated Erk1, MAPK and Abl (Allen *et al.*, 2007) are promising.

Phosphorylation and cell cycle progression: Lats2

In our quest for Lats2 substrate proteins, Cdc2 (also called Cdk1; cyclin dependent kinase 1) was amongst the candidates identified (Chapter 2). Cdks control transitions between successive stages of the cell cycle. In mammalian cells, Cdk2 is responsible for G1/S transition, whereas Cdc2/Cdk1 is responsible for the G2/M transition. Interestingly, transient Lats2 expression in HeLa Tet-off cells caused a cell cycle arrest at the G2/M transition (Kamikubo *et al.*, 2003), which fits with a model that is built on an interaction between Lats2 and Cdc2. Indeed, Cdc2 activity was shown to be inhibited by Lats2 due to increased phosphorylation of Cdc2, but a direct interaction was not reported (Kamikubo *et al.*, 2003). Cdc2 does form a complex with Lats1 (Morisaki *et al.*, 2002) however, and the considerable homology between Lats1 and Lats2 therefore supports the identification of Cdc2 as an interaction partner and candidate substrate of Lats2. Furthermore, these data hint at a possible mechanism by which Lats2 may act on G2/M transition, but whether Lats2 directly phosphorylates Cdc2 remains to be demonstrated.

Chapter 5 also touches upon the involvement of Lats2 in the cell cycle by demonstrating that Lats2 overexpression induces a G1/S arrest, which corroborates

findings by others (Li *et al.*, 2003). This G1/S transition block suggests that Lats2 exerts its effects via candidates other than Cdc2/Cdk1, most likely Cdk2. Indeed Cdk2 activity was shown to be downregulated in Lats2 transduced NIH3T3/v-ras cells (Li *et al.*, 2003).

What determines whether the effect of Lats2 (over)expression becomes apparent at the G1/S or at the G2/M transition? One possible explanation might be that epigenetic differences between various cell lines give rise to differences in expression levels of Lats2 targets, causing cells to respond differently to the same signal. Another explanation could be that expression levels of Lats2 itself vary between different studies, either due to differences in cell-specific factors or due to differences in promoter use in expression plasmids. One would need to compare in one study effects of different Lats2 expression levels on both Cdk1 and Cdk2 activity in a variety of cell lines to obtain more insight into this matter.

A role for Lats2 in regulation of the cell cycle would be supported by cell cycle-dependent phosphorylation of Lats2 itself, since this modulates Lats2 activity. Data presented in Chapters 2 and 5 reveal that serine/threonine and tyrosine phosphorylation of Lats2 are specific events. In order for Lats2 to become activated, cells have to be treated with the serine/threonine phosphatase inhibitor okadaic acid (Chapter 2) and tyrosine phosphorylation is detectable only after cells are treated with protein tyrosine phosphatase inhibitor BpV(phen) (Chapter 5). This raises the question whether Lats2 phosphorylation is regulated in a spatiotemporal manner. Lats2 is being phosphorylated during mitosis (Hori *et al.*, 2000; Toji *et al.*, 2004), but whether this occurs at the Lats2 activating MST1/2 target site (Thr999) was not investigated. For MST3, an upstream activator of Lats family member NDR2, cell cycle-dependent activity was found (Cornils *et al.*, 2011), but whether MST1 and MST2 exhibit cell-cycle dependent activation is not known. For Lats1 such a cell cycle-dependent phosphorylation was observed (Nishiyama *et al.*, 1999; Tao *et al.*, 1999) but its autophosphorylation activity, which depends on MST1/2 target site phosphorylation, did not change during the cell cycle (Chan *et al.*, 2005a). These data imply that localization rather than timing is the determining factor for Lats2 activity. Several reports describe localization of Lats2 at centrosomes (Abe *et al.*, 2006; McPherson *et al.*, 2004; Toji *et al.*, 2004). Analysis of the phosphorylation state of the centrosomal Lats2 pool compared to the cytoplasmic pool might provide interesting views on the regulation of its activity.

Binding of MOB1 to the Lats2 SMA domain promotes Lats2 activity (Bao *et al.*, 2009; Hergovich and Hemmings, 2009). The ability of okadaic acid to activate both the full-length and the truncated form of Lats2 - lacking half of the SMA domain - implies that MOB1 binding to the Lats2 SMA domain is not essential for activation under our experimental conditions. However, we did observe that the specific activity

of full-length Lats2 is much higher than that of the truncated Lats2 variant (data not shown), suggesting that MOB1 binding may be a regulatory event. Alternatively, the more upstream protein parts in Lats2 promote its activity. For other NDR kinase family members, MOB1 binding could also not be demonstrated to be absolutely required for their activation (Bichsel *et al.*, 2004; Zhou *et al.*, 2009). Finally, other proteins than MOB proteins can also be involved in the stimulation of Lats2 autophosphorylation activity.

Besides the many similarities in Lats1 and Lats2 structure and function, there are also interesting differences. One is the influence of kinase activity on their PDZ binding properties. In Chapter 5 we demonstrated that binding of Lats2 to PDZ domains is independent of Lats2 kinase activity. In contrast, in another study it was found that only enzymatically active Lats1 binds Omi/HtrA2 via a PDZ-mediated interaction (Kuninaka *et al.*, 2005). Lats1 kinase activity may thus be linked to a conformational state which allows exposure of Lats1's C-terminus to the Omi/HtrA2 PDZ domain. Alternatively, Omi/HtrA2 may need to be phosphorylated by Lats1 before its PDZ domain becomes functional. Together, our findings and the data of others suggest that PDZ domain-binding involves distinct regulatory mechanisms for Lats1 and -2. Studies on the structure of active and inactive Lats1 and Lats2 and identification of upstream tyrosine kinases will be necessary to elucidate specific modes of regulation and hence specific functions for these two homologous kinases. A candidate upstream tyrosine kinase for phosphorylation of the penultimate tyrosine in both Lats proteins is CSK (C-terminal Src kinase), since it was identified as the kinase responsible for phosphorylation of the C-terminal tyrosine residue in *Drosophila* lats/warts (Stewart *et al.*, 2003).

Lats2-induced cell cycle arrest is more profound when interactions with PDZ domain proteins are abolished (Chapter 5). A function for phosphorylation of the PDZ-BM - the motif responsible for interaction with PDZ domains - could not be demonstrated. YAP and TAZ are the only two identified *in vivo* Lats2 substrate proteins at present. Since they both contain a PDZ-BM too, Lats2's PDZ-BM may contribute to the phosphorylation of YAP and TAZ by facilitating docking to a shared PDZ domain scaffold protein. YAP and TAZ both can bind to the first of three PDZ domains in ZO-2 (Oka *et al.*, 2010; Remue *et al.*, 2010). Investigation of Lats2's binding capacity to ZO-2 PDZ domains should reveal whether ZO-2 indeed could function as a scaffold and organizing platform for YAP, TAZ and Lats2 interactions.

Phosphorylation and cell cycle progression: DMPK

In Chapter 2, I report on the search for substrates for the second member of the AGC kinase group that was central in my PhD study: DMPK E. MLC2 was put forward as a candidate. The biological relevance of the interaction between DMPK E and

MLC2 was investigated in Chapter 3 and a role in the regulation of centrosomes and formation of the mitotic spindle during M-phase was postulated.

The generally accepted model for DM1 pathogenesis assumes that expanded DMPK transcripts are retained in the nucleus (Davis *et al.*, 1997; Taneja *et al.*, 1995). At the protein level, this may lead to a downregulation of DMPK expression (note that reliable studies on DMPK protein levels in patients are scarce and have given contradictory results (Wansink and Wieringa, 2003)). An interesting publication on tumour incidence in literature and registered in the NIH National Registry of DM and FSHD (Facioscapulohumeral Muscular Dystrophy) patients and their family members unveils a susceptibility of DM1 patients to an unusual spectrum of neoplasms (Mueller *et al.*, 2009), suggesting that deregulation of DMPK could also contribute to tumourigenesis. Together with the findings as detailed in Chapter 3, this could mean that a tight balance in DMPK E expression is required and that both up- and downregulation of its expression levels could contribute to tumourigenesis.

DMPK E expression resulted in MLC2 hyperphosphorylation, formation of aberrant mitotic spindles and multinucleated cells. Although multinucleation is a physiological phenomenon in certain cell types and during different stages of development (Edgar and Orr-Weaver, 2001), it is also associated with tumourigenesis. Multinucleation results in formation of polyploid cells. The presence of extra centrosomes frequently leads to formation of an aberrant mitotic spindle and thus to improper chromosome segregation in the next round(s) of cell division (Storchova and Kuffer, 2008). A link between aneuploidy and tumourigenesis was already described over 100 years ago (Holland and Cleveland, 2009).

Interestingly, three different mutations in DMPK protein in tumour tissues from non-DM1 patients were identified (<http://www.sanger.ac.uk/genetics/CGP/cosmic/>). These mutations are (i) L438V, a rather conserved mutation in a low-conserved region, (ii) T544M, a mutation in a region absent in isoforms E and F, (iii) Q560Q, a silent mutation in the coding region of long isoforms, but in the 3' UTR of short isoforms. Detailed analysis of the influence of these mutations on functioning of different DMPK isoforms and on their expression levels in tumours and healthy tissues should shed light on a possible specific tumourigenic effect of mutations in DMPK E.

It is the cytosolic DMPK E isoform, but not the membrane-bound isoforms A and C, that induces mitotic aberrancies. This implies that localization of DMPK is a crucial factor for the cell division defects to occur. Remarkably, during mitosis the localization of DMPK C is cytosolic, similar to DMPK E. So, why then does only DMPK E affect the mitotic process and not DMPK A or C? Perhaps, the interaction between MLC2 and DMPK E during earlier stages in the cell cycle is important to induce the observed cell division effects. Alternatively, the C-terminal tail of DMPK C may prevent MLC2 interaction and MLC2 is therefore not a substrate for the C isoform (note that

also MYPT1 was phosphorylated by DMPK E, but not C (Wansink *et al.*, 2003)). A third possibility is that there are subtle differences in DMPK E and C localization that were not observed with microscopy. Analysis of the molecular complexes in which the various DMPK splice isoforms reside during distinct phases of the cell cycle should provide detailed information required to answer this question.

DMPK^{-/-} myoblasts, which totally lack DMPK protein, can divide normally, indicating that DMPK isoforms are dispensable for completion of cell division. Also in many other cell lines where DMPK expression is undetectable cell division proceeds normally (Oude Ophuis *et al.*, 2009a). Since other DMPK kinase family members, like ROCK, MRCK and CRICK are also implicated in cell division and MLC2 and MYPT phosphorylation (Matsumura, 2005), functional redundancy within this kinase family is likely. At present not much is known about cell-type specific expression of individual DMPK family members and to what extent activities are shared or truly redundant. Next to DMPK kinase family members, also MLCK, PAK, DAK and ILK are able to phosphorylate MLC2 (Matsumura, 2005). Existence of such a diverse set of MLC2 kinases suggests that temporal and spatial regulation of MLC2 is crucial for control of cell fate and behaviour. The various kinases are probably expressed in different cell types and participate in distinct complexes and microdomains to fine-tune activity of MLC2 when and where required.

In Chapter 3 it was demonstrated that DMPK E highly likely phosphorylates the smooth muscle MLC2 isoform, which is involved in cell division and, in addition, in smooth muscle contraction (Eddinger and Meer, 2007). Evidence that DMPK indeed also affects smooth muscle contraction comes from a study with DMPK overexpressor mice (O’Cochlain *et al.*, 2004). The reduced blood pressure in these mice was assigned to a deficit in smooth muscle functioning. Effects of DMPK knockout on smooth muscle functioning have not been investigated yet. Histological evidence that DMPK influences the architecture of smooth muscle also remains to be provided. A function of DMPK E in the regulation of skeletal muscle contraction is less likely, because this is not depending on MLC2 phosphorylation, but rather on Ca²⁺-induced conformational changes of troponin, an actin-bound protein (Kamm and Stull, 2011). Moreover, DMPK E expression levels are undetectable in skeletal muscle (Groenen *et al.*, 2000).

Phosphorylation and cell cycle progression: MLC2

A function during cell division for MLC2 in formation of the actomyosin contractile ring, in which myosin II is a main component (Eggert *et al.*, 2006; Glotzer, 2005; Guertin *et al.*, 2002), has been reviewed extensively (Matsumura, 2005; Matsumura *et al.*, 2001). Myosin II also plays a role in centrosomal positioning during mitosis (Rosenblatt *et al.*, 2004). A centriolar localization for 2P-MLC2 was claimed earlier by Yamashiro *et al.*

(Yamashiro *et al.*, 2003), but double staining experiments with specific markers to substantiate the observation were lacking. A detailed picture of 2P-MLC2 centrosomal localization is given for the first time in Chapter 3 of this thesis. YFP fusion proteins of all non-sarcomeric MLC2 isoforms - whether phosphorylated or not - reside primarily at polar crescents, a location that differs from the unique centrosomal positioning of 2P-MLC2 (Chapter 4). A detailed study of NuMa localization demonstrated that polar crescents form an insoluble matrix surrounding the centrosomes. This matrix is distinct from the pericentriolar material and anchors the microtubule ends of the mitotic spindle (Dionne *et al.*, 1999). Our observation of MLC2 localization in the centrosome area supports a function of MLC2 in mitotic spindle organization.

What could cause the difference in localization between endogenous 2P-MLC2, revealed by a phospho-specific antibody, and the pool of phosphorylated and non-phosphorylated YFP-MLC2 during transient transfection? Tagging MLC2 (~20 kDa) with YFP (~29 kDa) might generate a fusion protein too big for targeting to centrosomes. This would imply that the fluorescent signal observed at the crescents represents diphosphorylated MLC2, since for endogenous MLC2 only the 2P-fraction was found in centrosomes. Immunofluorescence of YFP-MLC2 expressing cells with the 2P-MLC2 antibody should be performed to test this hypothesis. The possibility that the YFP tag interferes with MLC2 phosphorylation seems unlikely, since our *in vitro* kinase assays showed that wild type YFP-MLC2 was readily phosphorylated. In addition, urea/glycerol-PAGE analysis of YFP-MLC2 transfected cells revealed three phosphorylation states for YFP-MLC2 (data not shown), indicating that YFP-MLC2 is also subject of phosphorylation in cells. MLC2 phosphorylation biosensors provide suitable and elegant tools to monitor phosphorylation-dependent MLC2 localization during different stages of the cell cycle *in vivo* (Post *et al.*, 1995; Yamada *et al.*, 2005). An MLC2 phosphorylation biosensor that monitors both mono- and diphosphorylation, however, has not been developed yet.

Diphosphorylation of MLC2 occurs in a sequential manner, with phosphorylation of Ser19 occurring first, followed by phosphorylation of Thr18 (Ikebe and Hartshorne, 1985; Ikebe *et al.*, 1986). Our *in vitro* data indicate that Ser19 and Thr18 are both target sites for DMPK E. Absence of 1P-MLC2 in centrosomes may indicate that the kinase responsible for phosphorylation of residue Thr18 specifically resides or is activated in that area. Conversely, the protein phosphatase (MYPT) that is involved in this process might be absent there. We have shown earlier that DMPK E is present throughout the cytosol, including the centrosome area (van Herpen, 2006; van Herpen *et al.*, 2005). It is not known yet where in the cell DMPK is active and how it is activated. Certain DMPK-specific activators may be located at centrosomes. A second possibility could be that phosphorylation of Thr18 on 1P-MLC2 results in translocation of 2P-MLC2 to centrosomes, but evidence to support this is lacking. Furthermore,

2P-MLC2 phosphorylation by Citron-kinase did not result in centrosomal targeting of MLC2 (Yamashiro *et al.*, 2003). Perhaps DMPK activity needs to be combined with that of a second kinase *in vivo*, given the many kinases that are able to phosphorylate MLC2 and/or 1P-MLC2.

In vitro kinase assays strongly suggest that DMPK E favours Thr18 and Ser19 over Thr9 (Chapter 3). An MLC2 peptide containing Thr9, but not Thr18 and Ser19, was represented on the peptide array and phosphorylated by DMPK E. Thr9 phosphorylation has not been reported for any of the other DMPK kinase family members. The choice to include the Thr9 peptide as the only MLC2 substrate seems irrational, since experimental support for *in vivo* Thr9 phosphorylation is rather limited (Shuster and Burgess, 1999), whereas evidence for a biological role of Thr18/Ser19 phosphorylation is overwhelming (Eddinger and Meer, 2007; Komatsu *et al.*, 2000; Matsumura, 2005; Matsumura *et al.*, 2001; Vicente-Manzanares *et al.*, 2009). The triphosphorylated MLC2 form identified upon DMPK E expression *in vivo* is indicative of an additional phosphosite next to Thr18 and Ser19. Triphosphorylated MLC2 has been reported before and contained phosphate groups on Thr9 (a known PKC site (Bengur *et al.*, 1987; Kawamoto *et al.*, 1989; Nishikawa *et al.*, 1984; Obara *et al.*, 2008)), Thr18 and Ser19 (Obara *et al.*, 2008; Obara *et al.*, 2010). Simultaneous phosphorylation of these three residues is surprising, since Thr18/Ser19 phosphorylation causes activation of myosin II, whereas Thr9 phosphorylation inhibits myosin II activity (Ikebe *et al.*, 1987). Whether Thr9 indeed is the third phosphorylated residue that is involved in our observations must be investigated, for instance by mass spectrometry. Next, by generating specific point mutants, one also could investigate whether this phosphoacceptor site is a true DMPK E site or requires another kinase (e.g. PKC).

Why do higher vertebrates express three homologous MLC2 genes, which encode almost identical proteins (Chapter 4)? In evolutionary biology it is generally accepted that after a duplication event both gene copies are retained only when this is neutral or beneficial to the organism. If both copies are indeed preserved, this will result in (i) silencing of one copy (pseudogenization), (ii) increased protein amounts, (iii) partitioning of the ancestral gene's subfunctions over the duplicated genes (subfunctionalization) or (iv) development towards a new function for one of the copies (neofunctionalization) (Innan, 2009). Obviously, the first option does not apply to the nm-/nml-/sm-MLC2 trio. The second option is also not likely, since expression of sm- and nm-MLC2 seemed to be mutually exclusive. Thus we are left with two options to consider: sub- or neofunctionalization. The most likely explanation would be that different MLC2 isoforms confer different contractile properties to myosin II or form distinct complexes with certain MHCII and ELC isoforms. Studies on the contractility of distinct myosin II complexes composed of fixed MHCII and ELC combinations and either nm-,

nml-, or sm-MLC2 should provide interesting details on these characteristics. Another interesting possibility is that MLC2 proteins fulfil a role outside the context of the myosin II complex, but experimental evidence for this scenario is scarce (Bajaj *et al.*, 2010).

Chapter 4 reports on the differential expression of nm-, nml- and sm-MLC2 isoforms in tumour- and nontumour-derived cells. Other examples of contractile proteins whose expression levels change with tumourigenicity are caldesmon, tropomyosin and vimentin (Cobellis *et al.*, 2001), suggesting a more general role for contractile proteins in tumourigenesis. It would be interesting to investigate whether changes in MLC2 isoform expression contribute to tumourigenic characteristics or are a mere consequence of tumourigenicity. To answer this question, one would need a non-tumourigenic cell line in which expression levels of MLC2 isoforms can be manipulated and changes in tumourigenic cell characteristics can be monitored (e.g., growth rate, anchorage independent growth, cell shape, cell size). This should also reveal whether the MLC2 isoform expression profile can be used as an oncogenic marker.

Concluding remarks

My studies provide evidence that both kinase-substrate interactions as well as non-enzymatic protein-protein interactions strongly impact on the functioning of two AGC kinases - DMPK E and Lats2 - during cell cycle progression. Lats2 was found to lead to a cell cycle arrest at the G1/S transition and an interaction with PDZ domain-containing proteins via a newly identified PDZ-binding motif in Lats2 plays a role in this process. DMPK E was found to influence different aspects of mitosis and cytokinesis, presumably via phosphorylation of the newly identified substrate MLC2. In addition, three MLC2 isoforms were found to be differentially expressed in transformed and non-transformed cells. These data contribute to the delineation of different kinase signalling pathways and therewith to a more detailed understanding of processes that are essential for health and disease in higher organisms.

references

Nederlandse samenvatting

abbreviations

publications

curriculum vitae

dankwoord

[illegible]

REFERENCES

- Abe Y, Ohsugi M, Haraguchi K, Fujimoto J, Yamamoto T: LATS2-Ajuba complex regulates gamma-tubulin recruitment to centrosomes and spindle organization during mitosis. *FEBS Lett.* 2006, 580:782-788.
- Abrantes J, Posada D, Guillon P, Esteves PJ, Le Pendu J: Widespread gene conversion of alpha-2-fucosyltransferase genes in mammals. *J Mol Evol.* 2009, 69:22-31.
- Alberts B, Johnson, A., Lewis, J., Raff, M., Roberts, K., Walter, P.: *Molecular Biology of the Cell* 4th edn. New York: Garland Science; 2002.
- Allen JJ, Lazerwith SE, Shokat KM: Bio-orthogonal affinity purification of direct kinase substrates. *J Am Chem Soc.* 2005, 127:5288-5289.
- Allen JJ, Li M, Brinkworth CS, Paulson JL, Wang D, Hubner A, Chou WH, Davis RJ, Burlingame AL, Messing RO, et al: A semisynthetic epitope for kinase substrates. *Nat Methods* 2007, 4:511-516.
- Amano M, Fukata Y, Kaibuchi K: Regulation and functions of Rho-associated kinase. *Exp Cell Res* 2000, 261:44-51.
- Amano M, Ito M, Kimura K, Fukata Y, Chihara K, Nakano T, Matsuura Y, Kaibuchi K: Phosphorylation and activation of myosin by Rho-associated kinase (Rho-kinase). *J Biol Chem.* 1996, 271:20246-20249.
- Amigo M, Schalkwijk J, Olthuis D, De Rosa S, Paya M, Terencio MC, Lamme E: Identification of avarol derivatives as potential antipsoriatic drugs using an in vitro model for keratinocyte growth and differentiation. *Life Sci.* 2006, 79:2395-2404.
- Arner A, Lofgren M, Morano I: Smooth, slow and smart muscle motors. *J Muscle Res Cell Motil.* 2003, 24:165-173.
- Aylon Y, Michael D, Shmueli A, Yabuta N, Nojima H, Oren M: A positive feedback loop between the p53 and Lats2 tumor suppressors prevents tetraploidization. *Genes Dev.* 2006, 20:2687-2700.
- Aylon Y, Ofir-Rosenfeld Y, Yabuta N, Lapi E, Nojima H, Lu X, Oren M: The Lats2 tumor suppressor augments p53-mediated apoptosis by promoting the nuclear proapoptotic function of ASPP1. *Genes Dev.* 2010, 24:2420-2429.
- Azimzadeh J, Bornens M: Structure and duplication of the centrosome. *J Cell Sci* 2007, 120:2139-2142.
- Babu GJ, Warshaw DM, Periasamy M: Smooth muscle myosin heavy chain isoforms and their role in muscle physiology *Microsc Res Tech.* 2000, 50:532-540.
- Bajaj G, Rodriguez-Proteau R, Venkataraman A, Fan Y, Kioussi C, Ishmael JE: MDR1 function is sensitive to the phosphorylation state of myosin regulatory light chain. *Biochem Biophys Res Commun.* 2010, 398:7-12.
- Bannon JH, Mc Gee MM: Understanding the role of aneuploidy in tumorigenesis *Biochem Soc Trans.* 2009, 37:910-913.
- Bao J, Oishi K, Yamada T, Liu L, Nakamura A, Uchida MK, Kohama K: Role of the short isoform of myosin light chain kinase in the contraction of cultured smooth muscle cells as examined by its down-regulation. *Proc Natl Acad Sci USA.* 2002, 99 9556-9561.
- Bao Y, Sumita K, Kudo T, Withanage K, Nakagawa K, Ikeda M, Ohno K, Wang Y, Hata Y: Roles of

- mammalian sterile 20-like kinase 2-dependent phosphorylations of Mps one binder 1B in the activation of nuclear Dbf2-related kinases. *Genes Cells*. 2009, 14:1369-1381
- Barber TD, McManus K, Yuen KW, Reis M, Parmigiani G, Shen D, Barrett I, Nouhi Y, Spencer F, Markowitz S, et al: Chromatid cohesion defects may underlie chromosome instability in human colorectal cancers. *Proc Natl Acad Sci U S A*. 2008, 105:3443-3448
- Benders AA, Groenen PJ, Oerlemans FT, Veerkamp JH, Wieringa B: Myotonic dystrophy protein kinase is involved in the modulation of the Ca²⁺ homeostasis in skeletal muscle cells. *J Clin Invest*. 1997, 100:1440-1447.
- Bengur AR, Robinson EA, Appella E, Sellers JR: Sequence of the sites phosphorylated by protein kinase C in the smooth muscle myosin light chain. *J Biol Chem*. 1987, 262:7613-7617.
- Berg JS, Powell BC, Cheney RE: A millennial myosin census. *Mol Biol Cell*. 2001, 12:780-794
- Berul CI, Maguire CT, Aronovitz MJ, Greenwood J, Miller C, Gehrmann J, Housman D, Mendelsohn ME, Reddy S: DMPK dosage alterations result in atrioventricular conduction abnormalities in a mouse myotonic dystrophy model. *J Clin Invest*. 1999, 103:R1-7.
- Bettencourt BR, Feder ME: Rapid concerted evolution via gene conversion at the *Drosophila* hsp70 genes. *J Mol Evol*. 2002, 54:569-586
- Bichsel SJ, Tamaskovic R, Stegert MR, Hemmings BA: Mechanism of activation of NDR (nuclear Dbf2-related) protein kinase by the hMOB1 protein. *J Biol Chem*. 2004, 279:35228-35235
- Birrane G, Chung J, Ladias JA: Novel mode of ligand recognition by the Erbin PDZ domain. *J Biol Chem*. 2003, 278:1399-1402.
- Breitenlechner CB, Friebe WG, Brunet E, Werner G, Graul K, Thomas U, Kunkele KP, Schafer W, Gassel M, Bossemeyer D, et al: Design and crystal structures of protein kinase B-selective inhibitors in complex with protein kinase A and mutants. *J Med Chem*. 2005, 48:163-170.
- Broers JL, Machiels BM, van Eys GJ, Kuipers HJ, Manders EM, van Driel R, Ramaekers FC: Dynamics of the nuclear lamina as monitored by GFP-tagged A-type lamins. *J Cell Sci*. 1999, 112 (Pt 20):3463-3475.
- Brook JD, McCurrach ME, Harley HG, Buckler AJ, Church D, Aburatani H, Hunter K, Stanton VP, Thirion JP, Hudson T, et al: Molecular basis of myotonic dystrophy: expansion of a trinucleotide (CTG) repeat at the 3' end of a transcript encoding a protein kinase family member. *Cell*. 1992, 68:799-808.
- Brown DD, Wensink PC, Jordan E: A comparison of the ribosomal DNA's of *Xenopus laevis* and *Xenopus mulleri*: the evolution of tandem genes. *J Mol Biol*. 1972, 63:57-73.
- Burgess SA, Yu S, Walker ML, Hawkins RJ, Chalovich JM, Knight PJ: Structures of smooth muscle myosin and heavy meromyosin in the folded, shutdown state. *J Mol Biol*. 2007, 372:1165-1178.
- Burnett G, Kennedy EP: The enzymatic phosphorylation of proteins. *J Biol Chem*. 1954, 211:969-980.
- Bush EW, Helmke SM, Birnbaum RA, Perryman MB: Myotonic dystrophy protein kinase domains mediate localization, oligomerization, novel catalytic activity, and autoinhibition. *Biochemistry*. 2000, 39:8480-8490.
- Campbell JH, Kocher O, Skalli O, Gabbiani G, Campbell GR: Cytodifferentiation and expression of alpha-

- smooth muscle actin mRNA and protein during primary culture of aortic smooth muscle cells
Correlation with cell density and proliferative state. *Arteriosclerosis* 1989, 9:633-643.
- Cao TT, Deacon HW, Reczek D, Bretscher A, von Zastrow M: A kinase-regulated PDZ-domain interaction controls endocytic sorting of the beta2-adrenergic receptor. *Nature*. 1999, 401:286-290.
- Carrasco M, Canicio J, Palacin M, Zorzano A, Kaliman P: Identification of intracellular signaling pathways that induce myotonic dystrophy protein kinase expression during myogenesis. *Endocrinology*. 2002, 143:3017-3025.
- Chahine M, George AL, Jr.: Myotonic dystrophy kinase modulates skeletal muscle but not cardiac voltage-gated sodium channels. *FEBS Lett* 1997, 412:621-624.
- Chan EH, Nousiainen M, Chalamalasetty RB, Schafer A, Nigg EA, Sillje HH: The Ste20-like kinase Mst2 activates the human large tumor suppressor kinase Lats1 *Oncogene*. 2005a, 24:2076-2086.
- Chan W, Calderon G, Swift AL, Moseley J, Li S, Hosoya H, Arias IM, Ortiz DF: Myosin II regulatory light chain is required for trafficking of bile salt export protein to the apical membrane in Madin-Darby canine kidney cells. *J Biol Chem* 2005b, 280:23741-23747.
- Chan KF, Hurst MO, Graves DJ: Phosphorylase kinase specificity A comparative study with cAMP-dependent protein kinase on synthetic peptides and peptide analogs of glycogen synthase and phosphorylase. *J Biol Chem*. 1982, 257:3655-3659.
- Chan SW, Lim CJ, Chen L, Chong YF, Huang C, Song H, Hong W: The Hippo pathway in biological control and cancer development. *J Cell Physiol*. 2011, 226:928-939.
- Chan SW, Lim CJ, Guo K, Ng CP, Lee I, Hunziker W, Zeng Q, Hong W: A role for TAZ in migration, invasion, and tumorigenesis of breast cancer cells. *Cancer Res*. 2008, 68:2592-2598.
- Chang F, Drubin D, Nurse P: cdc12p, a protein required for cytokinesis in fission yeast, is a component of the cell division ring and interacts with profilin. *J Cell Biol* 1997, 137:169-182
- Chen X-Q, Tan I, Leung T, Lim L: The Myotonic Dystrophy Kinase-related Cdc42-binding Kinase Is Involved in the Regulation of Neurite Outgrowth in PC12 Cells. *J Biol Chem*. 1999, 274:19901-19905.
- Chen X-q, Tan I, Ng CH, Hall C, Lim L, Leung T: Characterization of RhoA-binding Kinase ROKalpha Implication of the Pleckstrin Homology Domain in ROKalpha Function Using Region-specific Antibodies. *J Biol Chem*. 2002, 277:12680-12688
- Chevrier V, Piel M, Collomb N, Saoudi Y, Frank R, Paintrand M, Narumiya S, Bornens M, Job D: The Rho-associated protein kinase p160ROCK is required for centrosome positioning. *J Cell Biol* 2002, 157:807-817
- Chi YH, Jeang KT: Aneuploidy and cancer. *J Cell Biochem*. 2007, 102:531-538.
- Cho DH, Tapscott SJ: Myotonic dystrophy: emerging mechanisms for DM1 and DM2. *Biochim Biophys Acta* 2007, 1772:195-204.
- Cho W, Shin J, Kim J, Lee M, Hong K, Lee J-H, Koo K, Park J, Kim K-S: miR-372 regulates cell cycle and apoptosis of ags human gastric cancer cell line through direct regulation of LATS2. *Mol Cells*. 2009, 28:521-527.
- Choi J, Ko J, Park E, Lee JR, Yoon J, Lim S, Kim E: Phosphorylation of stargazin by protein kinase A regulates its interaction with PSD-95. *J Biol Chem*. 2002, 277:12359-12363.

- Chung HJ, Xia J, Scannevin RH, Zhang X, Huganir RL Phosphorylation of the AMPA receptor subunit GluR2 differentially regulates its interaction with PDZ domain-containing proteins *J Neurosci* 2000, 20 7258-7267
- Ciesla J, Fraczyk T, Rode W Phosphorylation of basic amino acid residues in proteins important but easily missed *Acta Biochim Pol* 2011, 58 137-148
- Cimini D Merotelic kinetochore orientation, aneuploidy, and cancer *Biochim Biophys Acta* 2008, 1786 32-40
- Cimini D, Howell B, Maddox P, Khodjakov A, Degrossi F, Salmon ED Merotelic kinetochore orientation is a major mechanism of aneuploidy in mitotic mammalian tissue cells *J Cell Biol* 2001, 153 517-527
- Cobellis G, Missero C, Simionati B, Valle G, Di Lauro R Immediate early genes induced by H-Ras in thyroid cells *Oncogene* 2001, 20 2281-2290
- Cohen NA, Brenman JE, Snyder SH, Brecht DS Binding of the inward rectifier K⁺ channel Kir 2.3 to PSD-95 is regulated by protein kinase A phosphorylation *Neuron* 1996, 17 759-767
- Collins JH Myoinformatics report myosin regulatory light chain paralogs in the human genome *J Muscle Res Cell Motil* 2006, 27 69-74
- Compton DA, Yen TJ, Cleveland DW Identification of novel centromere/kinetochore-associated proteins using monoclonal antibodies generated against human mitotic chromosome scaffolds *J Cell Biol* 1991, 112 1083-1097
- Conti MA, Kawamoto S, Adelstein RS Non-muscle myosin II In *Myosins A Superfamily of Molecular Motors* Volume 7 Edited by Colluccio LM Dordrecht Springer, 2008 223-264 *Proteins and Cell regulation*
- Cooper GM *The cell a molecular approach* 2nd edn Sunderland Sinauer Associates, 2000
- Cornils H, Kohler RS, Hergovich A, Hemmings BA Human NDR kinases control G1/S cell cycle transition by directly regulating p21 stability *Mol Cell Biol* 2011, 31 1382-1395
- Craig R, Woodhead JL Structure and function of myosin filaments *Curr Opin Struct Biol* 2006, 16 204-212
- Cuppen E, Gerrits H, Pepers B, Wieringa B, Hendriks W PDZ motifs in PTP-BL and RIL bind to internal protein segments in the LIM domain protein RIL *Mol Biol Cell* 1998, 9 671-683
- Cuppen E, van Ham M, Wansink DG, de Leeuw A, Wieringa B, Hendriks W The zyxin-related protein TRIP6 interacts with PDZ motifs in the adaptor protein RIL and the protein tyrosine phosphatase PTP-BL *Eur J Cell Biol* 2000, 79 283-293
- Das Thakur M, Feng Y, Jagannathan R, Seppa MJ, Skeath JB, Longmore GD Ajuba LIM proteins are negative regulators of the Hippo signaling pathway *Curr Biol* 2010, 20 657-662
- Davis BM, McCurrach ME, Taneja KL, Singer RH, Housman DE Expansion of a CUG trinucleotide repeat in the 3' untranslated region of myotonic dystrophy protein kinase transcripts results in nuclear retention of transcripts *Proc Natl Acad Sci U S A* 1997, 94 7388-7393
- de Groof AJ, te Lindert MM, van Dommelen MM, Wu M, Willemse M, Smift AL, Winer M, Oerlemans F, Pluk H, Fransen JA, Wieringa B Increased OXPHOS activity precedes rise in glycolytic rate in

- H-RasV12/E1A transformed fibroblasts that develop a Warburg phenotype. *Mol Cancer*. 2009, 8:54
- De Lozanne A, Spudich JA: Disruption of the Dictyostelium myosin heavy chain gene by homologous recombination. *Science*. 1987, 236:1086-1091.
- Dean SO, Spudich JA: Rho kinase's role in myosin recruitment to the equatorial cortex of mitotic Drosophila S2 cells is for myosin regulatory light chain phosphorylation. *PLoS One*. 2006, 1:e131
- Debec A, Sullivan W, Bettencourt-Dias M: Centrioles: active players or passengers during mitosis? *Cell Mol Life Sci*. 2010, 67:2173-2194.
- DeBiasio RL, LaRocca GM, Post PL, Taylor DL: Myosin II transport, organization, and phosphorylation: evidence for cortical flow/solution-contraction coupling during cytokinesis and cell locomotion *Mol Biol Cell*. 1996, 7:1259-1282.
- Dereeper A, Guignon V, Blanc G, Audic S, Buffet S, Chevenet F, Dufayard JF, Guindon S, Lefort V, Lescot M, et al: Phylogeny.fr: robust phylogenetic analysis for the non-specialist. *Nucleic Acids Res*. 2008, 36:W465-469.
- Di Ciano-Oliveira C, Sirokmany G, Szasz K, Arthur WT, Masszi A, Peterson M, Rotstein OD, Kapus A: Hyperosmotic stress activates Rho: differential involvement in Rho kinase-dependent MLC phosphorylation and NKCC activation. *Am J Physiol Cell Physiol*. 2003, 285:C555-566
- Di Cunto F, Calautti E, Hsiao J, Ong L, Topley G, Turco E, Dotto GP: Citron rho-interacting kinase, a novel tissue-specific ser/thr kinase encompassing the Rho-Rac-binding protein Citron *J Biol Chem*. 1998, 273:29706-29711.
- Dionne MA, Howard L, Compton DA: NuMA is a component of an insoluble matrix at mitotic spindle poles *Cell Motil Cytoskeleton*. 1999, 42:189-203.
- Distelmaier F, Visch HJ, Smeitink JA, Mayatepek E, Koopman WJ, Willems PH: The antioxidant Trolox restores mitochondrial membrane potential and Ca²⁺-stimulated ATP production in human complex I deficiency. *J Mol Med*. 2009, 87 515-522.
- Dong J, Feldmann G, Huang J, Wu S, Zhang N, Comerford SA, Gayyed MF, Anders RA, Maitra A, Pan D: Elucidation of a universal size-control mechanism in Drosophila and mammals. *Cell*. 2007, 130:1120-1133.
- Dunne PW, Ma L, Casey DL, Harati Y, Epstein HF: Localization of myotonic dystrophy protein kinase in skeletal muscle and its alteration with disease *Cell Motil Cytoskeleton*. 1996, 33:52-63.
- Ebralidze A, Wang Y, Petkova V, Ebralidze K, Junghans RP: RNA leaching of transcription factors disrupts transcription in myotonic dystrophy. *Science*. 2004, 303:383-387.
- Eddinger TJ, Meer DP: Myosin II isoforms in smooth muscle: heterogeneity and function. *Am J Physiol Cell Physiol*. 2007, 293:C493-508
- Edgar BA, Orr-Weaver TL: Endoreplication cell cycles: more for less. *Cell*. 2001, 105:297-306.
- Eggert US, Mitchison TJ, Field CM: Animal cytokinesis: from parts list to mechanisms. *Annu Rev Biochem*. 2006, 75:543-566.
- Elkins JM, Amos A, Niesen FH, Pike AC, Fedorov O, Knapp S: Structure of dystrophin myotonic protein kinase. *Protein Sci*. 2009, 18:782-791.

- Etienne-Manneville S, Hall A: Rho GTPases in cell biology. *Nature* 2002, 420:629-635.
- Fabian L, Forer A: Possible roles of actin and myosin during anaphase chromosome movements in locust spermatocytes. *Protoplasma* 2007, 231:201-213.
- Fanning AS, Anderson JM: PDZ domains: fundamental building blocks in the organization of protein complexes at the plasma membrane *J Clin Invest*. 1999, 103:767-772.
- Feng W, Zhang M: Organization and dynamics of PDZ-domain-related supramodules in the postsynaptic density. *Nat Rev Neurosci* 2009, 10:87-99.
- Fliegauf M, Benzing T, Omran H: When cilia go bad: cilia defects and ciliopathies. *Nat Rev Mol Cell Biol*. 2007, 8:880-893.
- Forner F, Furlan S, Salvatori S: Mass spectrometry analysis of complexes formed by myotonic dystrophy protein kinase (DMPK). *Biochim Biophys Acta*. 2010, 1804:1334-1341.
- Fu YH, Pizzuti A, Fenwick RG, Jr., King J, Rajnarayan S, Dunne PW, Dubel J, Nasser GA, Ashizawa T, de Jong P, et al.: An unstable triplet repeat in a gene related to myotonic muscular dystrophy. *Science*. 1992, 255:1256-1258
- Fujiwara K, Pollard TD: Simultaneous localization of myosin and tubulin in human tissue culture cells by double antibody staining. *J Cell Biol* 1978, 77:182-195.
- Gaglio T, Saredi A, Compton DA: NuMA is required for the organization of microtubules into aster-like mitotic arrays *J Cell Biol*. 1995, 131:693-708.
- Gally C, Wissler F, Zahreddine H, Quintin S, Landmann F, Labouesse M: Myosin II regulation during *C. elegans* embryonic elongation: LET-502/ROCK, MRCK-1 and PAK-1, three kinases with different roles *Development*. 2009, 136:3109-3119.
- Ganem NJ, Godinho SA, Pellman D: A mechanism linking extra centrosomes to chromosomal instability. *Nature* 2009, 460:278-282.
- Garcia JG, Davis HW, Patterson CE: Regulation of endothelial cell gap formation and barrier dysfunction: role of myosin light chain phosphorylation. *J Cell Physiol*. 1995, 163:510-522.
- Gaylinn BD, Eddinger TJ, Martino PA, Monical PL, Hunt DF, Murphy RA: Expression of nonmuscle myosin heavy and light chains in smooth muscle. *Am J Physiol*. 1989, 257:C997-1004.
- Geering K: FXYP proteins: new regulators of Na-K-ATPase. *Am J Physiol Renal Physiol*. 2006, 290:F241-250
- Gerrits L, Venselaar H, Wieringa B, Wansink DG, Henriks WJAJ: phosphorylation target site specificity for AGC kinases DMPK E and Lats2. *J Cell Biochem*. 2012a, in press.
- Gerrits L, Overheul GJ, Derks RC, Wieringa B, Hendriks WJAJ, Wansink DG: Gene duplication and conversion events shaped three homologous, differentially expressed myosin regulatory light chain (MLC2) genes. *Eur J Cell Biol*. 2012b, in press.
- Gimona M: The microfilament system in the formation of invasive adhesions. *Semin Cancer Biol* 2008, 18:23-34
- Glotzer M: The molecular requirements for cytokinesis. *Science*. 2005, 307:1735-1739.
- Glotzer M: The 3Ms of central spindle assembly: microtubules, motors and MAPs. *Nat Rev Mol Cell Biol*. 2009, 10:9-20.

- Grant JW, Taubman MB, Church SL, Johnson RL, Nadal-Ginard B: Mammalian nonsarcomeric myosin regulatory light chains are encoded by two differentially regulated and linked genes *J Cell Biol.* 1990, 111:1127-1135
- Gregan J, Polakova S, Zhang L, Tolic-Norrelykke IM, Cimini D: Merotelic kinetochore attachment: causes and effects. *Trends Cell Biol.* 2011, 21:374-381.
- Grodsky N, Li Y, Bouzida D, Love R, Jensen J, Nodes B, Nonomiya J, Grant S: Structure of the catalytic domain of human protein kinase C beta II complexed with a bisindolylmaleimide inhibitor *Biochemistry.* 2006, 45:13970-13981.
- Groenen P, Wieringa B: Expanding complexity in myotonic dystrophy. *Bioessays.* 1998, 20:901-912.
- Groenen PJ, Wansink DG, Coerwinkel M, van den Broek W, Jansen G, Wieringa B: Constitutive and regulated modes of splicing produce six major myotonic dystrophy protein kinase (DMPK) isoforms with distinct properties *Hum Mol Genet.* 2000, 9:605-616.
- Guertin DA, Trautmann S, McCollum D: Cytokinesis in eukaryotes. *Microbiol Mol Biol Rev.* 2002, 66:155-178
- Guo A, Villen J, Kornhauser J, Lee KA, Stokes MP, Rikova K, Possemato A, Nardone J, Innocenti G, Wetzell R, et al: Signaling networks assembled by oncogenic EGFR and c-Met. *Proc Natl Acad Sci U S A* 2008, 105:692-697
- Guo Y, Ramachandran C, Satpathy M, Srinivas SP: Histamine-induced myosin light chain phosphorylation breaks down the barrier integrity of cultured corneal epithelial cells. *Pharm Res.* 2007, 24:1824-1833.
- Gyuris J, Golemis E, Chertkov H, Brent R: Cdi1, a human G1 and S phase protein phosphatase that associates with Cdk2. *Cell.* 1993, 75:791-803.
- Haklai R, Weisz MG, Elad G, Paz A, Marciano D, Egozi Y, Ben-Baruch G, Kloog Y: Dislodgment and accelerated degradation of Ras. *Biochemistry.* 1998, 37:1306-1314.
- Hall RA, Ostedgaard LS, Premont RT, Blitzer JT, Rahman N, Welsh MJ, Lefkowitz RJ: A C-terminal motif found in the beta2-adrenergic receptor, P2Y1 receptor and cystic fibrosis transmembrane conductance regulator determines binding to the Na⁺/H⁺ exchanger regulatory factor family of PDZ proteins *Proc Natl Acad Sci U S A.* 1998a, 95:8496-8501
- Hall RA, Premont RT, Chow CW, Blitzer JT, Pitcher JA, Claing A, Stoffel RH, Barak LS, Shenolikar S, Weinman EJ, et al: The beta2-adrenergic receptor interacts with the Na⁺/H⁺-exchanger regulatory factor to control Na⁺/H⁺ exchange. *Nature.* 1998b, 392:626-630
- Halle M, Liu YC, Hardy S, Theberge JF, Blanchetot C, Bourdeau A, Meng TC, Tremblay ML: Caspase-3 regulates catalytic activity and scaffolding functions of the protein tyrosine phosphatase PEST, a novel modulator of the apoptotic response. *Mol Cell Biol.* 2007, 27:1172-1190
- Hamshire MG, Newman EE, Alwazzan M, Athwal BS, Brook JD: Transcriptional abnormality in myotonic dystrophy affects DMPK but not neighboring genes. *Proc Natl Acad Sci U S A.* 1997, 94:7394-7399.
- Hanks SK, Hunter T: Protein kinases 6 The eukaryotic protein kinase superfamily: kinase (catalytic) domain structure and classification. *Faseb J.* 1995, 9:576-596.

- Hao Y, Chun A, Cheung K, Rashidi B, Yang X: Tumor suppressor LATS1 is a negative regulator of oncogene YAP *J Biol Chem.* 2008, 283:5496-5509.
- Harmon EB, Harmon ML, Larsen TD, Yang J, Glasford JW, Perryman MB: Myotonic dystrophy protein kinase is critical for nuclear envelope integrity. *J Biol Chem.* 2011, 286:40296-40306.
- Harris BZ, Lim WA: Mechanism and role of PDZ domains in signaling complex assembly *J Cell Sci.* 2001, 114:3219-3231.
- Harrison SC: Peptide-surface association: the case of PDZ and PTB domains *Cell.* 1996, 86:341-343.
- Hashimoto M, Matsui T, Iwabuchi K, Date T: PKU-beta/TLK1 regulates myosin II activities, and is required for accurate equaled chromosome segregation. *Mutat Res* 2008, 657:63-67.
- Hauge C, Antal TL, Hirschberg D, Doehn U, Thorup K, Idrissova L, Hansen K, Jensen ON, Jorgensen TJ, Biondi RM, Frodin M: Mechanism for activation of the growth factor-activated AGC kinases by turn motif phosphorylation. *EMBO J.* 2007, 26:2251-2261
- Hergovich A, Cornils H, Hemmings BA: Mammalian NDR protein kinases: from regulation to a role in centrosome duplication *Biochim Biophys Acta* 2008, 1784:3-15.
- Hergovich A, Hemmings BA: Mammalian NDR/LATS protein kinases in hippo tumor suppressor signaling. *Biofactors.* 2009, 35:338-345.
- Hergovich A, Lamla S, Nigg EA, Hemmings BA: Centrosome-associated NDR kinase regulates centrosome duplication. *Mol Cell.* 2007, 25:625-634.
- Hergovich A, Schmitz D, Hemmings BA: The human tumour suppressor LATS1 is activated by human MOB1 at the membrane. *Biochem Biophys Res Commun.* 2006a, 345:50-58.
- Hergovich A, Stegert MR, Schmitz D, Hemmings BA: NDR kinases regulate essential cell processes from yeast to humans. *Nat Rev Mol Cell Biol.* 2006b, 7:253-264.
- Hillier BJ, Christopherson KS, Prehoda KE, Bredt DS, Lim WA: Unexpected modes of PDZ domain scaffolding revealed by structure of nNOS-syntrophin complex. *Science.* 1999, 284:812-815.
- Hirota T, Morisaki T, Nishiyama Y, Marumoto T, Tada K, Hara T, Masuko N, Inagaki M, Hatakeyama K, Saya H: Zyxin, a regulator of actin filament assembly, targets the mitotic apparatus by interacting with h-warts/LATS1 tumor suppressor. *J Cell Biol.* 2000, 149:1073-1086.
- Holland AJ, Cleveland DW: Boveri revisited: chromosomal instability, aneuploidy and tumorigenesis *Nat Rev Mol Cell Biol.* 2009, 10:478-487.
- Hori T, Takaori-Kondo A, Kamikubo Y, Uchiyama T: Molecular cloning of a novel human protein kinase, kpm, that is homologous to warts/lats, a Drosophila tumor suppressor *Oncogene* 2000, 19:3101-3109.
- Huang QQ, Fisher SA, Brozovich FV: Unzipping the role of myosin light chain phosphatase in smooth muscle cell relaxation. *J Biol Chem.* 2004, 279:597-603.
- Hunter T: Signaling--2000 and beyond. *Cell.* 2000, 100:113-127.
- Huxley AF: Mechanics and models of the myosin motor. *Philos Trans R Soc Lond B Biol Sci.* 2000, 355:433-440
- Huxley HE: Fifty years of muscle and the sliding filament hypothesis. *Eur J Biochem* 2004, 271:1403-1415
- Ikebe M, Hartshorne DJ: Phosphorylation of smooth muscle myosin at two distinct sites by myosin light

- chain kinase. *J Biol Chem* 1985, 260:10027-10031.
- Ikebe M, Hartshorne DJ, Elzinga M: Identification, phosphorylation, and dephosphorylation of a second site for myosin light chain kinase on the 20,000-dalton light chain of smooth muscle myosin. *J Biol Chem* 1986, 261:36-39.
- Ikebe M, Hartshorne DJ, Elzinga M: Phosphorylation of the 20,000-dalton light chain of smooth muscle myosin by the calcium-activated, phospholipid-dependent protein kinase. Phosphorylation sites and effects of phosphorylation. *J Biol Chem* 1987, 262:9569-9573.
- Innan H: A two-locus gene conversion model with selection and its application to the human RHCE and RHD genes. *Proc Natl Acad Sci USA*. 2003, 100:8793-8798.
- Innan H: Population genetic models of duplicated genes. *Genetica*. 2009, 137:19-37.
- Inomata N, Shibata H, Okuyama E, Yamazaki T: Evolutionary relationships and sequence variation of alpha-amylase variants encoded by duplicated genes in the Amy locus of *Drosophila melanogaster*. *Genetics*. 1995, 141:237-244.
- Inoue A, Yanagisawa M, Masaki T: Differential tissue expression of multiple genes for chicken smooth muscle/nonmuscle myosin regulatory light chains. *Biochim Biophys Acta*. 1992, 1130:197-202.
- Ishizaki T, Maekawa M, Fujisawa K, Okawa K, Iwamatsu A, Fujita A, Watanabe N, Saito Y, Kakizuka A, Morii N, Narumiya S: The small GTP-binding protein Rho binds to and activates a 160 kDa Ser/Thr protein kinase homologous to myotonic dystrophy kinase. *Embo J* 1996, 15:1885-1893.
- Iyer D, Belaguli N, Fluck M, Rowan BG, Wei L, Weigel NL, Booth FW, Epstein HF, Schwartz RJ, Balasubramanyam A: Novel phosphorylation target in the serum response factor MADS box regulates alpha-actin transcription. *Biochemistry*. 2003, 42:7477-7486.
- Jacobs AE, Benders AA, Oosterhof A, Veerkamp JH, van Mier P, Wevers RA, Joosten EM: The calcium homeostasis and the membrane potential of cultured muscle cells from patients with myotonic dystrophy. *Biochim Biophys Acta*. 1990, 1096:14-19.
- Jansen G, Groenen PJ, Bachner D, Jap PH, Coerwinkel M, Oerlemans F, van den Broek W, Gohlsch B, Pette D, Plomp JJ, et al: Abnormal myotonic dystrophy protein kinase levels produce only mild myopathy in mice. *Nat Genet*. 1996, 13:316-324.
- Jelen F, Oleksy A, Smietana K, Otlewski J: PDZ domains - common players in the cell signaling. *Acta Biochim Pol*. 2003, 50:985-1017.
- Jiang Z, Li X, Hu J, Zhou W, Jiang Y, Li G, Lu D: Promoter hypermethylation-mediated down-regulation of LATS1 and LATS2 in human astrocytoma. *Neurosci Res*. 2006, 56:450-458.
- Jimenez-Velasco A, Roman-Gomez J, Agirre X, Barrios M, Navarro G, Vazquez I, Prosper F, Torres A, Heiniger A: Downregulation of the large tumor suppressor 2 (LATS2/KPM) gene is associated with poor prognosis in acute lymphoblastic leukemia. *Leukemia*. 2005, 19:2347-2350.
- Jin S, Shimizu M, Balasubramanyam A, Epstein HF: Myotonic dystrophy protein kinase (DMPK) induces actin cytoskeletal reorganization and apoptotic-like blebbing in lens cells. *Cell Motil Cytoskeleton*. 2000, 45:133-148.
- Jordan P, Karess R: Myosin light chain-activating phosphorylation sites are required for oogenesis in *Drosophila*. *J Cell Biol* 1997, 139:1805-1819.

- Jung HS, Burgess SA, Billington N, Colegrave M, Patel H, Chalovich JM, Chantler PD, Knight PJ: Conservation of the regulated structure of folded myosin 2 in species separated by at least 600 million years of independent evolution. *Proc Natl Acad Sci USA*. 2008a, 105:6022-6026.
- Jung HS, Komatsu S, Ikebe M, Craig R: Head-head and head-tail interaction: a general mechanism for switching off myosin II activity in cells. *Mol Biol Cell*. 2008b, 19:3234-3242.
- Kaliman P, Catalucci D, Lam JT, Kondo R, Gutierrez JC, Reddy S, Palacin M, Zorzano A, Chien KR, Ruiz-Lozano P: Myotonic dystrophy protein kinase phosphorylates phospholamban and regulates calcium uptake in cardiomyocyte sarcoplasmic reticulum. *J Biol Chem*. 2005, 280:8016-8021.
- Kaliman P, Llagostera E: Myotonic dystrophy protein kinase (DMPK) and its role in the pathogenesis of myotonic dystrophy 1. *Cell Signal*. 2008, 20:1935-1941.
- Kamikubo Y, Takaori-Kondo A, Uchiyama T, Hori T: Inhibition of cell growth by conditional expression of kpm, a human homologue of Drosophila warts/lats tumor suppressor. *J Biol Chem*. 2003, 278:17609-17614.
- Kamm KE, Stull JT: Signaling to myosin regulatory light chain in sarcomeres. *J Biol Chem*. 2011, 286:9941-9947.
- Kanai F, Marignani PA, Sarbassova D, Yagi R, Hall RA, Donowitz M, Hisaminato A, Fujiwara T, Ito Y, Cantley LC, Yaffe MB: TAZ: a novel transcriptional co-activator regulated by interactions with 14-3-3 and PDZ domain proteins. *EMBO J*. 2000, 19:6778-6791.
- Karagiannis P, Brozovich FV: The kinetic properties of smooth muscle. how a little extra weight makes myosin faster. *J Muscle Res Cell Motil*. 2003, 24:157-163.
- Kawamoto S, Bengur AR, Sellers JR, Adelstein RS: In situ phosphorylation of human platelet myosin heavy and light chains by protein kinase C. *J Biol Chem*. 1989, 264:2258-2265.
- Kawano Y, Fukata Y, Oshiro N, Amano M, Nakamura T, Ito M, Matsumura F, Inagaki M, Kaibuchi K: Phosphorylation of myosin-binding subunit (MBS) of myosin phosphatase by Rho-kinase in vivo. *J Cell Biol*. 1999, 147:1023-1038.
- Ke H, Pei J, Ni Z, Xia H, Qi H, Woods T, Kelekar A, Tao W: Putative tumor suppressor Lats2 induces apoptosis through downregulation of Bcl-2 and Bcl-x(L). *Exp Cell Res*. 2004, 298:329-338.
- Kennedy MB: Origin of PDZ (DHR, GLGF) domains. *Trends Biochem Sci*. 1995, 20:350.
- Kimura K, Ito M, Amano M, Chihara K, Fukata Y, Nakafuku M, Yamamori B, Feng J, Nakano T, Okawa K, et al: Regulation of myosin phosphatase by Rho and Rho-associated kinase (Rho-kinase). *Science*. 1996, 273:245-248.
- Knehr M, Poppe M, Enulescu M, Eickelbaum W, Stoehr M, Schroeter D, Paweletz N: A critical appraisal of synchronization methods applied to achieve maximal enrichment of HeLa cells in specific cell cycle phases. *Exp Cell Res*. 1995, 217:546-553.
- Kolodner RD, Cleveland DW, Putnam CD: Cancer. Aneuploidy drives a mutator phenotype in cancer. *Science*. 2011, 333:942-943.
- Komander D, Garg R, Wan PT, Ridley AJ, Barford D: Mechanism of multi-site phosphorylation from a ROCK-I:RhoE complex structure. *EMBO J*. 2008, 27:3175-3185.
- Komander D, Kular G, Deak M, Alessi DR, van Aalten DM: Role of T-loop phosphorylation in PDK1

- activation, stability, and substrate binding. *J Biol Chem.* 2005, 280:18797-18802
- Komatsu S, Yano T, Shibata M, Tuft RA, Ikebe M: Effects of the regulatory light chain phosphorylation of myosin II on mitosis and cytokinesis of mammalian cells. *J Biol Chem.* 2000, 275:34512-34520.
- Kops GJ, Weaver BA, Cleveland DW: On the road to cancer: aneuploidy and the mitotic checkpoint. *Nat Rev Cancer.* 2005, 5:773-785
- Kosako H, Goto H, Yanagida M, Matsuzawa K, Fujita M, Tomono Y, Okigaki T, Odai H, Kaibuchi K, Inagaki M: Specific accumulation of Rho-associated kinase at the cleavage furrow during cytokinesis: cleavage furrow-specific phosphorylation of intermediate filaments. *Oncogene* 1999, 18:2783-2788.
- Kovacs M, Wang F, Hu A, Zhang Y, Sellers JR: Functional divergence of human cytoplasmic myosin II: kinetic characterization of the non-muscle IIA isoform. *J Biol Chem.* 2003, 278:38132-38140.
- Kozlov G, Banville D, Gehring K, Ekiel I: Solution structure of the PDZ2 domain from cytosolic human phosphatase hPTP1E complexed with a peptide reveals contribution of the beta2-beta3 loop to PDZ domain-ligand interactions. *J Mol Biol.* 2002, 320:813-820.
- Krebs EG, Beavo JA: Phosphorylation-dephosphorylation of enzymes. *Annu Rev Biochem.* 1979, 48:923-959.
- Kreis TE: Microinjected antibodies against the cytoplasmic domain of vesicular stomatitis virus glycoprotein block its transport to the cell surface. *Embo J.* 1986, 5:931-941.
- Krieger E, Koraimann G, Vriend G: Increasing the precision of comparative models with YASARA NOVA--a self-parameterizing force field. *Proteins.* 2002, 47:393-402.
- Kumar CC, Chang C: Human smooth muscle myosin light chain-2 gene expression is repressed in ras transformed fibroblast cells. *Cell Growth Differ.* 1992, 3:1-10
- Kunda P, Baum B: The actin cytoskeleton in spindle assembly and positioning. *Trends Cell Biol.* 2009, 19:174-179.
- Kuninaka S, Nomura M, Hirota T, Iida S, Hara T, Honda S, Kunitoku N, Sasayama T, Arima Y, Marumoto T, et al: The tumor suppressor WARTS activates the Omi / HtrA2-dependent pathway of cell death. *Oncogene.* 2005, 24:5287-5298.
- Lash JA, Helper DJ, Klug M, Nicolozakes AW, Hathaway DR: Nucleotide and deduced amino acid sequence of cDNAs encoding two isoforms for the 17,000 dalton myosin light chain in bovine aortic smooth muscle. *Nucleic Acids Res.* 1990, 18:7176.
- Lazzaro BP, Clark AG: Evidence for recurrent paralogous gene conversion and exceptional allelic divergence in the Attacin genes of *Drosophila melanogaster*. *Genetics.* 2001, 159:659-671.
- Lee KH, Goan YG, Hsiao M, Lee CH, Jian SH, Lin JT, Chen YL, Lu PJ: MicroRNA-373 (miR-373) post-transcriptionally regulates large tumor suppressor, homolog 2 (LATS2) and stimulates proliferation in human esophageal cancer. *Exp Cell Res.* 2009, 315:2529-2538.
- Lei QY, Zhang H, Zhao B, Zha ZY, Bai F, Pei XH, Zhao S, Xiong Y, Guan KL: TAZ promotes cell proliferation and epithelial-mesenchymal transition and is inhibited by the hippo pathway. *Mol Cell Biol.* 2008, 28:2426-2436.
- Lenz S, Lohse P, Seidel U, Arnold HH: The alkali light chains of human smooth and nonmuscle myosins

- are encoded by a single gene. Tissue-specific expression by alternative splicing pathways. *J Biol Chem* 1989, 264:9009-9015
- Leung T, Chen XQ, Manser E, Lim L. The p160 RhoA-binding kinase ROK alpha is a member of a kinase family and is involved in the reorganization of the cytoskeleton. *Mol Cell Biol*. 1996, 16:5313-5327.
- Leung T, Chen XQ, Tan I, Manser E, Lim L: Myotonic dystrophy kinase-related Cdc42-binding kinase acts as a Cdc42 effector in promoting cytoskeletal reorganization. *Mol Cell Biol*. 1998, 18:130-140.
- Levene PA, Alsberg CL: The cleavage products of vitellin. *J Biol Chem*. 1906, 2:127-133
- Li Y, Pei J, Xia H, Ke H, Wang H, Tao W: Lats2, a putative tumor suppressor, inhibits G1/S transition *Oncogene* 2003, 22:4398-4405.
- Llagostera E, Carmona MC, Vicente M, Escorihuela RM, Kaliman P: High-fat diet induced adiposity and insulin resistance in mice lacking the myotonic dystrophy protein kinase *FEBS Lett* 2009, 583:2121-2125.
- Llagostera E, Catalucci D, Marti L, Liesa M, Camps M, Ciaraldi TP, Kondo R, Reddy S, Dillmann WH, Palacin M, et al: Role of myotonic dystrophy protein kinase (DMPK) in glucose homeostasis and muscle insulin action *PLoS One* 2007, 2:e1134.
- Mabuchi I, Okuno M: The effect of myosin antibody on the division of starfish blastomeres *J Cell Biol*. 1977, 74:251-263.
- Mack G, Rattner JB. Centrosome repositioning immediately following karyokinesis and prior to cytokinesis *Cell Motil Cytoskeleton*. 1993, 26:239-247.
- Madaule P, Eda M, Watanabe N, Fujisawa K, Matsuoka T, Bito H, Ishizaki T, Narumiya S: Role of citron kinase as a target of the small GTPase Rho in cytokinesis. *Nature*. 1998, 394:491-494.
- Madaule P, Furuyashiki T, Eda M, Bito H, Ishizaki T, Narumiya S: Citron, a Rho target that affects contractility during cytokinesis. *Microsc Res Tech*. 2000, 49:123-126.
- Maekawa K, Imagawa N, Naito A, Harada S, Yoshie O, Takagi S: Association of protein-tyrosine phosphatase PTP-BAS with the transcription-factor-inhibitory protein IkappaBalpha through interaction between the PDZ1 domain and ankyrin repeats. *Biochem J* 1999, 337 (Pt 2):179-184.
- Mah AS, Elia AE, Devgan G, Piatek J, Schutkowski M, Snyder M, Yaffe MB, Deshaies RJ: Substrate specificity analysis of protein kinase complex Dbf2-Mob1 by peptide library and proteome array screening *BMC Biochem*. 2005, 6:22.
- Mahadevan M, Tsiflidis C, Sabourin L, Shutler G, Amemiya C, Jansen G, Neville C, Narang M, Barcelo J, O'Hoy K, et al.: Myotonic dystrophy mutation: an unstable CTG repeat in the 3' untranslated region of the gene. *Science*. 1992, 255:1253-1255.
- Maly DJ, Allen JA, Shokat KM: A mechanism-based cross-linker for the identification of kinase-substrate pairs. *J Am Chem Soc*. 2004, 126:9160-9161.
- Manning G, Whyte DB, Martinez R, Hunter T, Sudarsanam S. The protein kinase complement of the human genome. *Science* 2002, 298:1912-1934.
- Matsuda S, Mikawa S, Hirai H: Phosphorylation of serine-880 in GluR2 by protein kinase C prevents

- its C terminus from binding with glutamate receptor-interacting protein. *J Neurochem.* 1999, 73:1765-1768.
- Matsumura F: Regulation of myosin II during cytokinesis in higher eukaryotes. *Trends Cell Biol.* 2005, 15:371-377.
- Matsumura F, Hartshorne DJ: Myosin phosphatase target subunit: Many roles in cell function. *Biochem Biophys Res Commun* 2008, 369:149-156.
- Matsumura F, Ono S, Yamakita Y, Totsukawa G, Yamashiro S: Specific localization of serine 19 phosphorylated myosin II during cell locomotion and mitosis of cultured cells. *J Cell Biol.* 1998, 140:119-129.
- Matsumura F, Totsukawa G, Yamakita Y, Yamashiro S: Role of myosin light chain phosphorylation in the regulation of cytokinesis. *Cell Struct Funct.* 2001, 26:639-644.
- McPherson JP, Tamblyn L, Elia A, Migon E, Shehabeldin A, Matysiak-Zablocki E, Lemmers B, Salmena L, Hakem A, Fish J, et al: Lats2/Kpm is required for embryonic development, proliferation control and genomic integrity. *Embo J.* 2004, 23:3677-3688.
- Millward TA, Heizmann CW, Schafer BW, Hemmings BA: Calcium regulation of Ndr protein kinase mediated by S100 calcium-binding proteins. *Embo J.* 1998, 17:5913-5922.
- Millward TA, Hess D, Hemmings BA: Ndr protein kinase is regulated by phosphorylation on two conserved sequence motifs. *J Biol Chem.* 1999, 274:33847-33850.
- Mizutani T, Kawabata K, Koyama Y, Takahashi M, Haga H: Regulation of cellular contractile force in response to mechanical stretch by diphosphorylation of myosin regulatory light chain via RhoA signaling cascade. *Cell Motil Cytoskeleton.* 2009, 66:389-397.
- Monical PL, Owens GK, Murphy RA: Expression of myosin regulatory light-chain isoforms and regulation of phosphorylation in smooth muscle. *Am J Physiol.* 1993, 264:C1466-1472.
- Montagnac G, Echard A, Chavrier P: Endocytic traffic in animal cell cytokinesis. *Curr Opin Cell Biol.* 2008, 20:454-461.
- Morisaki T, Hirota T, Iida S, Marumoto T, Hara T, Nishiyama Y, Kawasaki M, Hiraoka T, Mimori T, Araki N, et al: WARTS tumor suppressor is phosphorylated by Cdc2/cyclin B at spindle poles during mitosis. *FEBS Lett* 2002, 529:319-324.
- Moritz A, Li Y, Guo A, Villen J, Wang Y, MacNeill J, Kornhauser J, Sprott K, Zhou J, Possemato A, et al: Akt-RSK-S6 kinase signaling networks activated by oncogenic receptor tyrosine kinases. *Sci Signal.* 2010, 3:ra64.
- Mounsey JP, John JE, 3rd, Helmke SM, Bush EW, Gilbert J, Roses AD, Perryman MB, Jones LR, Moorman JR: Phospholemman is a substrate for myotonic dystrophy protein kinase. *J Biol Chem* 2000a, 275:23362-23367.
- Mounsey JP, Mistry DJ, Ai CW, Reddy S, Moorman JR: Skeletal muscle sodium channel gating in mice deficient in myotonic dystrophy protein kinase. *Hum Mol Genet* 2000b, 9:2313-2320.
- Mounsey JP, Xu P, John JE, 3rd, Horne LT, Gilbert J, Roses AD, Moorman JR: Modulation of skeletal muscle sodium channels by human myotonic protein kinase. *J Clin Invest.* 1995, 95:2379-2384.
- Mueller CM, Hilbert JE, Martens W, Thornton CA, Moxley RT, 3rd, Greene MH: Hypothesis: neoplasms in myotonic dystrophy. *Cancer Causes Control.* 2009, 20:2009-2020.

- Mulders SA, van Horsen R, Gerrits L, Bennink MB, Pluk H, de Boer-van Huizen RT, Croes HJ, Wijers M, van de Loo FA, Fransen J, et al: Abnormal actomyosin assembly in proliferating and differentiating myoblasts upon expression of a cytosolic DMPK isoform. *Biochim Biophys Acta*. 2011, 1813:867-877.
- Muranyi A, Zhang R, Liu F, Hirano K, Ito M, Epstein HF, Hartshorne DJ: Myotonic dystrophy protein kinase phosphorylates the myosin phosphatase targeting subunit and inhibits myosin phosphatase activity. *FEBS Lett* 2001, 493:80-84.
- Murthy KK, Clark K, Fortin Y, Shen SH, Banville D: ZRP-1, a zyxin-related protein, interacts with the second PDZ domain of the cytosolic protein tyrosine phosphatase hPTP1E. *J Biol Chem*. 1999, 274:20679-20687
- Mussini I, Biral D, Marin O, Furlan S, Salvatori S: Myotonic dystrophy protein kinase expressed in rat cardiac muscle is associated with sarcoplasmic reticulum and gap junctions. *J Histochem Cytochem*. 1999, 47:383-392
- Nabeshima Y, Nonomura Y, Fujii-Kuriyama Y: Nonmuscle and smooth muscle myosin light chain mRNAs are generated from a single gene by the tissue-specific alternative RNA splicing. *J Biol Chem*. 1987, 262:10608-10612.
- Naumanen P, Lappalainen P, Hotulainen P: Mechanisms of actin stress fibre assembly *J Microsc*. 2008, 231:446-454.
- Ng Y, Tan I, Lim L, Leung T: Expression of the Human Myotonic Dystrophy Kinase-related Cdc42-binding Kinase {gamma} Is Regulated by Promoter DNA Methylation and Sp1 Binding. *J Biol Chem*. 2004, 279:34156-34164.
- Nishikawa M, Sellers JR, Adelstein RS, Hidaka H: Protein kinase C modulates in vitro phosphorylation of the smooth muscle heavy meromyosin by myosin light chain kinase. *J Biol Chem* 1984, 259:8808-8814.
- Nishiyama Y, Hirota T, Morisaki T, Hara T, Marumoto T, Iida S, Makino K, Yamamoto H, Hiraoka T, Kitamura N, Saya H: A human homolog of Drosophila warts tumor suppressor, h-warts, localized to mitotic apparatus and specifically phosphorylated during mitosis. *FEBS Lett*. 1999, 459:159-165.
- Normand G, King RW: Understanding cytokinesis failure. *Adv Exp Med Biol*. 2010, 676:27-55.
- O'Cochlain DF, Perez-Terzic C, Reyes S, Kane GC, Behfar A, Hodgson DM, Strommen JA, Liu XK, van den Broek W, Wansink DG, et al: Transgenic overexpression of human DMPK accumulates into hypertrophic cardiomyopathy, myotonic myopathy and hypotension traits of myotonic dystrophy. *Hum Mol Genet*. 2004, 13:2505-2518.
- Obara K, Ito Y, Shimada H, Nakayama K: The relaxant effect of okadaic acid on canine basilar artery involves activation of PKCalpha and phosphorylation of the myosin light chain at Thr-9. *Eur J Pharmacol*. 2008, 598:87-93.
- Obara K, Mitate A, Nozawa K, Watanabe M, Ito Y, Nakayama K: Interactive role of protein phosphatase 2A and protein kinase Calpha in the stretch-induced triphosphorylation of myosin light chain in canine cerebral artery. *J Vasc Res*. 2010, 47:115-127.
- Obara K, Uchino M, Koide M, Yamanaka A, Nakayama K: Stretch-induced triphosphorylation of myosin

- light chain and myogenic tone in canine basilar artery. *Eur J Pharmacol.* 2006, 534:141-151
- Oka T, Remue E, Meerschaert K, Vanloo B, Boucherie C, Gfeller D, Bader GD, Sidhu SS, Vandekerckhove J, Gettemans J, Sudol M: Functional complexes between YAP2 and ZO-2 are PDZ domain-dependent, and regulate YAP2 nuclear localization and signalling. *Biochem J.* 2010, 432 461-472.
- Oka T, Sudol M: Nuclear localization and pro-apoptotic signaling of YAP2 require intact PDZ-binding motif. *Genes Cells.* 2009, 14:607-615.
- Oude Ophuis RJ, Mulders SA, van Herpen RE, van de Vorstenbosch R, Wieringa B, Wansink DG: DMPK protein isoforms are differentially expressed in myogenic and neural cell lineages. *Muscle Nerve* 2009a, 40:545-555.
- Oude Ophuis RJ, Wijers M, Bennink MB, van de Loo FA, Fransen JA, Wieringa B, Wansink DG: A tail-anchored myotonic dystrophy protein kinase isoform induces perinuclear clustering of mitochondria, autophagy, and apoptosis. *PLoS One.* 2009b, 4:e8024
- Pall GS, Johnson KJ, Smith GL: Abnormal contractile activity and calcium cycling in cardiac myocytes isolated from DMPK knockout mice. *Physiol Genomics.* 2003, 13:139-146
- Park I, Han C, Jin S, Lee B, Choi H, Kwon JT, Kim D, Kim J, Lifirsu E, Park WJ, et al: Myosin regulatory light chains are required to maintain the stability of myosin II and cellular integrity. *Biochem J.* 2011, 434:171-180
- Park I, Hong SE, Kim TW, Lee J, Oh J, Choi E, Han C, Lee H, Han Kim D, Cho C: Comprehensive identification and characterization of novel cardiac genes in mouse. *J Mol Cell Cardiol.* 2007, 43 93-106
- Parker PJ, Parkinson SJ: AGC protein kinase phosphorylation and protein kinase C. *Biochem Soc Trans.* 2001, 29:860-863.
- Pawson T, Nash P: Assembly of cell regulatory systems through protein interaction domains. *Science.* 2003, 300:445-452.
- Pearce LR, Komander D, Alessi DR: The nuts and bolts of AGC protein kinases. *Nat Rev Mol Cell Biol.* 2010, 11:9-22.
- Pei L, Melmed S: Isolation and characterization of a pituitary tumor-transforming gene (PTTG). *Mol Endocrinol.* 1997, 11:433-441
- Peters JM: The anaphase-promoting complex: proteolysis in mitosis and beyond. *Mol Cell.* 2002, 9:931-943.
- Pham YC, Man N, Lam LT, Morris GE: Localization of myotonic dystrophy protein kinase in human and rabbit tissues using a new panel of monoclonal antibodies. *Hum Mol Genet.* 1998, 7:1957-1965.
- Piel M, Nordberg J, Euteneuer U, Bornens M: Centrosome-dependent exit of cytokinesis in animal cells. *Science.* 2001, 291:1550-1553.
- Plotnikova OV, Kondrashov FA, Vlasov PK, Grigorenko AP, Ginter EK, Rogaev EI: Conversion and compensatory evolution of the gamma-crystallin genes and identification of a cataractogenic mutation that reverses the sequence of the human CRYGD gene to an ancestral state. *Am J Hum Genet.* 2007, 81:32-43.

- Pollard TD Mechanics of cytokinesis in eukaryotes. *Curr Opin Cell Biol.* 2010, 22:50-56.
- Popovic M, Bella J, Zlatev V, Hodnik V, Anderluh G, Barlow PN, Pintar A, Pangor S: The interaction of Jagged-1 cytoplasmic tail with afadin PDZ domain is local, folding-independent, and tuned by phosphorylation. *J Mol Recognit.* 2010, 24 245-253.
- Post PL, DeBiasio RL, Taylor DL: A fluorescent protein biosensor of myosin II regulatory light chain phosphorylation reports a gradient of phosphorylated myosin II in migrating cells. *Mol Biol Cell* 1995, 6:1755-1768.
- Powzaniuk M, McElwee-Witmer S, Vogel RL, Hayami T, Rutledge SJ, Chen F, Harada S, Schmidt A, Rodan GA, Freedman LP, Bai C: The LATS2/KPM tumor suppressor is a negative regulator of the androgen receptor. *Mol Endocrinol.* 2004, 18:2011-2023.
- Ranum LP, Cooper TA: RNA-mediated neuromuscular disorders. *Annu Rev Neurosci.* 2006, 29:259-277.
- Reddy S, Smith DB, Rich MM, Leferovich JM, Reilly P, Davis BM, Tran K, Rayburn H, Bronson R, Cros D, et al: Mice lacking the myotonic dystrophy protein kinase develop a late onset progressive myopathy. *Nat Genet.* 1996, 13:325-335.
- Reiser PJ, Bicer S: Multiple isoforms of myosin light chain 1 in pig diaphragm slow fibers: correlation with maximal shortening velocity and force generation. *Arch Biochem Biophys.* 2006, 456:112-118.
- Remue E, Meerschaert K, Oka T, Boucherie C, Vandekerckhove J, Sudol M, Gettemans J: TAZ interacts with zonula occludens-1 and -2 proteins in a PDZ-1 dependent manner. *FEBS Lett* 2010, 584:4175-4180.
- Riento K, Ridley AJ: Rocks: multifunctional kinases in cell behaviour. *Nat Rev Mol Cell Biol.* 2003, 4:446-456.
- Roberts R, Timchenko NA, Miller JW, Reddy S, Caskey CT, Swanson MS, Timchenko LT: Altered phosphorylation and intracellular distribution of a (CUG)_n triplet repeat RNA-binding protein in patients with myotonic dystrophy and in myotonin protein kinase knockout mice. *Proc Natl Acad Sci U S A.* 1997, 94:13221-13226.
- Rosenblatt J, Cramer LP, Baum B, McGee KM: Myosin II-dependent cortical movement is required for centrosome separation and positioning during mitotic spindle assembly. *Cell* 2004, 117:361-372.
- Ruchaud S, Carmena M, Earnshaw WC: Chromosomal passengers: conducting cell division. *Nat Rev Mol Cell Biol* 2007, 8:798-812.
- Saba S, Vanderbrink BA, Luciano B, Aronovitz MJ, Berul CI, Reddy S, Housman D, Mendelsohn ME, Estes NA, 3rd, Wang PJ: Localization of the sites of conduction abnormalities in a mouse model of myotonic dystrophy. *J Cardiovasc Electrophysiol* 1999, 10:1214-1220.
- Salvatori S, Biral D, Furlan S, Marin O: Evidence for localization of the myotonic dystrophy protein kinase to the terminal cisternae of the sarcoplasmic reticulum. *J Muscle Res Cell Motil.* 1997, 18:429-440.
- Satterwhite LL, Lohka MJ, Wilson KL, Scherson TY, Cisek LJ, Corden JL, Pollard TD: Phosphorylation of myosin-II regulatory light chain by cyclin-p34cdc2: a mechanism for the timing of cytokinesis. *J Cell Biol.* 1992, 118:595-605.
- Scholey JM, Taylor KA, Kendrick-Jones J: Regulation of non-muscle myosin assembly by calmodulin-

dependent light chain kinase *Nature*. 1980, 287:233-235.

Schutzowski M, Reineke U, Reimer U: Peptide arrays for kinase profiling. *ChemBiochem*. 2005, 6:513-521

Scruggs SB, Solaro RJ: The significance of regulatory light chain phosphorylation in cardiac physiology
Arch Biochem Biophys. 2011, 510:129-134

Sedzinski J, Biro M, Oswald A, Tinevez JY, Salbreux G, Paluch E: Polar actomyosin contractility destabilizes the position of the cytokinetic furrow. *Nature* 2011, 476:462-466

Sellers JR: Myosins: a diverse superfamily. *Biochim Biophys Acta* 2000, 1496:3-22.

Seto M, Sasaki Y: Alteration in the myosin phosphorylation pattern of smooth muscle by phorbol ester. *Am J Physiol*. 1990, 259:C769-774

Sheng M, Sala C: PDZ domains and the organization of supramolecular complexes. *Annu Rev Neurosci* 2001, 24:1-29.

Shi Q, King RW: Chromosome nondisjunction yields tetraploid rather than aneuploid cells in human cell lines. *Nature*. 2005, 437:1038-1042.

Shimizu M, Wang W, Walch ET, Dunne PW, Epstein HF: Rac-1 and Raf-1 kinases, components of distinct signaling pathways, activate myotonic dystrophy protein kinase. *FEBS Lett*. 2000, 475:273-277.

Shimokawa M, Ishiura S, Kameda N, Yamamoto M, Sasagawa N, Saitoh N, Sorimachi H, Ueda H, Ohno S, Suzuki K, Kobayashi T: Novel isoform of myotonic protein kinase: gene product of myotonic dystrophy is localized in the sarcoplasmic reticulum of skeletal muscle. *Am J Pathol*. 1997, 150:1285-1295.

Shivanna M, Jalimarada SS, Srinivas SP: Lovastatin inhibits the thrombin-induced loss of barrier integrity in bovine corneal endothelium. *J Ocul Pharmacol Ther*. 2010, 26:1-10.

Shuster CB, Burgess DR: Parameters that specify the timing of cytokinesis. *J Cell Biol* 1999, 146:981-992.

Sicot G, Gourdon G, Gomes-Pereira M: Myotonic dystrophy, when simple repeats reveal complex pathogenic entities: new findings and future challenges. *Hum Mol Genet* 2011, 15:R116-123.

Simoni RD, Hill RL, Vaughan M: Carbohydrate Metabolism: Glycogen Phosphorylase and the Work of Carl F and Gerty T. Cori. *J Biol Chem* 2002, 277:e18.

Snyder JA, Ha Y, Olsofka C, Wahdan R: Both actin and myosin inhibitors affect spindle architecture in PtK1 cells: does an actomyosin system contribute to mitotic spindle forces by regulating attachment and movements of chromosomes in mammalian cells? *Protoplasma*. 2010, 240:57-68

Songyang Z, Fanning AS, Fu C, Xu J, Marfatia SM, Chishti AH, Crompton A, Chan AC, Anderson JM, Cantley LC: Recognition of unique carboxyl-terminal motifs by distinct PDZ domains. *Science*. 1997, 275:73-77.

Spudich JA: How molecular motors work. *Nature*. 1994, 372:515-518.

Statsuk AV, Maly DJ, Seeliger MA, Fabian MA, Biggs WH, 3rd, Lockhart DJ, Zarrinkar PP, Kuriyan J, Shokat KM: Tuning a three-component reaction for trapping kinase substrate complexes. *J Am Chem Soc*. 2008, 130:17568-17574

Steeg PS, Palmieri D, Ouatas T, Salerno M: Histidine kinases and histidine phosphorylated proteins in mammalian cell biology, signal transduction and cancer. *Cancer Lett*. 2003, 190:1-12.

Steigemann P, Gerlich DW: Cytokinetic abscission: cellular dynamics at the midbody. *Trends Cell Biol*. 2009,

Stewart RA, Li DM, Huang H, Xu T: A genetic screen for modifiers of the *lats* tumor suppressor gene identifies C-terminal Src kinase as a regulator of cell proliferation in *Drosophila*. *Oncogene*. 2003, 22:6436-6444.

Storchova Z, Kuffer C: The consequences of tetraploidy and aneuploidy. *J Cell Sci*. 2008, 121:3859-3866.

Stull JT, Kamm KE, Vandenboom R: Myosin light chain kinase and the role of myosin light chain phosphorylation in skeletal muscle. *Arch Biochem Biophys*. 2011, 510:120-128.

Sulka B, Lortat-Jacob H, Terreux R, Letourneur F, Rousselle P: Tyrosine dephosphorylation of the syndecan-1 PDZ binding domain regulates syntenin-1 recruitment. *J Biol Chem*. 2009, 284:10659-10671.

Suzuki A, Sugiyama Y, Hayashi Y, Nyu-i N, Yoshida M, Nonaka I, Ishiura S, Arahata K, Ohno S. MKBP, a novel member of the small heat shock protein family, binds and activates the myotonic dystrophy protein kinase. *J Cell Biol*. 1998, 140:1113-1124.

Takahashi Y, Miyoshi Y, Takahata C, Irahara N, Taguchi T, Tamaki Y, Noguchi S: Down-regulation of LATS1 and LATS2 mRNA expression by promoter hypermethylation and its association with biologically aggressive phenotype in human breast cancers. *Clin Cancer Res*. 2005, 11:1380-1385.

Takashima S: Phosphorylation of myosin regulatory light chain by myosin light chain kinase, and muscle contraction. *Circ J*. 2009, 73:208-213

Tamaskovic R, Bichsel SJ, Hemmings BA: NDR family of AGC kinases--essential regulators of the cell cycle and morphogenesis. *FEBS Lett*. 2003a, 546:73-80.

Tamaskovic R, Bichsel SJ, Rogniaux H, Stegert MR, Hemmings BA: Mechanism of Ca²⁺-mediated Regulation of NDR Protein Kinase through Autophosphorylation and Phosphorylation by an Upstream Kinase. *J Biol Chem*. 2003b, 278:6710-6718.

Tan I, Lai J, Yong J, Li SF, Leung T: Chelerythrine perturbs lamellar actomyosin filaments by selective inhibition of myotonic dystrophy kinase-related Cdc42-binding kinase. *FEBS Lett*. 2011.

Tan I, Ng CH, Lim L, Leung T. Phosphorylation of a novel myosin binding subunit of protein phosphatase 1 reveals a conserved mechanism in the regulation of actin cytoskeleton. *J Biol Chem*. 2001a, 276:21209-21216

Tan I, Seow KT, Lim L, Leung T: Intermolecular and intramolecular interactions regulate catalytic activity of myotonic dystrophy kinase-related Cdc42-binding kinase alpha. *Mol Cell Biol*. 2001b, 21:2767-2778.

Tanaka M, Gupta R, Mayer BJ: Differential inhibition of signaling pathways by dominant-negative SH2/SH3 adapter proteins. *Mol Cell Biol*. 1995, 15:6829-6837.

Taneja KL, McCurrach M, Schalling M, Housman D, Singer RH: Foci of trinucleotide repeat transcripts in nuclei of myotonic dystrophy cells and tissues. *J Cell Biol*. 1995, 128:995-1002.

Tao W, Zhang S, Turenchalk GS, Stewart RA, St John MA, Chen W, Xu T: Human homologue of the *Drosophila melanogaster lats* tumour suppressor modulates CDC2 activity. *Nat Genet*. 1999, 21:177-181.

Taylor SS, Scott MI, Holland AJ: The spindle checkpoint: a quality control mechanism which ensures accurate chromosome segregation. *Chromosome Res*. 2004, 12 599-616

- Teshima KM, Innan H: The effect of gene conversion on the divergence between duplicated genes. *Genetics*. 2004, 166:1553-1560.
- Thiele A, Stangl GI, Schutkowski M: Deciphering Enzyme Function Using Peptide Arrays. *Mol Biotechnol* 2011.
- Tiganis T, Bennett AM: Protein tyrosine phosphatase function: the substrate perspective. *Biochem J*. 2007, 402 1-15.
- Tiscornia G, Mahadevan MS: Myotonic dystrophy: the role of the CUG triplet repeats in splicing of a novel DMPK exon and altered cytoplasmic DMPK mRNA isoform ratios. *Mol Cell* 2000, 5:959-967.
- Toji S, Yabuta N, Hosomi T, Nishihara S, Kobayashi T, Suzuki S, Tamai K, Nojima H: The centrosomal protein Lats2 is a phosphorylation target of Aurora-A kinase. *Genes Cells*. 2004, 9:383-397.
- Torshin I. Direct and reversed amino acid sequence pattern analysis: structural reasons for activity of reversed sequence sites and results of kinase site mutagenesis. *Biochem J*. 2000, 345 Pt 3:733-740.
- Totsukawa G, Yamakita Y, Yamashiro S, Hosoya H, Hartshorne DJ, Matsumura F: Activation of myosin phosphatase targeting subunit by mitosis-specific phosphorylation. *J Cell Biol*. 1999, 144:735-744.
- Tsuji K, Yamauchi K, Yang M, Jiang P, Bouvet M, Endo H, Kanai Y, Yamashita K, Moossa AR, Hoffman RM: Dual-color imaging of nuclear-cytoplasmic dynamics, viability, and proliferation of cancer cells in the portal vein area. *Cancer Res*. 2006, 66:303-306.
- Turner MS, Fen Fen L, Trauger JW, Stephens J, LoGrasso P: Characterization and purification of truncated human Rho-kinase II expressed in Sf-21 cells. *Arch Biochem Biophys*. 2002, 405:13-20.
- Ubersax JA, Ferrell JE, Jr.: Mechanisms of specificity in protein phosphorylation. *Nat Rev Mol Cell Biol* 2007, 8:530-541.
- Ueda H, Shimokawa M, Yamamoto M, Kameda N, Mizusawa H, Baba T, Terada N, Fujii Y, Ohno S, Ishiura S, Kobayashi T: Decreased expression of myotonic dystrophy protein kinase and disorganization of sarcoplasmic reticulum in skeletal muscle of myotonic dystrophy. *J Neurol Sci*. 1999, 162:38-50.
- Vaccaro P, Dente L: PDZ domains. troubles in classification. *FEBS Lett*. 2002, 512:345-349.
- Vakifahmetoglu H, Olsson M, Zhivotovsky B: Death through a tragedy: mitotic catastrophe. *Cell Death Differ*. 2008, 15:1153-1162.
- van den Berk LC: Binding characteristics of PTP-BL PDZ domains. *Ph.D. Thesis*. Radboud University Nijmegen Medical Centre, Cell Biology, 2005.
- van den Berk LC, Landi E, Harmsen E, Dente L, Hendriks WJ: Redox-regulated affinity of the third PDZ domain in the phosphotyrosine phosphatase PTP-BL for cysteine-containing target peptides. *FEBS J*. 2005, 272:3306-3316.
- van den Berk LC, Landi E, Walma T, Vuister GW, Dente L, Hendriks WJ: An allosteric intramolecular PDZ-PDZ interaction modulates PTP-BL PDZ2 binding specificity. *Biochemistry*. 2007, 46:13629-13637.
- van den Berk LC, van Ham MA, te Lindert MM, Walma T, Aelen J, Vuister GW, Hendriks WJ: The interaction of PTP-BL PDZ domains with RIL: an enigmatic role for the RIL LIM domain. *Mol Biol Rep*. 2004,

- van Ham M, Croes H, Schepens J, Fransen J, Wieringa B, Hendriks W: Cloning and characterization of mCRIP2, a mouse LIM-only protein that interacts with PDZ domain IV of PTP-BL. *Genes Cells*. 2003, 8:631-644
- van Ham M, Hendriks W: PDZ domains-glue and guide. *Mol Biol Rep*. 2003, 30:69-82.
- van Herpen RE: Myotonic Dystrophy Protein Kinase Splice Isoforms. *Ph.D. Thesis*. Radboud University Nijmegen Medical Centre, Cell Biology; 2006
- van Herpen RE, Oude Ophuis RJ, Wijers M, Bennink MB, van de Loo FA, Fransen J, Wieringa B, Wansink DG: Divergent mitochondrial and endoplasmic reticulum association of DMPK splice isoforms depends on unique sequence arrangements in tail anchors. *Mol Cell Biol*. 2005, 25:1402-1414.
- Vazquez F, Grossman SR, Takahashi Y, Rokas MV, Nakamura N, Sellers WR: Phosphorylation of the PTEN tail acts as an inhibitory switch by preventing its recruitment into a protein complex. *J Biol Chem*. 2001, 276:48627-48630.
- Velasco G, Armstrong C, Morrice N, Frame S, Cohen P: Phosphorylation of the regulatory subunit of smooth muscle protein phosphatase 1M at Thr850 induces its dissociation from myosin. *FEBS Lett*. 2002, 527:101-104
- Via A, Diella F, Gibson TJ, Helmer-Citterich M: From sequence to structural analysis in protein phosphorylation motifs. *Front Biosci*. 2011, 16:1261-1275.
- Vicente-Manzanares M, Ma X, Adelstein RS, Horwitz AR: Non-muscle myosin II takes centre stage in cell adhesion and migration. *Nat Rev Mol Cell Biol*. 2009, 10:778-790.
- Voorhoeve PM, le Sage C, Schrier M, Gillis AJ, Stoop H, Nagel R, Liu YP, van Duijse J, Drost J, Griekspoor A, et al: A genetic screen implicates miRNA-372 and miRNA-373 as oncogenes in testicular germ cell tumors. *Cell*. 2006, 124:1169-1181.
- Vriend G: WHAT IF: a molecular modeling and drug design program. *J Mol Graph*. 1990, 8:52-56, 29
- Walma T, Spronk CA, Tessari M, Aelen J, Schepens J, Hendriks W, Vuister GW: Structure, dynamics and binding characteristics of the second PDZ domain of PTP-BL. *J Mol Biol*. 2002, 316:1101-1110.
- Wansink DG, van Herpen RE, Coerwinkel-Driessen MM, Groenen PJ, Hemmings BA, Wieringa B: Alternative splicing controls myotonic dystrophy protein kinase structure, enzymatic activity, and subcellular localization. *Mol Cell Biol*. 2003, 23 5489-5501.
- Wansink DG, van Herpen, R.E M.A., Wieringa, B.: Normal and pathophysiological significance of myotonic dystrophy protein kinase. In *Genetic Instabilities and Neurological Diseases* 2nd edition Edited by Wells RD, Ashizawa, T. San Diego, CA: Elsevier-Academic Press; 2006: 79-97
- Wansink DG, Wieringa B: Transgenic mouse models for myotonic dystrophy type 1 (DM1). *Cytogenet Genome Res*. 2003, 100:230-242.
- Weisz B, Giehl K, Gana-Weisz M, Egozi Y, Ben-Baruch G, Marciano D, Gierschik P, Kloog Y: A new functional Ras antagonist inhibits human pancreatic tumor growth in nude mice. *Oncogene*. 1999, 18:2579-2588
- Wendt T, Taylor D, Trybus KM, Taylor K: Three-dimensional image reconstruction of dephosphorylated smooth muscle heavy meromyosin reveals asymmetry in the interaction between myosin heads

- and placement of subfragment 2. *Proc Natl Acad Sci U S A*. 2001, 98:4361-4366
- Wheeler TM, Thornton CA: Myotonic dystrophy: RNA-mediated muscle disease. *Curr Opin Neurol*. 2007, 20:572-576.
- Whitehead CM, Winkfein RJ, Fritzler MJ, Rattner JB: The spindle kinesin-like protein HsEg5 is an autoantigen in systemic lupus erythematosus. *Arthritis Rheum*. 1996, 39:1635-1642.
- Wieland T, Hippe HJ, Ludwig K, Zhou XB, Korth M, Klumpp S: Reversible histidine phosphorylation in mammalian cells: a teeter-totter formed by nucleoside diphosphate kinase and protein histidine phosphatase 1. *Methods Enzymol*. 2010, 471:379-402.
- Wilkinson S, Paterson HF, Marshall CJ: Cdc42-MRCK and Rho-ROCK signalling cooperate in myosin phosphorylation and cell invasion. *Nat Cell Biol*. 2005, 7:255-261.
- Woodhead JL, Zhao FQ, Craig R, Egelman EH, Alamo L, Padron R: Atomic model of a myosin filament in the relaxed state. *Nature*. 2005, 436:1195-1199.
- Wu Q, Sahasrabudhe RM, Luo LZ, Lewis DW, Gollin SM, Saunders WS: Deficiency in myosin light-chain phosphorylation causes cytokinesis failure and multipolarity in cancer cells. *Oncogene*. 2010, 29:4183-4193.
- Xia H, Winokur ST, Kuo WL, Altherr MR, Bredt DS: Actinin-associated LIM protein: identification of a domain interaction between PDZ and spectrin-like repeat motifs. *J Cell Biol*. 1997, 139:507-515.
- Yabuta N, Fujii T, Copeland NG, Gilbert DJ, Jenkins NA, Nishiguchi H, Endo Y, Toji S, Tanaka H, Nishimune Y, Nojima H: Structure, expression, and chromosome mapping of LATS2, a mammalian homologue of the *Drosophila* tumor suppressor gene *lats/warts*. *Genomics*. 2000, 63:263-270.
- Yabuta N, Okada N, Ito A, Hosomi T, Nishihara S, Sasayama Y, Fujimori A, Okuzaki D, Zhao H, Ikawa M, et al: Lats2 is an essential mitotic regulator required for the coordination of cell division. *J Biol Chem*. 2007, 282:19259-19271.
- Yamada A, Hirose K, Hashimoto A, Iino M: Real-time imaging of myosin II regulatory light-chain phosphorylation using a new protein biosensor. *Biochem J*. 2005, 385:589-594.
- Yamakita Y, Yamashiro S, Matsumura F: In vivo phosphorylation of regulatory light chain of myosin II during mitosis of cultured cells. *J Cell Biol*. 1994, 124:129-137.
- Yamashiro S, Totsukawa G, Yamakita Y, Sasaki Y, Madaule P, Ishizaki T, Narumiya S, Matsumura F: Citron kinase, a Rho-dependent kinase, induces di-phosphorylation of regulatory light chain of myosin II. *Mol Biol Cell*. 2003, 14:1745-1756.
- Yang J, Cron P, Good VM, Thompson V, Hemmings BA, Barford D: Crystal structure of an activated Akt/protein kinase B ternary complex with GSK3-peptide and AMP-PNP. *Nat Struct Biol*. 2002a, 9:940-944.
- Yang J, Cron P, Thompson V, Good VM, Hess D, Hemmings BA, Barford D: Molecular mechanism for the regulation of protein kinase B/Akt by hydrophobic motif phosphorylation. *Mol Cell*. 2002b, 9:1227-1240.
- Yang X, Yu K, Hao Y, Li DM, Stewart R, Insogna KL, Xu T: LATS1 tumour suppressor affects cytokinesis by inhibiting LIMK1. *Nat Cell Biol*. 2004, 6:609-617.
- Yasui Y, Amano M, Nagata K-i, Inagaki N, Nakamura H, Saya H, Kaibuchi K, Inagaki M: Roles of Rho-

references, Nederlandse samenvatting, abbreviations, publications, curriculum vitae, dankwoord

associated Kinase in Cytokinesis, Mutations in Rho-associated Kinase Phosphorylation Sites Impair Cytokinetic Segregation of Glial Filaments *J Cell Biol.* 1998, 143:1249-1258.

Yokoyama T, Goto H, Izawa I, Mizutani H, Inagaki M. Aurora-B and Rho-kinase/ROCK, the two cleavage furrow kinases, independently regulate the progression of cytokinesis: possible existence of a novel cleavage furrow kinase phosphorylates ezrin/radixin/moesin (ERM) *Genes Cells.* 2005, 10:127-137.

Yu R, Lu W, Chen J, McCabe CJ, Melmed S: Overexpressed pituitary tumor-transforming gene causes aneuploidy in live human cells *Endocrinology.* 2003, 144:4991-4998.

Yuce O, Piekny A, Glotzer M: An ECT2-centralspindlin complex regulates the localization and function of RhoA. *J Cell Biol.* 2005, 170:571-582.

Yuen SL, Ogut O, Brozovich FV: Nonmuscle myosin is regulated during smooth muscle contraction. *Am J Physiol Heart Circ Physiol.* 2009, 297:H191-199.

Zaliani A, Pinori M, Ball HL, DiGregorio G, Cremonesi P, Mascagni P: The interaction of myristylated peptides with the catalytic domain of protein kinase C revealed by their sequence palindromy and the identification of a myristyl binding site. *Protein Eng.* 1998, 11:803-810.

Zeng C: NuMA: a nuclear protein involved in mitotic centrosome function. *Microsc ResTech.* 2000, 49:467-477

Zhang N, Ge G, Meyer R, Sethi S, Basu D, Pradhan S, Zhao YJ, Li XN, Cai WW, El-Naggar AK, et al: Overexpression of Separase induces aneuploidy and mammary tumorigenesis. *Proc Natl Acad Sci U S A.* 2008, 105:13033-13038.

Zhao B, Wei X, Li W, Udan RS, Yang Q, Kim J, Xie J, Ikenoue T, Yu J, Li L, et al: Inactivation of YAP oncoprotein by the Hippo pathway is involved in cell contact inhibition and tissue growth control. *Genes Dev.* 2007, 21:2747-2761.

Zhao Z, Manser E: PAK and other Rho-associated kinases--effectors with surprisingly diverse mechanisms of regulation *Biochem J.* 2005, 2.201-214.

Zhou D, Conrad C, Xia F, Park JS, Payer B, Yin Y, Lauwers GY, Thasler W, Lee JT, Avruch J, Bardeesy N: Mst1 and Mst2 maintain hepatocyte quiescence and suppress hepatocellular carcinoma development through inactivation of the Yap1 oncogene. *Cancer Cell.* 2009, 16:425-438

Zimmermann P, Meerschaert K, Reekmans G, Leenaerts I, Small JV, Vandekerckhove J, David G, Gettemans J. PIP(2)-PDZ domain binding controls the association of syntenin with the plasma membrane. *Mol Cell* 2002, 9:1215-1225.

NEDERLANDSE SAMENVATTING

Celdeling is een proces dat essentieel is voor het voortbestaan van zowel eenvoudige eencelligen alsook hogere multicellulaire organismen. Voor multicellulaire organismen is celdeling ook noodzakelijk voor de instandhouding van het organisme zelf. Een goede communicatie tussen de verschillende componenten in de cel en tussen cellen onderling (in het geval van multicellulaire organismen) is van belang om het delingsproces betrouwbaar te laten verlopen. Hierbij wordt gebruikt gemaakt van zogenaamde signaaltransductie-routes. Deze routes zorgen ervoor dat extracellulaire signalen (bv. steroïden) worden omgezet naar intracellulaire signalen, die uiteindelijk leiden tot een bepaalde respons in de cel. Binnen deze routes zijn eiwitten actief die signalen aan elkaar doorgeven in de vorm van kleine moleculen, zoals Ca^{2+} , cAMP en IP_3 . Bij veel signaaltransductiepaden spelen tevens reversibele eiwitmodificaties een rol. Deze veranderen de lokalisatie, stabiliteit of activiteit van een betreffend eiwit. Een veelvoorkomende reversibele eiwitmodificatie is fosforylering: het plaatsen van een fosfaatgroep op de reactieve hydroxylgroep van een tyrosine-, threonine- of serine-residu.

Fosforylering van eiwitten wordt uitgevoerd door bepaalde enzymen, kinases genoemd. In het menselijk genoom coderen meer dan 500 genen voor kinases. Op basis van overeenkomsten in hun aminozuurvolgorde zijn deze kinases onderverdeeld in verschillende groepen. Eén groep daarvan wordt gevormd door de AGC-kinases. Gefosforyleerde eiwitten kunnen ook weer van hun fosfaatgroepen worden ontdaan. Hiervoor is een andere klasse van enzymen, de fosfatases, verantwoordelijk.

Aangezien fosforylering een algemeen mechanisme is om de activiteit van eiwitten te reguleren, speelt het een essentiële rol in het goed functioneren van diverse cellulaire processen, zoals metabolisme, celdifferentiatie en de regulatie van celdeling en celdood. Afwijkingen in de werking van kinases liggen vaak aan de basis van het ontstaan van ziektes. Kanker, bijvoorbeeld, kan worden veroorzaakt door abnormale werking van kinases die een rol spelen bij de controle van ontwikkeling en groei, in het bijzonder in de regulatie van de celcyclus.

De celcyclus omvat een serie processen die achtereenvolgens doorlopen moeten worden alvorens een cel kan delen of kan besluiten voor langere tijd in rust te gaan. Aan het eind van de celcyclus is de celdeling voltooid en zijn twee identieke dochtercellen ontstaan die beide aan een nieuwe celcyclus kunnen beginnen. Uit eerder onderzoek op de afdeling celbiologie is naar voren gekomen dat twee AGC-kinases, Lats2 (uit de NDR-familie) en DMPK-E (uit de DMPK-familie), mogelijk een rol spelen bij het reguleren van de celcyclus. Het doel van het in dit proefschrift beschreven

promotieonderzoek was om meer inzicht te krijgen in de signaaltransductiepaden waarin Lats2 en DMPK-E een rol spelen, opdat we hun invloed op de voortgang van de celcyclus beter kunnen begrijpen.

Hiertoe is allereerst gezocht naar mogelijke substraten van Lats2 en DMPK-E door middel van een grootschalige analyse gebruikmakend van een peptide-array (Hoofdstuk 2). Deze array bevat peptides die afgeleid zijn van bekende cellulaire eiwitten. Voor een viertal peptides die positief uit de test kwamen is van de corresponderende complete eiwitten - PTP-PEST, Cdc2, Lamine-A en MLC2 - onderzocht of deze gefosforyleerd kunnen worden door DMPK-E. Alleen voor MLC2 kon dit worden aangetoond. Een andere benadering om aan de hand van de peptide-array-data mogelijke substraten voor Lats2 en DMPK-E te identificeren was het opstellen van een standaard herkenningsequentie waarmee een eiwitdatabase kon worden doorzocht op eiwitten die deze sequentie bevatten. Zowel DMPK-E als Lats2 bleek een voorkeur te hebben voor een aminozuurvolgorde die aan de N-terminale kant basische aminozuren (arginine of lysine) bevat. Omdat de gevonden standaardherkenningsequentie voor beide kinases in een grote hoeveelheid eiwitten aanwezig bleek, heeft deze benadering niet geleid tot het vinden van concrete nieuwe kandidaatsubstraten. Vervolgonderzoek met specifiek voor Lats2 en DMPK-E ontworpen peptidesequenties zal moeten bijdragen aan het vaststellen van een beter gedefinieerde standaardherkenningsequentie.

Aan de hand van bestaande modellen van de 3D-structuur van beide kinases is bestudeerd of de gevonden kandidaatsubstraten pasten op het enzymatische domein van de kinases. Zowel Lats2 als DMPK-E bevat twee negatieve gebieden waar de N-terminus van het te fosforyleren peptide in het kinasedomein bindt, wat de voorkeur voor positief geladen aminozuren op die lokatie in het substraat verklaart. Beide kinases hebben een hydrofoob stuk waar het C-terminale uiteinde van het substraatpeptide bindt. Een duidelijke voorkeur voor hydrofobe aminozuren op die plek in het substraat kon met de peptide array echter niet aangetoond worden.

MLC2, de regulerende lichte keten van myosine-II kwam naar voren als kandidaatsubstraat van DMPK-E. Het is bekend dat fosforylering van MLC2 in een myosine-II-complex verantwoordelijk is voor regulatie van diens activiteit. Er zijn verschillende fosforyleringplekken in MLC2 bekend, waarvan de threonine op positie 18 (Thr18) en de serine op positie 19 (Ser19) het best bestudeerd zijn. Fosforylering van deze twee residuen leidt tot activering van myosine-II.

Additionele experimenten hebben laten zien dat MLC2 ook in de cel door DMPK-E kan worden gefosforyleerd (Hoofdstuk 3). Wanneer DMPK-E in relatief grote hoeveelheden in de cel aanwezig was, leidde dit tot afwijkingen tijdens de delingsfase van de celcyclus. Voorbeelden zijn de vorming van een afwijkende mitotische

spoelfiguur, celdood tijdens mitose en het ontstaan van cellen met twee kernen. Ook kon aangetoond worden dat dubbelgefosforyleerd MLC2 (P-Thr18/P-Ser19) zich in de contractiele ring en de centrosomen bevindt, twee cytoskeletaire structuren die essentieel zijn voor een correct verloop van de celdeling. Deze observaties hebben geleid tot de hypothese dat DMPK-E in staat is MLC2-eiwit te fosforyleren in centrosomen en in de contractiele ring. Abnormale fosforylering van MLC2 zal resulteren in een abnormaal functioneren van deze structuren en kan het optreden van afwijkende mitotische spoelfiguren, afgebroken celdeling, vorming van cellen met twee kernen en celdood tijdens mitose verklaren.

Bij het bestuderen van de interactie tussen DMPK-E en MLC2 werd duidelijk dat er drie nauwelijks van elkaar te onderscheiden MLC2-varianten bestaan, te weten het zogenaamde gladde-spier (smooth-muscle), niet-spier (non-muscle) en niet-spiergelijkend (nonmuscle-like) MLC2. Deze drie MLC2-eiwitvarianten zijn producten van drie verschillende genen. Analyse van de coderende DNA volgordes en de lokatie van de MLC2-genen in de genomen van een grote verscheidenheid aan dieren wees uit dat deze drie genen zijn ontstaan uit één MLC2-oergen dat twee duplicaties heeft ondergaan. De laatste duplicatie heeft ertoe geleid dat twee MLC2-genen (non-muscle en nonmuscle-like) naast elkaar gelegen zijn in het genoom. De coderende DNA-volgorde van deze twee genen is nagenoeg identiek. Wij denken dat dit verklaard kan worden via een evolutionair mechanisme dat bekend staat als genconversie. Hierbij dienen sterk homologe stukken DNA als elkaars voorbeeld-sjabloon en worden basepaarveranderingen in elk van de twee stukken regelmatig uitgewisseld, wat ertoe leidt dat de twee sequenties gedurende zeer lange tijd gezamenlijk kunnen evolueren.

Aangezien de coderende DNA-sequenties van smooth-muscle, non-muscle en nonmuscle-like MLC2 zeer veel gelijkenis vertonen, zijn de overeenkomsten op eiwitniveau groot (Hoofdstuk 4). Isovorm-specifieke antilichamen om de drie varianten te onderscheiden zijn niet beschikbaar. Om de drie isovormen toch apart aan te kunnen tonen is gebruik gemaakt van een scheidingsmethode waarbij eiwitten van dezelfde grootte gescheiden worden op basis van ladingsverschillen. Omdat nonmuscle MLC2 één negatieve lading minder bevat dan smooth-muscle en nonmuscle-like MLC2, kon deze isovorm gescheiden worden van de andere twee varianten. Door deze vinding konden ook de expressieniveaus van de verschillende MLC2-varianten in diverse cellijnen onderzocht worden. Hierbij vonden we dat specifiek de expressie van smooth-muscle MLC2 sterk gereduceerd is in tumorcellen van muizen.

Naast interacties met substraten, kunnen kinases ook interacties met eiwitten aangaan die niet afhankelijk zijn van het enzymatische domein. Ook deze laatstgenoemde interacties zijn afhankelijk van eiwit-eiwit interactiedomeinen die binden aan specifieke aminozuurvolgordes in hun interactiepartner. Eén van de meest voorkomende niet-enzymatische interactiedomeinen is het PDZ-domein. In Hoofdstuk

5 wordt aangetoond dat het AGC-kinase Lats2 een motief bevat in de C-terminus dat kan binden aan PDZ-domeinen van andere eiwitten. Bovendien bleek dat fosforylering van een tyrosine in dit motief leidde tot een verzwakking van de interactie. Al eerder is aangetoond dat Lats2-overexpressie resulteert in een vertraging in de celcyclus op de overgang van de G1-fase naar de S-fase. Verwijdering van het PDZ-bindende motief van Lats2 versterkt deze blokkade.

Samengevat, in dit proefschrift is aangetoond dat twee kinases van de AGC-groep - Lats2 en DMPK-E - een vergelijkbare, maar niet identieke standaardsequentie herkennen en fosforyleren. Beide kinases kunnen het verloop van de celcyclus beïnvloeden. DMPK-E bewerkstelligt dit mogelijk door fosforylering van MLC2, dat in drie nagenoeg identieke isovormen voorkomt die elk een celtype-afhankelijke expressie vertonen. Lats2 kan via de C-terminus, die interacties aangaat met PDZ-domeinen, de overgang van G1- naar S-fase beïnvloeden. De hier gepresenteerde data dragen bij aan de vergroting van de fundamentele kennis van signaal-transductieroutes, in het bijzonder tijdens de celcyclus. Deze kennis is nodig om beter te kunnen begrijpen hoe signaaloverdracht verloopt in cellen van zowel gezonde als zieke individuen.

ABBREVIATIONS

OP	unphosphorylated	CBB	Coomassie Brilliant Blue
1P	monophosphorylated	CD	catalytic domain
2P	diphosphorylated	Cdc	cell division cycle
3D	three-dimensional	Cdk	cyclin-dependent kinase
3P	triphosphorylated	cDNA	copy DNA
<i>A. carolinensis</i>	<i>Anolis carolinensis</i> (anole lizard)	CRIK	citron kinase
Abl	Abelson	CSK	c-terminal src kinase
AGC	protein kinase A/protein kinase G/protein kinase C	C-terminal	carboxyl terminal
AIS	autoinhibitory sequence	CTG	cytosine-thymine-guanine
Ala	alanine	CUG	cytosine-uracil-guanine
aLRT	approximate likelihood-ratio test	CUG-BP	CUG binding protein
APC	anaphase promoting complex	<i>D. discoideum</i>	<i>Dictyostelium discoideum</i> (slime mold)
<i>A. queenslandica</i>	<i>Amphimedon queenslandica</i> (sponge)	<i>D. melanogaster</i>	<i>Drosophila melanogaster</i> (fruit fly)
Arg	arginine	<i>D. rerio</i>	<i>Danio rerio</i> (zebra fish)
ASPP1	apoptosis stimulating protein of p53	DAK	death associated kinase
ATCC	American Type Culture Collection	DAPI	4',6-diamidino-2-phenylindole
ATP	adenosine triphosphate	DEAE	diethylaminoethyl
AU	arbitrary units	del.	deletion
<i>B. floridae</i>	<i>Branchiostoma floridae</i> (Florida lancelet)	DM1	myotonic dystrophy type 1
<i>B. taurus</i>	<i>Bos taurus</i> (cattle)	DMEM	Dulbecco's modified Eagle's medium
BpV(phen)	bisperoxovanadium 1,10-phenanthroline	DMPK	dystrophin myotonia protein kinase
BSA	bovine serum albumin	DMSO	dimethylsulfoxide
<i>C. elegans</i>	<i>Caenorhabditis elegans</i>	DNA	deoxyribonucleic acid
<i>C. intestinalis</i>	<i>Ciona intestinalis</i> (vase tunicate)	DTT	dithiothreitol
cAMP	cyclic adenosine monophosphate	ECT	epithelial cell transforming protein
		EDTA	ethylenediaminetetraacetic acid
		ER	endoplasmic reticulum
		Erk	extracellular signal-regulated kinase

references, Nederlandse samenvatting, abbreviations, publications, curriculum vitae, dankwoord

EST	expressed sequence tag	MAGI	MAGUK proteins with inverted
FACS	fluorescence activated cell		domain arrangement
	sorting	MAPK	mitogen-activated protein
FCS	fetal calf serum		kinase
FERM	4.1 protein, ezrin, radixin,	MBS	myosin binding subunit
	moesin	MDM2	murine double minute 2
FSHD	facioscapulohumeral	MEF	mouse embryonic fibroblast
	muscular dystrophy	MH2	mad homology 2
<i>G. gallus</i>	<i>Gallus gallus</i> (chicken)	MHC	myosin heavy chain
GEO	gene expression omnibus	miRNA	microRNA
GFP	green fluorescent protein	MKBP	DMPK binding protein
Glu	glutamate	MLC1	myosin essential light chain
Gly	glycine	MLC2	myosin regulatory light chain
GSK	glycogen synthase kinase	MLCK	myosin light chain kinase
GST	glutathione-S-transferase	MMT	mouse mammary tumour
GTP	guanosine triphosphate	MOB	mps one binder
<i>H. sapiens</i>	<i>Homo sapiens</i> (human)	MRCK	myotonic dystrophy kinase-
HeLa	Henrietta Lacks		related Cdc42-binding kinase
HEPES	(4-(2-hydroxyethyl)-1-	mRNA	messenger ribonucleic acid
	piperazineethanesulfonic acid	MST	mammalian Ste20-like
hsp	heat shock protein	MTOC	microtubule organizing centre
ILK	integrin-linked kinase	MUSCLE	multiple sequence comparison
Imm	immortalized		by log-expectation
IP	immunoprecipitation	MYPT	myosin phosphatase targeting
IP3	inositol 1,4,5-trisphosphate		subunit
IPTG	isopropyl β -D-1-	NCBI	National Centre for
	thiogalactopyranoside		Biotechnology Information
KD/kd	kinase dead	NDR	nuclear Dbf2-related
KIND	kinase non-catalytic C-lobe	NIH	National Institutes of Health
	domain	nm	nonmuscle
KO	knockout	nml	nonmuscle-like
LamA	Lamine A	NRK	normal rat kidney
Lats	large tumour suppressor	N-terminal	amino terminal
LB	luria broth	NTR	N-terminal regulatory
LIM	Lin11, Isl-1, Mec-3	NuMa	nuclear mitotic apparatus
LIMK	LIM kinase	Omi/HtrA2	high temperature requirement
Lys	lysine		protein-2
<i>M. musculus</i>	<i>Mus musculus</i> (mouse)	PAK	p21-activated protein kinase
		PBS	phosphate buffered saline

PCM	pericentriolar material	<i>S. kowalevskii</i>	<i>Saccoglossus kowalevskii</i>
PCR	polymerase chain reaction		(acorn worm)
PDB	protein data bank	SD	standard deviation
PDZ	PSD-95/SAP90, Discs-large, ZO-1	SDS-PAGE	sodium dodecyl sulphate polyacrylamide gel electrophoresis
PDZ-BM	PDZ binding motif		
PEI	polyethyleneimine	SEM	standard error of the mean
PH	pleckstrin homology	Ser	serine
PIP2	phosphatidylinositol 4,5-bisphosphate	SH2	src homology 2
		SH3	src homology 3
PKA/B/C	protein kinase A/B/C	sm	smooth muscle
PMSF	phenylmethylsulfonyl fluoride	SMA	S100B/hMOB1 association
PP	protein phosphatase	SRF	serum response factor
Prim	primary	SSC	saline-sodium citrate
PSD-95/SAP90	postsynaptic density protein 95/synapse-associated protein 90	<i>T. guttata</i>	<i>Taeniopygia guttata</i> (zebra finch)
		<i>T. nigroviridis</i>	<i>Tetraodon nigroviridis</i> (green spotted puffer fish)
PTB	phosphotyrosine-binding domain	TAZ	transcriptional co-activator with PDZ-binding motif
PTEN	phosphatase and tensin homologue	TBS	tris-buffered saline
PTP	protein tyrosine phosphatase	TBS-T	TBS with Tween
PTP-BL	protein tyrosine phosphatase BAS-like	TBX2	T-box 2
		TCA	trichloroacetic acid
PTP-PEST	protein tyrosine phosphatase, non-receptor type 12	Thr	threonine
		UG-PAGE	urea/glycerol polyacrylamide gel electrophoresis
PVDF	polyvinylidene fluoride		
Rac	Ras-related C3 botulinum toxin substrate	UTR	untranslated region
		Val	valine
Raf	rapidly accelerated fibrosarcoma	VSGGG motif	Val-Ser-Gly-Gly-Gly motif
		VSV	vesicular stomatitis virus
Ras	rat sarcoma	WB	Western blot
Rho	Ras homologue gene family	WT/wt	wild type
RNA	ribonucleic acid	<i>X. tropicalis</i>	<i>Xenopus tropicalis</i> (African clawed frog)
ROCK	Rho-associated coiled coil containing kinase	YAP	yes-associated protein
RT-PCR	reverse transcription polymerase chain reaction	YFP	yellow fluorescent protein
		ZO	zonula occludens

references, Nederlandse samenvatting, abbreviations, publications, curriculum vitae, dankwoord

PUBLICATIONS

Gerrits L, Venselaar H, Wieringa B, Wansink DG, Hendriks WJAJ: Phosphorylation target site specificity for AGC kinases DMPK E and Lats2. *J. Cell Biochem.* 2012, in press.

Gerrits L, Overheul GJ, Derks RC, Wieringa B, Hendriks WJAJ, Wansink DG: Gene duplication and conversion events shaped three homologous, differentially expressed myosin regulatory light chain (MLC2) genes. *Eur J Cell Biol.* 2012, in press.

Mulders SA, van Horssen R, **Gerrits L**, Bennink MB, Pluk H, de Boer-van Huizen RT, Croes HJ, Wijers M, van de Loo FA, Fransen J, Wieringa B, Wansink DG: Abnormal actomyosin assembly in proliferating and differentiating myoblasts upon expression of a cytosolic DMPK isoform. *Biochim Biophys Acta.* 2011, 1813:867-877.

Te Velthuis AJ, Isogai T, **Gerrits L**, Bagowski CP: Insights into the molecular evolution of the PDZ/LIM family and identification of a novel conserved protein motif. *PLoS One.* 2007, 2:e189.

references, Nederlandse samenvatting,
publications,
curriculum vitae, dankwoord

Lieke Gerrits is geboren op 26 augustus 1981 in Noordwijkerhout. Na het behalen van het VWO-diploma in 1999 aan het Teylingen College te Noordwijkerhout, is zij begonnen aan de opleiding HBO-Verpleegkunde aan de Haagse Hogeschool in Den Haag. Na twee jaar vindt een overstap plaats naar de studie Biologie en Medisch Laboratoriumonderzoek aan de Hogeschool Leiden. Met het voltooien van een afstudeerstage op de afdeling Moleculaire Virologie van het Leids Universitair Medisch Centrum (Prof. dr. W. Spaan) is het diploma voor deze studie in 2004 *cum laude* behaald. Aansluitend stroomt ze door in de Masterfase van de studie Biologie aan de Universiteit Leiden, waar zij voor de specialisatie Moleculaire Biologie en Celbiologie kiest. In 2006 wordt, na een afstudeerstage bij het Instituut Biologie Leiden op de afdeling Moleculaire Celbiologie (Prof. dr. H. Spaink), ook deze studie *cum laude* afgesloten.

In oktober 2006 begint Lieke Gerrits als junioronderzoeker aan een promotieproject op de afdeling Celbiologie van het Universitair Medisch Centrum St. Radboud te Nijmegen onder supervisie van Prof. dr. Bé Wieringa, Dr. Wiljan Hendriks en Dr. Rick Wansink. Het werk verricht op deze afdeling staat beschreven in dit proefschrift. Tijdens deze periode heeft ze drie HLO-studenten begeleid bij hun hoofdvakstages. Ook heeft zij bij praktisch onderwijs voor studenten Biomedische Wetenschappen en Geneeskunde geassisteerd.

Van augustus 2011 tot januari 2012 heeft Lieke Gerrits als Regulatory Affairs Manager bij MSD te Oss gewerkt. Vanaf 1 januari 2012 is zij werkzaam als Regulatory Affairs Manager bij Synthon in Nijmegen.

Na vijf en een half jaar is het moment dan eindelijk aangebroken: ik mag het dankwoord schrijven. In gedachten ben ik hier al zo vaak mee bezig geweest en toch kan ik nog steeds niet geloven dat het er nu echt van gekomen is.

In het voorjaar van 2006 kwam ik naar Nijmegen voor een eerste sollicitatiegesprek met Rick en Wiljan en ongeveer een week later mocht ik terugkomen om een presentatie te geven over mijn afstudeerstage in Leiden. Na afloop hadden Wiljan, Rick, Bé en ik een kort gesprek op een zonovergoten dakterras van de NCMLS-toren en een paar dagen later werd ik gebeld door Wiljan met de vraag of ik de baan wilde accepteren. Daar hoefde ik niet lang over na te denken en ik zei dan ook meteen dat ik dat wilde. En zodoende kwam ik op maandag 2 oktober 2006 naar de 6^e verdieping van de toren om te beginnen aan mijn promotieonderzoek. En nu, ruim vijf jaar later is het eindresultaat daar: dit proefschrift. In de tussentijd heb ik veel leuke, nieuwe en uitdagende, maar ook moeilijke en frustrerende momenten meegemaakt. Dit proefschrift zou er nooit gekomen zijn zonder de hulp en steun van velen, die ik daarom graag in dit hoofdstuk wil bedanken.

Bé, allereerst wil ik jou bedanken voor de mogelijkheid om mijn promotieonderzoek bij jou te voltooien, voor je bijdrage aan alle individuele hoofdstukken en het tot een geheel maken van deze hoofdstukken tot dit boekje.

Rick en Wiljan, ook jullie wil ik uiteraard heel erg bedanken: voor het altijd meedenken met experimenten en het steeds weer met nieuwe ideeën komen, voor jullie grote bijdrage aan het schrijfwerk van de verschillende hoofdstukken en voor alles wat ik van jullie geleerd heb. Jullie hebben elk je eigen manier van begeleiden waardoor ik van jullie allebei verschillende dingen heb geleerd. Wiljan, van jou heb ik geleerd dat een goede voorbereiding essentieel is en dat je nooit teveel controles kunt meenemen. En natuurlijk dat de gitaar een geweldig instrument is! Rick, het belangrijkste dat ik van jou heb geleerd is dat ik soms iets minder kritisch moet zijn op mijn eigen werk en dat elk hoogtepunt, hoe klein ook, de moeite waard is om van te genieten en om te vieren.

Relativering is onmisbaar geweest voor het voltooien van mijn promotieproject. De vrijdagmiddagborrels (voorafgegaan door de you-tube-knaller) waren hiervoor bij uitstek geschikt. Ik denk ook met ontzettend veel plezier terug aan alle filmavonden, kerstdiners, paaslunches, dagjes-uit, Sinterklaasvieringen en het onvergetelijke feestje met Gordon in Groesbeek.

Jan, Irene, Mirthe, Susan, Walther, Anke, Anchel, Ralph, Marieke, Mietske,

Huib, Rinske, Magda, Steffi, Gerda, Remco, Jack, Mariska, Frank, Ineke, Monique: bedankt voor al jullie praktische adviezen, gezelligheid en goede gesprekken. Ook de andere "bewoners" van de zesde verdieping (Marieke deV, Peter deB, de Moldiertjes en de Friedls) wil ik bedanken: een goede buur is beter dan een verre vriend, dat hebben jullie absoluut bewezen.

Ook wil ik op deze plek mijn stagiaires Ronny, Gijs en Michael bedanken voor hun bijdrage aan de verschillende hoofdstukken. Alledrie werken jullie inmiddels als analist bij het UMC St. Radboud en ik wens jullie daarbij veel succes en plezier. Gijs, jouw appeltaartrecept is inmiddels legendarisch. Michael, ik heb nooit een vrolijker en enthousiaster persoon dan jij meegemaakt. En je hebt nog maar eens bewezen dat ethanol inderdaad brandbaar is...

Lieke van den Berk, bedankt voor de totstandkoming van het Lieke & Lieke hoofdstuk. Ook wil ik Piet van Erp bedanken voor zijn hulp met de FACS-experimenten uit hoofdstuk 5 en Hanka Venselaar voor haar hulp bij hoofdstuk 2, mijn eerste gepubliceerde hoofdstuk!

Marieke en Mirthe, ik ben heel erg blij dat jullie mijn paranimfen willen zijn. Voor mij staat dit symbool voor wat jullie tijdens mijn promotie voor mij betekend hebben: het bieden van een luisterend oor (tijdens jullie spreekuren in het celkweeklab) bij persoonlijke en wetenschappelijke dieptepunten, het samen vieren van de hoogtepunten en mij ervan verzekeren dat "het altijd goed komt". Ik ben jullie heel dankbaar voor jullie vriendschap die zich ook buiten het werk ontwikkeld heeft en ik hoop dat die zal blijven voortbestaan. Ik wens jullie allebei heel veel geluk toe met jullie gezin. Marieke, ik bewonder je altijd positieve kijk op de dingen en je directheid. Mirthe, ik heb ontzag voor je enthousiasme, gevoel voor humor en je pragmatische instelling. Heel veel succes met het afronden van je eigen promotieproject.

Natuurlijk zijn ook mijn vrienden erg belangrijk geweest. Door mijn vertrek naar Nijmegen, werden de bezoeken aan de vrienden in Noordwijkerhout minder frequent. Ad, Elise, Jeroen, Josien en Bart, ik ben heel blij dat jullie me altijd overal bij zijn blijven betrekken en dat we nog steeds een goed contact met elkaar hebben.

Wendy, ook wij hebben na al die jaren nog steeds contact met elkaar. En ik ben blij dat we door jouw initiatief om een boekenclub op te richten elkaar weer wat vaker zien!

Margje, onze vriendschap is juist ontstaan doordat ik in Nijmegen ben komen wonen. Ik hoop dat we ook in de toekomst een hoop lol zullen beleven.

Ook wil ik Opa en Oma en alle ooms en tantes bedanken voor de altijd getoonde interesse in mijn werk. Geregeld werd mij door jullie gevraagd hoe het ging met

"afstuderen" en ik ben blij dat ik nu eindelijk kan antwoorden dat het klaar is.

Joep en Gijs, ik ben blij dat ik jullie zus(je) ben en ik wens jullie een hele gelukkige toekomst toe met Sietske en Linda. Ook jullie bedankt voor jullie interesse en steun.

Pappa en mamma, mijn laatste woorden van dit hoofdstuk wil ik graag tot jullie richten. Jullie hebben mij alle kansen en mogelijkheden gegeven om te studeren en me te ontwikkelen tot wie ik nu ben. Ookal moeten jullie het niet makkelijk hebben gevonden dat ik naar het "verre" Nijmegen vertrok, jullie hebben me hierin altijd gesteund en waren en zijn altijd vol belangstelling. Voor dit alles en het feit dat jullie altijd voor me klaar staan, ben ik jullie ontzettend dankbaar. Ik hou van jullie!

Dit hoofdstuk nog eens nalezend besef ik des te meer dat ik veel mensen erg dankbaar ben: door jullie is mijn promotietijd een tijd waar ik met heel veel plezier aan terug zal denken!

Hieke

*And the hardest part
Was letting go, not taking part
Was the hardest part
Coldplay - The hardest part*

